DUZCE MEDICAL JOURNAL

DÜZCE TIP FAKÜLTESİ DERGİSİ

Indexed in / Tarandığı indeksler

CINAHL, CrossRef, DOAJ, EBSCO, EBSCOhost, EMBASE, ICMJE, Scopus, Türkiye Atıf Dizini, Türk Medline, ULAKBİM TR Dizin, Web of Science: E-SCI

An international peer-reviewed journal published three times a year. / Yılda üç kez yayınlanan uluslararası hakemli bir dergidir.
The authors are responsible for their articles. / Makalelerin sorumluluğu yazarlarına aittir.

Contact / İletişim

Düzce Üniversitesi Tıp Fakültesi Konuralp Yerleşkesi, Düzce   e-mail: duzcetipdergisi@duzce.edu.tr   web: https://dergipark.org.tr/en/pub/dtfd

CONTENTS / İÇİNDEKİLER

CONTENTS / İÇİNDEKİLER

Assessment of Anticancer Properties of Synthesized Pyrazole-Acridine Derivative on SH-SY5Y Human Neuroblastoma Cells

Sentezlenen Pirazol-Akridin Türevinin SH-SY5Y İnsan Nöroblastoma Hücrelerinde Antikanser Özelliklerinin Değerlendirilmesi

Yusuf KÜÇÜKBAĞRIAÇIK[1]
0000-0002-4909-2669
Muna ELMUSA[2]
0000-0003-4087-4944
Fatıma ELMUSA[3]
0000-0001-6645-5487
Hümeyra YILMAZ[4]
0000-0001-7530-4568
Rahmi KASIMOĞULLARI[5]
0000-0001-6391-7121
Mohammadreza DASTOURI[4]
0000-0003-3882-0728

[1]Department of Biophysics, Health Sciences University Gülhane Faculty of Medicine, Ankara, Türkiye

[2]Elfurat Engineering Research and Development Limited Company, Ankara, Türkiye

[3]Department of Molecular Biology, Eskisehir Technical University Institution of Graduate Schools, Eskisehir, Türkiye

[4]Department of Medical Biology, Ankara Medipol University School of Medicine, Ankara, Türkiye

[5]Department of Chemistry, Dumlupınar University Faculty of Art and Science, Kütahya, Türkiye

Corresponding Author
Sorumlu Yazar
Yusuf KÜÇÜKBAĞRIAÇIK
yusuf.kucukbagriacik@sbu.edu.tr

ABSTRACT

Aim: This study aimed to synthesize a novel pyrazole acridine derivative (3-ACH) and evaluate its anticancer properties on SH-SY5Y human neuroblastoma cells.

Material and Methods: The pyrazole-4-carbaldehyde derivative was cyclized with dimedone and p-nitroaniline to synthesize the 3-ACH. Characterization of the compound was performed using FT-IR, NMR, HPLC-Q-TOF/MS, and elemental analysis. The cytotoxic impact of the 3-ACH compound on SH-SY5Y human neuroblastoma cells was evaluated using the WST-1 assay in a dose- (50, 100, and 150 µg/mL) and time-dependent (12, 24, and 48 hours) manner. The impact of 3-ACH on apoptosis was investigated through immunostaining for Caspase-3, -8, and -9, and BAX proteins.

Results: 3-ACH reduced SH-SY5Y cell viability with the rate of 89.89±7.63% (p=0.002) at 100 µg/mL concentration after 24 hours of treatment. While a higher (150 µg/mL) concentration showed a similar reduction (90.53±2.88%, p=0.004), the lower (50 µg/mL) concentration maintained high cell viability (98.37±1.67%, p=0.903) at 24 hours. All doses of 50 µg/mL (94.55±0.65%), 100 µg/mL (95.18±1.41%), and 150 µg/mL (95.28±2.57%) significantly reduced cell viability rates, at 48 hours (all p<0.001). Immunostaining revealed a significant upregulation in the synthesis of BAX, Caspase-3, -8, and -9 proteins in cells treated with 3-ACH (100 µg/mL) for 24 hours compared to the control group.

Conclusion: These results indicate that 3-ACH has the potential to induce apoptosis in SH-SY5Y cells by activating both the intrinsic and extrinsic pathways, which may contribute to its cytotoxic effects. This study provides promising evidence supporting the potential of the 3-ACH compound as an anticancer therapeutic agent.

Keywords: Chemical synthesis; antineoplastic agents; neuroblastoma; pyrazoles; acridines; cytotoxicity; apoptosis.

ÖZ

Amaç: Bu çalışmanın amacı yeni bir pirazol akridin türevi (3-ACH) sentezlemek ve bu bileşiğin SH-SY5Y insan nöroblastoma hücreleri üzerindeki antikanser özelliklerini değerlendirmektir.

Gereç ve Yöntemler: Pirazol-4-karbaldehit türevi, 3-ACH sentezlemek için dimedon ve p-nitroanilin ile siklize edildi. Bileşiğin karakterizasyonu FT-IR, NMR, HPLC-Q-TOF/MS ve element analizi kullanılarak yapıldı. 3-ACH bileşiğinin SH-SY5Y insan nöroblastoma hücreleri üzerindeki sitotoksik etkisi, doz (50, 100 ve 150 µg/mL) ve zaman (12, 24 ve 48 saat) bağımlı bir şekilde WST-1 testi kullanılarak değerlendirildi. 3-ACH'nin apoptoz üzerindeki etkisi, Kaspaz-3, -8, -9 ve BAX proteinleri için immün boyama yolu ile araştırıldı.

Bulgular: 3-ACH, 100 µg/mL konsantrasyonda 24 saatlik tedaviden sonra SH-SY5Y hücre canlılığını %89,89±7,63 (p=0,002) oranında azaltmıştır. 24 saatte, daha yüksek (150 µg/mL) konsantrasyon benzer bir azalma gösterirken (%90,53±2,88, p=0,004), daha düşük (50 µg/mL) konsantrasyon hücre canlılığını korumuştur (%98,37±1,67, p=0,903). 50 µg/mL (%94,55±0,65), 100 µg/mL (%95,18±1,41) ve 150 µg/mL (%95,28±2,57) dozlarının tümü, 48 saatte hücre canlılık oranlarını önemli ölçüde azaltmıştır (tüm p<0,001). İmmün boyama, 24 saat boyunca 3-ACH (100 µg/mL) ile muamele edilen hücrelerde, BAX, Kaspaz-3, -8 ve -9 proteinlerinin sentezinde kontrol grubuna kıyasla önemli bir artış olduğunu ortaya koymuştur.

Sonuç: Bu sonuçlar, 3-ACH'nin hem intrinsik hem de ekstrinsik yolları aktive ederek SH-SY5Y hücrelerinde, sitotoksik etkilerine katkıda bulunabilecek olan, apoptozu indükleme potansiyeline sahip olduğunu göstermektedir. Bu çalışma, 3-ACH bileşiğinin antikanser terapötik ajan olarak potansiyelini destekleyen umut verici kanıtlar sunmaktadır.

Anahtar kelimeler: Kimyasal sentez; antineoplastik ajanlar; nöroblastoma; pirazoller; akridinler; sitotoksisite; apoptoz.

INTRODUCTION

Pyrazole is a 5-membered organic heterocyclic compound containing nitrogen and carbon atoms, with the chemical formula $C_3H_3N_2$ (1). The pyrazole ring closely resembles the imidazole compound, but with the substitution of a nitrogen atom by a carbon atom. Pyrazole and its derivatives have been reported to be present in various natural products (2). Due to the chemical diversity of pyrazoles, they have been extensively investigated and found to exhibit various pharmacological properties, including anti-inflammatory, anti-cancer, anti-viral, and anti-bacterial effects (3). Moreover, certain pyrazoles have exhibited inhibitory properties against cancer cell proliferation, positioning them as viable candidates for anti-tumor agents (4). Additionally, there is a need to explore innovative strategies to optimize the side effect profile, pharmacokinetics, and pharmacodynamics of pyrazoles (5), including enhancing pyrazole activity, reducing toxicity, and increasing water solubility (6,7).

Acridine is a heterocyclic compound belonging to the class of organic compounds known as polycyclic aromatic hydrocarbons (8). Its unique molecular structure has attracted significant attention, leading to extensive investigations regarding its potential applications in various fields. Acridine and its derivatives have been the subject of numerous studies due to their interactions with DNA and RNA, notable fluorescence properties, and enzyme inhibition capabilities, particularly against topoisomerases (9). The intercalation of acridine with DNA is believed to underlie its anticancer activity, as it can disrupt DNA replication and induce cell death (10). Encouraging results have emerged from preclinical and clinical trials, demonstrating the efficacy of acridine-based drugs in inhibiting tumor growth and achieving successful cancer treatment across various types, including breast, lung, and colon cancers.

Pyrazoloacridine, a compound that combines acridine with the pyrazole ring, belongs to the class of anthrapyrazoles, which have shown antitumor activity similar to doxorubicin but with reduced cardiotoxicity (11,12). It has been extensively studied in vitro and in vivo against various cancer types, particularly leukemia, and has demonstrated promising effectiveness (12).

While various pyrazole-acridine derivatives have been investigated for their biological activities, the specific compound 9-(1-(benzo[d]thiazol-2-yl)-3-(4-chlorophenyl)-1H-pyrazol-4-yl)-3,3,6,6-tetramethyl-10-(4-nitrophenyl)-3,4,6,7,9,10-hexahydroacridine-1,8(2H,5H)-dione (3-ACH) represents a novel molecular entity that was first synthesized by Elmusa et al. (13). Their initial study focused exclusively on the compound's acetylcholinesterase inhibitory properties through in vitro and in silico approaches. However, the potential anticancer properties of 3-ACH, particularly against neuroblastoma cells, have not been previously investigated. The unique structural features of 3-ACH, including the benzothiazole moiety and the specific substitution pattern of the pyrazole-acridine scaffold, distinguish it from other previously reported pyrazole-acridine derivatives. This structural novelty, combined with the unexplored anticancer potential, presents an opportunity to evaluate 3-ACH as a potential therapeutic agent against neuroblastoma, thereby expanding the understanding of structure-activity relationships in this class of compounds.

In this study, the goal was to develop new agents with improved anticancer activity by integrating pyrazole and acridine, which individually exhibit anticancer properties, within a single molecule. To achieve this, hydrazone synthesis was initially conducted, followed by the synthesis of the compound referred to as 1-(benzo[d]thiazol-2-yl)-3-(4-chlorophenyl)-1H-pyrazole-4-carbaldehyde (P4C) using the hydrazone as a precursor. Subsequently, cyclization of the synthesized pyrazole-4-carbaldehyde was accomplished by utilizing dimedone and p-nitroaniline, leading to the formation of 3-ACH, the pyrazole-acridine derivative. Following synthesis, the obtained pyrazole-acridine derivative was subjected to characterization using FT-IR, NMR, HPLC-Q-TOF/MS, and elemental analysis techniques. Subsequently, the anticancer activity of the obtained pyrazole-acridine derivative was tested against the SH-SY5Y neuroblastoma cell line. Test concentrations of 50, 100, and 150 µg/mL were employed, and the assessment was conducted over incubation durations of 12, 24, and 48 hours. The WST-1 assay was employed to evaluate the cytotoxic impact of the pyrazole-acridine derivative on the SH-SY5Y cell line. Additionally, immunostaining techniques were employed to evaluate the expression levels of proteins associated with the apoptotic pathway, including Caspase-3, -8, and -9, and BAX. These investigations aimed to provide insights into the apoptotic mechanism of 3-ACH on human neuroblastoma cancer cell lines.

MATERIAL AND METHODS

Chemical Synthesis

The chemicals used in this study were obtained from Sigma, Aldrich, Fluka, and Merck companies. The solvents employed were distilled prior to use. All compounds are >95% pure by HPLC analysis. The synthesis of the pyrazole-acridine derivative was performed in two stages. In the first stage, the hydrazone compound was synthesized by employing 4-chloroacetophenone and 2-hydrazinobenzothiazole as precursors. Subsequently, the Vilsmeier-Haack reagent was introduced to the hydrazone compound to facilitate the synthesis of P4C, which served as the initial compound containing the benzothiazole moiety. In the second stage, the synthesized P4C was activated through its reaction with dimedone and p-nitroaniline, resulting in the conversion to the desired pyrazole-acridine derivative, 3-ACH.

For the synthesis of 2-(2-(1-(4-chlorophenyl)ethylidine)hydrazino)benzo[d]thiazole compound, 1 g (6 mmol) of 2-hydrazinobenzothiazole and 0.94 g (6 mmol) of 4-chloroacetophenone were mixed in a flask and dissolved in 20 mL of ethanol. Subsequently, 0.4 mL of acetic acid was added to the mixture, which was then refluxed for 3 hours. The resulting beige precipitate was washed with a 2:1 mixture of water and ethanol, followed by purification through crystallization in butanol.

For the synthesis of P4C, 0.55 mL (6 mmol) of phosphoryl chloride ($POCl_3$) was kept in an ice bath for 20 minutes, and then 2 mL of cooled N, N-dimethylformamide (DMF) was added dropwise. After stirring for a few minutes, 0.301 g (1 mmol) of the compound 2-(2-(1-(4-chlorophenyl)ethylidine)hydrazino)benzo[d]thiazole was added to the mixture. The reaction mixture was stirred in an ice bath for

30 minutes, followed by an additional 30 minutes at room temperature. It was subsequently refluxed in an oil bath at 80-90 °C for 5 hours. After cooling the mixture to room temperature, ice water was added, resulting in the formation of a brown precipitate, which was further purified by crystallization from toluene.

To synthesize 3-ACH, a solution was prepared by dissolving 0.340 g (1 mmol) of P4C and 0.019 g (0.1 mmol) of p-toluenesulfonic acid (TSA) in 10 mL of tetrahydrofuran (THF). 0.280 g (2 mmol) of dimedone was added to this solution and stirred for 5 minutes. Next, 0.138 g (1 mmol) of p-nitroaniline was introduced into the solution, followed by refluxing for 6 hours. The resultant yellow precipitate was washed with water and further purified through crystallization from ethanol (13).

Characterization

DC-Alufolien 20x20 cm Kieselgel 60 F254 analytical thin-layer chromatography (TLC) plates and a Camag UV lamp (254-366 nm) were utilized to monitor the progress of the reactions conducted in this study. The melting points of the synthesized compounds were measured using the Barnstead Electrothermal 9200 instrument. Fourier-transform infrared spectroscopy (FT-IR) was conducted using the Bruker Optics Vertex 70 instrument, providing valuable information about the functional groups present in the compounds. High-performance liquid chromatography quadrupole time-of-flight mass spectrometry (HPLC-Q-TOF/MS) was performed using the Agilent 1260 infinity HPLC system coupled with a 6210 time of flight (TOF) LC/MS detector to analyze the mass of the synthesized compounds. Nuclear magnetic resonance (NMR) spectroscopy was employed for detailed structural analysis, with ^{1}H-NMR analysis conducted at 600 MHz and ^{13}C-NMR analysis at 150 MHz. In NMR analyses, $CDCl_3$ was used as the solvent, providing a chemical shift reference of 7.26 ppm for ^{1}H-NMR and 77.2 ppm for ^{13}C-NMR. Finally, elemental analysis of the compounds was performed using the Leco CHNS-932 device (13).

Sample Size

Sample size calculation was performed using G*Power software v.3.1.9.7. For one-way ANOVA comparison between groups with $\alpha=0.05$, power $(1-\beta)=0.80$, effect size $f=0.6$, and four experimental groups (one control and three treatment groups), the minimum required total sample size was calculated as 36 (9 samples per group). In our experimental design, we conducted six independent biological replicates for each group, with each replicate consisting of three technical replicates, resulting in a total of 18 measurements per group. This sample size exceeded the minimum requirement, achieving an actual statistical power of 0.82, which ensured robust statistical analysis of the experimental data.

Cell Culture

The SH-SY5Y human neuroblastoma cell line (ATCC® CRL-2266™) was cultured in DMEM high glucose medium (Sigma-D6429-500 ML), supplemented with 10% heat-inactivated fetal bovine serum (Biowest, S181H-500), 1% L-glutamine (Gibco, 25030081), and 1% penicillin-streptomycin (Gibco, 10378016). The cells were kept in a 37 °C incubator with 5% CO_2, and observations related to cell viability and growth rates were conducted using a microscope.

Study Design and Experimental Groups

The study was designed to evaluate both the dose- and time-dependent effects of 3-ACH on SH-SY5Y human neuroblastoma cells. The experimental design consisted of four groups: a control group (0.1% DMSO) and three treatment groups receiving different concentrations of 3-ACH (50, 100, and 150 µg/mL). These concentrations were selected based on our previous study where these doses showed significant cytotoxic effects against SKBR-3 human breast cancer cells (14). Time points (12, 24, and 48 hours) were chosen to evaluate both early and late effects of the compound. Cell viability was assessed using WST-1 assay and expressed as a percentage of viable cells relative to control (100%). For apoptosis-related protein expression studies, the 24-hour time point and 100 µg/mL concentration were selected based on the optimal cytotoxic response observed in viability assays. Each experiment was performed with six independent biological replicates per group.

Cell Viability/Cytotoxicity Assay (WST-1)

The WST-1 assay is used to assess cell viability and cytotoxicity. In this study, we employed the WST-1 to evaluate the cytotoxic effects of different doses and durations of 3-ACH administration on human neuroblastoma cells. To assess the anticancer potential of 3-ACH, we conducted cell viability measurements using the WST-1 assay (Takara Premix WST-1 Cell Proliferation Assay System MK400), following the manufacturer's guidelines. The assay is based on the conversion of tetrazolium salt into formazan by mitochondrial dehydrogenases within the cells. Stock solutions of the tested compounds were diluted in complete medium to final concentrations of 50, 100, and 150 µg/mL. The cells were exposed to various concentrations of the compounds or a maximum vehicle dose (0.1% DMSO). After incubation periods of 12, 24, and 48 hours, cell viability was assessed. The cells were treated with the WST-1 reagent and incubated for 4 hours at 37 °C. Absorbance was then measured at 450 nm using a microplate reader (Tecan Infinite 200pro) (15).

Immunostaining

Immunostaining is a technique that depends on the creation of antigen-antibody complexes. In this study, we employed immunostaining to investigate the apoptotic pathways activated in SH-SY5Y cells following the administration of 3-ACH. The aim was to elucidate the process of cell death associated with apoptosis using this methodology.

Based on cytotoxicity results, SH-SY5Y cells were treated with 3-ACH at 100 µg/mL for 24 hours. The cells cultured on coverslips were fixed with a 3.5% paraformaldehyde solution (Sigma-158127). After fixation, the cells were rinsed with PBS (Gibco,14190-094) and immersed in PBS azide (Chemcruz, SC-296028). The fixed cells were incubated individually with primary antibodies against BAX (Abcam, ab32503, rabbit), Caspase-3 (Abcam, ab13847, rabbit), Caspase-8 (Abcam, ab32125, rabbit), and Caspase-9 (Abcam, ab202068, rabbit) for 24 hours at +4 °C. Subsequently, the coverslips were washed twice with PBS to remove unbound antibodies. The cells were then treated with FITC-labeled secondary antibody (Sigma, F9887, anti-rabbit) for 2 hours at 37 °C. Following another round of PBS washing, the cells were stained with 7-amino actinomycin D (7-AAD), a DNA dye, for 30 minutes at 37 °C (15).

Cell nuclei were stained with 7-AAD dye, producing a red signal, while target proteins were labeled with a FITC-conjugated antibody, emitting a green signal. The intensity of these signals was analyzed using ImageJ software, and the images of nuclei and cytoplasm were merged. Immunofluorescence images were qualitatively evaluated by visually comparing fluorescence signals between the control and treatment groups.

The immunostained cells were visualized and photographed using an inverted fluorescence microscope (ZEISS Axioscope 5) equipped with appropriate filter sets for FITC (excitation: 495 nm/emission: 519 nm) and 7-AAD (excitation: 546 nm/emission: 647 nm). Representative images were captured at 100X magnification. The green fluorescence (FITC signal) indicated the presence and relative expression levels of target proteins (BAX, Caspase-3, -8, and -9), while the red fluorescence (7-AAD) showed nuclear staining. The relative protein expression levels were evaluated by comparing the intensity of green fluorescence between control and treated groups in representative fields. An increase in green fluorescence intensity indicated elevated protein expression compared to control cells.

Ethics Statement

This study utilized commercially available cell lines and did not involve human subjects or animal experiments. Therefore, ethics committee approval was not required.

Statistical Analysis

Statistical analysis of cytotoxicity data obtained in the study was performed using IBM SPSS Statistics Version 27.0 software. Data normality was assessed using the Shapiro-Wilk test, and homogeneity of variances was evaluated using the Levene test. One-way ANOVA followed by Tukey's post-hoc test was used for multiple comparisons. Results are expressed as mean±standard deviation. Statistical significance was determined at a threshold of $p < 0.05$ for all results.

RESULTS

The synthesis of the pyrazole-acridine derivative was completed in two stages (Figure 1). The yield of the synthesized P4C compound was 83%, with a melting point range of 224-225 ℃. The yield of the synthesized 3-ACH compound was 62%, with a melting point range of 280-282 ℃.

Fourier-Transform Infrared Spectroscopy (FT-IR)

The FTIR spectrum of P4C exhibited a distinctive absorption at 3066 cm^{-1}, indicating aromatic C-H bonds. The identified peak at 1696 cm^{-1} confirmed the existence of a carbonyl group associated with the aldehyde moiety in P4C. Additionally, the peaks in the range of 1600-1450 cm^{-1} corresponded to C=C and C=N bonds, consistent with the anticipated compound structure (Figure 2).

Similarly, 3-ACH, a derivative of P4C, displayed the characteristic peak for aromatic C-H bonds at 3066 cm^{-1}. Additional absorptions at 2959 cm^{-1} and 2869 cm^{-1} suggested aliphatic C-H bonds. The peak at 1656 cm^{-1} provided confirmation of the carbonyl group's existence, which is linked to the ketone group within the compound. Furthermore, the peaks in the 1600-1450 cm^{-1} range corresponded to C=C and C=N bonds present within the compound. Finally, the absorption peaks at 1532 cm^{-1} and 1388 cm^{-1} were attributed to the presence of nitro groups within the molecular structure (Figure 2) (16).

Nuclear Magnetic Resonance (NMR)

The ^{1}H-NMR spectrum of the P4C showed a singlet at 10.08 ppm, indicating the presence of the aldehyde proton (CHO), while the proton bonded to the carbon atom in the pyrazole ring (C5H) resonated as a singlet at 9.08 ppm. The aromatic protons exhibited a complex pattern of absorption, appearing as multiplets within the range of 7.97-7.42 ppm (Figure 3a). In the ^{1}H-NMR spectrum of 3-ACH, the proton attached to the pyrazole ring's carbon (C5H) appeared as a single signal at 7.99 ppm. Multiplet signals observed in the 7.98-7.40 ppm range were assigned to aromatic protons (Ar-H). The singlet at 5.57 ppm originated from the proton associated with the C9H carbon in the acridine ring. Singular signals at 2.66 and 2.61 ppm were assigned to protons at carbons C2-C7H and C4-C5H of the acridine ring, respectively. Furthermore, single peaks at 1.54 ppm and 1.13 ppm corresponded to methyl protons (CH3) in the molecule (Figure 3b).

The ^{13}C-NMR spectrum of P4C displayed a signal at 183.73 ppm for the aldehyde carbon atom (C=O). The peaks at 168.19 ppm and 153.94 ppm were attributed to carbon 2 and 9 in the benzothiazole ring, respectively. The 12 peaks observed between 150.64 and 121.78 ppm were assigned to the aromatic carbons (Figure 3c). The ^{13}C-NMR spectrum of 3-ACH revealed a signal at 197.62 ppm, indicating the presence of the ketone (C=O) carbonyl within
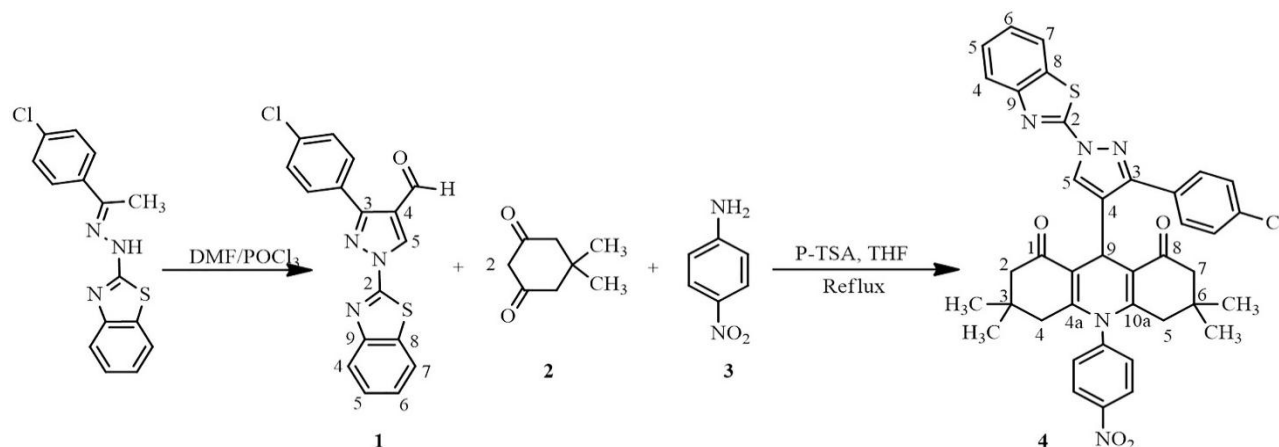
Figure 1. Synthesis of pyrazole-acridine derivative from hydrazone (1: P4C, 2: dimedone, 3: p-nitroaniline, 4: 3-ACH)
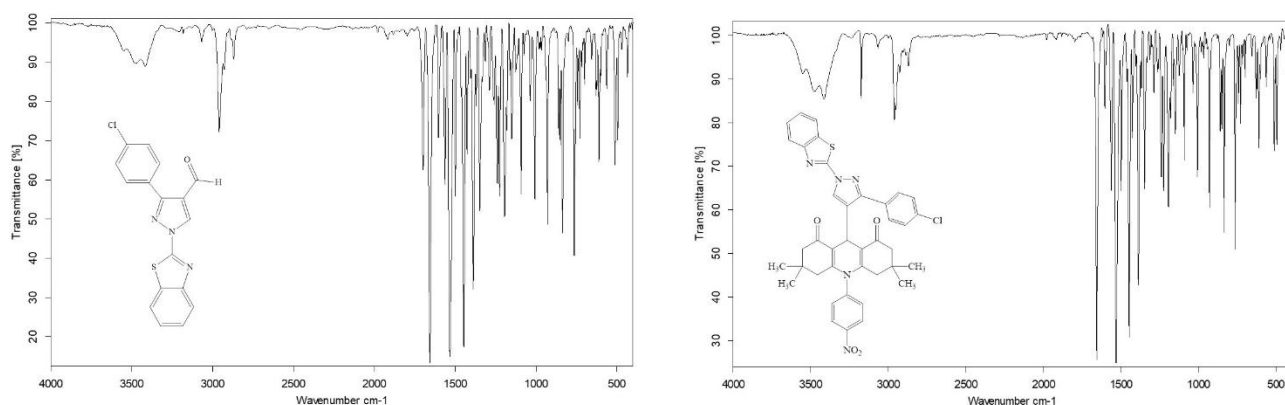
Figure 2. Fourier-transform infrared spectroscopy (FT-IR) spectrum of P4C and 3-ACH
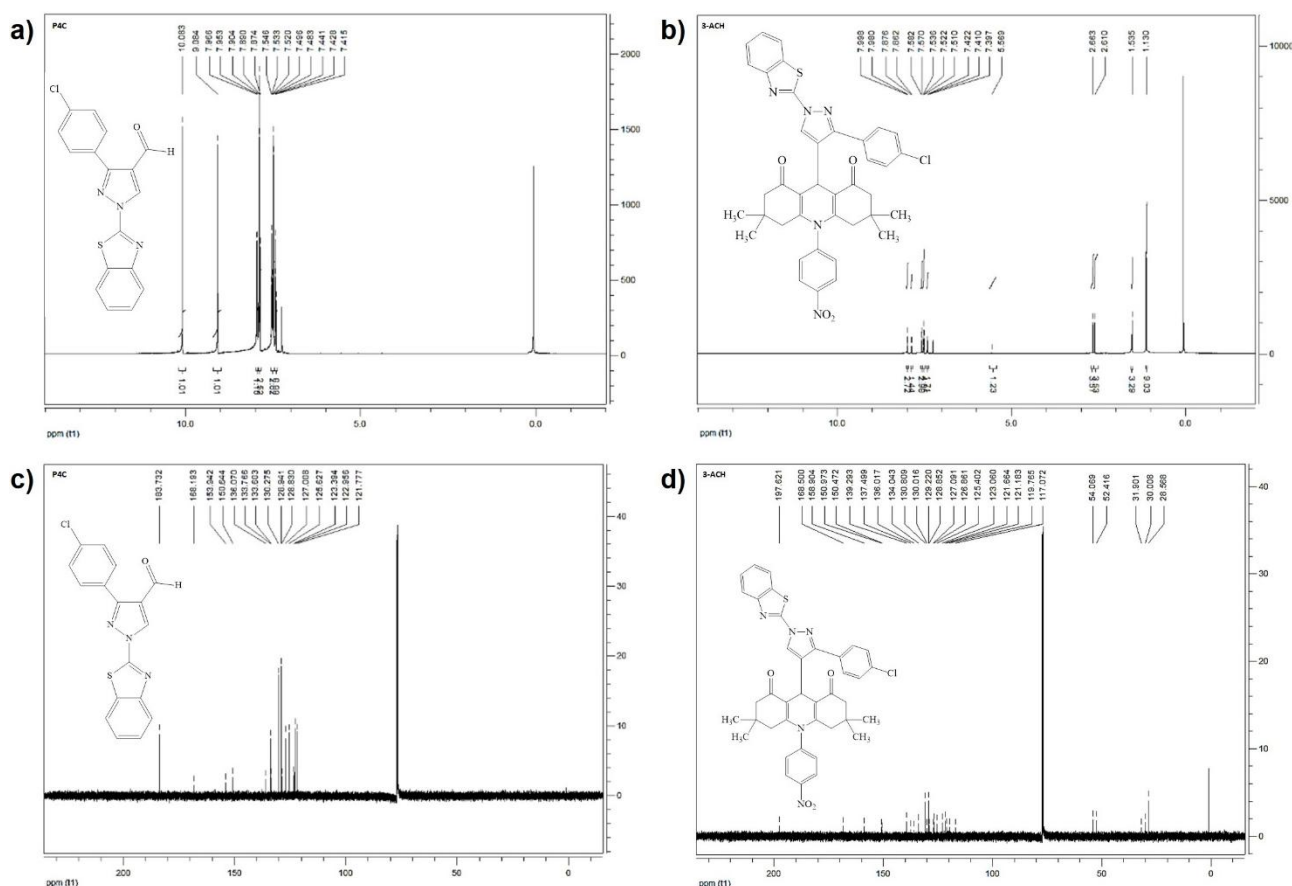
Figure 3. Nuclear magnetic resonance (NMR) spectra of synthesized compounds at 600 MHz and 150 MHz; **a)** ^{1}H-NMR spectrum of P4C, **b)** ^{1}H-NMR spectrum of 3-ACH, **c)** ^{13}C-NMR spectrum of P4C, **d)** ^{13}C-NMR spectrum of 3-ACH

the acridine ring. Signals at 168.50 ppm and 150.97 ppm were attributed to carbon 2 and carbon 9 in the benzothiazole ring, respectively. Furthermore, signals at 158.90 ppm and 158.70 ppm arose from the C4a and C10a carbons in the acridine ring, while the signal at 150.47 ppm denoted the carbon linked to the nitro atom (C-NO$_2$). Aliphatic carbon atoms were represented by signals at 54.07 ppm (C2 and C7), 52.42 ppm (C4 and C5), 31.90 ppm (C9), and 30.01 ppm (C3 and C6), all located in the acridine ring. Finally, the signal at 28.57 ppm in the spectrum originated from the methyl carbons within the molecule (Figure 3d) (17).

Mass Spectrometry (High-Performance Liquid Chromatography Quadrupole Time-of-Flight Mass Spectrometry, HPLC-Q-TOF/MS) Analysis
In the mass spectrum of P4C, the molecular ion peak was identified at m/z 338.33 [M-1], corresponding to the molecular formula C$_{17}$H$_{10}$ClN$_3$OS and possessing a mass of 338.02. The close agreement between the experimental and theoretical molecular ion peaks indicated a high level of purity for P4C (Figure 4). However, the theoretical mass of 3-ACH could not be directly confirmed due to its fragmentation during analysis. Therefore, elemental analysis was performed to further characterize 3-ACH (13).
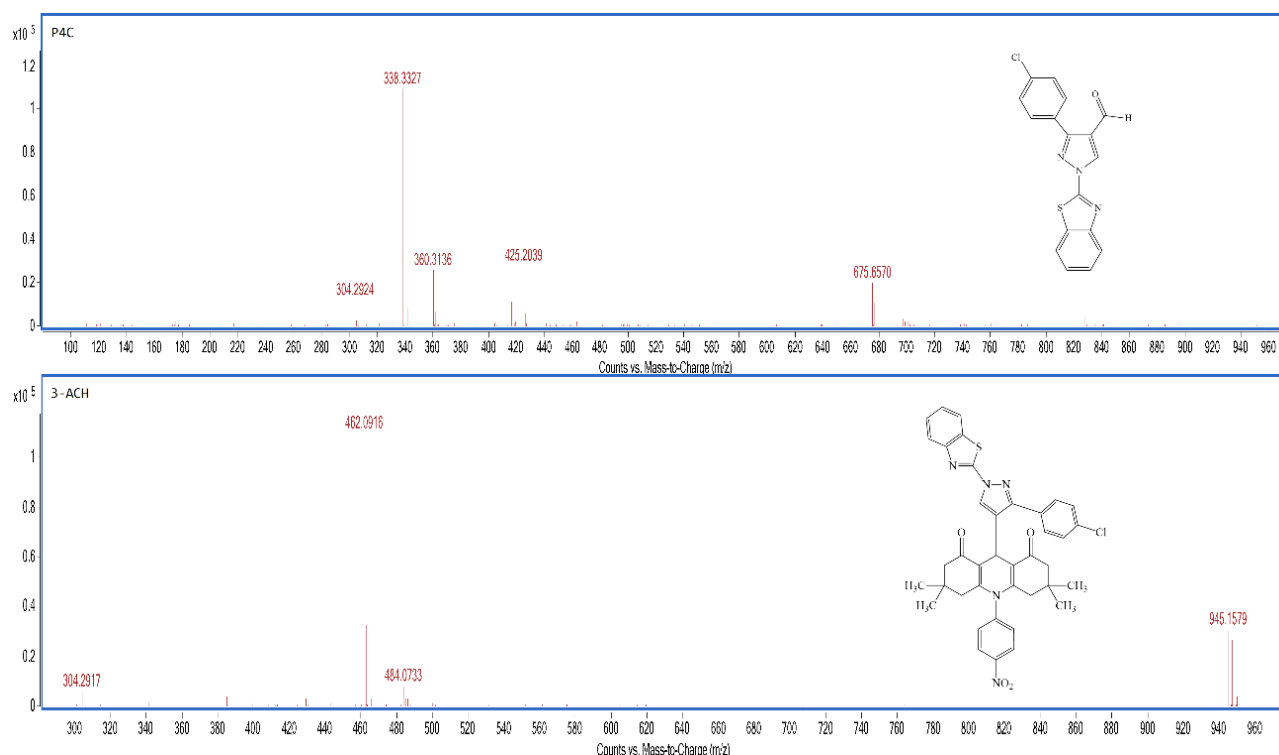
Figure 4. The mass spectrum of P4C and 3-ACH

Elemental Analysis

The results demonstrated close agreement between the calculated values and the experimental analysis for both P4C and 3-ACH (Table 1). These findings offer strong confirmation of the purity of the synthesized compounds and support the accuracy of their chemical structures.

Upon comprehensive evaluation of the combined FT-IR, NMR, mass spectra, and elemental analysis data, it can be concluded that the target compounds were successfully synthesized, with values consistent with previous research findings. This thorough analysis provides robust evidence regarding the successful synthesis and characterization of the compounds following established scientific knowledge.

Cell Viability

The application of 3-ACH for 12 hours resulted in a statistically significant decrease in cell viability rates of $94.54\pm2.50\%$ ($p=0.015$) and $94.33\pm1.84\%$ ($p=0.011$) at doses of 100 µg/mL and 150 µg/mL, respectively. However, applying 50 µg/mL of 3-ACH for the same duration did not result in a significant decrease in cell viability rates ($98.28\pm4.69\%$, $p=0.718$) compared to the control group. While extending the exposure time to 24 hours, doses of 100 µg/mL ($89.89\pm7.63\%$, $p=0.002$) and 150 µg/mL ($90.53\pm2.88\%$, $p=0.004$) of 3-ACH continued to show a statistically significant reduction in cell viability compared to the control group, there was no statistically significant decrease observed when 50 µg/mL of 3-ACH

was applied for 24 hours ($98.37\pm1.67\%$, $p=0.903$). Additionally, both 100 µg/mL and 150 µg/mL doses showed significant decreases compared to the 50 µg/mL group ($p=0.011$ and $p=0.019$, respectively). Comparing the exposure times, the 24-hour application of 3-ACH at 100 µg/mL and 150 µg/mL resulted in a more substantial reduction in cell viability compared to the 12-hour application of 3-ACH at the same doses. After exposing the cells to 3-ACH for 48 hours, a notable and statistically significant reduction in cell viability was observed across all dosage levels when compared to the control group, $94.55\pm0.65\%$ for 50 µg/mL, $95.18\pm1.41\%$ for 100 µg/mL, and $95.28\pm2.57\%$ for 150 µg/mL (all $p<0.001$, Figure 5). The overall effect of the 3-ACH treatment was significant at all time points ($p=0.004$ for 12 hours, $p<0.001$ for both 24 and 48 hours, Table 2).

Table 1. P4C and 3-ACH elemental analysis

	P4C ($C_{17}H_{10}ClN_3OS$)		3-ACH ($C_{39}H_{34}ClN_5O_4S$)	
	Calculated	**Found**	**Calculated**	**Found**
% C	60.09	59.93	66.51	66.32
% H	2.97	3.01	4.87	4.90
% N	12.37	12.42	9.94	10.02
% S	9.44	9.47	4.55	4.61

Table 2. Cell survival rates (%) of SH-SY5Y cells treated with different doses of 3-ACH at different time points

Time	Control	3-ACH 50 µg/mL	3-ACH 100 µg/mL	3-ACH 150 µg/mL	p
12-hour	100.00±0.00	98.28±4.69	94.54±2.50 [*##]	94.33±1.84 [*##]	**0.004**
24-hour	100.00±0.00	98.37±1.67	89.89±7.63 [**#]	90.53±2.88 [**#]	**<0.001**
48-hour	100.00±0.00	94.55±0.65 [***]	95.18±1.41 [***]	95.28±2.57 [***]	**<0.001**

Values are presented as mean±standard deviation, *: different from control, #: different from 3-ACH 50 µg/mL, 1 symbol p<0.05, 2 symbols p<0.005, and 3 symbols p<0.001
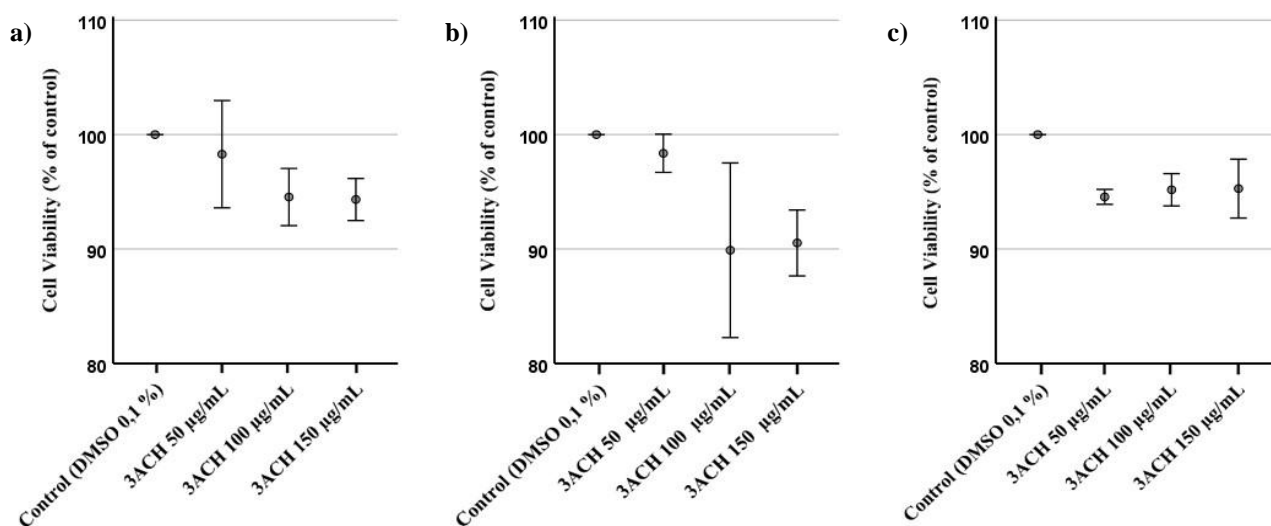
Figure 5. The cytotoxic impact of 3-ACH on SH-SY5Y cells was assessed at **a)** 12 hours, **b)** 24 hours, and **c)** 48 hours

3-ACH Stimulates Cell Death in SH-SY5Y Human Neuroblastoma Cells by Triggering Apoptosis

Immunofluorescence analysis revealed that BAX protein expression was significantly elevated in SH-SY5Y cells treated with 3-ACH (100 µg/mL) for 24 hours compared to untreated controls. Similarly, the expression levels of Caspase-3, -8, and -9 were markedly increased in treated cells compared to the control groups (Figure 6). These elevated levels of both intrinsic (BAX, Caspase-9) and extrinsic (Caspase-8) pathway proteins, together with the executioner caspase (Caspase-3), suggested comprehensive activation of apoptotic pathways.

DISCUSSION

Cancer is the uncontrolled movement of abnormal cells, which reduces the standard of living and is an important cause of death in both developed and developing countries. The core structure of pyrazole serves as the foundation for a class of medications employed in addressing various medical conditions. These conditions include cardiovascular diseases, neurological disorders, tumors, respiratory ailments, endocrine disorders, and metabolic abnormalities.

In recent years, research interest in pyrazole derivatives has been increasing due to their diverse biological activities. Currently, there are 34 pyrazole-based therapeutic drugs under investigation in clinical practice or clinical trials (18). Pyrazole is a significant heterocyclic structure with a potent pharmacological profile and can serve as a crucial pharmacophore in the drug discovery procedure, particularly for the development of anti-cancer and anti-inflammatory drugs (19). The pyrazolic analogue with different pharmacophoric subunits has been tested in numerous cancer cell lines, including neuroblastoma. The lethal effect of bis(pyrazolyl)alkanes co-synthesized with Pd (II) dichloride and diacetate complexes on SH-SY5Y has been demonstrated using the 3-(4,5-dimethylthiazol-2-yl)-2,5-diphenyltetrazolium bromide (MTT) cytotoxicity test. However, their cytotoxic impact was less pronounced compared to cisplatin (20). A novel series of 1,2,4-oxadiazoles incorporating 1,2,3-triazole-pyrazoles was synthesized, and cytotoxicity tests were performed on cancer cell lines, including A549 (lung cancer), DU-145 and
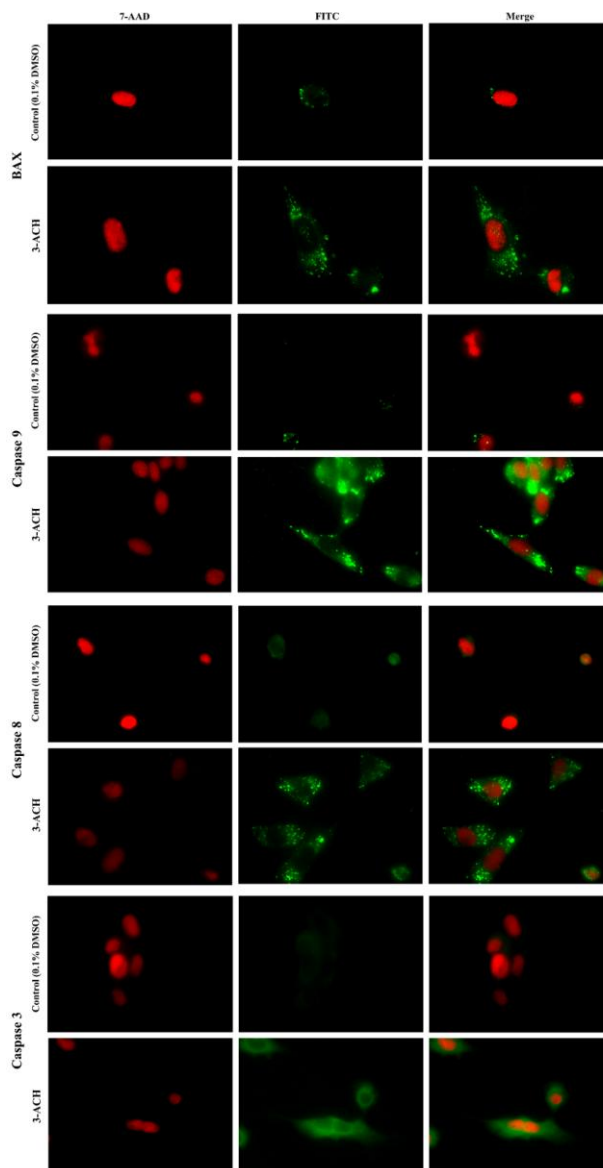
Figure 6. Expression level of the BAX, Caspase-3, -8, and -9 proteins in SH-SY5Y cells (x100). Cell nuclei were stained using the 7-AAD dye, producing a red signal, the BAX, Caspase-3, -8, and -9 proteins were detected using a FITC-labeled antibody, represented by a green signal

PC3 (prostate cancer), and MCF-7 (breast cancer) human cancer cell lines. Many of the synthesized compounds showed activity against all cell lines, while some demonstrated a more potent cytotoxic effect (21). In the study by Akhtar et al. (22), specific pyrazole-pyrazoline hybrid derivatives targeting the COX-2 enzyme were synthesized. They demonstrated strong anticancer potential against A549, SiHa (cellosaurus cancer cell line), HepG2 (hepatocellular carcinoma), and COLO205 (colon cancer) cell lines, as evidenced by the MTT assay (with IC50 values of approximately 4.94 μM, 4.94 μM, 2.09 μM, and 4.86 μM, respectively). Given the specificity of these compounds towards the COX-2 enzyme, it can be inferred that they exerted their anticancer effects through COX-2 inhibition.

Acridine, a crystalline compound discovered by Graebe and Caro in 1870 from coal tar, has many uses, including medicine and industry. Acridine has been the subject of research with its antibacterial, antiparasitic, antiviral, and antimalarial properties. The anticancer effect of acridine derivatives has been investigated due to interactions with DNA and DNA-related enzymes, topoisomerase II, and telomerase (23,24). Hybrid compounds of 9-aminoacridine and artemisinin-acridine were synthesized and the cytotoxic and apoptotic activity of HepG2 and SH-SY5Y were evaluated against CHO cells (Chinese hamster ovary cells), and both acridine and artemisinin pharmacophores showed hepatotoxicity and neurotoxicity (25).

Recent studies have highlighted the therapeutic potential of combining the pyrazole and acridine pharmacophores. Hu et al. (26) demonstrated that pyrazoloacridine exhibits synergistic cytotoxicity when combined with conventional anticancer agents like doxorubicin, etoposide, and topotecan, particularly in drug-resistant tumor cells. Their research showed that these combinations could effectively overcome drug resistance mechanisms. Additionally, Adjei (12) reported that pyrazoloacridine represents a novel class of anticancer agents with distinct advantages, including activity against solid tumors, effectiveness in hypoxic conditions, and ability to target drug-resistant cells. Notably, pyrazoloacridine maintains its activity against cells that are resistant to other agents due to P-glycoprotein overexpression or topoisomerase deficiency. Building on these promising findings, phase 2 clinical studies have been conducted evaluating pyrazole-acridine derivatives in breast and ovarian cancer (27,28). In a pioneering study, Sugaya et al. (29) demonstrated significant inhibition of Hela S3 cell proliferation in vitro and remarkable suppression of P388 leukemia and sarcoma 180 solid tumors in vivo using novel pyrazole-acridine derivatives. Notably, these compounds exhibited superior antitumor activity at lower doses compared to adriamycin.

Our results indicate that 3-ACH holds promise as a potential anticancer agent for targeting SH-SY5Y human neuroblastoma cells. The cytotoxic effects of pyrazole derivatives on neuroblastoma cells have been demonstrated in the literature. In our study, we similarly confirmed the anticancer properties of the pyrazole-acridine compounds that we synthesized on neuroblastoma cells. Furthermore, we elucidated the underlying apoptotic mechanism of cell death through immunostaining. Apart from its cytotoxic impact, we additionally noticed that the administration of 3-ACH activated several apoptosis-associated proteins,

such as BAX, Caspase-9, -8, and -3. These proteins have well-established roles in both the intrinsic and extrinsic apoptotic pathways, which are tightly regulated mechanisms of programmed cell death frequently disrupted in cancer cells.

Apoptosis is a complex process with two main pathways: the intrinsic (mitochondrial) pathway and the extrinsic (cell surface receptor-mediated) pathway. When these apoptotic processes work in balance, they contribute to healthy tissue homeostasis, being a natural part of the cell's life cycle (30). Compared to the control group, there was an increase in the synthesis of proteins involved in the intrinsic pathway components, BAX and Caspase-9. Additionally, the synthesis of Caspase-8, an extrinsic pathway component, and Caspase-3, which plays a role in both intrinsic and extrinsic pathways, significantly increased. These results indicate that 3-ACH may exert its cytotoxic effect by activating both intrinsic and extrinsic pathways.

We have synthesized a novel pyrazole-acridine derivative using a four-step synthetic process and characterized its structure using FT-IR, NMR, HPLC-Q-TOF/MS, and elemental analysis techniques. This development is particularly significant given the current limitations of chemotherapy, which despite being the prevailing approach in cancer treatments, suffers from several drawbacks including high toxicity, side effects, costly nature, and limited targeting specificity. Our findings suggest that pyrazole-acridine hybrids may offer a promising alternative therapeutic approach for cancer treatment, with the potential for enhanced efficacy and improved selectivity. However, it is important to acknowledge certain limitations of our study and address future research directions. The current investigation primarily focused on in vitro analyses, and while these results are promising, they represent only the initial steps in understanding the therapeutic potential of 3-ACH. Several critical aspects require further investigation: First, additional experimental approaches, such as intracellular calcium imaging and Western blot analysis, are needed to provide stronger validation of the apoptotic pathways we observed. Second, the compound's ability to cross the blood-brain barrier, which is crucial for treating neuroblastoma, remains to be determined. Third, whether 3-ACH acts as a prodrug requiring metabolic activation or functions directly in its current form is yet to be established. To address these questions, comprehensive in vivo studies will be necessary to assess both the compound's efficacy and safety profile in animal models. Additionally, investigating potential synergistic effects with existing chemotherapeutic agents could provide valuable insights for combination therapy approaches. These future investigations would significantly enhance our understanding of 3-ACH's therapeutic potential and guide its development as an anticancer agent.

CONCLUSIONS
Our research illustrates that 3-ACH has cytotoxic effects on SH-SY5Y human neuroblastoma cells, which are dependent on both the dosage and duration of exposure. Additionally, we noted activation of apoptosis-associated proteins, such as BAX, Caspase-3, -8, and -9, upon exposure to 3-ACH. These proteins are crucial in the intrinsic and extrinsic apoptotic pathways, which are tightly regulated

mechanisms of programmed cell death that are often disrupted in cancerous cells. The stimulation of these proteins indicates that 3-ACH possesses the capability to trigger apoptosis, serving as the underlying mechanism responsible for its cytotoxic impact on SH-SY5Y human neuroblastoma cells. Further investigations are necessary to elucidate the precise mechanisms through which 3-ACH acts on neuroblastoma cancer cells.

REFERENCES
1. Nandurkar D, Danao K, Rokde V, Shivhare R, Mahajan U. Pyrazole scaffold: Strategies toward the synthesis and their applications. In: Kumari P, Patel AB, editors. Strategies for the synthesis of heterocycles and their applications. London, UK: IntechOpen; 2022. p15-38.
2. Kumar V, Kaur K, Gupta GK, Sharma AK. Pyrazole containing natural products: Synthetic preview and biological significance. Eur J Med Chem. 2013;69:735-53.
3. Karrouchi K, Radi S, Ramli Y, Taoufik J, Mabkhot YN, Al-Aizari FA, et al. Synthesis and pharmacological activities of pyrazole derivatives: A review. Molecules. 2018;23(1):134.
4. Nitulescu GM. Quantitative and qualitative analysis of the anti-proliferative potential of the pyrazole scaffold in the design of anticancer agents. Molecules. 2022;27(10):3300.
5. Costa RF, Turones LC, Cavalcante KVN, Rosa Júnior IA, Xavier CH, Rosseto LP, et al. Heterocyclic compounds: Pharmacology of pyrazole analogs from rational structural considerations. Front Pharmacol. 2021;12:666725.
6. Alfei S, Brullo C, Caviglia D, Piatti G, Zorzoli A, Marimpietri D, et al. Pyrazole-based water-soluble dendrimer nanoparticles as a potential new agent against staphylococci. Biomedicines. 2021;10(1):17.
7. Kornis GI. Pyrazoles, pyrazolines, and pyrazolones. In: Kirk-Othmer encyclopedia of chemical technology. 3rd ed. New York: John Wiley & Sons; 2000. p.436-53.
8. National Center for Biotechnology Information. PubChem compound summary for CID 9215, Acridine. 2023. [Cited: 2024 Jul 23]. Available from: https://pubchem.ncbi.nlm.nih.gov/compound/Acridine
9. Prasher P, Sharma M. Medicinal chemistry of acridine and its analogues. Medchemcomm. 2018;9(10):1589-618.
10. Varakumar P, Rajagopal K, Aparna B, Raman K, Byran G, Gonçalves Lima CM, et al. Acridine as an anti-tumour agent: A critical review. Molecules. 2022;28(1):193.
11. Gackowski M, Szewczyk-Golec K, Pluskota R, Koba M, Mądra-Gackowska K, Woźniak A. Application of multivariate adaptive regression splines (MARSplines) for predicting antitumor activity of anthrapyrazole derivatives. Int J Mol Sci. 2022;23(9):5132.
12. Adjei AA. Current status of pyrazoloacridine as an anticancer agent. Invest New Drugs. 1999;17(1):43-8.
13. Elmusa M, Elmusa S, Mert S, Kasımoğulları R, Türkan F, Atalar MN, et al. One-pot three-component synthesis of novel pyrazolo-acridine derivatives and assessment of their acetylcholinesterase inhibitory properties: An in vitro and in silico study. J Mol Struct. 2023;1274(1):134553.
14. Küçükbağrıaçık Y, Dastouri MR, Elmusa M, Elmusa F, Yılmaz H, Kasımoğulları R. Evaluation of the potential anticancer activity of pyrazole-acridine derivative synthesis on SKBR-3 human breast cancer cell line. KÜ Tıp Fak Derg. 2024;26(1):76-85. Turkish.
15. Kucukbagriacik Y, Dastouri M, Yilmaz H, Altuntas EG. The apoptotic effect of the Lycopodium clavatum extracts on MCF-7 human breast cancer cells. Med Oncol. 2023;40(10):289.
16. Nandiyanto ABD, Oktiani R, Ragadhita R. How to read and interpret FTIR spectroscope of organic material. Indonesian J Sci Technol. 2019;4(1):97-118.
17. Gunawan R, Nandiyanto ABD. How to read and interpret ^{1}H-NMR and ^{13}C-NMR spectrums. Indonesian J Sci Technol. 2021;6(2):267-98.
18. Zhai H, Zhang S, Ampomah-Wireko M, Wang H, Cao Y, Yang P, et al. Pyrazole: An important core in many marketed and clinical drugs. Russ J Bioorg Chem. 2022;48(6):1175-89.
19. Alam MJ, Alam O, Naim MJ, Nawaz F, Manaithiya A, Imran M, et al. Recent advancement in drug design and discovery of pyrazole biomolecules as cancer and inflammation therapeutics. Molecules. 2022;27(24):8708.
20. Di Nicola C, Marchetti F, Pettinari C, Pettinari R, Brisdelli F, Crucianelli M, et al. Synthesis and characterization of a new alkyne functionalized bis(pyrazolyl)methane ligand and of its Pd(II) complexes: Evaluation of their in vitro cytotoxic activity. Inorganica Chim Acta. 2017;455(2):677-82.
21. Mohan G, Sridhar G, Laxminarayana E, Chary MT. Synthesis and biological evaluation of 1,2,4-oxadiazole incorporated 1,2,3-triazole-pyrazole derivatives as anticancer agents. Chem Data Coll. 2021;34:100735.
22. Akhtar W, Marella A, Alam MM, Khan MF, Akhtar M, Anwer T, et al. Design and synthesis of pyrazole-pyrazoline hybrids as cancer-associated selective COX-2 inhibitors. Arch Pharm (Weinheim). 2021;354(1):e2000116.

23. Varakumar P, Rajagopal K, Aparna B, Raman K, Byran G, Gonçalves Lima CM, et al. Acridine as an anti-tumour agent: A critical review. Molecules. 2022;28(1):193.

24. Rupar JS, Dobričić VD, Aleksić MM, Brborić JS, Čudina OA. A review of published data on acridine derivatives with different biological activities. Kragujevac J Sci. 2018;40:83-101.

25. Joubert JP, Smit FJ, du Plessis L, Smith PJ, N'Da DD. Synthesis and in vitro biological evaluation of aminoacridines and artemisinin-acridine hybrids. Eur J Pharm Sci. 2014;56:16-27.

26. Hu Y, Krishan A, Nie W, Sridhar KS, Mayer LD, Bally M. Synergistic cytotoxicity of pyrazoloacridine with doxorubicin, etoposide, and topotecan in drug-resistant tumor cells. Clin Cancer Res. 2004;10(3):1160-9.

27. Plaxe SC, Blessing JA, Bookman MA, Creasman WT. Phase II trial of pyrazoloacridine in recurrent platinum-sensitive ovarian cancer: a Gynecologic Oncology Group study. Gynecol Oncol. 2002;84(1):32-5.

28. Ramaswamy B, Mrozek E, Kuebler JP, Bekaii-Saab T, Kraut EH. Phase II trial of pyrazoloacridine (NSC#366140) in patients with metastatic breast cancer. Invest New Drugs. 2011;29(2):347-51.

29. Sugaya T, Mimura Y, Shida Y, Osawa Y, Matsukuma I, Ikeda S, et al. 6H-pyrazolo[4,5,1-de]acridin-6-ones as a novel class of antitumor agents. Synthesis and biological activity. J Med Chem. 1994;37(7):1028-32.

30. Jan R, Chaudhry GE. Understanding apoptosis and apoptotic pathways targeted cancer therapeutics. Adv Pharm Bull. 2019;9(2):205-18.

Prognostic Value of Geriatric Nutritional Risk Index and Prognostic Nutritional Index in Geriatric Orthopedic Trauma Patients in the Surgical Intensive Care Unit

Cerrahi Yoğun Bakım Ünitesindeki Geriatrik Ortopedik Travma Hastalarında Geriatrik Nutrisyonel Risk İndeksi ile Prognostik Nutrisyonel İndeksin Prognostik Değeri

Kadir ARSLAN
0000-0003-4061-0746
Ayça Sultan ŞAHİN
0000-0002-7765-5297

Department of Anesthesiology and Reanimation, University of Health Sciences Kanuni Sultan Süleyman Training and Research Hospital, İstanbul, Türkiye

ABSTRACT

Aim: Malnutrition is associated with postoperative morbidity and mortality in geriatric patients. This study investigated the prognostic value of geriatric nutritional risk index (GNRI) and prognostic nutritional index (PNI) in geriatric orthopedic trauma patients.
Material and Methods: Geriatric (≥65 years old) patients followed in the surgical intensive care unit after orthopedic trauma surgery between June 2019 and June 2022 were evaluated retrospectively. Patients were classified into mortality and survivor groups. GNRI was calculated according to the ratio of serum albumin level and actual body weight to ideal body weight. PNI was obtained from serum albumin level and blood lymphocyte count.
Results: The study included 371 patients. American Society of Anesthesiologists (ASA) IV status was significantly higher in the mortality group (p<0.001). Mean BMI, albumin, lymphocyte levels, PNI, and GNRI were significantly lower in the mortality group (p=0.009, p=0.008, p=0.030, p=0.001, and p=0.003, respectively). While the median Glasgow coma scale (GCS) score was significantly lower, the median acute physiology and chronic health evaluation (APACHE)-II score and median injury severity score (ISS) were significantly higher in the mortality group (p<0.001 for all). Regression analysis revealed that ASA IV status, APACHE-II score, and ISS were independent predictors of mortality. In ROC curve analysis, the area under the curve (AUC) for GNRI was 0.660 (95% CI, 0.553-0.768), and the AUC for PNI was 0.654 (95% CI, 0.566-0.743).
Conclusion: In geriatric orthopedic trauma patients, nutritional scores GNRI and PNI help predict in-hospital mortality. Although their prognostic values are not high, they are similar.
Keywords: Trauma; malnutrition; geriatric nutritional risk index; prognostic nutritional index; mortality.

ÖZ

Amaç: Malnutrisyon, geriatrik hastalarda postoperatif morbidite ve mortalite ile ilişkilidir. Bu çalışmada, geriatrik ortopedik travmalı hastalarda geriatrik nutrisyonel risk indeksi (GNRI) ve prognostik nutrisyonel indeksin (PNI) prognostik değeri araştırılmıştır.
Gereç ve Yöntemler: Haziran 2019 ile Haziran 2022 tarihleri arasında ortopedik travma cerrahisi sonrasında cerrahi yoğun bakım ünitesinde takip edilen geriatrik (≥65 yaş) hastalar retrospektif olarak değerlendirildi. Hastalar mortalite ve yaşayan grupları olarak sınıflandırıldı. GNRI, serum albümin düzeyi ile gerçek vücut ağırlığının ideal vücut ağırlığına oranına göre hesaplandı. PNI ise serum albumin düzeyi ve kan lenfosit sayısından elde edildi.
Bulgular: Çalışmaya 371 hasta dahil edildi. Mortalite grubunda Amerikan Anestezistler Derneği (American Society of Anesthesiologists, ASA) IV statüsü anlamlı olarak daha yüksekti (p<0,001). Mortalite grubunda ortalama BMI, albumin, lenfosit düzeyleri ile PNI ve GNRI anlamlı şekilde daha düşüktü (sırasıyla p=0,009, p=0,008, p=0,030, p=0,001 ve p=0,003). Mortalite grubunda ortanca Glasgow koma skalası (GKS) skoru anlamlı şekilde daha düşükken, ortanca akut fizyoloji ve kronik sağlık değerlendirmesi (acute physiology and chronic health evaluation, APACHE)-II skoru ve ortanca yaralanma şiddet skoru (injury severity score, ISS) anlamlı olarak daha yüksekti (hepsi için p<0,001). Regresyon analizinde ASA IV statüsü, APACHE-II skoru ve ISS'nin mortalitenin bağımsız prediktörleri olduğu belirlendi. ROC eğrisi analizinde, eğri altında kalan alan (area under the curve, AUC), GNRI için 0,660 (%95 GA, 0,553-0,768) ve PNI için 0,654 (%95 GA, 0,566-0,743) saptandı.
Sonuç: Geriatrik ortopedik travmalı hastalarda, nutrisyonel skorlardan GNRI ve PNI, hastane içi mortalitenin öngörülmesinde faydalıdır. Prognostik değerleri yüksek olmamakla birlikte benzer saptanmıştır.
Anahtar kelimeler: Travma; malnütrisyon; geriatrik nutrisyonel risk indeks; prognostik nutrisyonel indeks; mortalite.

Corresponding Author
Sorumlu Yazar
Kadir ARSLAN
kadir.arslan@sbu.edu.tr

INTRODUCTION

Trauma is on the rise in the geriatric population, leading to functional limitations, morbidity, and mortality (1,2). Visual impairments, musculoskeletal problems, comorbidities, and polypharmacy are contributing factors to this trend (3). Low-energy traumas, such as hip fractures, are a common consequence of osteoporosis in geriatric patients, while craniofacial traumas carry the highest mortality rates (4). There is an increased risk of complications in patients with geriatric trauma. These patients require intensive care unit (ICU) care and may have long lengths of stay (5). The treatment and care process in critical geriatric trauma patients negatively affects the patient and their relatives physically, psychologically, and socially.

Malnutrition in geriatric patients occurs due to inadequate or excessive energy consumption or imbalance in food consumption. It can cause physical and cognitive dysfunction, decreased quality of life, postoperative complications, and increased mortality in elderly individuals (6). Malnutrition is also associated with higher levels of frailty. Nutritional deficiencies in functionally limited geriatric patients with comorbidities should be prevented. In addition to body mass index, anthropometric measurements, and biochemical markers, various nutritional screening tests are used to assess malnutrition. However, there is yet to be an ideal method on which there is a consensus to assess malnutrition in geriatric patients. The lack of consensus on this issue is a significant challenge that needs to be addressed. The geriatric nutritional risk index (GNRI) and prognostic nutritional index (PNI) are associated with poor prognosis in both trauma patients and critically ill patients, followed by non-traumatic reasons, and are predictors of mortality (7,8). PNI helps evaluate preoperative nutritional status and may help determine the geriatric population's postoperative delirium and ICU requirements (9,10). However, there are not enough studies comparing the prognostic value of GNRI and PNI in geriatric trauma patients in the postoperative period, further highlighting the need for more research in this area.

This study aimed to compare the prognostic value of GNRI and PNI on mortality in critically ill geriatric trauma patients followed in the surgical ICU (SICU) during the postoperative period.

MATERIAL AND METHODS

This retrospective observational study complied with the principles of the Declaration of Helsinki. It was initiated after the approval of the scientific research ethics committee of İstanbul Kanuni Sultan Süleyman Training and Research Hospital (27.03.2024, 55). Patients who underwent surgery due to geriatric trauma at the University of Health Sciences, İstanbul Kanuni Sultan Süleyman Training and Research Hospital between June 2019 and June 2022 and whose postoperative follow-up and treatment were performed in the SICU were included in the study. Study data were obtained from the hospital information system and patient follow-up forms.

Inclusion criteria were: 1) ≥65 years of age, 2) orthopedic trauma patients undergoing surgery. Exclusion criteria included: 1) preoperative albumin transfusion, 2) undergoing major surgery within the last month, 3) chronic renal failure,

4) severe liver dysfunction, 5) not checking albumin level during SICU admission, 6) viral and bacterial infection within the last month, and 7) missing data.

Along with demographic data, comorbidities, American Society of Anesthesiologists (ASA) status, Glasgow coma scale (GCS) score, acute physiology and chronic health evaluation (APACHE)-II score, injury severity score (ISS), hemoglobin, albumin, and lymphocyte levels on admission to SICU and in-hospital mortality of geriatric patients who underwent surgery after trauma and were followed in SICU were recorded. GNRI and PNI were calculated from the patient's blood results at admission to the SICU. The patients were classified as survivor and mortality groups, and the data were compared.

Prognostic Nutritional Index (PNI)

A PNI based on serum albumin and lymphocyte concentrations is a new inflammation-based risk score that predicts prognosis in various patient populations. PNI has also been reported to predict postoperative morbidity and mortality in geriatric trauma patients (8-10). It is calculated from the formula PNI = (10 × serum albumin (g/dL) + 0.005 × total lymphocyte count).

Geriatric Nutritional Risk Index (GNRI)

The GNRI, a practical and effective tool, is used to identify patients at risk of morbidity and mortality due to malnutrition. Calculated using albumin and ideal body weight (IBW), this score can be readily applied in daily practice, providing a valuable tool for patient care. GNRI= [1.489 × albumin (g/L)] + [41.7 × (weight/IBW)]. GNRI has been shown to have prognostic value in geriatric trauma patients and patients with malignancy (6,7,11,12). IBW was calculated using the following formula in male and female, widely accepted and used in the literature due to its accuracy and simplicity (7). IBW male= (height-80) × 0.7, IBW female= (height-70) × 0.6

This was a retrospective observational study aimed to compare the effectiveness of the GNRI and the PNI in predicting in-hospital mortality among elderly patients with orthopedic trauma, and all patients who met the inclusion and exclusion criteria during three years between June 2019 and June 2022 were included.

Statistical Analysis

The statistical analyses were performed using IBM SPSS Statistics, Version 27.0 (IBM Corp., Armonk, NY). The Kolmogorov-Smirnov test, histogram, skewness, and kurtosis values assessed the conformity of the data to normal distribution. Descriptive statistics of the data according to normality were expressed as mean±standard deviation, and median (interquartile range) [min-max]. The independent samples t-test was used to analyze quantitative data showing a normal distribution, and the Mann-Whitney U test was used to analyze data not showing a normal distribution. Qualitative data were expressed as the number of patients, and percentage, and analyzed using the Pearson chi-square test and Fisher's exact test. Multivariate logistic regression analysis was performed to evaluate independent factors of mortality. Receiver operating characteristics (ROC) curve analysis was performed to determine the prognostic value of GNRI and PNI. Youden index was used to determine the cut-off values of GNRI and PNI. The statistical significance level for all analyses was set at $p < 0.05$.

RESULTS

Between June 2019 and June 2022, 371 patients who underwent surgery for geriatric orthopedic trauma and were followed up in the SICU postoperatively were included in the study (Figure 1). The mean age of the patients was 78.5±8.4 years, and 61.7% (n=229) were female. Age and gender did not differ significantly between the groups (p=0.229 and p=0.607, respectively). Median BMI was significantly lower in the mortality group (24.1 vs. 25.7 kg/m², p=0.009). ASA IV status was significantly higher in the mortality group than in the survivor group (18.2% vs. 2.7%, p<0.001). In the mortality

group, median GCS score were significantly lower, while APACHE-II score and ISS at admission were significantly higher (p<0.001 for all). While hemoglobin levels at SICU admission did not differ significantly (p=0.857) between the groups, albumin (2.8±0.6 vs. 3.1±0.5 g/dL, p=0.008) and lymphocyte (1.4±0.6 vs. 1.7±0.6 x10⁹/L, p=0.030) levels were significantly lower in the mortality group. In the mortality group, median PNI (27.9 vs. 31.2, p=0.001) and median GNRI (51.2 vs. 54.4, p=0.003) were found significantly lower (Table 1).

Hypertension was found in 67.9% (n=252) of the patients, diabetes mellitus in 34% (n=126), coronary artery disease/heart failure in 31.5% (n=117), asthma/chronic obstructive pulmonary disease in 12.9% (n=48), hemorrhagic and ischemic stroke in 9.7% (n=36), and chronic renal failure in 7.3% (n=27). No significant difference was found between the groups regarding comorbidities (Table 2).

Multivariate regression analysis was performed for ASA status, GCS, APACHE-II score, and ISS, which are prognostic scoring systems in trauma patients and show significant differences in mortality in patients followed in SICU, and nutritional scores GNRI and PNI. The enter method was used in regression analysis. ASA IV status, APACHE-II score, and ISS were found as independent predictors of mortality (p=0.038, p=0.004, and p<0.001, respectively). Multicollinearity between GNRI and PNI was evaluated using the Pearson correlation analysis. A weak correlation coefficient (r=0.15) was detected between
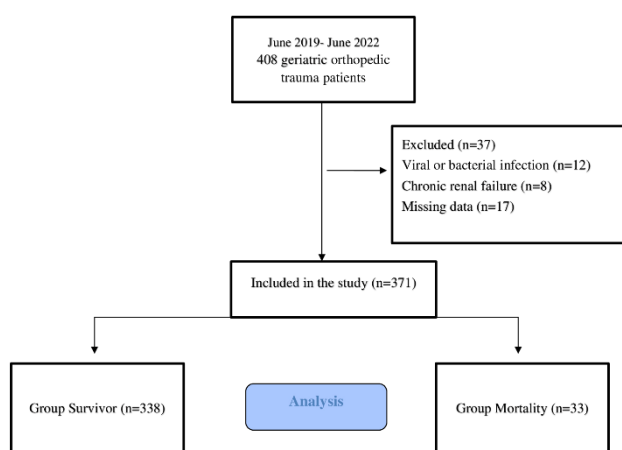
Figure 1. Flow chart of the study

Table 1. Clinical characteristics of the patients and comparison of groups

	Survivor Group (n=338)	Mortality Group (n=33)	p	Overall (n=371)
Age (year)	78.3±8.3	80.1±8.8	0.229	78.5±8.4
Gender, n (%)				
Female	210 (62.1)	19 (57.6)	0.607	229 (61.7)
Male	128 (37.9)	14 (42.4)		142 (38.3)
BMI (kg/m²)	25.7 (23-28) [16-44]	24.1 (22-24) [21-34]	**0.009**	25.5 (23-27) [16-44]
Weight (kg)	69.5±12.7	66.1±10.5	0.090	69.2±12.6
IBW (kg)	56.7±5.0	57.6±5.3	0.403	56.8±5.0
ASA Status, n (%)				
I	4 (1.2)	0 (0.0)		4 (1.1)
II	65 (19.2)	2 (6.1)	**<0.001**	67 (18.1)
III	260 (76.9)	25 (75.7)		285 (76.8)
IV	9 (2.7)	6 (18.2)		15 (4.0)
GCS	15 (12-15) [3-15]	12 (3-12) [3-15]	**<0.001**	15 (12-15) [3-15]
APACHE-II	13 (9-18) [6-37]	29 (22-32) [11-46]	**<0.001**	14 (10-19) [6-46]
ISS	9 (9-9) [4-25]	25 (25-25) [9-25]	**<0.001**	9 (9-9) [4-25]
ISS, n (%)				
1-15	292 (86.4)	1 (3.0)		293 (79.0)
16-24	44 (13.0)	7 (21.2)	**<0.001**	51 (13.7)
≥25	2 (0.6)	25 (75.8)		27 (7.3)
Duration of ICU (days)	3 (1-8) [1-81]	12 (5-17) [2-82]	**<0.001**	3 (2-9) [1-82]
Hemoglobin (g/dL)	10.9±1.7	10.8±1.9	0.857	10.9±1.7
Albumin (g/dL)	3.1±0.5	2.8±0.6	**0.008**	3.1±0.5
Lymphocyte (x10⁹/L)	1.7±0.6	1.4±0.6	**0.030**	1.7±0.6
PNI	31.2 (28-35) [14-45]	27.9 (23-32) [16-42]	**0.001**	30.9 (28-35) [14-45]
GNRI	54.4 (50-59) [33-94]	51.2 (47-53) [45-72]	**0.003**	54.2 (50-59) [33-94]

BMI: body mass index, IBW: ideal body weight, ASA: American Society of Anesthesiologists, GCS: Glasgow coma scale, APACHE-II: acute physiology and chronic health evaluation-II, ISS: injury severity score, ICU: intensive care unit, PNI: prognostic nutritional index, GNRI: geriatric nutritional risk index, data were expressed as number of patients (percentage), mean±standard deviation, and median (interquartile range) [min-max]

Table 2. Comparison of comorbid diseases between the groups

Comorbidity	Survivor Group (n=338)	Mortality Group (n=33)	p	Overall (n=371)
Hypertension, n (%)	231 (68.3)	21 (63.6)	0.580	252 (67.9)
Diabetes, n (%)	112 (33.1)	14 (42.4)	0.282	126 (34.0)
CAD/HF, n (%)	109 (32.2)	8 (24.2)	0.345	117 (31.5)
Asthma/COPD, n (%)	47 (13.9)	1 (3.0)	0.076	48 (12.9)
Stroke, n (%)	34 (10.1)	2 (6.1)	0.459	36 (9.7)
Chronic renal failure, n (%)	24 (7.1)	3 (9.1)	0.674	27 (7.3)

CVD/HF: coronary artery disease/heart failure, COPD: chronic obstructive pulmonary disease

the two. PNI and GNRI were not independent predictors of mortality (Table 3). The regression analysis determined that -2 Log likelihood= 28.992, Nagelkerke R square= 0.901. For the Hosmer and Lemeshow test, p=1.000.

The PNI and GNRI prognostic values used to predict mortality were evaluated with ROC curve analysis. The optimal cut-off value for PNI was 26, and the area under the curve (AUC) was 0.660 (95% CI, 0.553-0.768). The AUC was 0.654 (95% CI, 0.566-0.743) and the cut-off value was 53.1 for GNRI (Table 4, Figure 2). PNI and GNRI help predict mortality in geriatric orthopedic patients. Although their prognostic values are not high, they are close to each other.

DISCUSSION

In this study conducted in a tertiary center, ASA IV status, GCS, APACHE-II score, and ISS at admission to SICU, albumin, lymphocyte levels, and PNI and GNRI helped predict mortality in geriatric trauma patients. ASA IV status, APACHE-II score, and ISS were independent predictors of mortality, while PNI and GNRI were not independent predictors of mortality. At the same time, GNRI and PNI were found to have similar prognostic values in predicting mortality.

The elderly population is increasing worldwide in parallel with the increase in average life expectancy, improvement in quality of life due to significant medical developments, and the decrease in population growth rate. Falls and fall-related injuries are common in the elderly geriatric population. Falls are seen in approximately 30% of adults aged 60 and over every year (13). It has been reported that geriatric trauma patients have orthopedic trauma most frequently and are primarily patients with hip (proximal femur) fractures (10,14). It has been stated that geriatric traumas are more common in females, and 60% occur due to falls (14). The present study included patients with orthopedic trauma. In line with the literature, the female gender ratio (61.7%) was found to be higher, but gender did not show a significant effect on mortality. Hip fractures affect more than 1 million people annually globally, with the highest mortality occurring within the first 30 days (15). Geriatric patients are at high risk for nutritional deficiencies and malnutrition due to their low functional capacity, multiple comorbidities, polypharmacy, inadequate nutrition, and dysphagia (16). Malnutrition is a serum albumin level of <3.5 g/dL or a peripheral blood lymphocyte count of <1500 cells per mm³ (17). Malnutrition is associated with increased risk of complications, increased length of hospital stay, readmission to the ICU, increased infection rates, and higher mortality rates in hospitalized

Table 3. Regression analysis for mortality

	OR	95% CI	p
ASA IV	4.621	1.311-12.188	**0.038**
GCS	0.951	0.727-1.243	0.713
APACHE-II	1.365	1.103-1.690	**0.004**
ISS	1.978	1.463-2.673	**<0.001**
PNI	0.888	0.722-1.093	0.263
GNRI	0.890	0.763-1.039	0.141

OR: odds ratio, CI: confidence interval, ASA: American Society of Anesthesiologists, GCS: Glasgow coma scale, APACHE-II: acute physiology and chronic health evaluation-II, ISS: injury severity score, PNI: prognostic nutritional index, GNRI: geriatric nutritional risk index

Table 4. Mortality prediction performance of PNI and GNRI

	Cut-off	AUC (95% CI)	Sensitivity	Specificity
PNI	26.0	0.660 (0.553-0.768)	45.5	85.5
GNRI	53.1	0.654 (0.566-0.743)	75.8	59.5

PNI: prognostic nutritional index, GNRI: geriatric nutritional risk index, AUC: area under the curve, CI: confidence interval
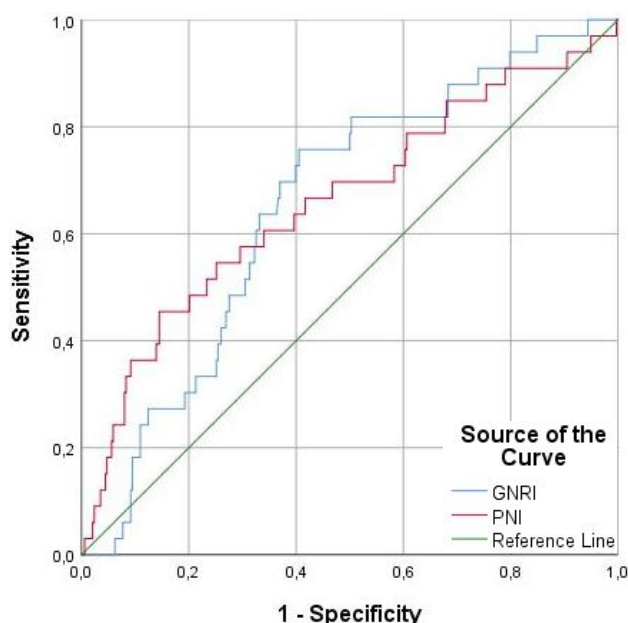
Figure 2. ROC curve analysis of PNI and GNRI

ROC: receiver operating characteristic, PNI: prognostic nutritional index, GNRI: geriatric nutritional risk index

patients (18-20). While mortality rate is around 13% in patients with hip fractures within the first month, this rate can increase to 25% in geriatric hip fracture patients with

malnutrition (21,22). Low albumin and lymphocyte levels, essential markers in evaluating malnutrition in patients with geriatric hip fractures, are prognostic factors in determining 1-year mortality (23). In the present study, the in-hospital mortality rate in geriatric orthopedic trauma patients was found to be 8.9%. In line with the literature, albumin, and lymphocyte levels at admission to the SICU were significantly low in the mortality group. However, their prognostic value is limited due to many factors that can affect albumin and lymphocyte levels. Although the patients had various comorbidities, they did not show a significant effect on mortality.

Prognostic scoring systems are used to plan treatment and improve patient care in non-traumatic or trauma patients monitored in the ICU. In addition to non-trauma-specific scores (GCS, APACHE-II), various trauma-specific scores (ISS and revised trauma score) are used to predict mortality (2,3,10,24). In addition to these scores, nutritional scores such as PNI and GNRI have recently been reported to have prognostic value in various clinical situations in the geriatric population, where malnutrition is frequently seen (6-10). PNI is a simple measurement used to assess the patient's nutritional status. It can be easily calculated using serum albumin and lymphocyte count. Low PNI values have been reported to be an independent predictor of 6-month mortality after cancer surgery (8). It has also been reported that the preoperative PNI value, which can be easily calculated in geriatric hip fracture patients, is valid in predicting postoperative ICU requirements and mortality (10). In another study, low preoperative PNI values in geriatric hip fracture patients were associated with increased hospital stay, postoperative delirium, and increased mortality (25). Another nutritional indicator with prognostic value in geriatric patients is the GNRI, calculated using serum albumin level, body weight, and IBW. It has been reported that GNRI has prognostic value in heart failure (26), chronic obstructive pulmonary disease (27), some malignancies (11,28), and trauma patients (7,29). Su et al. (30) reported that in geriatric patients with femoral fractures, GNRI helps to classify malnourished patients and that low GNRI scores lead to a significant increase in mortality. Kregel et al. (31) reported that infectious complications are higher, hospital stays are more extended, and mortality is higher in geriatric trauma patients with low GNRI scores. To our knowledge, the prognostic value of GNRI and PNI has not been compared in geriatric trauma patients. Our study found that GNRI and PNI calculated at the time of admission to SICU were helpful in predicting in-hospital mortality, and their prognostic values were similar. However, it was determined that both GNRI and GNRI have lower prognostic value than the APACHE-II and ISS scores currently used to determine prognosis in the ICU.

The main limitation of the study is that it is retrospective and single-center design. Secondly, in-hospital mortality was evaluated to determine the prognosis in the study, and data over 28 days were not recorded. Thirdly, patients other than orthopedic trauma patients (such as intracranial trauma patients) were not included in the study. Fourthly, serum albumin levels of some patients were not measured during admission to the SICU. Excluding these patients may have affected the study results.

CONCLUSION
Orthopedic traumas, especially hip fractures, are primarily seen in geriatric trauma patients due to falls. Malnutrition is frequently seen in geriatric patients who undergo surgery due to orthopedic trauma and is associated with postoperative complications and mortality. In orthopedic trauma patients followed in the postoperative SICU, GNRI, and PNI at admission help predict in-hospital mortality and have similar predictive values. It should be remembered that the detection and treatment of nutritional deficiencies in the geriatric population is not just effective, but also brings hope and optimism for the patient's prognosis.

REFERENCES
1. Clare D, Zink KL. Geriatric trauma. Emerg Med Clin North Am. 2021;39(2):257-71.
2. Arslan K, Sahin AS, Yalcın N, Kaya E. Evaluation of trauma patients followed up and treated in intensive care unit: the sample of İstanbul province training and research hospital. Turk J Intensive Care. 2023;21(1):41-7.
3. Kirshenbom D, Ben-Zaken Z, Albilya N, Niyibizi E, Bala M. Older age, comorbid illnesses, and injury severity affect immediate outcome in elderly trauma patients. J Emerg Trauma Shock. 2017;10(3):146-50.
4. Gioffre-Florio M, Murabito LM, Visalli C, Pergolizzi FP, Fama F. Trauma in elderly patients: a study of prevalence, comorbidities and gender differences. G Chir. 2018;39(1):35-40.
5. Arslan K, Kaya E, Şahin AS. Classical blind percutaneous dilatational tracheostomy vs fiberoptic bronchoscopy guided percutaneous dilatational tracheostomy in the intensive care unit: Complications, mortality, and outcomes. Duzce Med J. 2023;25(3):273-8.
6. Phan K, Ranson W, White SJW, Cheung ZB, Kim J, Shin JI, et al. Thirty-day perioperative complications, prolonged length of stay, and readmission following elective posterior lumbar fusion associated with poor nutritional status. Global Spine J. 2019;9(4):417-23.

7. Rau CS, Tsai CH, Chou SE, Su WT, Hsu SY, Hsieh CH. The addition of the geriatric nutritional risk index to the prognostic scoring systems did not improve mortality prediction in trauma patients in the intensive care unit. Emerg Med Int. 2023;2023:3768646.

8. Cadwell JB, Afonso AM, Shahrokni A. Prognostic nutritional index (PNI), independent of frailty is associated with six-month postoperative mortality. J Geriatr Oncol. 2020;11(5):880-4.

9. Xing H, Xiang D, Li Y, Ji X, Xie G. Preoperative prognostic nutritional index predicts postoperative delirium in elderly patients after hip fracture surgery. Psychogeriatrics. 2020;20(4):487-94.

10. Arslan K, Celik S, Arslan HC, Sahin AS, Genc Y, Erturk C. Predictive value of prognostic nutritional index on postoperative intensive care requirement and mortality in geriatric hip fracture patients. North Clin Istanb. 2024;11(3):249-57.

11. Ozturk E, Elibol T, Kilicaslan E, Kabayuka B, Erdogan Ozunal I. Prognostic nutritional index predicts early mortality in diffuse large B-cell lymphoma. Medeni Med J. 2022;37(1):85-91.

12. Hanada M, Yamauchi K, Miyazaki S, Hirasawa J, Oyama Y, Yanagita Y, et al. Geriatric nutritional risk index, a predictive assessment tool, for postoperative complications after abdominal surgery: A prospective multicenter cohort study. Geriatr Gerontol Int. 2019;19(9):924-9.

13. Montero-Odasso MM, Kamkar N, Pieruccini-Faria F, Osman A, Sarquis-Adamson Y, Close J, et al. Evaluation of clinical practice guidelines on fall prevention and management for older adults: A systematic review. JAMA Netw Open. 2021;4(12):e2138911. Erratum in: JAMA Netw Open. 2023;6(8):e2332257.

14. Baykan N, Durukan P, Salt O, Yakar S, Kantar Y, Kaymaz ND, et al. Examination of geriatric trauma patients presenting to the emergency department. Phnx Med J. 2022;4(1):22-6.

15. Abrahamsen B, van Staa T, Ariely R, Olson M, Cooper C. Excess mortality following hip fracture: a systematic epidemiological review. Osteoporos Int. 2009;20(10):1633-50.

16. Bouillanne O, Morineau G, Dupant C, Coulombel I, Vincent JP, Nicolis I, et al. Geriatric nutritional risk index: A new index for evaluating at-risk elderly medical patients. Am J Clin Nutr. 2005;82(4):777-83.

17. Morey VM, Song YD, Whang JS, Kang YG, Kim TK. Can serum albumin level and total lymphocyte count be surrogates for malnutrition to predict wound complications after total knee arthroplasty? J. Arthroplasty. 2016;31(6):1317-21.

18. Dudrick SJ. Nutrition management of geriatric surgical patients. Surg Clin North Am. 2011;91(4):877-96.

19. Lew CCH, Yandell R, Fraser RJL, Chua AP, Chong MFF, Miller M. Association between malnutrition and clinical outcomes in the intensive care unit: A systematic review. J Parenter Enteral Nutr. 2017;41(5):744-58.

20. Inciong JFB, Chaudhary A, Hsu HS, Joshi R, Seo JM, Trung LV, et al. Hospital malnutrition in northeast and southeast Asia: A systematic literature review. Clin Nutr ESPEN. 2020;39:30-45.

21. Hu F, Jiang C, Shen J, Tang P, Wang Y. Preoperative predictors for mortality following hip fracture surgery: a systematic review and meta-analysis. Injury. 2012;43(6):676-85.

22. Wilson JM, Boissonneault AR, Schwartz AM, Staley CA, Schenker ML. Frailty and malnutrition are associated with inpatient postoperative complications and mortality in hip fracture patients. J Orthop Trauma. 2019;33(3):143-8.

23. Lu J, Chen YY, Zhang L, Li YG, Wang C. Laboratory nutritional parameters predict one-year mortality in elderly patients with intertrochanteric fracture. Asia Pac J Clin Nutr. 2016;25(3):457-63.

24. Arslan K, Arslan HC, Sahin AS. Evaluation of critically ill obstetric patients treated in an intensive care unit during the COVID-19 pandemic. Ann Saudi Med. 2023;43(1):10-6.

25. Canbolat N, Büyük D, Sulejmani İ, Sağlam Y, Altun D, Durmaz H, et al. The relationship between preoperative prognostic nutritional index and postoperative mortality in patients with hip fracture. Turk J Intensive Care. 2022;20(Suppl 1):7-13.

26. Nishi I, Seo Y, Hamada-Harimura Y, Yamamoto M, Ishizu T, Sugano A, et al. Geriatric nutritional risk index predicts all-cause deaths in heart failure with preserved ejection fraction. ESC Heart Fail. 2019;6(2):396-405.

27. Matsumura T, Mitani Y, Oki Y, Fujimoto Y, Ohira M, Kaneko H, et al. Comparison of geriatric nutritional risk index scores on physical performance among elderly patients with chronic obstructive pulmonary disease. Heart Lung. 2015;44(6):534-8.

28. Lidoriki I, Schizas D, Frountzas M, Machairas N, Prodromidou A, Kapelouzou A, et al. GNRI as a prognostic factor for outcomes in cancer patients: A systematic review of the literature. Nutr Cancer. 2021;73(3):391-403.

29. Liu HT, Wu SC, Tsai CH, Li C, Chou SE, Su WT, et al. Association between geriatric nutritional risk index and mortality in older trauma patients in the intensive care unit. Nutrients. 2020;12(12):3861.

30. Su WT, Wu SC, Huang CY, Chou SE, Tsai CH, Li C, et al. Geriatric nutritional risk index as a screening tool to identify patients with malnutrition at a high risk of in-hospital mortality among elderly patients with femoral fractures-A retrospective study in a level I trauma center. Int J Environ Res Public Health. 2020;17(23):8920.

31. Kregel HR, Murphy PB, Attia M, Meyer DE, Morris RS, Onyema EC, et al. The Geriatric Nutritional Risk Index as a predictor of complications in geriatric trauma patients. J Trauma Acute Care Surg. 2022;93(2):195-9.

The Effect of Antibiotic Use on Intensive Care Unit Admission and Mortality in Inpatients with COVID-19 Diagnosis

COVID-19 Tanısıyla Yatan Hastalarda Antibiyotik Kullanımının Yoğun Bakım Ünitesine Yatış ve Mortalite Üzerine Etkisi

Taliha KARAKÖK[1]
 0000-0003-4369-229X
Ahmet DOĞAN[1]
 0000-0001-5110-4027
Onur ACAR[2]
 0000-0003-3561-3192

[1]Infectious Diseases and Clinical Microbiology Clinic, Fatsa State Hospital, Ordu, Türkiye

[2]Public Health Specialist, Bursa Orhangazi District Health Management, Bursa, Türkiye

ABSTRACT

Aim: The coronavirus disease 2019 (COVID-19) pandemic had and continues to directly impact antibiotic management. This study aimed to evaluate antibiotic use and its impact on intensive care unit (ICU) admission and mortality in COVID-19 patients.

Material and Methods: The medical records of 324 COVID-19 patients aged ≥18 years who had clinical signs of infection and were followed up in the service were retrospectively evaluated. Patients were divided into two groups, those who received antibiotics and those who did not. Patients transferred from the ICU to the ward, discharged on the first day, or had missing data were excluded from the study.

Results: Of the patients, 172 (53.1%) were male, 152 (46.9%) were female, and 212 (65.4%) received antibiotic treatment. Hospitalization longer than one week (p<0.001), pulse steroid use (p=0.011), ICU admission (p=0.002) and mortality (p<0.001) were significantly higher in patients receiving antibiotics. While CRP (p<0.001), PCT (p=0.001), and ferritin (p=0.017) values obtained at admission and 48-72 hours were also found to be higher in antibiotic-using patients, there was no difference in CRP value (p=0.052) at discharge. Duration of hospitalization, antibiotic use, pulse steroid use, and being 60 years and older were found to be risk factors for mortality and ICU admission.

Conclusion: Overusing antibiotics in COVID-19 patients did not have a positive effect on mortality and ICU requirements. Considering the harms of excessive antibiotic use, recommendations and practices that lead to rational antibiotic use are needed. Furthermore, factors predicting mortality and ICU can be used in clinical practice.

Keywords: Antibiotics; COVID-19; intensive care unit; mortality.

ÖZ

Amaç: Koronavirüs hastalığı 2019 (coronavirus disease 2019, COVID-19) pandemisinin antibiyotik yönetimi üzerinde doğrudan bir etkisi olmuştur ve olmaya devam etmektedir. Bu çalışmanın amacı, COVID-19 hastalarında antibiyotik kullanımı ve bunun yoğun bakım ünitesine (YBÜ) yatış ve mortalite üzerindeki etkisini değerlendirmektir.

Gereç ve Yöntemler: Enfeksiyonun klinik bulguları olan ve serviste takip edilen ≥18 yaş 324 COVID-19 hastasının tıbbi kayıtları geriye dönük olarak değerlendirildi. Hastalar antibiyotik tedavisi alanlar ve almayan olmak üzere iki ayrı gruba ayrıldı. YBÜ'den servise devredilen, birinci gün taburcu edilen veya eksik verisi olan hastalar çalışma dışı bırakıldı.

Bulgular: Hastaların 172'si (%53,1) erkek, 152'si (%46,9) kadın ve 212'si (%65,4) antibiyotik tedavisi almıştı. Bir haftadan uzun hastanede yatış (p<0,001), pulse steroid kullanımı (p=0,011), yoğun bakım yatışı (p=0,002) ve mortalite (p<0,001) antibiyotik kullanan hastalarda anlamlı olarak daha yüksekti. Antibiyotik kullanan hastalarda yatışta ve 48-72. saatlerde elde edilen CRP (p<0,001), PCT (p=0,001) ve ferritin (p=0,017) değerleri de daha yüksek bulunurken, taburculuktaki CRP değeri (p=0,052) açısından fark yoktu. Hastanede yatış süresi, antibiyotik kullanımı, pulse steroid kullanımı ve 60 yaş ve üzeri olmak mortalite ve YBÜ yatış için risk faktörleri olarak bulunmuştur.

Sonuç: COVID-19 hastalarında aşırı antibiyotik kullanımının, mortalite ve YBÜ gereksinimi üzerinde olumlu bir etkisi olmamıştır. Aşırı antibiyotik kullanımının zararları göz önüne alınarak akılcı antibiyotik kullanımına yönlendiren öneri ve uygulamalara ihtiyaç vardır. Bununla birlikte mortalite ve YBÜ yatışı yordayan faktörlerin klinik pratikte kullanımı fayda sağlayabilir.

Anahtar kelimeler: Antibiyotik; COVID-19; yoğun bakım ünitesi; mortalite.

Corresponding Author
Sorumlu Yazar
Taliha KARAKÖK
talihapala@hotmail.com

INTRODUCTION

The coronavirus disease 2019 (COVID-19), which has caused the deaths of millions of people since the day it was identified, was removed as an international health emergency by the World Health Organization (WHO) on 5 May 2023. Although the disease is not an emergency, the whole world is still experiencing the effects of the pandemic, both in health systems and economically. In the process, health systems have been put under unprecedented stress and have been experimenting with non-evidence-based practices. Since 2019, much literature has been published on COVID-19, including treatment protocols. Antimicrobial drugs were frequently used for anti-inflammatory effects and to treat secondary bacterial infections. The new guidelines do not recommend antibacterial agents for COVID-19 treatment unless there is strong evidence of super-infection or co-infection (1). However, in clinical practice, antibacterial drugs are still used in COVID-19 cases (1). As the rate of antibiotic use in COVID-19 patients has increased, studies on the collateral effects of this practice on the health system, especially antimicrobial resistance, have started to be published (2-4). Unnecessary antibiotic use was observed in many patients (5,6). Despite these publications, still some clinicians have started antibiotics in the treatment of COVID-19. The fact that super-infection and worsening of the course of COVID-19 show similar clinical and laboratory findings and the lack of tests that can be used in differential diagnosis leads many physicians to unnecessary antibiotic use. Elevated C-reactive protein (CRP) and procalcitonin (PCT) levels, which are frequently used in follow-up, are known to be predictive of bacterial infection rather than viral infection in clinical practice, but both tests can reach high levels in COVID-19 patients. Especially high CRP in COVID-19 patients may be misleading for antibiotic use (7). This study aimed to determine the characteristics of antibiotic use in COVID-19 patients and to investigate the effect of antibiotic use on intensive care unit (ICU) admission and mortality, which has a high rate of antibiotic use.

MATERIAL AND METHODS

The study was designed as a retrospective, cross-sectional study. The medical records of patients aged 18 years and older who tested positive for severe acute respiratory syndrome coronavirus 2 (SARS-CoV-2) polymerase chain reaction (PCR) and had signs of COVID-19 infection (fever, fatigue, dyspnea, cough, digestive symptoms) and were followed up in the service between 01.04.2021 and 01.03.2022 in the 370-bed Fatsa State Hospital, a secondary care hospital, were retrospectively scanned from the hospital information system. The inclusion and exclusion criteria for the study were as follows.

Inclusion criteria:
- 18 years of age or older
- Positive SARS-CoV-2 PCR test
- To be followed up in the pandemic service

Exclusion criteria:
- COVID-19 patients hospitalized in ICU
- Patients admitted to the ward after ICU follow-up
- Patients discharged within the first 24 hours of admission
- Patients with incomplete treatment and clinical information in the epicrisis

According to the information obtained from the records and patient files, the patients were analyzed in two groups: patients who received antibiotics and patients who did not receive antibiotics. In patients requiring ICU, only the treatments and cultures administered in the ward were evaluated. The culture and blood values of the patients who were transferred to the ICU after service follow-up were not analyzed in the study. Since the primary outcome was determined as ICU requirement and mortality, only the pre-ICU processes of the patients were analyzed after transfer to the ICU. Mortality was evaluated as all causes of mortality regardless of ward and ICU.

Demographic information, comorbidities, treatments received, whether the patients received pulse steroid treatment during hospitalization (pulse steroid defined as methylprednisolone 250 mg or more at least once during hospitalization), duration of hospitalization, duration of antibiotic treatment, culture results if any, and clinical results were recorded. White blood cell (WBC), lymphocyte, platelet, PCT, CRP, aspartate aminotransferase (AST), alanine aminotransferase (ALT), ferritin, D-dimer values (taken during the first 48 hours of admission) were recorded. To evaluate CRP dynamics in the antibiotic and non-antibiotic group, patients' CRP values at 48-72 hours, on the 7th day of admission, and the last CRP value analyzed (before discharge, before ICU admission, or as the last value before mortality for cases with a mortal course during service follow-up) were noted. The first 28-day mortality in the service or ICU was analyzed. The duration of antibiotic use was recorded as the total duration of antibiotic use (e.g., for a patient who received ceftriaxone for 3 days and moxifloxacin for 2 days, the duration of antibiotic use was 5 days).

A power analysis was conducted using G*Power v.3.1. The study's power was calculated to be 98.9% for an independent samples t-test, conducted post hoc, with an effect size of 0.5, a type-1 error (α) level of 0.05, and sample sizes of 212 in the antibiotic-using group and 112 in the non-using group (8).

The study was conducted by the Declaration of Helsinki. Approval for the study was received from the Ordu University Ethics Committee (27.10.2022, 21/235).

Statistical Analysis

Data were analyzed using IBM SPSS Statistics for Windows, v.20.0. Descriptive statistics were presented as frequency, percentage, mean, standard deviation, median, quartile, minimum, and maximum values. The conformity of the variables to the normal distribution was evaluated by visual (histogram and probability graphs) and analytical methods (Kolmogorov-Smirnov and Shapiro-Wilk tests). Group comparisons were done with an independent samples t-test when data were distributed normally and a Mann-Whitney U test when data were non-normally distributed. The chi-square test or Fisher's exact test was used for categorical variables. A multivariable logistic regression model was used to assess independent variables. In logistic regression analysis, two different models were created by considering the need for ICU and death as the dependent variables. The multivariate model included variables found to be statistically significant in univariate analyses and known to be related to mortality and ICU admission. Final models were computed with the enter

procedure. Clinically relevant variables and those with p<0.05 were incorporated through a backward step-wise approach. The Hosmer-Lemeshow test was applied to evaluate the goodness of fit of the model. The results were evaluated within a 95% confidence interval and the statistical significance level was accepted as p<0.05.

RESULTS

A total of 324 COVID-19 patients, 172 (53.1%) male and 152 (46.9%) female, were included in the study. Of the patients, 212 (65.4%) received antibiotic treatment. The mean age was 65.14±15.91 years in the antibiotic-using group and 62.99±14.98 years in the non-using group. Mean age (p=0.239) and gender (p=0.565) were not found statistically significantly different between the two groups. Hospitalization longer than one week (p<0.001), pulse steroid use (p=0.011), ICU admission (p=0.002), and mortality (p<0.001) were found statistically significantly higher in the group receiving antibiotics than in the group non-using. Demographic and clinical data of the patients and characteristics of the antibiotic-using and non-using groups were presented in Table 1.

When the cases were evaluated in terms of comorbidity, there was no difference between the two groups (p=0.559). There were patients with more than one comorbid disease. Hypertension 156 (48.1%), diabetes mellitus 76 (23.5%), and chronic obstructive pulmonary disease 67 (20.7%) were the most common comorbidities (Table 2).

When the laboratory parameters of the cases were compared according to the antibiotic use, it was found that CRP (p<0.001), PCT (p=0.001), ferritin (p=0.017), and D-dimer (p=0.018) values obtained at admission and 48-72 hours were statistically significantly higher in the group receiving antibiotics. No significant difference was observed in terms of other parameters (Table 3).

When the antibiotics used by the patients were analyzed, it was found that 212 (65.4%) patients used at least one antibiotic and 112 (34.6%) patients had received combined

Table 1. Comparison of cases according to antibiotic use

	Using (n=212)	Non-using (n=112)	p
Age (year), mean±SD	65.14±15.91	62.99±14.98	0.239
Age group, n (%)			
23-39 years	14 (6.6)	8 (7.1)	
40-59 years	56 (26.4)	38 (33.9)	0.333
≥60 years	142 (67.0)	66 (59.0)	
Gender, n (%)			
Male	115 (54.2)	57 (50.9)	0.565
Female	97 (45.8)	55 (49.1)	
Duration of hospitalization (day), median (Q1-Q3) [min-max]	7 (5-10) [1-30]	5 (3-6) [1-21]	**<0.001**
Hospitalization ≥1 week, n (%)	116 (54.7)	27 (24.1)	**<0.001**
Comorbidity, n (%)	156 (73.6)	79 (70.5)	0.559
ICU admission, n (%)	37 (17.5)	6 (5.4)	**0.002**
Pulse steroid treatment, n (%)	61 (28.8)	18 (16.1)	**0.011**
Presence of culture, n (%)	73 (34.4)	9 (8.0)	**<0.001**
Blood culture positivity* (n=39 vs n=2), n (%)	6 (20.7)	1 (50.0)	0.406
Urine culture positivity* (n=58 vs n=6), n (%)	16 (27.6)	0 (0.0)	0.323
Mortality, n (%)	37 (17.4)	4 (3.6)	**<0.001**

SD: standard deviation, ICU: intensive care unit, *: there were 29 antibiotic-using and 2 non-using patients with blood culture, and 58 antibiotic-using and 6 non-using patients with urine culture, percentages for these comparisons were calculated accordingly

antibiotic treatment. The median duration of antibiotic use was 6 (interquartile range, 4-9) days. The most commonly used antibiotics were ceftriaxone at 112 (34.6%) patients and moxifloxacin at 93 (28.7%) patients (Table 4).

When the factors affecting the need for ICU were analyzed, logistic regression analysis revealed that being over 60 years of age (p=0.002), hospitalization duration of more than one week (p<0.001), pulse steroid use (p<0.001), and history of antibiotic use (p=0.002) were independent risk factors (Table 5).

When the associated factors with mortality were analyzed by logistic regression analysis, again being over 60 years of age (p=0.002), hospitalization duration of more than one week (p=0.002), pulse steroid use (p<0.001), and history of antibiotic use (p=0.001) were detected as the factors affecting mortality (Table 6).

Table 2. Comorbid diseases of the cases

Comorbidity	n (%)
Hypertension	156 (48.1)
Diabetes Mellitus	76 (23.5)
Chronic Obstructive Pulmonary Disease	67 (20.7)
Coronary Artery Disease	51 (15.7)
Congestive Heart Failure	23 (7.1)
Cerebrovascular Disease	16 (4.9)
Alzheimer	8 (2.5)
Malignancy	6 (1.9)
Epilepsy	5 (1.5)
Thyroid Disease	4 (1.2)
Other Disease	39 (12.0)

Table 3. Comparison of laboratory parameters according to antibiotic treatment status

	Using (n=212)	Non-using (n=112)	p
WBC (μl)	7445 (5498-10445) [770-29050]	6800 (5500-8990) [1100-84700]	0.127
Lymphocyte (μl)	1075 (728-1423) [200-22300]	1130 (810-1610) [220-3320]	0.072
Platelet (μl)	198500 (158000-239250) [11000-498000]	196000 (161000-249000) [59000-465000]	0.584
CRP (mg/L)			
First arrival	108 (53-171) [2-370]	68 (31-113) [0-239]	**<0.001**
Third day	66 (35-128) [0-320]	29 (13-59) [0-142]	**<0.001**
Seventh day	17 (6-49) [1-233]	5 (2-16) [1-179]	**0.006**
At discharge	11 (5-36) [0-219]	8 (3-25) [0-343]	0.052
PCT (μg/L)	0.11 (0.06-0.24) [0.01-4.21]	0.06 (0.04-0.14) [0.01-1.62]	**0.001**
AST (IU/L)	29 (20-41) [8-165]	26 (21-38) [11-133]	0.579
ALT (IU/L)	20 (13-32) [5-201]	20 (15-29) [6-440]	0.771
Ferritin (ng/mL)	331 (166-607) [16-3140]	252 (133-454) [8-1863]	**0.017**
D-dimer (ng/mL)	548 (293-1067) [84-8858]	420 (256-803) [70-6331]	**0.018**

WBC: white blood cell, CRP: C-reactive protein, PCT: procalcitonin, AST: aspartate aminotransferase, ALT: alanine aminotransferase, descriptive statistics were presented as median (25th-75th percentile) [minimum-maximum]

Table 4. Antibiotics used in order of frequency

Antibiotics	n (%)
Ceftriaxone	112 (34.6)
Moxifloxacin	93 (28.7)
Piperacillin-tazobactam	55 (17.0)
Levofloxacin	27 (8.3)
Meropenem	21 (6.5)
Ertapenem	16 (4.9)
Clarithromycin	9 (2.8)
Amikacin	6 (1.9)
Vancomycin	5 (1.5)
Azithromycin	5 (1.5)
Ciprofloxacin	5 (1.2)
Metronidazole	4 (1.2)
Other	8 (2.5)

Table 5. Associated factors with ICU admission

Independent Variables	p	OR	%95 CI
Age ≥60 years	**0.002**	5.989	1.961 - 18.286
Hospitalization ≥1 week	**<0.001**	5.075	2.130 - 12.091
Pulse steroid treatment	**<0.001**	6.954	3.086 - 15.672
Antibiotic treatment	**0.002**	4.650	1.748 - 12.372

ICU: intensive care unit, OR: odds ratio, CI: confidence interval

Table 6. Associated factors with mortality

Independent Variables	p	OR	%95 CI
Age ≥60 years	**0.002**	5.507	1.822 - 16.643
Hospitalization ≥1 week	**0.002**	3.554	1.569 - 8.051
Pulse steroid treatment	**<0.001**	4.449	2.014 - 9.829
Antibiotic treatment	**0.001**	6.728	2.215 - 20.434

OR: odds ratio, CI: confidence interval

DISCUSSION

This study found that mortality did not increase significantly in the group that did not receive antibiotics, but on the contrary, antibiotic treatment was found to be 6.728 and 4.650 times higher in terms of mortality and ICU admission in logistic regression, respectively. In addition to antibiotic use, pulse steroid use, being 60 years of age or older, and long hospital stays were found to be other factors predicting mortality and ICU admission. Although antibiotics were used in 65.4% (n=212) of all patients, culture was ordered in only 25.3% (n=82) of patients, and growth was detected in any culture in only 10.4% (n=22) of the patients who received antibiotics. These data show that there is a high rate of inappropriate antibiotic use in COVID-19 management in the study center.

Similar to this study, studies have shown that antibiotic use in COVID-19 patients is associated with the severity of the disease and the need for mechanical ventilation (9-11). In a study to detect co-infections during hospital admission for COVID-19, co-infections were detected in less than 4% of cases. In addition, the efficiency of routine diagnostic testing for pneumonia was low (12). In the present study,

the causative agent was detected in the culture of only 10.4% (n=22) of the patients in total (at the time of admission or during hospitalization). This is an indication of how low the co-infection rate is in the first presentation of COVID-19 cases. Although ICU patients were excluded from the study, it was observed that broad-spectrum antibiotics such as piperacillin-tazobactam, meropenem, and vancomycin were preferred at a considerable rate. In addition, while atypical agents were expected less frequently, it was observed that quinolone group antibiotics were preferred at a high rate in the study center despite the cautions regarding the use of quinolone group antibiotics. In the COVID-19 patient group, the lack of a clear indicator to differentiate between bacterial co-infection or super-infection and deterioration due to COVID-19 results in a high rate of unnecessary antibiotic use. Incorrect or unnecessary use of antibiotics may have multifaceted results. One of these is the increasing antimicrobial resistance (13-17). Another result is the worsening of the clinic in COVID-19 patients due to the disruption of the microbiota (18).

The long duration of hospitalization, pulse steroid treatment, and high baseline CRP and PCT values, which were found to be significantly higher in the group receiving antibiotics, are factors defined in COVID-19 patients in terms of ICU admission and mortality. Therefore, mortality was found to be high in this group. The estimated relative risk of antibiotic treatment in patients with a mortal course was high. This may be due to clinicians' suspicion of bacterial infection secondary to COVID-19 when initiating antibiotics or empirical antibiotic initiation practices in patients with severe progression. During the pandemic, due to the disease burden, many branch physicians have followed primary COVID-19 patients, and the principles and perspectives of antibiotic use of each branch physician have been different. This makes the reasons and patterns of antibiotic use in COVID-19 patients heterogeneous and makes it difficult to distinguish whether the high use of antibiotics in the mortality group is due to inappropriate use or a genuine need for antibiotics. The independent impact of antibiotic-related adverse effects on mortality is difficult to determine in this complicated patient group. In COVID-19 patients, elevated levels of PCT as well as CRP without bacterial infection have been reported with clinical severe progression (19). CRP and PCT may contribute to the diagnosis of lower respiratory tract infection, but it is not possible to make a definitive distinction (20,21). Because inflammation, which is a natural consequence of COVID-19 pathophysiology, can also increase acute phase parameters (22). Nevertheless, studies show that PCT values are particularly useful in shortening the duration of antibiotic treatment (23-25). A cohort study showed that PCT-guided antibiotic prescription reduced antibiotic prescription rates in hospitalized COVID-19 patients (26). However, baseline and third-day CRP were higher in the group receiving antibiotics, while there was no difference in seventh-day and discharge CRP. This supports the inappropriateness of antibiotic treatment based on CRP. The similar decline in seventh-day and discharge CRP in the group not receiving antibiotics indicates that elevated CRP should not be an indication for antibiotics alone in COVID-19 patients. It is noticeable that antibiotic use is higher in the group with high acute-phase reactants. However, as can be understood from the studies, acute phase reactants alone are insufficient to diagnose co-infection or super-infection in COVID-19 cases (19-22). Studies are showing that CRP trajectory in the first week of hospitalization is an important factor in predicting microbiology culture positivity and outcome in patients hospitalized with COVID-19 (27). For the prediction of clinical outcome and co-infection, the dynamism of CRP over time as well as the absolute value of CRP should be interpreted.

The main limitation of the study is that the results represent more regional data since it is a single-centered study. Secondly, the study was limited to 324 cases so this reduces the strength of the study. Thirdly, patients hospitalized in the ICU and pediatric age group were not included.

CONCLUSION

As a result, the present study center was found to have a very high rate of antibiotic use during the COVID-19 pandemic. Although the number of cultures gained was relatively small, it was observed that a considerable amount of broad-spectrum antibiotics were used. Since the COVID-19 pandemic has been managed according to the guidelines of the Ministry of Health in Türkiye from the beginning, we guess that similar results will be obtained throughout the country. The high acute phase values in COVID-19 cases contributed to this result. The lack of a definitive algorithm for antibiotic management in COVID-19 cases and the limitations in microbiologic detection of bacterial pneumonia agents are other factors of this problem. It is possible to predict that the rates of antibiotic use will be much higher in retrospective studies, especially in cases followed up in ICUs in Türkiye. During the COVID-19 pandemic, many negative consequences of high antibiotic use in this patient group in Türkiye, especially resistance, will be revealed more clearly in the future. These effects should be investigated with further analyses such as antibiotic resistance, side effects of treatments, and cost. In addition, the principles of antibiotic use in the COVID-19 patient group should be presented in a way to guide clinicians with clear and applicable recommendation articles based on Türkiye.

REFERENCES

1. Bartoletti M, Azap O, Barac A, Bussini L, Ergonul O, Krause R, et al. ESCMID COVID-19 living guidelines: drug treatment and clinical management. Clin Microbiol Infect. 2022;28(2):222-38.
2. Mahida N, Winzor G, Wilkinson M, Jumaa P, Gray J. Antimicrobial stewardship in the post COVID-19 pandemic era: an opportunity for renewed focus on controlling the threat of antimicrobial resistance. J Hosp Infect. 2022;129:121-3.
3. Calderón-Parra J, Muiño-Miguez A, Bendala-Estrada AD, Ramos-Martínez A, Muñez-Rubio E, Fernández Carracedo E, et al. Inappropriate antibiotic use in the COVID-19 era: Factors associated with inappropriate prescribing and secondary complications. Analysis of the registry SEMI-COVID. PLoS One. 2021;16(5):e0251340.
4. Murray AK. The novel coronavirus COVID-19 outbreak: Global implications for antimicrobial resistance. Front Microbiol. 2020;11:1020.

5. Langford BJ, So M, Raybardhan S, Leung V, Soucy JR, Westwood D, et al. Antibiotic prescribing in patients with COVID-19: rapid review and meta-analysis. Clin Microbiol Infect. 2021;27(4):520-31.

6. Martin AJ, Shulder S, Dobrzynski D, Quartuccio K, Pillinger KE. Antibiotic use and associated risk factors for antibiotic prescribing in COVID-19 hospitalized patients. J Pharm Pract. 2023;36(2):256-63.

7. Carbonell R, Urgelés S, Salgado M, Rodríguez A, Reyes LF, Fuentes YV, et al. Negative predictive value of procalcitonin to rule out bacterial respiratory co-infection in critical COVID-19 patients. J Infect. 2022;85(4):374-81.

8. Faul F, Erdfelder E, Lang AG, Buchner A. G*Power 3: a flexible statistical power analysis program for the social, behavioral, and biomedical sciences. Behav Res Methods. 2007;39(2):175-91.

9. Chaaban T, Ezzeddine Z, Ghssein G. Antibiotic misuse during the COVID-19 pandemic in Lebanon: a cross-sectional study. COVID. 2024;4(7):921-9.

10. Şencan İ, Çağ Y, Karabay O, Kurtaran B, Güçlü E, Öğütlü A, et al. Antibiotic use and influencing factors among hospitalized patients with COVID-19: a multicenter point-prevalence study from Turkey. Balkan Med J. 2022;39(3):209-17.

11. Popp M, Stegemann M, Riemer M, Metzendorf MI, Romero CS, Mikolajewska A, et al. Antibiotics for the treatment of COVID-19. Cochrane Database Syst Rev. 2021;10(10):CD015025.

12. Westblade LF, Simon MS, Satlin MJ. Bacterial coinfections in coronavirus disease 2019. Trends Microbiol. 2021;29(10):930-41.

13. Ukuhor HO. The interrelationships between antimicrobial resistance, COVID-19, past, and future pandemics. J Infect Public Health. 2021;14(1):53-60.

14. Ghosh S, Bornman C, Zafer MM. Antimicrobial resistance threats in the emerging COVID-19 pandemic: Where do we stand? J Infect Public Health. 2021;14(5):555-60.

15. Haqqi A, Awan UA, Ahmed H, Afzal MS. Antimicrobial resistance vs COVID-19: A bigger challenge in the post-pandemic era! J Formos Med Assoc. 2021;120(7):1537-8.

16. Ma ESK, Kung KH, Chen H. Combating antimicrobial resistance during the COVID-19 pandemic. Hong Kong Med J. 2021;27(6):396-8.

17. Rickard J, Boulware DR, Guan W, Ntirenganya F, Kline S. Has there been exacerbation of disparities in antimicrobial resistance during the SARS-CoV-2 pandemic? Surg Infect (Larchmt). 2022;23(7):613-5.

18. Rosca A, Balcaen T, Lanoix JP, Michaud A, Moyet J, Marcq I, et al. Mortality risk and antibiotic use for COVID-19 in hospitalized patients over 80. Biomed Pharmacother. 2022;146:112481.

19. Wu HY, Chang PH, Chen KY, Lin IF, Hsih WH, Tsai WL, et al. Coronavirus disease 2019 (COVID-19) associated bacterial coinfection: Incidence, diagnosis and treatment. J Microbiol Immunol Infect. 2022;55(6 Pt 1):985-92.

20. Galli F, Bindo F, Motos A, Fernández-Barat L, Barbeta E, Gabarrús A, et al. Procalcitonin and C-reactive protein to rule out early bacterial coinfection in COVID-19 critically ill patients. Intensive Care Med. 2023;49(8):934-45.

21. Wolfisberg S, Gregoriano C, Schuetz P. Procalcitonin for individualizing antibiotic treatment: an update with a focus on COVID-19. Crit Rev Clin Lab Sci. 2022;59(1):54-65.

22. Roy A, Powers HR, Craver EC, Nazareno MD, Yarrarapu SNS, Sanghavi DK. Antibiotic stewardship: Early discontinuation of antibiotics based on procalcitonin level in COVID-19 pneumonia. J Clin Pharm Ther. 2022;47(2):243-7.

23. Covington EW, Roberts MZ, Dong J. Procalcitonin monitoring as a guide for antimicrobial therapy: A review of current literature. Pharmacotherapy. 2018;38(5):569-81.

24. Lee CC, Chang JC, Mao XW, Hsu WT, Chen SY, Chen YC, et al. Combining Procalcitonin and rapid multiplex respiratory virus testing for antibiotic stewardship in older adult patients with severe acute respiratory infection. J Am Med Dir Assoc. 2020;21(1):62-7.

25. Smith SE, Muir J, Kalabalik-Hoganson J. Procalcitonin in special patient populations: Guidance for antimicrobial therapy. Am J Health Syst Pharm. 2020;77(10):745-58.

26. Hessels LM, Speksnijder E, Paternotte N, van Huisstede A, Thijs W, Scheer M, et al. Procalcitonin-guided antibiotic prescription in patients with COVID-19: a multicenter observational cohort study. Chest. 2023;164(3):596-605.

27. Ming DK, Myall AC, Hernandez B, Weiße AY, Peach RL, Barahona M, et al. Informing antimicrobial management in the context of COVID-19: understanding the longitudinal dynamics of C-reactive protein and procalcitonin. BMC Infect Dis. 2021;21(1):932. Erratum in: BMC Infect Dis. 2021;21(1):988.

Determination of Serum Interleukin-36 Alpha, Beta, Gamma, and Interleukin-17 Levels in Patients with Non-Hodgkin Lymphoma

Non-Hodgkin Lenfoma'lı Hastaların Serum İnterlökin-36 Alfa, Beta, Gamma ve İnterlökin-17 Düzeylerinin Belirlenmesi

Hatice TERZİ[1]
 0000-0003-3471-1305
Ecem DEMİR[2]
 0000-0001-9714-0672
Halef Okan DOĞAN[3]
 0000-0001-8738-0760
Mehmet ŞENCAN[1]
 0000-0002-1459-3906

[1]Department of Internal Medicine, Division of Hematology, Sivas Cumhuriyet University Faculty of Medicine, Sivas, Türkiye

[2]Department of Statistics, Sivas Cumhuriyet University, Sivas, Türkiye

[3]Department of Medical Biochemistry, Sivas Cumhuriyet University Faculty of Medicine, Sivas, Türkiye

ABSTRACT

Aim: Non-Hodgkin lymphoma (NHL) is a diverse group of hematologic cancers characterized by uncontrolled proliferation of lymphoid cells. This study aimed to evaluate the relationship between serum concentrations of interleukin-36 alpha (IL-36α), interleukin-36 beta (IL-36β), interleukin-36 gamma (IL-36γ), and interleukin-17 (IL-17), which play an important role in the immune system, in NHL patients and whether these cytokines can serve as potential biomarkers or therapeutic targets for NHL.

Material and Methods: A total of 88 individuals, including 55 NHL patients diagnosed and followed up in the Department of Hematology, Sivas Cumhuriyet University Medical Faculty, and 33 healthy controls, were included in the study. Blood samples were collected from patients at the time of diagnosis and from individuals in the control group for hemogram and biochemistry tests and serum IL-17, IL-36α, IL-36β, and IL-36γ levels. Patients were divided into three groups, complete remission (CR), partial remission (PR), and progression according to interim positron emission tomography/computed tomography (PET/CT) results.

Results: Serum IL-36α (p<0.001), IL-36β (p=0.022), IL-36γ (p<0.001), and IL-17 (p<0.001) concentrations were statistically significantly higher in NHL patients compared to healthy controls. Although IL-17, IL-36α, IL-36β, and IL-36γ levels were lower in patients with progression compared to the CR and PR groups, these differences were not statistically significant (p=0.065, p=0.186, p=0.151, and p=0.065, respectively).

Conclusion: These cytokines may influence the etiopathogenesis and even the progression of NHL. However, since NHL constitutes a highly heterogeneous disease group, more extensive in-vivo and in-vitro studies are needed.

Keywords: Interleukin; non-Hodgkin lymphoma; therapeutic targets.

ÖZ

Amaç: Non-Hodgkin lenfoma (NHL), lenfoid hücrelerin kontrolsüz çoğalmasıyla tanımlanan çeşitli bir hematolojik kanser grubudur. Bu çalışmanın amacı, NHL hastalarında immün sistemde önemli bir rol oynayan interlökin-36 alfa (IL-36α), interlökin-36 beta (IL-36β), interlökin-36 gama (IL-36γ) ve interlökin-17 (IL-17) serum konsantrasyonları arasındaki ilişkiyi ve bu sitokinlerin NHL için potansiyel biyobelirteçler veya tedavi hedefleri olarak hizmet edip edemeyeceğini değerlendirmektir.

Gereç ve Yöntemler: Çalışmaya Sivas Cumhuriyet Üniversitesi Tıp Fakültesi Hematoloji bölümünde tanı almış ve takip edilmiş 55 NHL hastası ve 33 sağlıklı kontrol olmak üzere toplam 88 birey dahil edildi. Hastaların tanı anındaki ve kontrol grubundaki bireylerin hemogram ve biyokimya tetkikleri ile serum IL-17, IL-36α, IL-36β ve IL-36γ düzeylerinin çalışılması için kan örnekleri alındı. Hastalar interim pozitron emisyon tomografisi/bilgisayarlı tomografi (PET/BT) sonuçlarına göre komplet remisyon (CR), parsiyel remisyon (PR) ve progresyon olmak üzere üç gruba ayrıldı.

Bulgular: Serum IL-36α (p<0,001), IL-36β (p=0,022), IL-36γ (p<0,001) ve IL-17 (p<0,001) konsantrasyonları NHL hastalarında sağlıklı kontrollere kıyasla istatistiksel olarak anlamlı derecede daha yüksekti. Progresyon gösteren hastalarda IL-17, IL-36α, IL-36β ve IL-36γ düzeyleri CR ve PR gruplarına göre daha düşük olmasına rağmen bu farklar istatistiksel olarak anlamlı değildi (sırasıyla p=0,065; p=0,186; p=0,151 ve p=0,065).

Sonuç: Bu sitokinler NHL'nin etyopatogenezi ve hatta progresyonu üzerinde etkili olabilir. Ancak, NHL oldukça heterojen bir hastalık grubunu oluşturduğundan, daha geniş kapsamlı in-vivo ve in-vitro çalışmalara ihtiyaç vardır.

Anahtar kelimeler: İnterlökin; non-Hodgkin lenfoma; terapötik hedefler.

Corresponding Author
Sorumlu Yazar
Hatice TERZİ
dr.terzi@hotmail.com

INTRODUCTION

Non-Hodgkin lymphoma (NHL) encompasses diverse malignancies originating from lymphoid tissues. NHL are among the most prevalent cancers worldwide and represent a broad spectrum of malignancies derived from lymphoid tissue. This category encompasses around 60 subtypes with clinical and biological profiles (1). While precise classification of NHL subtypes is essential for accurate diagnosis and effective treatment, conducting risk assessments specific to each subtype poses significant difficulties. These challenges arise from the limited number of cases and the relative rarity of each subtype (2). Interleukin-36 (IL-36) is a pro-inflammatory cytokine that is part of the interleukin-1 (IL-1) superfamily, consisting of three agonists (IL-36α, IL-36β, IL-36γ) and one antagonist (IL-36Ra) (3). IL-36 activates the MAPK and NF-kB pathways, essential in innate and adaptive immunity. It is primarily expressed at barrier sites such as the bronchial, intestinal, and dermal epithelium, linking innate and adaptive immune responses. IL-36 is associated with various inflammatory conditions and cancer (4). Interleukin-17 (IL-17), mainly produced by Th17 cells, has a multifaceted role in cancer progression. It supports tumor growth by enhancing angiogenesis, cell proliferation, and metastasis and inhibiting apoptosis (5). The network of cytokines plays a crucial role in the development and progression of these lymphomas by affecting both tumor growth and the immune response (6). Cytokines such as IL-36α, IL-36β, IL-36γ, and IL-17 are known to be involved in various inflammatory and autoimmune disorders (7). Despite their significant roles in these conditions, their specific contributions to NHL are poorly understood. This study sought to evaluate the serum levels of IL-36α, IL-36β, IL-36γ, and IL-17 in patients with NHL and to investigate their potential associations with disease features and outcomes.

MATERIAL AND METHODS

The single-center, multidisciplinary, and cross-sectional study project was conducted by the Department of Internal Medicine, Hematology Division, and the Department of Medical Biochemistry at Sivas Cumhuriyet University Medical Faculty Hospital, and commenced following the approval from Sivas Cumhuriyet University Clinical Research Ethics Committee, dated September 12, 2023, with decision number 2023-09/03.

Study Groups

Patients diagnosed with NHL according to the 2016/2022 lymphoma classification of the World Health Organization (WHO), and histopathologically confirmed, not receiving any NHL treatment, aged 18 years and over and admitted to the Hematology Department of the Sivas Cumhuriyet University, Faculty of Medicine Hospital between February 6, 2022, and February 6, 2023, were included in the study as the patient group. As the control group, healthy individuals had a similar mean age to the patient group were included. Patients with known additional hematological malignancies and healthy individuals with any hematological or rheumatological diseases were excluded from the study. Also, the presence of any known acute and/or chronic disease, having a solid and/or hematological malignancy, regular medication use, pregnancy, breastfeeding, or smoking were additional

exclusion criteria for healthy individuals. Based on this framework, adjustments to the number of patients and healthy individuals included in the study were deemed necessary. For the sample calculation, it was decided to include 56 patients in the NHL group and 34 people in the control group by taking α=0.05, β=0.10, (1-β)=0.90, and R=1.62 with the Epi Info 7.2.6.0 program. One person in each patient and control group was excluded from the study due to insufficient data. The study finally involved 88 participants, comprising 55 individuals with NHL and 33 healthy controls. These participants' comprehensive clinical, laboratory, and imaging data were retrieved from patient records. For NHL patients, venous blood samples were collected at the time of diagnosis before initiating any treatment. Serum levels of IL-36α, IL-36β, IL-36γ, and IL-17 were quantified in both NHL patient and healthy control groups. The clinical data and performance status of the patients at the time of diagnosis were recorded during their first admission, and the routine biochemical test results were accessed through the automation system.

Patients diagnosed with NHL were grouped according to histologic subtypes. Patients were classified according to the Ann-Arbor staging system based on positron emission tomography/computed tomography (PET/CT) imaging at the time of diagnosis. According to the treatment response evaluation based on the Lugano revised response criteria, patients were categorized into three groups, complete response (CR), partial response (PR), and progression at the interim PET evaluation.

Sample Collection and Cytokine Measurement

Peripheral blood was collected from new patients diagnosed with NHL and healthy controls. Blood samples were drawn into appropriate tubes for measuring IL-36α, IL-36β, IL-36γ, IL-17 levels, and other laboratory parameters. The collected blood samples were centrifuged at 4000 G for 10 minutes and stored at -80°C in Eppendorf tubes for the measurement of IL-36α, IL-36β, IL-36γ, and IL-17, SunRed brand enzyme-linked immunosorbent assay (ELISA) kits were used.

Statistical Analysis

Data analysis was conducted using IBM SPSS v.26.0, with a confidence level set at 95%. The Kolmogorov-Smirnov test assessed whether the data followed a normal distribution. Since the data were not normally distributed, the Mann-Whitney U test was used for two-group comparisons, and the Kruskal-Wallis H test was used for more than two-group comparisons. Descriptive statistics of the median, 25th-75th percentiles, minimum, and maximum were calculated for the measurements and frequency and percentages for the categorical variables.

RESULTS

Demographic and Clinical Characteristics

Out of 55 NHL patients, 22 (40%) were female, 33 (60%) were male. There were 33 individuals in the control group, of whom 20 (60.6%) were female and 13 (39.4%) were male. The median age of individuals in the patient group was 65 (range, 34-88) years, while the median age in the control group was 53 (range, 37-63) years. While the gender was homogeneously distributed between the two groups (p=0.052), the patient group with NHL had a higher median age (p=0.001).

Out of 55 patients histologically diagnosed with NHL, except for one with NK/T-cell lymphoma, the rest were classified as B-cell lymphomas according to cell origin. Among these, diffuse large B-cell lymphoma (DLBCL) was the most common histopathologic subtype with a frequency of 65.5% (n=36). The other histological subtypes were follicular lymphoma (FL) with 16.4% (n=9), mantle cell lymphoma (MCL) with 12.7% (n=7), and marginal zone lymphoma (MZL) with 3.6% (n=2). The distribution of histopathological subtypes and the treatment protocols applied to the patients were presented in Table 1.

Comparison of Cytokine Levels and Laboratory Parameters

Serum levels of the IL-36α (p<0.001), IL-36β (p=0.022), IL-36γ (p<0.001), and IL-17 (p<0.001) were significantly elevated in NHL patients compared to healthy controls. In comparing laboratory data between the patient and control groups, statistically significant differences were observed in white blood cells (p=0.005), neutrophils (p=0.001), lymphocytes (p=0.002), monocytes (p=0.001), and hemoglobin (p=0.015) values. The comparison results of the hemogram parameters and IL-17, IL-36α, IL-36β, and IL-36γ levels between the patient and control groups were presented in Table 2. In the patient group, when laboratory parameters and IL-17, IL-36α, IL-36β, and IL-36γ levels were compared by gender, statistically significant differences were found between the two groups for hemoglobin and creatinine values. Hemoglobin (p=0.001), and creatinine (p=0.009) levels were significantly higher in males compared to females (Table 3).

Comparison Based on Clinical Parameters

Patients were classified into three groups (CR, PR, and progression) based on the interim PET results during the first-line treatment. There were 40 patients in the CR group, 10 in the PR group, and 5 in the progression group. When IL-17, IL-36α, IL-36β, and IL-36γ levels were compared according to the interim PET/CT responses, no statistically significant differences were observed. The comparison of interleukin levels according to interim PET/CT results was presented in Table 4. The levels of

IL-17 and IL-36γ were found to be considerably lower in the progression group compared to the other groups, however, this difference was not statistically significant.

Table 1. Histopathologic subtypes of patients and treatments

	n=55
Subtype, n (%)	
DLBCL	36 (65.5)
FL	9 (16.4)
MCL	7 (12.7)
MZL	2 (3.6)
TL	1 (1.8)
First-Line Treatment, n (%)	
CHOP	1 (1.8)
R-Bendamustine	3 (5.5)
R-Bendamustine + Rituximab Maintenance	5 (9.1)
R-CHOP	22 (40.0)
R-CHOP + Intrathecal Methotrexate	9 (16.4)
R-CHOP/R-DHAP Protocol	6 (10.9)
R-CNOP	2 (3.6)
R-CVP + Rituximab Maintenance Therapy	1 (1.8)
R-EPOCH	1 (1.8)
R-EPOCH + Intrathecal Methotrexate	1 (1.8)
R-MiniCHOP	3 (5.5)
No Therapy	1 (1.8)
Second-Line Treatment, n (%)	
DeAngelis protocol (8)	1 (1.8)
R-DHAP	4 (7.3)
R-ICE	2 (3.6)
Rituximab-Ibrutinib	2 (3.6)
R-VCD	1 (1.8)
Radiotherapy	1 (1.8)
Third-Line Treatment, n (%)	
Autologous Stem Cell Transplant	7 (12.7)
Lenalidomide + Obinutuzumab	1 (1.8)
Fourth-Line and Beyond Treatment, n (%)	
R-GemOx	1 (1.8)

DLBCL: diffuse large B-cell lymphoma, FL: follicular lymphoma, MCL: mantle cell lymphoma, MZL: marginal zone lymphoma, TL: T-cell lymphoma, R: rituximab, CHOP: cyclophosphamide- doxorubicin- vincristine- prednisone, DHAP: dexamethasone-cytarabine- cisplatin, CNOP: cyclophosphamide- mitoxantrone- vincristine- prednisone, CVP: cyclophosphamide- vincristine- prednisone, EPOCH: etoposide- prednisone-vincristine- cyclophosphamide- doxorubicin, ICE: ifosfamide- carboplatin- etoposide, VCD: bortezomib- cyclophosphamide- dexamethasone, GemOx: gemcitabine- oxaliplatin

Table 2. Comparison of hemogram and interleukin values between patient and healthy groups

	Patient (n=55)	Control (n=33)	p
WBC (10^9/L)	7.78 (6.29-10.30) [1.87-34.65]	6.45 (5.43-7.41) [3.81-10.59]	**0.005**
Neu (10^9/L)	5.39 (3.50-6.84) [0.04-13.11]	3.46 (2.69-4.60) [2.02-6.82]	**0.001**
Lymp (10^9/L)	1.48 (0.99-2.25) [0.31-20.44]	2.16 (1.73-2.58) [1.15-3.08]	**0.002**
Mono (10^9/L)	0.57 (0.46-0.92) [0.10-1.77]	0.47 (0.36-0.56) [0.30-0.83]	**0.001**
Hgb (g/dL)	13.2 (11.5-14.6) [7.2-17.0]	13.9 (13.1-15.4) [10.4-16.7]	**0.015**
Plt (10^9/L)	255 (200-327) [34-829]	291 (245-342) [188-409]	0.115
Cre (mg/dL)	0.83 (0.67-1.03) [0.31-6.88]	0.76 (0.64-0.88) [0.50-1.16]	0.063
LDH (U/L)	240 (185-343) [128-1340]	167 (153-181) [124-242]	**<0.001**
IL-17 (pg/ml)	111.5 (90.4-138.4) [15.0-819.1]	298.3 (136.6-607.7) [70.9-1000.0]	**<0.001**
IL-36α (ng/L)	11.99 (9.18-15.77) [0.27-57.77]	23.44 (12.57-41.31) [5.36-73.97]	**<0.001**
IL-36β (ng/L)	6.27 (4.94-8.22) [0.17-39.32]	14.57 (5.42-27.33) [1.92-55.50]	**0.022**
IL-36γ (ng/L)	5.57 (4.63-6.80) [0.23-34.51]	12.97 (7.31-36.77) [4.30-59.94]	**<0.001**
Age (year)	65 (52-73) [34-88]	53 (51-57) [37-63]	**0.001**

WBC: white blood cell, Neu: neutrophil, Lymp: lymphocyte, Mono: monocyte, Hgb: hemoglobin, Plt: platelet, Cre: creatinine, LDH: lactate dehydrogenase, IL: interleukin, IL-17: interleukin-17, IL-36α: interleukin-36 alpha, IL-36β: interleukin-36 beta, IL-36γ: interleukin-36 gamma

Table 3. Comparison of hemogram and interleukin values between genders in the patient group

	Female (n=22)	Male (n=33)	p
WBC (10^9/L)	8.30 (6.23-11.20) [1.87-16.64]	7.58 (6.22-9.36) [3.22-34.65]	0.437
Neu (10^9/L)	5.56 (3.22-8.01) [0.04-10.31]	5.30 (3.69-6.35) [2.38-13.11]	0.618
Lymp (10^9/L)	1.47 (0.66-2.99) [0.31-7.90]	1.51 (1.07-2.09) [0.53-20.44]	0.979
Mono (10^9/L)	0.52 (0.45-0.74) [0.10-1.77]	0.63 (0.50-0.95) [0.28-1.72]	0.120
Hgb (g/dL)	11.7 (10.0-13.8) [7.2-15.2]	13.8 (12.5-15.3) [8.0-17.0]	**0.001**
Plt (10^9/L)	274 (201-430) [34-543]	245 (192-293) [48-829]	0.213
Cre (mg/dL)	0.64 (0.55-0.96) [0.31-6.88]	0.92 (0.78-1.10) [0.54-1.44]	**0.009**
LDH (U/L)	259 (183-478) [128-926]	240 (191-326) [143-1340]	0.594
IL-17 (pg/ml)	114.5 (93.2-267.3) [57.4-819.1]	106.5 (84.3-130.4) [15.0-794.1]	0.192
IL-36α (ng/L)	11.87 (10.16-27.95) [6.84-57.77]	12.16 (8.97-15.27) [0.27-53.24]	0.303
IL-36β (ng/L)	6.12 (4.92-13.89) [3.13-37.98]	6.27 (4.74-8.03) [0.17-39.32]	0.718
IL-36γ (ng/L)	5.85 (4.57-11.89) [3.05-34.51]	5.37 (4.47-6.57) [0.23-32.57]	0.405
Age (year)	57 (47-71) [34-86]	63 (56-73) [34-88]	0.191

WBC: white blood cell, Neu: neutrophil, Lymp: lymphocyte, Mono: monocyte, Hgb: hemoglobin, Plt: platelet, Cre: creatinine, LDH: lactate dehydrogenase, IL: interleukin, IL-17: interleukin-17, IL-36α: interleukin-36 alpha, IL-36β: interleukin-36 beta, IL-36γ: interleukin-36 gamma

Table 4. Comparison of hemogram and interleukin values according to the interim PET results in the patient group

	CR (n=40)	PR (n=10)	Progression (n=5)	p
WBC (10^9/L)	7.82 (6.34-9.51) [1.87-16.55]	7.45 (4.98-11.02) [3.22-34.65]	7.53 (6.97-13.37) [6.94-16.64]	0.812
Neu (10^9/L)	5.55 (3.63-6.82) [0.04-10.31]	3.77 (1.92-6.65) [1.38-13.11]	5.42 (4.97-9.39) [4.55-9.71]	0.305
Lymp (10^9/L)	1.44 (0.97-2.19) [0.50-7.35]	1.94 (1.26-4.86) [0.83-20.44]	1.07 (0.36-3.91) [0.31-5.66]	0.203
Mono (10^9/L)	0.56 (0.46-0.81) [0.25-1.72]	0.61 (0.45-0.97) [0.31-1.51]	0.56 (0.29-1.39) [0.10-1.77]	0.909
Hgb (g/dL)	12.8 (11.2-14.6) [7.2-17.0]	13.5 (11.7-14.3) [8.0-15.7]	12.4 (10.8-15.5) [9.9-16.6]	0.940
Plt (10^9/L)	264 (224-341) [34-650]	174 (128-204) [49-829]	279 (221-369) [173-411]	**0.010**
Cre (mg/dL)	0.82 (0.67-1.02) [0.31-6.88]	0.90 (0.74-1.08) [0.55-1.17]	0.84 (0.69-2.55) [0.59-4.18]	0.842
LDH (U/L)	230 (186-337) [128-1340]	263 (177-330) [143-380]	455 (197-692) [180-926]	0.495
IL-17 (pg/ml)	109.8 (90.4-145.8) [15.0-819.1]	120.7 (103.3-201.9) [86.9-521.7]	77.7 (60.6-107.1) [57.4-111.5]	0.065
IL-36α (ng/L)	12.07 (9.17-16.01) [0.27-57.77]	14.37 (10.19-19.71) [9.08-34.25]	10.33 (6.71-11.85) [6.58-12.76]	0.186
IL-36β (ng/L)	6.13 (4.96-8.67) [0.17-39.32]	7.01 (5.71-11.87) [4.55-22.05]	4.33 (3.02-6.55) [1.80-7.28]	0.151
IL-36γ (ng/L)	5.73 (4.32-7.14) [0.23-34.51]	6.27 (5.16-12.14) [4.94-15.24]	4.67 (2.62-5.30) [2.20-5.72]	0.065

PET: positron emission tomography, CR: complete remission, PR: partial remission, WBC: white blood cell, Neu: neutrophil, Lymp: lymphocyte, Mono: monocyte, Hgb: hemoglobin, Plt: platelet, Cre: creatinine, LDH: lactate dehydrogenase, IL: interleukin, IL-17: interleukin-17, IL-36α: interleukin-36 alpha, IL-36β: interleukin-36 beta, IL-36γ: interleukin-36 gamma

A total of 14 patients received second-line treatment, including 5 patients who progressed according to interim PET/CT results and 9 patients who experienced treatment failure based on PET/CT evaluation at the end of first-line therapy. Following second-line treatment, 7 (12.7%) patients underwent autologous stem cell transplantation (Table 1).

Survival Status

When evaluating NHL patients' survival status, 34 (61.8%) were alive, while 21 (38.2%) had exitus. As of July 2024, a reassessment of the patients revealed that out of 55 patients, 21 had deceased, while 34 were alive. It was determined that all 34 surviving patients were in remission. Among the deceased, 6 patients had achieved a CR response in the interim PET evaluation. However, 1 patient died due to pulmonary thromboembolism, 1 due to liver failure, and 4 due to febrile neutropenia and sepsis. The remaining 15 deceased patients were found to have died from non-treatment-related causes such as cerebrovascular disease, respiratory failure, myocardial infarction, and traffic accidents.

DISCUSSION

Non-Hodgkin lymphomas (NHLs) represent a diverse collection of malignancies that arise from lymphoid tissue, consisting of around 60 distinct subtypes, each exhibiting different clinical and biological characteristics (9). NHL is a heterogeneous group of tumors caused by the malignant transformation of mature and immature cells of the lymphoid system, primarily originating from B lymphocytes (in 85-90% of cases) and, to a lesser extent, from T lymphocytes and natural killer (NK) cells. NHL is an extremely heterogeneous group of diseases, with the clinical courses and treatment responses of different subtypes varying significantly (10).

Recent studies have explored the role of interleukins in lymphomas and other cancers. IL-36, comprising three subforms (α, β, γ), has been implicated in chronic inflammation and cancer, activating various immune and non-immune cells (11). IL-36 cytokines belong to the IL-1 family and have various roles in inflammatory diseases and cancer. A meta-analysis indicated that elevated IL-36α expression correlates with improved overall survival in

cancer patients, while the effect of IL-36γ differs depending on the type of cancer. IL-36 signaling promotes pro-tumorigenic characteristics in colon cancer cells, and the administration of IL-36R antagonists has been shown to reduce tumor burden in vivo (12,13). In multiple myeloma, serum levels of the IL-36α, IL-36β, IL-36γ, and IL-17 were significantly lower in patients than in healthy controls, suggesting a potential role in the disease's etiopathogenesis (14). In non-small cell lung cancer, IL-36γ expression was higher in tumor tissues than adjacent normal tissues, with elevated protein levels associated with higher tumor grade in lung adenocarcinoma (15). IL-17 plays a crucial role in cancer progression, especially in lung, colorectal, and breast cancers. IL-17 facilitates tumor angiogenesis, cell proliferation, and metastasis while suppressing apoptosis through inflammatory signaling pathways (5,16). The role of IL-17 in cancer is multifaceted, with some evidence indicating possible antitumor effects during cancer therapies (17).

Among NHL patients included in the present study, significant differences were observed in hemoglobin levels and monocyte counts between those who survived and those who did not. Based on existing literature, we believe these hematological parameters may impact the prognosis of the disease (18,19).

These findings highlight the complex roles of interleukins in various cancers and their potential as prognostic markers or therapeutic targets. In the present study, IL-17 and IL-36α, IL-36β, and IL-36γ levels were found higher in NHL patients compared to the control group, suggesting that these interleukins may play a role in the etiopathogenesis of NHL. However, during interim evaluations of patients undergoing treatment, it was noted that IL-17 and IL-36γ levels were markedly lower in the progression group compared to those who achieved CR or PR. Although this difference was not statistically significant, it is considered a noteworthy finding.

NHL represents a heterogeneous group of diseases with various subtypes characterized by distinct clinical courses and biological features. This heterogeneity can lead to different responses to treatment and varying prognoses across subtypes (1,2). Therefore, future studies involving larger cohorts of NHL patients with more homogenous distribution are needed to clarify the potential prognostic impact of IL-17 and IL-36 levels on disease progression.

Previous studies have shown that IL-17 and IL-36 have diverse roles in different types of cancer, influencing tumor development, progression, and response to therapy with both tumor-promoting and anti-tumor effects. Based on the findings of the present study, it can be suggested that IL-17 and IL-36α, IL-36β, and IL-36γ may play a role in the etiopathogenesis and prognosis of NHL. However, it is important to acknowledge that the heterogeneity of the NHL and the limited sample size may have influenced the results.

CONCLUSION

Further comprehensive in vivo and in vitro studies are necessary to better understand the roles of IL-17 and IL-36 in the pathogenesis and prognosis of NHL. These interleukins hold promise as potential therapeutic targets, and future research should focus on investigating their utility as biomarkers for cancer diagnosis, prognosis, and treatment strategies.

Author Contributions: Idea/Concept: HT, HOD; Design: HT, HOD, MŞ; Data Collection/Processing: HT, ED; Analysis/Interpretation: HT, ED, HOD; Literature Review: ED, MŞ; Drafting/Writing: HT, ED; Critical Review: HT, MŞ.

REFERENCES

1. Howlader N, Morton LM, Feuer EJ, Besson C, Engels EA. Contributions of subtypes of non-Hodgkin lymphoma to mortality trends. Cancer Epidemiol Biomarkers Prev. 2016;25(1):174-9.
2. Moubadder L, McCullough LE, Flowers CR, Koff JL. Linking environmental exposures to molecular pathogenesis in non-Hodgkin lymphoma subtypes. Cancer Epidemiol Biomarkers Prev. 2020;29(10):1844-55.
3. Yuan ZC, Xu WD, Liu XY, Liu XY, Huang AF, Su LC. Biology of IL-36 signaling and its role in systemic inflammatory diseases. Front Immunol. 2019;10:2532.
4. Wang X, Yi P, Liang Y. The role of IL-36 in infectious diseases: a potential target for COVID-19? Front Immunol. 2021;12:662266.
5. Yang B, Kang H, Fung A, Zhao H, Wang T, Ma D. The role of interleukin 17 in tumor proliferation, angiogenesis, and metastasis. Mediators Inflamm. 2014;2014:623759.
6. Sheu BC, Chang WC, Cheng CY, Lin HH, Chang DY, Huang SC. Cytokine regulation networks in the cancer microenvironment. Front Biosci. 2008;13:6255-68.
7. Ding L, Wang X, Hong X, Lu L, Liu D. IL-36 cytokines in autoimmunity and inflammatory disease. Oncotarget. 2018;9(2):2895-901.
8. Shahzadi M, Ahmed D, Sawani S, Moosajee M. Outcome of primary CNS lymphoma; a retrospective analysis. Asian Pac J Cancer Care. 2022;7(1):41-6.
9. Shingleton J, Wang J, Baloh C, Dave T, Davis N, Happ L, et al. Non-Hodgkin lymphomas: Malignancies arising from mature B cells. Cold Spring Harb Perspect Med. 2021;11(3):a034843.
10. Terzi H, Oral K, Yılmaz H, Demir Yurtseven E, Şencan M. Single-center experience in relapsed/refractory non-Hodgkin's lymphoma. Cumhuriyet Med J. 2022;44(1):51-6.
11. Neurath MF. IL-36 in chronic inflammation and cancer. Cytokine Growth Factor Rev. 2020;55:70-9.

12. Baker K, O'Donnell C, Bendix M, Keogh S, Byrne J, O'Riordain M, et al. IL-36 signalling enhances a pro-tumorigenic phenotype in colon cancer cells with cancer cell growth restricted by administration of the IL-36R antagonist. Oncogene. 2022;41(19):2672-84.

13. Zhang R, Jiang M, Huang M, Yang J, Liu Q, Zhao Z, et al. Prognostic value of Interleukin-36s in cancers: A systematic review and meta-analysis. Cytokine. 2023;172:156397.

14. Bilge Y, Terzi H, Doğan HO, Kablan D, Şencan M. Determination of serum interleukin-36 alpha, beta, gamma and interleukin-17 levels in patients with multiple myeloma. Cumhuriyet Med J. 2024;46(1):57-65.

15. Liu L, He H, Xu D, Feng Y, Zhou H, Shi L, et al. Association between interleukin 36γ and tumor progression in non-small cell lung cancer. Oncol Lett. 2020;19(3):2457-65.

16. Wu F, Xu J, Huang Q, Han J, Duan L, Fan J, et al. The role of interleukin-17 in lung cancer. Mediators Inflamm. 2016;2016:8494079.

17. Welte T, Zhang XH. Interleukin-17 could promote breast cancer progression at several stages of the disease. Mediators Inflamm. 2015;2015:804347.

18. Lim EJ, Peh SC. Bone marrow and peripheral blood changes in non-Hodgkin's lymphoma. Singapore Med J. 2000;41(6):279-85.

19. Bari A, Tadmor T, Sacchi S, Marcheselli L, Liardo EV, Pozzi S, et al. Monocytosis has adverse prognostic significance and impacts survival in patients with T-cell lymphomas. Leuk Res. 2013;37(6):619-23.

Mycobacteria Presence and Anti-Tuberculosis Drug Resistance Profile in Düzce Region: 18 Years of Experience

Düzce Bölgesinde Mikobakteri Varlığı ve Antitüberküloz İlaç Direnci Profili: 18 Yıllık Deneyim

Emel AKBAŞ[1]
[ORCID] 0000-0001-6589-7734
Banu Hümeyra KESKİN[2]
[ORCID] 0000-0002-2102-3952
Emel ÇALIŞKAN[1]
[ORCID] 0000-0002-9451-7865
Şükrü ÖKSÜZ[1]
[ORCID] 0000-0002-4893-5564
İdris ŞAHİN[1]
[ORCID] 0000-0001-6203-5039
Cihadiye Elif ÖZTÜRK[3]
[ORCID] 0000-0002-4330-2864

[1]Department of Medical Microbiology, Düzce University Faculty of Medicine, Düzce, Türkiye

[2]Department of Medical Microbiology, Zonguldak Gynecology and Children's Disease Hospital, Zonguldak, Türkiye

[3]Department of Medical Microbiology, Arel University Faculty of Medicine, İstanbul, Türkiye

ABSTRACT

Aim: The aim of this study was to determine the frequency of *Mycobacterium tuberculosis* complex (MTBC) and non-tuberculous mycobacteria (NTM) growth among mycobacterial isolates collected over 18 years from patients suspected of having tuberculosis, and to evaluate the resistance rates of MTBC strains to first-line anti-tuberculosis drugs.

Material and Methods: A total of 17,199 clinical specimens, sent to the Mycobacteriology Laboratory, Department of Medical Microbiology, at Düzce University Health Application and Research Centre between 2004 and 2021 for suspected tuberculosis, were retrospectively analyzed in this study. To differentiate MTBC from NTM, the TBC Identification Test was performed to detect the MPT64 antigen of the MTBC. Ehrlich-Ziehl-Neelsen (EZN) staining method was used to detect the presence of acid-fast bacilli (AFB).

Results: Out of the samples with suspected tuberculosis, mycobacterial growth was detected in 896 (5.2%) cases. Among these, 824 (91.9%) were identified as MTBC, while 72 (8.1%) were classified as NTM. EZN staining revealed that 404 (45.1%) out of the 896 isolates were found AFB positive. Analysis of first-line anti-tuberculosis drug susceptibility in the 824 MTBC isolates revealed that 194 were resistant to at least one first-line anti-tuberculosis drug. Of these, 135 isolates showed resistance to a single drug, while 59 exhibited resistance to more than one drug.

Conclusion: Tuberculosis remains a significant public health problem both globally and in Türkiye. Regular investigation of local and regional growth patterns and resistance profiles is crucial for achieving the goals of tuberculosis elimination and eradication.

Keywords: Tuberculosis; non-tuberculous mycobacteria; anti-tuberculosis drug resistance.

ÖZ

Amaç: Bu çalışmanın amacı, tüberküloz şüphesi olan hastalardan 18 yıl boyunca toplanan mikobakteri izolatlarında *Mycobacterium tuberculosis* kompleks (MTBK) ve tüberküloz dışı mikobakteri (TDM) üreme sıklığını belirlemek ve MTBK olarak izole edilen suşların birinci basamak anti-tüberküloz ilaçlara direnç oranlarını değerlendirmektir.

Gereç ve Yöntemler: Bu çalışmada, Düzce Üniversitesi Sağlık Uygulama ve Araştırma Merkezi Tıbbi Mikrobiyoloji Anabilim Dalı Mikobakteriyoloji Laboratuvarı'na 2004 ve 2021 yılları arasında tüberküloz şüphesi ile gönderilen toplam 17.199 klinik örnek geriye dönük olarak analiz edildi. MTBK'yi TDM'den ayırt etmek için, MTBK'nin MPT64 antijenini tespit etmek amacıyla TBC Tanımlama Testi yapıldı. Asit-dirençli basillerin (ARB) varlığını tespit etmek amacıyla Ehrlich-Ziehl-Neelsen (EZN) boyama yöntemi kullanıldı.

Bulgular: Tüberküloz şüphesi ile gönderilen örneklerden 896 (%5,2) vakada mikobakteri üremesi tespit edildi. Bunlardan 824'ü (%91,9) MTBK olarak tanımlanırken 72'si (%8,1) TDM olarak sınıflandırıldı. EZN boyama sonucunda 896 izolatın 404'ünde (%45,1) ARB pozitifliği saptandı. 824 MTBK izolatında birinci basamak anti-tüberküloz ilaç duyarlılığının analizi, 194'ünün en az bir birinci basamak anti-tüberküloz ilaca dirençli olduğunu ortaya koydu. Bunlardan 135 izolat tek bir ilaca direnç gösterirken, 59'u birden fazla ilaca direnç göstermekteydi.

Sonuç: Tüberküloz, hem küresel olarak hem de Türkiye'de önemli bir halk sağlığı sorunu olmaya devam etmektedir. Tüberkülozun ortadan kaldırılması ve yok edilmesi hedeflerine ulaşmak için yerel ve bölgesel üreme kalıplarının ve direnç profillerinin düzenli olarak araştırılması hayati önem taşımaktadır.

Anahtar kelimeler: Tüberküloz; atipik mikobakteri; anti-tüberküloz ilaç direnci.

Corresponding Author
Sorumlu Yazar
Emel AKBAŞ
emel_kalkan@live.com

INTRODUCTION

Tuberculosis (TB) is one of the oldest infectious diseases, caused by *Mycobacterium tuberculosis* complex (MTBC), especially *M. tuberculosis* (1). Mycobacterial species that do not belong to this complex are referred to as non-TB mycobacteria (NTM), which are commonly found in the environment (2). While most NTM isolates are not clinically significant, recent studies have reported an increase in NTM infections, especially in the immunocompromised patients (3).

According to the World Health Organization (WHO), TB is the leading cause of death worldwide. Despite being both preventable and treatable, it still causes the death of approximately 1.5 million people every year (4).

The global effort to end the TB epidemic by 2030 was interrupted by the coronavirus disease 2019 (COVID-19) pandemic, resulting in a significant reduction in TB data. The number of newly reported TB cases dropped from 7.1 million in 2019 to 5.8 million in 2020, reverting to levels last seen in 2012. This reduction in access to TB diagnosis and treatment has caused an increase in deaths related to TB. In addition, it is estimated that these negative effects will worsen in the coming years (4).

Accurate and rapid diagnosis is the most important step in TB treatment and in preventing its transmission. While advancements in molecular methods have significantly improved TB diagnostics, the isolation of *M. tuberculosis* through culture remains the gold standard (5).

Delays in the diagnosis of TB and the emergence of drug-resistant strains pose significant challenges to eradicating the disease. Resistance to isoniazid and rifampicin, the most effective first-line treatments, is significantly concerning. Resistance to these drugs is classified as multidrug-resistant TB (MDR-TB). According to the WHO (4), an estimated half a million cases of MDR-TB have been reported in recent years, with 8.5% of these classified as extensively drug-resistant TB (XDR-TB).

This study aimed to determine the frequency of MTBC and NTM isolated from clinical samples with suspected TB over 18 years. Additionally, it sought to determine the resistance rates of MTBC species to first-line anti-TB drugs.

MATERIAL AND METHODS

A total of 17,199 clinical specimens sent to the Mycobacteriology Laboratory, Department of Medical Microbiology, at Düzce University Faculty of Medicine Health Application and Research Centre between 2004 and 2021 from various clinics and outpatient departments were retrospectively examined.

Lung specimens and non-sterile clinical specimens underwent homogenization and decontamination using conventional methods with N-acetyl-L-cysteine and 4% sodium hydroxide. Sterile samples, on the other hand, did not require decontamination. The processed samples were cultured on Löwenstein-Jensen (LJ) (Becton Dickinson, USA) as solid medium and Mycobacterium Growth Indicator Tube (BACTEC BD MGIT 320, Sparks, USA) as liquid medium following the manufacturer's instructions. Smear preparations were stained using Ehrlich-Ziehl-Neelsen (EZN) method and evaluated under a light microscope to detect the presence of acid-fast bacilli (AFB).

LJ media inoculated for bacterial growth were monitored weekly for up to eight weeks, and growth was evaluated accordingly. Similarly, the samples inoculated in the BACTEC MGIT BD 320 (Becton Dickinson, USA) automated system according to the manufacturer's recommendations were incubated for six weeks. Samples showing no growth by the end of these periods were considered negative. To differentiate MTBC from NTM, the TBC Identification Test (Becton Dickinson, USA) was performed to detect the MPT64 antigen of the MTBC, following the manufacturer's instructions (6). Drug susceptibility of the MTBC isolates, identified through differentiation against isoniazid (INH), streptomycin (SM), rifampicin (RIF), and ethambutol (EMB), was conducted using BACTEC MGIT 320 method with the SIRE kit containing first-line anti-TB drugs following the manufacturer's recommendations (5).

Prior to the study, permission was obtained from Düzce University Non-Interventional Ethics Committee, dated 25.07.2022, with reference number 138.

Statistical Analysis

The statistical analysis of the study was performed using IBM SPSS v.23.0 (IBM Corp. Released 2015. IBM SPSS Statistics for Windows, Version 23.0. Armonk, NY: IBM Corp.) software. Categorical data were summarized as frequencies and percentages. Chi-square, Fisher's exact and Fisher-Freeman-Halton tests were used for data analysis. $p < 0.05$ was considered statistically significant.

RESULTS

In this study, a total of 17,199 clinical samples sent to the Mycobacteriology Laboratory, Department of Medical Microbiology, at Düzce University Faculty of Medicine Health Application and Research Centre between 2004 and 2021, with a preliminary diagnosis of TB, were analyzed. Only 896 (5.2%) of the clinical samples showed growth. Of these, 824 (91.9%) were identified as MTBC and 72 (8.1%) as NTM. Of the 824 MTBC isolates, while 743 (90.2%) were isolated from lung specimens, 81 (9.8%) from extra-pulmonary specimens. In contrast, 68 (94.4%) of the NTM strains were isolated from lung specimens and 4 (5.6%) from extra pulmonary specimens (Table 1).

Staining of the samples using EZN method revealed that 404 (45.1%) out of the 896 isolates were found AFB positive. Among the samples with MTBC, 397 (48.2%) were AFB positive and seven (9.7%) NTM isolates were AFB positive (Table 1). The AFB positivity rate in MTBC-positive samples was statistically significantly higher than that of NTM isolates ($p < 0.001$).

The distribution of samples with mycobacterial growth according to patient gender was analyzed (Table 2). Among the patients with MTBC isolates, 546 (66.3%) were male and 278 (33.7%) were female, while 51 (70.8%) male and 21 (29.2%) female patients had NTM isolates. No statistically significant difference was found between genders in terms of MTBC and NTM growth in patients with mycobacterial growth ($p = 0.430$).

Analysis of the distribution of identified MTBC isolates over the years revealed that the highest number of isolates was obtained in 2010. Meanwhile, the number of isolates significantly decreased during the COVID-19 pandemic, reaching a minimum, especially in 2021.

Table 1. Distribution of mycobacteria according to sample type and EZN staining result

Sample	MTBC (n=824)		NTM (n=72)	
	N	AFB (+)	N	AFB (+)
Phlegm	577	319 (38.7)	40	4 (5.6)
BAL	140	41 (4.9)	25	1 (1.4)
GA	30	11 (1.3)	3	0 (0.0)
Biopsy	22	12 (1.5)	3	1 (1.4)
Urine	11	7 (0.9)	-	-
Body fluid	25	4 (0.5)	-	-
Wound	18	2 (0.2)	1	1 (1.4)
CSF	1	1 (0.1)	-	-
Total	**824**	**397 (48.2)**	**72**	**7 (9.7)**

N: number of isolated samples, EZN: Ehrlich-Ziehl-Neelsen, MTBC: mycobacterium tuberculosis complex, NTM: non-tuberculosis mycobacteria, AFB: acid-fast bacilli, BAL: bronchoalveolar lavage, GA: gastric aspirat, CSF: cerebrospinal fluid

Table 2. Comparison of patients with MTBC and NTM isolates according to the gender

	MTBC (n=824)	NTM (n=72)	p
Gender, n (%)			
Female	278 (33.7)	21 (29.2)	0.430
Male	546 (66.3)	51 (70.8)	

MTBC: mycobacterium tuberculosis complex, NTM: non-tuberculosis mycobacteria

Table 3. Resistance status of MTBC isolates

Anti-TB Drugs	MTBC (n=824)		Isolates with at least one resistance (n=194)
	n	%	%
INH	119	14.4	61.3
RIF	24	2.9	12.4
SM	77	9.3	39.7
EMB	54	6.5	27.8
Single Drug	135	16.4	69.6
INH	74	8.9	38.1
RIF	5	0.6	2.6
SM	32	3.9	16.5
EMB	24	2.9	12.4
Two Drug	40	4.8	20.6
INH+RIF	7	0.8	3.6
INH+SM	18	2.2	9.3
INH+EMB	4	0.5	2.1
RIF+SM	1	0.1	0.5
RIF+EMB	1	0.1	0.5
EMB+SM	9	1.1	4.6
Tree Drug	17	2.1	8.8
INH+RIF+SM	3	0.3	1.5
INH+RIF+EMB	2	0.2	1.0
INH+SM+EMB	9	1.1	4.6
RIF+SM+EMB	3	0.3	1.5
Four Drug	2	0.2	1.0

MTBC: mycobacterium tuberculosis complex, TB: tuberculosis, INH: isoniazid, RIF: rifampicin, SM: streptomycin, EMB: ethambutol

Analysis of the first-line anti-TB drug susceptibility of 824 MTBC isolates revealed that 194 of these isolates were resistant to at least one first-line anti-TB drug. The number of isolates resistant to INH, RIF, SM, and EMB were 119, 24, 77, and 54, respectively. Among the resistant MTBC isolates, 135 were resistant to a single drug, while 59 were resistant to more than one drug. Of the latter group, 14 were found to be MDR-TB due to concurrent resistance to both INH and RIF (Table 3).

The evaluation of anti-TB resistance over the years revealed that the resistance rates for years 2016, 2017, and 2021 were not statistically significantly different from one another (p=0.632), but were significantly higher compared to the other years (p<0.001). Additionally, 2016 was the only year in which resistance to all four anti-TB drugs was detected (Table 4).

DISCUSSION

Tuberculosis (TB) can affect individuals of any age or gender. According to the WHO Global Tuberculosis Report 2021, 56% of all TB cases in 2020 were in males, while 33% were in females. The same report also indicated that TB is more prevalent among individuals between the ages of 25-34 (4). In the Turkish Tuberculosis Control Report, 58.5% of all TB patients were male, and 41.5% were female (7). Kirui et al. (8) analyzed 120 TB cases in Nairobi and reported that 73% of the patients were male, while 27% were female. In Türkiye, Yazısız et al. (9) analyzed data from 974 patients and reported that 74.5% of TB cases were male and 25.5% were female. In this study, the gender distribution of TB patients revealed that 66.3% were male and 33.7% were female. Therefore, the findings in this study align with the literature.

TB is a systemic disease that typically affects the lungs but can also involve other organs and tissues. In 2020, 4.8 million new pulmonary TB cases were diagnosed worldwide, accounting for nearly half of all TB cases (4). According to the Tuberculosis Control Report in Türkiye, pulmonary TB cases constituted 60.9% of all TB cases (7). A study by Yazısız et al. (9) showed that lung samples comprised the majority (92.1%) of specimens from which MTBC was isolated. In this study, 743 (90.2%) out of 824 MTBC strains were isolated from lung samples. When compared to the data worldwide and in Türkiye, the pulmonary TB rates observed in the present study were found to be similar.

In the diagnosis of TB, searching for AFB using the EZN staining method is a simple, rapid, and inexpensive method. Kivihya-Ndugga et al. (10) reported that 332 (59.9%) out of 554 samples from which MTBC was isolated were AFB positive. Similarly, Yıldıran et al. (11) reported that 1,221 (71.8%) out of 1,701 samples with MTBC isolates were AFB positive. Tarhan et al. (12) reported 89 (86.4%) out of 103 MTBC isolates cultured were AFB positive. In the current study, 397 (48.2%) MTBC isolates and 7 (9.7%) NTM isolates were found to be AFB positive. Notably, the low positivity rate of EZN staining in samples with NTM isolates is remarkable. In the surveyed literature, no data on EZN staining results for NTM isolates were found. In this study, the findings revealed a lower AFB positivity rate compared to existing literature. The reason for this discrepancy may be attributed to factors such as the type of sample material, smear thickness, bacilli concentration

Table 4. Distribution of resistance in MTBC isolates according to years

Year	INH	RIF	SM	EMB	Two drug	Three drug	Four drug	Total
2004 (n=19)	4 (21.1)	2 (10.5)	0 (0.0)	1 (5.3)	1 (5.3)	1 (5.3)	0 (0.0)	4 (21.1)
2005 (n=41)	1 (2.4)	0 (0.0)	1 (2.4)	3 (7.3)	0 (0.0)	0 (0.0)	0 (0.0)	5 (12.2)
2006 (n=36)	0 (0.0)	1 (2.8)	1 (2.8)	3 (8.3)	0 (0.0)	0 (0.0)	0 (0.0)	5 (13.9)
2007 (n=47)	5 (10.6)	2 (4.3)	3 (6.4)	4 (8.5)	3 (6.4)	0 (0.0)	0 (0.0)	16 (34.0)
2008 (n=42)	6 (14.3)	1 (2.4)	2 (4.8)	2 (4.8)	1 (2.4)	0 (0.0)	0 (0.0)	10 (23.8)
2009 (n=60)	11 (18.3)	4 (6.7)	8 (13.3)	4 (6.7)	5 (8.3)	4 (6.7)	0 (0.0)	14 (23.3)
2010 (n=102)	6 (5.9)	2 (1.9)	9 (8.8)	4 (3.9)	3 (2.9)	2 (1.9)	0 (0.0)	13 (12.7)
2011 (n=75)	8 (10.7)	2 (2.7)	8 (10.7)	5 (6.7)	3 (4.0)	2 (2.7)	0 (0.0)	13 (17.3)
2012 (n=65)	15 (23.1)	2 (3.1)	2 (3.1)	2 (3.1)	4 (6.2)	0 (0.0)	0 (0.0)	16 (24.6)
2013 (n=37)	2 (5.4)	0 (0.0)	0 (0.0)	1 (2.7)	0 (0.0)	0 (0.0)	0 (0.0)	3 (8.1)
2014 (n=48)	6 (12.5)	2 (4.2)	8 (16.7)	0 (0.0)	3 (6.3)	0 (0.0)	0 (0.0)	13 (27.1)
2015 (n=37)	6 (16.2)	0 (0.0)	4 (10.8)	2 (5.4)	2 (5.4)	1 (2.7)	0 (0.0)	8 (21.6)
2016 (n=53)	19 (35.8)	5 (9.4)	11 (20.7)	9 (17.0)	5 (9.4)	4 (7.5)	2 (3.8)	**24 (45.3)**
2017 (n=44)	13 (29.5)	0 (0.0)	3 (6.8)	3 (6.8)	3 (6.8)	0 (0.0)	0 (0.0)	**18 (40.9)**
2018 (n=46)	3 (6.5)	0 (0.0)	7 (15.2)	5 (10.9)	2 (4.3)	0 (0.0)	0 (0.0)	13 (28.3)
2019 (n=33)	6 (18.2)	0 (0.0)	7 (21.2)	4 (12.1)	2 (6.1)	2 (6.1)	0 (0.0)	10 (30.3)
2020 (n=23)	4 (17.4)	0 (0.0)	0 (0.0)	0 (0.0)	0 (0.0)	0 (0.0)	0 (0.0)	4 (17.4)
2021 (n=16)	4 (25.0)	1 (6.3)	3 (18.8)	2 (12.5)	3 (18.8)	1 (6.3)	0 (0.0)	**5 (31.3)**
Total (n=824)	**119 (14.4)**	**24 (2.9)**	**77 (9.3)**	**54 (6.5)**	**40 (4.9)**	**17 (2.1)**	**2 (0.2)**	**194 (23.5)**

MTBC: mycobacterium tuberculosis complex, TB: tuberculosis, INH: isoniazid, RIF: rifampicin, SM: streptomycin, EMB: ethambutol

in the sample, and the experience of the person performing the microscopic examination.

Drug-resistant TB continues to be an important public health concern in Türkiye and many other countries worldwide. Detecting drug resistance in TB and initiating appropriate and effective treatment are critical steps in preventing infections and ensuring clinical recovery (5). Studies conducted in Türkiye and other countries have reported varying rates of resistance to anti-TB drugs. Arora et al. (13) evaluated 4,910 MTBC isolates and found that 3,941 isolates were resistant to at least one anti-TB drug. In the same study, resistance rates for INH, RIF, SM and EMB were reported as 8.3%, 0.44%, 0.16% and 1.9%, respectively. Similarly, He et al. (14) analyzed 13,486 TB cases in China and reported that 21.1% of the isolates were resistant to at least one first-line drug. Resistance rates for INH, RIF, SM and EMB were reported as 13.4%, 8.4%, 14.7% and 2.6%, respectively. In Türkiye, Yazısız et al. (9) investigated MTBC isolates at the Akdeniz University and reported that 26.7% were resistant to at least one of the first-line anti-TB drugs. In the aforementioned study, resistance rates for INH, RIF, SM and EMB were 9.1%, 1.3%, 4.4% and 0.5%, respectively. Yılmaz et al. (15) conducted a study in Erzurum and found that 19.6% of 419 MTBC strains were resistant to at least one drug. Analysis of resistance rates revealed that 1.9%, 4.1%, 11.7% and 3.6% for INH, RIF, SM and EMB, respectively. In the current study, among 824 MTBC strains isolated, 23.5% demonstrated resistance to at least one anti-TB drug. Resistance rates for INH, RIF, SM and EMB were 14.4%, 2.9%, 9.3% and 6.5%, respectively. Both in this study and in the previously mentioned literature, the most common resistance observed in MTBC isolates worldwide was against INH. This high resistance rate may be due to the

frequent use of INH both in treatment and prophylaxis, poor patient compliance to treatment regimens, and geographical differences in drug use and access.

MDR-TB is a condition where MTBC is resistant to INH and RIF, the two most effective first-line anti-TB drugs, with or without resistance to other anti-TB drugs. Globally, the prevalence of MDR-TB among newly diagnosed TB cases ranges from 3-4%, while it increases to 18-21% among previously treated TB patients (4). In a meta-analysis conducted in Pakistan, Molla et al. (16) showed that the prevalence of MDR-TB was 4% in new TB cases and 21%. Similarly, Yılmaz et al. (15) evaluated 419 MTBC strains in Erzurum, Türkiye, and found an MDR-TB prevalence rate of 3.6% which aligns with the national average in Türkiye. In the present study, the MDR-TB prevalence among MTBC strains was shown to be 1.6%. Compared to global and regional data, including data in Türkiye, MDR-TB prevalence rate in the present study is relatively lower. Moreover, the findings in this study show variations in TB resistance over the years. Specifically, resistance rates in 2016, 2017 and 2021 were statistically significantly higher compared to other years, while no significant differences were observed among themselves. These findings are consistent with previous studies conducted in Türkiye. This study suggests that incorporating these resistance rates to anti-TB drugs into treatment planning for TB patients would be beneficial. In addition, obtaining epidemiological data and understanding resistance rates in the laboratory, is necessary for evaluating regional, national, and international progress in the battle against TB and reaching potential targets.

Although NTMs are typically acquired from the environment, with no evidence of person-to-person transmission, their clinical importance has grown in recent

years. Moreover, the pathogenic roles of NTMs have been well established and they are known to cause serious clinical results, especially in immunocompromised individuals (17). The incidence, prevalence and strain distribution of NTM cases are highly variable among different geographical locations (3). However, accurately determining the prevalence and incidence of NTM infections remains challenging, as the microbiological isolation of these microbes does not always correspond to clinical infection. Recent guidelines recommend the use of clinical, radiographic, and microbiological criteria for the diagnosis of NTM-related lung disease. In a study by Özen et al. (5) involving 31,017 samples, 5.1% of the samples submitted with suspicion of TB were reported as MTBC, while 1.1% were identified as NTM. Similarly, Martínez González et al. (18) analyzed the distribution of NTM isolates according to sex and found that isolates were three times more common in males than females. In another study conducted in Japan, it was reported that there was a significant increase in lung disease cases due to NTM (19). In this study, 4.8% of the mycobacteria isolated were identified as MTBC and 0.4% as NTM, with 70.8% of the NTM strains isolated from male patients and 29.2% from female patients, primarily from respiratory tract samples. When compared to the existing literature, the MTBC and NTM rates in this study were found to be consistent with previously reported findings. The detection of NTMs in Düzce region emphasizes the clinical importance and frequency of these isolates. Notably, this is the first time infections caused by NTMs have been identified from clinical samples in Düzce region, which constitutes a strength of this study. However, the lack of relevant data on whether guidelines for differentiating NTMs as causative agents or contaminants were applied by clinics represents a limitation. Therefore, this study recommends more comprehensive, collaborative studies with clinical facilities to address this concern.

CONCLUSION

The findings in this study indicate that TB remains a significant public health concern in Düzce region, which can be classified as endemic for TB. Notably, resistance rates in 2016, 2017, and 2021 were significantly higher compared to other years, highlighting periods of increased TB burden. Interestingly, the number of TB isolates identified dropped to a minimum in 2021, coinciding with the onset of the COVID-19 pandemic. This demonstrates the impact of global health crises such as COVID-19 on the surveillance and management of other infectious diseases. Such health crises can unknowingly lead to a reemergence of neglected diseases, emphasizing the need for sustained focus on the control of TB. Moreover, this study highlights the significance of whether the NTMs detected represent infections or mere contaminants. Future research should assess the adherence of clinicians to diagnostic guidelines to ensure accurate identification and management of NTMs. The biggest obstacle in global TB control programs is the increasing prevalence of drug-resistant bacilli. In addition, the lack of new TB drugs intensifies this problem. To meet the elimination and eradication targets for TB by the WHO, it is necessary to prioritize prevention, diagnosis, and treatment algorithms. This includes investigating local and regional resistance profiles, focusing on research for new drugs, and ensuring that global infections, such as the COVID-19 pandemic, do not reduce the importance of eradicating other infectious diseases.

REFERENCES

1. Kanabalan RD, Lee LJ, Lee TY, Chong PP, Hassan L, Ismail R, et al. Human tuberculosis and mycobacterium tuberculosis complex: A review on genetic diversity, pathogenesis and omics approaches in host biomarkers discovery. Microbiol Res. 2021;246:126674.
2. Waters V, Ratjen F. Antibiotic treatment for nontuberculous mycobacteria lung infection in people with cystic fibrosis. Cochrane Database Syst Rev. 2020;6(6):CD010004.
3. Gopalaswamy R, Shanmugam S, Mondal R, Subbian S. Of tuberculosis and non-tuberculous mycobacterial infections - a comparative analysis of epidemiology, diagnosis and treatment. J Biomed Sci. 2020;27(1):74.
4. World Health Organization. Global tuberculosis report 2021. Geneva: World Health Organization; 2021.
5. Özen N, Kula Atik T, Çetin Duran A. Evaluation of mycobacterium tuberculosis culture and drug susceptibility test results and the distribution of nontuberculosis mycobacteria from the clinical specimens. Mikrobiyol Bul. 2020;54(4):559-74. Turkish.
6. T.C. Sağlık Bakanlığı. Ulusal Tüberküloz Tanı Rehberi. Türkiye Halk Sağlığı Kurumu, Sağlık Bakanlığı Yayın No: 935. Ankara; 2014. Turkish.
7. T.C. Sağlık Bakanlığı. Türkiye'de Verem Savaşı 2021 Raporu. Halk Sağlığı Genel Müdürlüğü, Sağlık Bakanlığı Yayın No: 1274. Ankara; 2023. Turkish.
8. Kirui JK, Nyamache AK, Maingi JM, Ogari C. Prevalence of multidrug resistant tuberculosis among previously treated TB patients in Nairobi county, Kenya. Int Clin Med Therp. 2019;1(1):4.

9. Yazısız H, Hırçın Cenger D, Yazısız V, Kılıç L, Altın S. First-line anti-tuberculosis drug resistance trends of mycobacterium tuberculosis complex isolates. A tertiary hospital study in Turkey. Tuberk Toraks. 2019;67(2):92-101.

10. Kivihya-Ndugga LE, van Cleeff MR, Githui WA, Nganga LW, Kibuga DK, Odhiambo JA, et al. A comprehensive comparison of Ziehl-Neelsen and fluorescence microscopy for the diagnosis of tuberculosis in a resource-poor urban setting. Int J Tuberc Lung Dis. 2003;7(12):1163-71.

11. Yıldıran ST, Özyurt M, Saraçlı MA, Gün H. The evaluation of the smear and culture results of mycobacteriological specimens in a seven-year study period: A retrospective study. İnfeksiyon Derg. 1998;12(2):151-5. Turkish.

12. Tarhan G, Ordulu L, Gümüşlü F, Ceyhan I, Cesur S. Comparison of auramine-rhodamine and Erlich-Ziehl-Neelsen staining methods for the diagnosis of tuberculosis. Mikrobiyol Bul. 2003;37(2-3):131-6. Turkish.

13. Arora J, Singhal R, Verma AK, Kumar G, Bhalla M, Sarin R, et al. Isoniazid resistance among rifampicin-susceptible mycobacterium tuberculosis isolates from tuberculosis patients. Int J Mycobacteriol. 2016;5(Suppl 1):S127-8.

14. He XC, Zhang XX, Zhao JN, Liu Y, Yu CB, Yang GR, et al. Epidemiological trends of drug-resistant tuberculosis in China from 2007 to 2014: A retrospective study. Medicine (Baltimore). 2016;95(15):e3336.

15. Yılmaz A, Afşin D. Investigation of the sensitivity of mycobacterium tuberculosis strains isolated from various clinical samples in eastern Turkey to major anti-tuberculosis drugs. J Contemp Med. 2021;11(1):92-6.

16. Molla KA, Reta MA, Ayene YY. Prevalence of multidrug-resistant tuberculosis in East Africa: A systematic review and meta-analysis. PLoS One. 2022;17(6):e0270272.

17. Liu H, Lian L, Jiang Y, Huang M, Tan Y, Zhao X, et al. Identification of species of nontuberculous mycobacteria clinical isolates from 8 provinces of China. Biomed Res Int. 2016;2016:2153910.

18. Martínez González S, Cano Cortés A, Sota Yoldi LA, García García JM, Alba Álvarez LM, Palacios Gutiérrez JJ. Non-tuberculous mycobacteria. An emerging threat? Arch Bronconeumol. 2017;53(10):554-60.

19. Daley CL, Iaccarino JM, Lange C, Cambau E, Wallace RJ Jr, Andrejak C, et al. Treatment of nontuberculous mycobacterial pulmonary disease: An official ATS/ERS/ESCMID/IDSA clinical practice guideline. Eur Respir J. 2020;56(1):2000535.

Gastrointestinal Symptoms in Pregnancy: The Influence of Thyroid-Stimulating Hormone and Modifiable Risk Factors

Gebelikte Gastrointestinal Semptomlar: Tiroid Uyarıcı Hormonun Etkisi ve Değiştirilebilir Risk Faktörleri

Büşra KÖRPE[1]
0000-0002-4315-5518
Caner KÖSE[1]
0000-0002-3044-4804
Sümeyye MERMİ[1]
0000-0002-3646-6465
Büşra DEMİR ÇENDEK[1]
0000-0002-6338-1408
Samet Kutluay ERGÖRÜN[1,2]
0000-0001-8498-7612
Kadriye ERDOĞAN[1]
0000-0002-8789-1875
Hüseyin Levent KESKİN[1]
0000-0002-2268-3821

[1]Department of Gynecology and Obstetrics, Ankara Etlik City Hospital, Ankara, Türkiye

[2]Department of Gynecology and Obstetrics, Düzce Atatürk State Hospital, Düzce, Türkiye

ABSTRACT

Aim: This study aimed to evaluate the prevalence of gastrointestinal (GI) symptoms during pregnancy and identify hormonal, nutritional, and lifestyle factors contributing to their severity.
Material and Methods: The study was conducted involving 612 pregnant women aged 20 to 40 years, with gestational ages between 5 and 36 weeks. Participants were categorized into three groups based on their trimester. GI symptoms were assessed using the gastrointestinal symptom rating scale (GSRS). A structured questionnaire was used to collect data on demographic characteristics, obstetric history, prior GI conditions, and lifestyle factors.
Results: The study found that indigestion (77.6%, n=475), reflux (68.5%, n=419), and abdominal pain (69.9%, n=428) were the most common GI symptoms reported. While indigestion (78.4%, n=171) followed by nausea (76.1%, n=166) was the most common symptoms in the first trimester, abdominal pain (78.1%, n=171) and reflux (76.3%, n=167) were most frequent in the second trimester, In the third trimester, indigestion (81.1%, n=142) was again the most common symptom, followed by reflux (76.6%, n=134). High GSRS scores were found to be significantly associated with excessive tea consumption (OR: 4.22, 95% CI: 1.44-12.35, p<0.001), employment status (OR: 2.32, 95% CI: 1.63-3.32, p<0.001), and TSH levels (OR: 1.26, 95% CI: 1.13-1.41, p<0.001).
Conclusion: GI symptoms are highly prevalent during pregnancy and are influenced by modifiable factors such as tea consumption, weight gain, and work-related stress. Monitoring thyroid function, managing weight, reducing tea intake, and addressing stress may help alleviate these symptoms, thereby improving the quality of life for pregnant women.
Keywords: Gastrointestinal diseases; pregnancy; risk factors.

ÖZ

Amaç: Bu çalışmanın amacı gebelik sırasında gastrointestinal (GI) semptomların yaygınlığını değerlendirmek ve bu semptomların şiddetine katkıda bulunan hormonal, beslenme ve yaşam tarzı faktörlerini belirlemektir.
Gereç ve Yöntemler: Bu çalışma, 20 ila 40 yaşları arasında, gestasyonel yaşları 5 ila 36 hafta arasında olan 612 gebe kadın ile yapılmıştır. Katılımcılar, trimesterlerine göre üç gruba ayrılmıştır. GI semptomlar, gastrointestinal semptom derecelendirme ölçeği (gastrointestinal symptom rating scale, GSRS) kullanılarak değerlendirilmiştir. Demografik özellikler, obstetrik geçmiş, önceki GI durumlar ve yaşam tarzı faktörleri hakkında veri toplamak amacıyla yapılandırılmış bir anket uygulanmıştır.
Bulgular: Çalışmada en sık görülen GI semptomların sindirim bozukluğu (%77,6, n=475), reflü (%68,5, n=419) ve karın ağrısı (%69,9, n=428) olduğu bulundu. İlk trimesterde sindirim bozukluğu (%78,4, n=171) ve bunu izleyen bulantı (%76,1, n=166) en sık görülen semptomlar iken, ikinci trimesterde karın ağrısı (%78,1, n=171) ve reflü (%76,3, n=167) en sık idi. Üçüncü trimesterde ise sindirim bozukluğu (%81,1, n=142) yine en sık görülen semptomdu ve bunu reflü (%76,6, n=134) izlemekteydi. Yüksek GSRS skorlarının aşırı çay tüketimi (OR: 4.22, %95 CI: 1.44-12.35, p<0.001), çalışma durumu (OR: 2.32, %95 CI: 1.63-3.32, p<0.001) ve TSH düzeyleri (OR: 1.26, %95 CI: 1.13-1.41, p<0.001) ile anlamlı şekilde ilişkili olduğu bulundu.
Sonuç: GI semptomlar gebelik sırasında oldukça yaygındır ve çay tüketimi, kilo artışı ve iş kaynaklı stres gibi değiştirilebilir faktörlerden etkilenmektedir. Tiroid fonksiyonlarının izlenmesi, kilo yönetimi, çay tüketiminin azaltılması ve stresle başa çıkma yöntemleri, bu semptomları hafifletmeye yardımcı olabilir ve böylece gebe kadınların yaşam kalitesini iyileştirebilir.
Anahtar kelimeler: Gastrointestinal hastalıklar; gebelik; risk faktörleri.

Corresponding Author
Sorumlu Yazar
Büşra KÖRPE
busraejderoglu@yahoo.com

INTRODUCTION

Pregnancy is characterized by a complex physiological change that can lead to a wide range of symptoms, including common gastrointestinal (GI) complaints such as heartburn, nausea, vomiting, and constipation (1). These GI disturbances are frequently encountered during pregnancy, with varying degrees of severity, and are typically managed by obstetricians (2-4). While many of these symptoms are considered mild to moderate, they can significantly impact a pregnant woman's quality of life (5,6).

Understanding the mechanisms behind these complaints is critical for effective management and improving maternal well-being. Hormonal fluctuations, particularly elevated levels of progesterone and human chorionic gonadotropin (hCG), play a central role in the development of GI symptoms (1,7,8). Progesterone delays gastric emptying by relaxing smooth muscle, which, combined with increased gastric acidity due to higher gastrin production by the placenta, contributes to the onset of gastroesophageal reflux disease (GERD) and other conditions (9,10).

GERD affects 40-85% of pregnant women, starting in the first trimester and often persisting throughout the pregnancy (9,10). Similarly, constipation, another frequent complaint, is thought to result from the relaxing effect of progesterone on intestinal smooth muscle, reduced bowel motility, and increased colonic water absorption (10,11). Iron supplementation, commonly prescribed during pregnancy, can further exacerbate constipation (12). Nausea and vomiting, which affect 50-80% of pregnant women, are among the most common medical conditions during pregnancy, peaking between the 8th and 12th weeks and generally subsiding by the 20th week (13). Although the exact mechanism is not fully understood, these symptoms are believed to result from the combined effects of hormonal changes, delayed gastric emptying, and psychological factors such as anxiety or depression (1,3,14). For most women, these symptoms resolve without the need for pharmacological intervention and can be managed through dietary adjustments and lifestyle modifications.

Despite the prevalence of these GI complaints, the underlying risk factors that predispose pregnant women to these conditions remain incompletely understood (1-4,15). This study aimed to evaluate the prevalence of GI symptoms during pregnancy and identify the lifestyle (tea consumption, employment status, weight gain), as well as hormonal (thyroid-stimulating hormone, TSH) and nutritional (iron supplements) factors contributing to their severity. By gaining a deeper understanding of these risk factors, the study hoped to inform more effective prevention and management strategies, ultimately improving the quality of care for pregnant women.

MATERIAL AND METHODS

This prospective observational study included 612 pregnant women, aged 20 to 40 years, with gestational ages ranging from 5 to 36 weeks, who attended antepartum clinics for routine prenatal care at Ankara Etlik City Hospital. Ethical approval was obtained from the local ethics committee (numbered AEŞH-BADEK-2024-016, dated 10.01.2024). Participants were categorized into three groups based on their trimester, 218 women in the first,

219 in the second, and 175 in the third trimester. All participants provided written informed consent prior to enrollment, in compliance with ethical standards.

GI symptoms were assessed using the gastrointestinal symptom rating scale (GSRS). GSRS is a validated and reliable instrument designed to evaluate GI complaints (16) and validated for use in the Turkish population (17). The GSRS consists of 15 questions, divided into five symptom clusters: Reflux (burning and discomfort related to reflux), Indigestion (gurgling in stomach, bloating), Abdominal Pain (nausea, pain due to hunger, pain in the upper part of the abdomen), Diarrhea, and Constipation. Each item is rated on a seven-point Likert scale, with 1 representing no symptoms and 7 indicating very troublesome symptoms. This scoring method allows for a comprehensive assessment of how GI symptoms affect the quality of life during pregnancy. The instrument helps to capture both the frequency and severity of these symptoms, providing a targeted measure for antepartum care.

In addition to these scales, a structured questionnaire was administered to collect data on participants' demographic characteristics (age, body mass index (BMI), educational status), obstetric history (gravidity, parity, previous pregnancies), previous GI conditions (such as peptic ulcers, irritable bowel syndrome), history of diagnostic procedures (e.g., gastroscopy, colonoscopy), and daily habits such as tea, coffee, and tobacco consumption, exercise routines, and the use of supplements (e.g., iron, multivitamins, and vitamin D).

Women with pre-existing chronic GI diseases requiring ongoing treatment, systemic conditions (e.g., diabetes, autoimmune diseases), multiple pregnancies, and use of medications known to affect GI function were excluded. Blood samples were collected from all participants during their first prenatal visit for routine biochemical analysis, including liver function tests, complete blood count, thyroid function tests, and serum electrolytes. These data, along with the GSRS scores and lifestyle information, were used to analyze the association between GI symptoms and potential metabolic and lifestyle factors.

Statistical Analysis

Data were analyzed using IBM SPSS v.26. Continuous variables were reported as mean±standard deviation, while categorical variables were expressed as frequencies and percentages. The normality of the data was assessed using the Kolmogorov-Smirnov test and the histogram and skewness-kurtosis values. The equality of variances was tested using Levene's test. Comparisons between trimesters were made using one-way ANOVA with post hoc Tukey analysis. The relationship between GSRS scores and potential risk factors was assessed using Pearson correlation coefficients. To identify independent predictors of higher GSRS scores, binary logistic regression analysis was conducted. The model included the following variables: age, BMI, gestational week, excessive tea consumption, employment status, and TSH levels. These variables were selected based on prior research and their theoretical relevance to GI symptoms during pregnancy. Age, BMI, and gestational week were included to control for potential confounders, as they are known to influence both GI symptoms and other risk factors. Model fit was evaluated using the Hosmer-Lemeshow test, which tests

the goodness-of-fit for the logistic regression model. The p-value for this test indicated whether the model fit the data well. The Nagelkerke R^2 statistic was reported to assess the proportion of variance explained by the model. The odds ratio (OR) with a 95% confidence interval (CI) was calculated for each independent variable to assess the strength and direction of the relationship between the predictors and GSRS scores. A p-value of less than 0.05 was considered statistically significant for all analyses.

RESULTS

The general characteristics and blood results of the study group were summarized in Table 1. Of the 612 participants, 29.9% (n=183) reported that they do not consume tea,

43.1% (n=264) of participants reported that they do not consume coffee, 73.0% (n=447) used antianemic drugs, 70.3% (n=430) took vitamin D supplement, 65.0% (n=398) did not engage in regular exercise, 6.2% (n=38) were current smokers, and 66.0% (n=404) were not employed during pregnancy (Table 2).

The GSRS responses of the participants and the comparison by trimester were presented in Table 3. The most frequently reported GI symptoms among the entire study group were indigestion (77.6%, n=475), reflux (68.5%, n=419), and abdominal pain (69.9%, n=428), including nausea. Indigestion (78.4%, n=171) was the most common symptom among women in the first trimester, followed by nausea (76.1%, n=166). In the second trimester, abdominal

Table 1. General characteristics and blood results of the study population, and comparison of groups by trimester

	1st trimester (n=218)	2nd trimester (n=219)	3rd trimester (n=175)	p	Study Group (n=612)
Age (year)	30.22±6.08	30.13±5.97	29.89±5.81	0.856	30.09±5.96
Weight gain (kg)	10.54±3.34[a]	15.21±4.26[b]	15.48±3.82[b]	**<0.001**	13.62±4.46
Pre-pregnancy weight (kg)	64.72±12.09[a]	59.18±12.39[b]	59.52±12.06[b]	**<0.001**	61.25±12.44
BMI (kg/m^2)	28.08±4.78	27.77±4.75	27.88±4.85	0.798	27.91±4.78
Glucose (mg/dL)	92.19±12.11	91.63±12.99	94.53±12.89	0.630	92.66±12.69
BUN (mg/dL)	27.11±6.74	27.15±6.44	26.49±6.93	0.556	26.95±6.69
Creatinine (mg/dL)	0.70±0.14	0.69±0.13	0.69±0.14	0.674	0.69±0.14
ALT (IU/L)	15.77±9.45	16.76±9.60	15.66±8.91	0.416	16.09±9.35
AST (IU/L)	17.27±9.93	17.02±9.76	17.10±10.00	0.965	17.13±10.00
Hb (mg/dL)	9.70±3.21	9.80±3.08	9.71±3.13	0.940	9.74±3.14
TSH (mU/ml)	1.83±1.27[a]	3.11±1.52[b]	3.02±1.53[b]	**<0.001**	3.07±1.57
T4 (ng/dL)	1.21±0.27[a]	1.15±0.26[b]	1.23±0.26[a]	**0.012**	1.20±0.26

BMI: body mass index, BUN: blood urea nitrogen, ALT: alanine transaminase, AST: aspartate aminotransferase, Hb: hemoglobin, TSH: thyroid-stimulating hormone, [a,b]: groups with different letters are significantly different from each other

Table 2. Daily lifestyle and nutritional factors study group

	n=612
Tea consumption, n (%)	
None	183 (29.9)
1-2 cups	257 (42.0)
3-4 cups	157 (25.7)
≥5 cups	15 (2.4)
Coffee consumption, n (%)	
None	264 (43.1)
1-2 cups	201 (32.8)
3-4 cups	143 (23.4)
≥5 cups	4 (0.7)
Smoking, n (%)	
None	459 (75.0)
Before pregnancy	115 (18.8)
1-2 per day	20 (3.3)
≥3 per day	18 (2.9)
Antianemic intake, n (%)	447 (73.0)
Vitamin D intake, n (%)	430 (70.3)
Exercise, n (%)	214 (35.0)
Working status, n (%)	208 (34.0)
Education, n (%)	
No	49 (8.0)
Primary school	153 (25.0)
High school	191 (31.2)
University	169 (27.6)
MSc/PhD	50 (8.2)

MSc/PhD: master of science/doctor of philosophy

pain (78.1%, n=171) and reflux (76.3%, n=167) were the most frequently reported symptoms, followed by indigestion (74.0%, n=162). In the third trimester, indigestion (81.1%, n=142) was again the most common symptom, followed by reflux (76.6%, n=134). The mean total GSRS scores of women in each trimester based on tea consumption were shown in Figure 1.
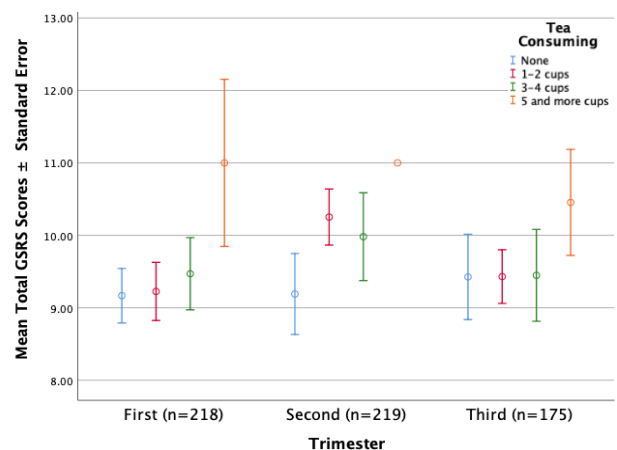
Figure 1. Gastrointestinal symptom rating scale scores in each trimester categorized by tea consumption habits

Table 3. Prevalence of gastrointestinal symptoms in the study group and by trimester, based on the GSRS score

	1st trimester (n=218)	2nd trimester (n=219)	3rd trimester (n=175)	p	Study Group (n=612)
Reflux, n (%)					
No discomfort at all	100 (45.9)[a]	52 (23.7)[b]	41 (23.4)[b]		193 (31.5)
Minor discomfort	53 (24.3)	66 (30.1)	49 (28.0)	<0.001	168 (27.5)
Mild discomfort	56 (25.7)	71 (32.4)	59 (33.7)		186 (30.4)
Moderate discomfort	9 (4.1)[a]	30 (13.7)[b]	26 (14.9)[b]		65 (10.6)
Indigestion, n (%)					
No discomfort at all	47 (21.6)	57 (26.0)	33 (18.9)		137 (22.4)
Minor discomfort	67 (30.7)	58 (26.5)	60 (34.3)		185 (30.2)
Mild discomfort	70 (32.1)	56 (25.6)	47 (26.9)	0.985	173 (28.3)
Moderate discomfort	32 (14.7)	43 (19.6)	31 (17.7)		106 (17.3)
Moderately severe discomfort	2 (0.9)	5 (2.3)	4 (2.3)		11 (1.8)
Abdominal Pain, n (%)					
No discomfort at all	52 (23.9)[a]	48 (21.9)[a]	84 (48.0)[b]		184 (30.1)
Minor discomfort	69 (31.7)	68 (31.1)	49 (28.0)	<0.001	186 (30.4)
Mild discomfort	55 (25.2)[ab]	61 (27.9)[b]	30 (17.1)[a]		146 (23.9)
Moderate discomfort	42 (19.3)[b]	42 (19.2)[b]	12 (6.9)[a]		96 (15.7)
Diarrhea, n (%)					
No discomfort at all	161 (73.9)	168 (76.7)	116 (66.3)	0.065	445 (72.7)
Minor discomfort	57 (26.1)	51 (23.3)	59 (33.7)		167 (27.3)
Constipation, n (%)					
No discomfort at all	152 (69.7)	143 (65.3)	117 (66.9)		412 (67.3)
Minor discomfort	59 (27.1)	61 (27.9)	41 (23.4)	0.607	161 (26.3)
Mild discomfort	7 (3.2)	15 (6.8)	17 (9.7)		39 (6.4)

GSRS: gastrointestinal symptom rating scale

There was a positive and weak correlation between the total GSRS score and TSH level (r=0.129, p=0.001). Weight gain (r=0.187, p<0.001), gestational week (r=0.167, p<0.001), and TSH level (r=0.082, p=0.043) were also found to be positively and weakly correlated with the reflux score. On the other hand, weight gain (r=-0.132, p<0.001) and gestational week (r=-0.206, p<0.001) were found negatively and weakly correlated with nausea score (Table 4).

Binary logistic regression analyses revealed several factors significantly associated with high GSRS score (Table 5). Consuming ≥5 cups of tea per day was associated with a high GSRS score (OR: 4.22, 95% CI: 1.44-12.35, p<0.001). Employment status was also significantly related to high GSRS score (OR: 2.32, 95% CI: 1.63-3.32, p<0.001), as were TSH level (OR: 1.26, 95% CI: 1.13-1.41, p<0.001). Furthermore, in terms of symptom clusters of the GSRS, weight gain (OR: 1.06, 95% CI: 1.02-1.10, p=0.001), gestational week (OR: 1.02, 95% CI: 1.01-1.04, p=0.002), and tea consumption exceeding 5 cups per day (OR: 7.26, 95% CI: 1.97-26.66, p=0.003) were the most strongly associated factors with higher reflux scores. Gestational age (OR: 0.965, 95% CI: 0.948-0.983, p<0.001) was found to be negatively associated with nausea scores.

DISCUSSION

The findings of this study indicate that GI symptoms, particularly indigestion, reflux, and abdominal pain including nausea, are highly prevalent during pregnancy, with notable variations across different trimesters. Additionally, we identified several key factors associated with increased severity of GI symptoms, including TSH levels, tea consumption, employment status, and weight gain.

Compared to Zielinski et al. (18), which focuses on common GI conditions in pregnancy like GERD, diarrhea, and constipation, the present study specifically highlights hormonal and lifestyle factors, such as tea consumption and

Table 4. Correlation analysis between variables and gastrointestinal symptom scores

		Weight Gain	Gestational week	TSH
Total GSRS score	r	0.056	0.031	0.129
	p	0.165	0.448	**0.001**
Reflux score	r	0.187	0.167	0.082
	p	**<0.001**	**<0.001**	**0.043**
Indigestion score	r	0.031	0.039	0.085
	p	0.447	0.336	**0.035**
Nausea score	r	-0.132	-0.206	0.020
	p	**0.001**	**<0.001**	0.628

GSRS: gastrointestinal symptom rating scale, TSH: thyroid-stimulating hormone

stress, influencing these symptoms. While both emphasize the variability of symptoms, this study offers more targeted management strategies. Naumann et al. (19) similarly address heartburn and nausea as common pregnancy symptoms but do not identify specific contributing factors. The present study adds depth by linking these symptoms to factors like weight gain, TSH levels, and tea intake, offering practical insights for symptom relief. In line with Zhang et al. (20), both studies recognize lifestyle factors in GI symptoms, though Zhang et al. (20) emphasize sedentary behavior and cold beverage consumption.

The weak but significant correlation between total GSRS scores and TSH levels suggests that thyroid function may play a role in the development of GI symptoms during pregnancy. This finding is consistent with previous studies that have demonstrated an association between altered thyroid hormone levels and GI disturbances such as constipation and reflux (21). Thyroid hormones can influence gut motility and the relaxation of the lower

Table 5. Univariate and multivariate logistic regression analysis results of the variables associated with high gastrointestinal symptom rating scale scores

Factor	Univariate Logistic Regression		Multivariate Logistic Regression	
	OR (95% CI)	p	OR (95% CI)	p
Age (year)	1.02 (0.99-1.05)	0.108	-	-
Weight gain (kg)	0.99 (0.95-1.03)	0.650	-	-
BMI (kg/m^2)	0.99 (0.96-1.03)	0.966	-	-
TSH (mU/ml)	1.26 (1.13-1.41)	**<0.001**	1.20 (1.07-1.35)	**<0.001**
Smoking (Yes)	1.22 (0.79-1.89)	0.352	-	-
Tea consumption (≥5 cups)	4.22 (1.44-12.35)	**<0.001**	2.84 (0.94-8.63)	**0.017**
Coffee consumption (Yes)	1.00 (0.74-1.35)	0.987	-	-
Exercise (Yes)	0.89 (0.61-1.28)	0.533	-	-
Employment status (Yes)	2.32 (1.63-3.32)	**<0.001**	2.15 (1.49-3.10)	**<0.001**

BMI: body mass index, TSH: thyroid-stimulating hormone, OR: odds ratio, CI: confidence interval

esophageal sphincter, contributing to the onset of symptoms such as heartburn and nausea (22). While the correlation was weak, it highlights the importance of monitoring thyroid function as part of prenatal care, especially in women presenting with GI complaints.

This study also found that weight gain and gestational week were positively correlated with reflux scores. As pregnancy progresses, the enlarging uterus exerts increased pressure on the stomach, contributing to gastroesophageal reflux (23). This mechanical factor, coupled with hormonal changes -particularly elevated progesterone levels- explains the high prevalence of reflux symptoms, especially in the third trimester. Weight gain further exacerbates this condition by increasing intra-abdominal pressure, a finding supported by prior research showing a similar association between BMI and reflux in non-pregnant populations (24,25).

The relationship between tea consumption and GI symptoms is a novel finding in this population. Women who consumed more than five cups of tea daily had significantly higher GSRS and reflux scores. Tea, particularly black tea, contains compounds like caffeine and theobromine, which can relax the lower esophageal sphincter and increase gastric acidity, contributing to reflux symptoms (26). While caffeine has been widely studied in relation to pregnancy outcomes, its impact on GI symptoms, specifically reflux, has received less attention (27). The results of the present study suggest that reducing tea consumption could be a simple and effective intervention for managing reflux symptoms during pregnancy.

Interestingly, employment status was another significant factor associated with higher GSRS scores. Women who were employed during pregnancy reported more severe GI symptoms, potentially reflecting the role of stress and time constraints in exacerbating these conditions. Work-related stress has been linked to the exacerbation of functional GI disorders, such as irritable bowel syndrome (IBS), and may similarly contribute to increased symptom severity in pregnant women (28,29). This finding suggests that managing stress, perhaps through relaxation techniques or modifications in workload, could help alleviate GI complaints during pregnancy.

One of the strengths of this study is its prospective design, which allowed for the assessment of GI symptoms throughout the different trimesters of pregnancy.

Additionally, the use of the validated GSRS ensured a comprehensive evaluation of symptom frequency and severity. However, there are some limitations. The study population was limited to women attending a tertiary hospital, which may not be representative of the broader pregnant population. Furthermore, while we identified several associations between lifestyle factors and GI symptoms, the study was observational, making it difficult to establish causal relationships.

CONCLUSION

This study highlights the high prevalence of GI symptoms during pregnancy and identifies several modifiable and non-modifiable risk factors. Monitoring thyroid function, managing weight gain, reducing tea consumption, and addressing work-related stress may help mitigate these symptoms. Future research should explore the underlying mechanisms linking these factors to GI symptoms and investigate the effectiveness of targeted interventions to improve maternal well-being during pregnancy.

Author Contributions: Idea/Concept: BK, CK, SM; Design: BK, SKE, KE; Data Collection/Processing: BK, CK, SM, SKE, BDÇ; Analysis/Interpretation: BK, CK, BDÇ, HLK; Literature Review: CK, SM, KE; Drafting/Writing: BK, CK, SKE, KE; Critical Review: KE, HLK.

The fifth author, Samet Kutluay ERGÖRÜN, was working at Ankara Etlik City Hospital during the study period, and relocated to a different city and currently is working at Düzce Atatürk State Hospital, which reflects his current place of employment.

REFERENCES

1. Gomes CF, Sousa M, Lourenço I, Martins D, Torres J. Gastrointestinal diseases during pregnancy: what does the gastroenterologist need to know?. Ann Gastroenterol. 2018;31(4):385-94.
2. Longo SA, Moore RC, Canzoneri BJ, Robichaux A. Gastrointestinal conditions during pregnancy. Clin Colon Rectal Surg. 2010;23(2):80-9.
3. Patrick SK, Schneider KM. Gastrointestinal disorders in pregnancy. In: Olsen M, editor. Obstetric care. Cambridge University Press; 2017. p.375-86.
4. Zielinski R, Searing K, Deibel M. Gastrointestinal distress in pregnancy: prevalence, assessment, and treatment of 5 common minor discomforts. J Perinat Neonatal Nurs. 2015;29(1):23-31.
5. Parangi S, Levine D, Henry A, Isakovich N, Pories S. Surgical gastrointestinal disorders during pregnancy. Am J Surg. 2007;193(2):223-32.
6. Boregowda G, Shehata HA. Gastrointestinal and liver disease in pregnancy. Best Pract Res Clin Obstet Gynaecol. 2013;27(6):835-53.
7. Liu C, Zhao G, Qiao D, Wang L, He Y, Zhao M, et al. Emerging progress in nausea and vomiting of pregnancy and hyperemesis gravidarum: challenges and opportunities. Front Med (Lausanne). 2022;8:809270.
8. Demirel F, Turkay Ü. The effect of inflammatory markers in the hemogram parameters of pregnant women with thyroid disease on obstetric and neonatal outcomes. Duzce Med J. 2023;25(3):231-5.
9. Alqudah M, Al-Shboul O, Al Dwairi A, Al-U´Datt DG, Alqudah A. Progesterone inhibitory role on gastrointestinal motility. Physiol Res. 2022;71(2):193-8.
10. Coquoz A, Regli D, Stute P. Impact of progesterone on the gastrointestinal tract: a comprehensive literature review. Climacteric. 2022;25(4):337-61.
11. Xiao ZL, Pricolo V, Biancani P, Behar J. Role of progesterone signaling in the regulation of G-protein levels in female chronic constipation. Gastroenterology. 2005;128(3):667-75.
12. Peña-Rosas JP, De-Regil LM, Garcia-Casal MN, Dowswell T. Daily oral iron supplementation during pregnancy. Cochrane Database Syst Rev. 2015;2015(7):CD004736.
13. Lee NM, Saha S. Nausea and vomiting of pregnancy. Gastroenterol Clin North Am. 2011;40(2):309-34, vii.
14. Biaggi A, Conroy S, Pawlby S, Pariante CM. Identifying the women at risk of antenatal anxiety and depression: A systematic review. J Affect Disord. 2016;191:62-77.
15. Nik Mazlan NAA, Mohamed Sidek AS, Zakaria AD, Zakaria Z, Yahya MM, Wan Zain WZ, et al. Proportion of colonic diverticulosis and its associated factors among patients underwent colonoscopy. Duzce Med J. 2024;26(1):9-14.
16. Kulich KR, Madisch A, Pacini F, Piqué JM, Regula J, Van Rensburg CJ, et al. Reliability and validity of the Gastrointestinal Symptom Rating Scale (GSRS) and Quality of Life in Reflux and Dyspepsia (QOLRAD) questionnaire in dyspepsia: a six-country study. Health Qual Life Outcomes. 2008;6:12.
17. Turan N, Aşt TA, Kaya N. Reliability and validity of the Turkish version of the gastrointestinal symptom rating scale. Gastroenterol Nurs. 2017;40(1):47-55.
18. Zielinski R, Searing K, Deibel M. Gastrointestinal distress in pregnancy: prevalence, assessment, and treatment of 5 common minor discomforts. J Perinat Neonatal Nurs. 2015;29(1):23-31.
19. Naumann CR, Zelig C, Napolitano PG, Ko CW. Nausea, vomiting, and heartburn in pregnancy: a prospective look at risk, treatment, and outcome. J Matern Fetal Neonatal Med. 2012;25(8):1488-93.
20. Zhang H, Wu S, Feng J, Liu Z. Risk factors of prolonged nausea and vomiting during pregnancy. Risk Manag Healthc Policy. 2020;13:2645-54.
21. Daher R, Yazbeck T, Jaoude JB, Abboud B. Consequences of dysthyroidism on the digestive tract and viscera. World J Gastroenterol. 2009;15(23):2834-8.
22. Xu GM, Hu MX, Li SY, Ran X, Zhang H, Ding XF. Thyroid disorders and gastrointestinal dysmotility: an old association. Front Physiol. 2024;15:1389113.
23. Altuwaijri M. Evidence-based treatment recommendations for gastroesophageal reflux disease during pregnancy: A review. Medicine (Baltimore). 2022;101(35):e30487.
24. Sucu ST, Karaman E, Kose C, Sucu S, Keskin HL. Is postpartum depression related to total weight gain during pregnancy and maternal anemia?. Rev Assoc Med Bras (1992). 2024;70(2):e20230908.
25. Jacobson BC, Somers SC, Fuchs CS, Kelly CP, Camargo CA Jr. Body-mass index and symptoms of gastroesophageal reflux in women. N Engl J Med. 2006;354(22):2340-8.
26. Cao H, Huang X, Zhi X, Han C, Li L, Li Y. Association between tea consumption and gastroesophageal reflux disease: A meta-analysis. Medicine (Baltimore). 2019;98(4):e14173.
27. Qian J, Chen Q, Ward SM, Duan E, Zhang Y. Impacts of caffeine during pregnancy. Trends Endocrinol Metab. 2020;31(3):218-27.
28. Huerta-Franco MR, Vargas-Luna M, Tienda P, Delgadillo-Holtfort I, Balleza-Ordaz M, Flores-Hernandez C. Effects of occupational stress on the gastrointestinal tract. World J Gastrointest Pathophysiol. 2013;4(4):108-18.
29. Sugaya N. Work-related problems and the psychosocial characteristics of individuals with irritable bowel syndrome: an updated literature review. Biopsychosoc Med. 2024;18(1):12.

Quantitative Assessment of the Distal Clavicle with Its Clinical Implications in Anatomical Reconstruction of the Coracoclavicular Ligament

Ligamentum Coracoclaviculare'nin Anatomik Rekonstruksiyonunda Klinik Etkisi Olan Distal Clavicula'nın Kantitatif Değerlendirilmesi

Hilal AKDEMİR AKTAŞ
ⓘ *0000-0002-7353-8069*
Helin YÜCEDAĞ GÜNDOĞDU
ⓘ *0000-0001-7724-6031*

Department of Anatomy, Hacettepe University Faculty of Medicine, Ankara, Türkiye

ABSTRACT

Aim: Anatomical reconstruction of the coracoclavicular ligament has recently become popular in the treatment of acromioclavicular joint injuries. To perform this procedure correctly, the anatomy of the conoid tubercle and trapezoid line, which are the attachment sites of the coracoclavicular ligament, should be known accurately. Therefore, this study aimed to evaluate the distal clavicle along with morphometry of the conoid tubercle and trapezoid line.

Material and Methods: In the present study, 77 human dry clavicles (39 right, 38 left) were examined using a digital caliper and digital thickness gauge. The clavicle length, thickness and width of the distal clavicle, morphometric features of the conoid tubercle, and trapezoid line were examined. Measurements were performed by two researchers independently.

Results: The clavicle length was 138.37±10.69 mm. Supero-inferior thickness of the distal clavicle was 9.08±1.69 mm, and the antero-posterior width was 17.70±2.37 mm. Medio-lateral and supero-inferior dimensions of the conoid tubercle were 17.17±3.58 mm and 7.59±1.38 mm, respectively. The distance between the clavicle acromial end and the center of the conoid tubercle was 34.43±5.41 mm. Medio-lateral dimension of trapezoid line was 16.69±2.73 mm, and antero-posterior dimension was 9.61±1.80 mm. The distance between the clavicle acromial end and the center of the trapezoid line was measured as 18.15±2.80 mm.

Conclusion: Accordingly, the tunnels for trapezoid and conoid ligaments should be created 18 mm and 34 mm medial from the clavicle acromial end, respectively. The measurements obtained in this study can be used as a guide for coracoclavicular ligament reconstruction.

Keywords: Anatomical reconstruction; conoid tubercle; coracoclavicular ligament; distal clavicle; morphometry; trapezoid line.

ÖZ

Amaç: Articulatio acromioclaviculare yaralanmalarının tedavisinde, ligamentum coracoclaviculare'nin anatomik rekonstrüksiyonu son zamanlarda popüler hale gelmiştir. Bu işlemin doğru şekilde yapılabilmesi için ligamentum coracoclaviculare'nin yapışma yerleri olan tuberculum conoideum ve linea trapezoidea'nın anatomisinin doğru şekilde bilinmesi gerekir. Bu nedenle, bu çalışmada tuberculum conoideum ve linea trapezoidea'nın morfometrisi ile birlikte distal clavicula'nın değerlendirilmesi amaçlandı.

Gereç ve Yöntemler: Bu çalışmada, 77 insan kuru clavicula kemiği (39 sağ, 38 sol) dijital kumpas ve dijital kalınlık ölçer kullanılarak incelendi. Clavicula uzunluğu, distal clavicula kalınlığı ve genişliği, tuberculum conoideum ve linea trapezoidea'nın morfometrik özellikleri incelendi. Ölçümler iki araştırmacı tarafından bağımsız olarak gerçekleştirildi.

Bulgular: Clavicula uzunluğu 138,37±10,69 mm idi. Distal clavicula'nın supero-inferior kalınlığı 9,08±1,69 mm ve antero-posterior genişliği ise 17,70±2,37 mm bulundu. Tuberculum conoideum'un medio-lateral ve supero-inferior boyutları sırasıyla 17,17±3,58 mm ve 7,59±1,38 mm idi. Clavicula extremitas acromialis'i ile tuberculum conoideum'un merkezi arasındaki mesafe 34,43±5,41 mm olarak ölçüldü. Linea trapezoidea'nın medio-lateral uzunluğu 16,69±2,73 mm ve antero-posterior uzunluğu ise 9,61±1,80 mm idi. Clavicula extremitas acromialis'i ile linea trapezoidea'nın merkezi arasındaki mesafe 18,15±2,80 mm olarak ölçüldü.

Sonuç: Bu çalışmadaki ölçümlere göre, ligamentum trapezoideum ve ligamentum conoideum için açılacak tüneller clavicula'nın extremitas acromialis'inden sırasıyla 18 mm ve 34 mm medialde oluşturulmalıdır. Bu çalışmadan elde edilen ölçümler, ligamentum coracoclaviculare'nin anatomik rekonstrüksiyonunda bir kılavuz olarak kullanılabilir.

Anahtar kelimeler: Anatomik rekonstrüksiyon; tuberculum conoideum; ligamentum coracoclaviculare; distal clavicula; morfometri; linea trapezoidea.

Corresponding Author
Sorumlu Yazar
Hilal AKDEMİR AKTAŞ
hakdemir06@hotmail.com

INTRODUCTION

The acromioclavicular joint is stabilized by the effects of the coracoclavicular ligaments and the capsule of the acromioclavicular joint. The coracoclavicular ligament restricts the distal clavicle's superior translation relative to the scapula (1,2). The coracoclavicular ligament is used effectively in various sports, particularly those involving significant shoulder activity and contacts, such as lacrosse, weightlifting, hockey, rugby, football, baseball, tennis, volleyball, and swimming (3,4). The coracoclavicular ligament is composed of the conoid and trapezoid ligaments and transmits the weight of the upper limb to the clavicle (5,6). The conoid ligament courses nearly vertically and attaches to the conoid tubercle, which is posteromedial to the trapezoid line. The trapezoid ligament attaches to the trapezoid line and angles anterolaterally away from the conoid ligament (7).

Acromioclavicular joint injuries are common among young athletes who engage in contact and overhead sports (8,9). Several surgical techniques have been described in the literature to treat the acromioclavicular joint (8,10). Recently, there has been a trend toward the anatomical reconstruction of the coracoclavicular ligament using free graft (1,10). Anatomical reconstruction has become popular due to successful clinical outcomes (11). This technique necessitates drilling clavicular bone tunnels and passing the graft through the clavicle and coracoid process of the scapula. The most precise method to restore the normal anatomy of the coracoclavicular ligaments involves creating bone tunnels at the residual stumps of the ruptured ligaments (1,10-12). Creating bone tunnels necessitates accurate morphometry of the conoid tubercle and trapezoid line. Therefore, the present study aimed to evaluate the morphometry of the conoid tubercle and the trapezoid line in order to create bone tunnels accurately for anatomical coracoclavicular ligament reconstructions.

MATERIAL AND METHODS

The present study was performed on 88 human dry clavicles which were obtained from the Department of Anatomy, Faculty of Medicine, Hacettepe University. Eleven clavicles with gross deformities were excluded from the study. Eventually, 77 human dry clavicles (39 right sides, 38 left sides) were examined. However, the sex and age of the bones used in the study were not known.

Measurements were performed using a digital caliper (150 mm, Insize 1195 IP 67 Waterproof Digital Calipers) and an outside diameter digital thickness gauge. Before measuring, the caliper and thickness gauge were calibrated. The boundaries of the conoid tubercle and trapezoid line were determined by following the rough footprints of the conoid and trapezoid ligaments. The measurements were carried out independently by two different researchers and an inter-rater reliability coefficient was >0.90 for all the parameters.

This study was performed in line with the principles of the Declaration of Helsinki. Consent to participate is not applicable for this study. Ethical approval for this study was obtained from the Health Sciences Research Ethics Committee of Hacettepe University (21 May 2024, SBA 24/549, 2024/09-18).

The measurements examined in the study were: *i)* the clavicle length: straight distance between the acromial and sternal ends of the clavicle (Figure 1). *ii)* supero-inferior thickness of the distal clavicle, measured from the midpoint between the conoid tubercle and trapezoid line (Figure 2A). *iii)* antero-posterior width of the distal clavicle, measured from the midpoint between the conoid tubercle and trapezoid line (Figure 2B). *iv)* the medio-lateral (Figure 3, EF), and *v)* the supero-inferior (Figure 3, GH) dimensions of the conoid tubercle. *vi)* distance between the clavicle acromial end and the center of the conoid tubercle (Figure 4, Z line). *vii)* a ratio calculated by dividing the distance from the clavicle acromial end to the conoid tubercle by the clavicle length. *viii)* the medio-lateral (Figure 3, AB) and *ix)* the antero-posterior (Figure 3, CD) dimensions of the trapezoid line, *x)* distance between the clavicle acromial end and the center of the trapezoid line (Figure 4, X line). *xi)* a ratio calculated by dividing the distance from the clavicle acromial end to the trapezoid line by the clavicle length. *xii)* distance between the center of the conoid tubercle and the center of the trapezoid line (Figure 4, Y line).

Statistical Analysis

Statistical analysis was performed using IBM SPSS version 21. The variables were assessed by histogram and Kolmogorov-Smirnov/Shapiro-Wilk methods for testing normal distribution. As they were normally distributed, the

Figure 1. Inferior view of the left clavicle. Clavicle length is a straight distance between the sternal and acromial ends of the clavicle. The inferior view of the acromial end includes the conoid tubercle for the conoid ligament and the trapezoid line for the trapezoid ligament
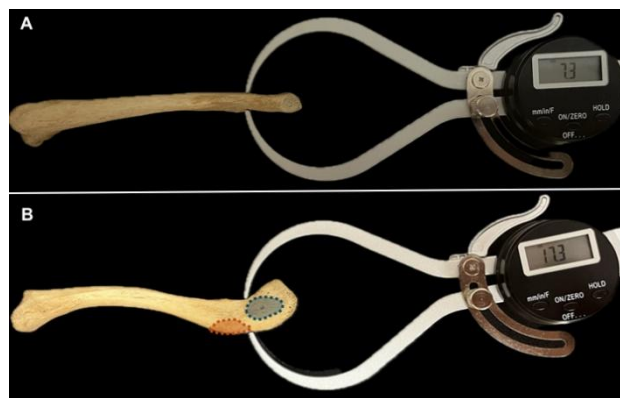
Figure 2. A) Supero-inferior thickness of the distal clavicle, measured from the midpoint between the conoid tubercle and trapezoid line, and **B)** antero-posterior width of the distal clavicle, measured from the midpoint between the conoid tubercle and trapezoid line utilizing an outside diameter digital thickness gauge

Figure 3. An inferior view of the left clavicle demonstrates the measurements of the trapezoid line and conoid tubercle, **AB)** medio-lateral and **CD)** antero-posterior dimensions of the trapezoid line, **EF)** medio-lateral and **GH)** supero-inferior dimensions of the conoid tubercle

Figure 4. The inferior view of the left clavicle shows the distances between **X)** the clavicle acromial end and the center of the trapezoid line, **Y)** the center of the conoid tubercle and the center of the trapezoid line, and **Z)** the clavicle acromial end and the center of the conoid tubercle

descriptive statistics were reported as mean±standard deviation. The groups were compared using the Student's t-test, and correlation analysis was conducted using Pearson's correlation. A p-value of less than 0.05 was considered statistically significant, and analyses were conducted using a 95% confidence interval.

RESULTS

In the present study, 77 human dry clavicles (39 right sides, 38 left sides) were examined. The mean clavicle length was found to be 138.37±10.69 mm. The mean supero-inferior thickness of the distal clavicle was measured as 9.46±1.36 mm on the right side, 8.69±1.92 mm on the left side, and 9.08±1.69 mm in general. There was a statistically significant difference in supero-inferior thickness of the distal clavicle between sides and right supero-inferior thickness was 0.77 mm thicker than the left side (p=0.044). The mean antero-posterior width of the distal clavicle was found to be 17.70±2.37 mm. Detailed measurements of these parameters were summarized in Table 1.

The mean value of the medio-lateral dimension of the conoid tubercle was 17.17±3.58 mm and the supero-inferior dimension was 7.59±1.38 mm. The mean distance between the clavicle acromial end and the center of the conoid

tubercle was found to be 36.70±5.00 mm on the right side, 32.10±4.83 mm on the left side, and 34.43±5.41 mm in general. There was a statistically significant difference between sides and the right side was 4.60 mm longer than the left side (p<0.001). A ratio representing the distance from the clavicle acromial end to the conoid tubercle divided by the clavicle length was calculated as 0.26±0.03 on the right side, 0.23±0.03 on the left side, and 0.25±0.03 in general. There was a statistically significant difference in ratios between sides (p<0.001). Detailed measurements of these parameters were summarized in Table 2.

The mean value of the medio-lateral dimension of the trapezoid line was 16.69±2.73 mm and, the antero-posterior dimension was 9.61±1.80 mm. The mean distance between the clavicle acromial end and the center of the trapezoid line was found to be 18.15±2.80 mm. A ratio representing the distance from the clavicle acromial end to the trapezoid line divided by the clavicle length was calculated as 0.13±0.02. There was no statistical difference between the sides in the measurements of the trapezoid line. The mean distance between the center of the conoid tubercle and the center of the trapezoid line was measured as 18.70±3.11 mm. Detailed measurements of these parameters were summarized in Table 3.

Table 1. Morphometric measurements of the distal clavicle

Measurements	Right (n=39)	Left (n=38)	p	General (n=77)
Clavicle length (mm)	139.44±10.11 (116.77-156.09)	137.27±11.27 (111.40-160.12)	0.375	138.37±10.69 (111.40-160.12)
Supero-inferior thickness of the distal clavicle (mm)	9.46±1.36 (6.58-12.52)	8.69±1.92 (6.40-17.60)	**0.044**	9.08±1.69 (6.40-17.60)
Antero-posterior width of the distal clavicle (mm)	18.19±2.25 (13.50-23.37)	17.20±2.40 (12.63-22.63)	0.065	17.70±2.37 (12.63-23.37)

Table 2. Morphometric measurements of the conoid tubercle

Measurements	Right (n=39)	Left (n=38)	p	General (n=77)
Medio-lateral dimension of the conoid tubercle (mm)	17.80±3.92 (12.20-30.63)	16.52±3.11 (11.10-23.42)	0.115	17.17±3.58 (11.10-30.63)
Supero-inferior dimension of the conoid tubercle (mm)	7.71±1.31 (4.36-10.20)	7.47±1.45 (4.74-10.27)	0.443	7.59±1.38 (4.36-10.27)
Distance between the clavicle acromial end and the center of the conoid tubercle (mm)	36.70±5.00 (24.55-48.11)	32.10±4.83 (23.26-41.24)	**<0.001**	34.43±5.41 (23.26-48.11)
Distance from acromial end to conoid/clavicle length	0.26±0.03 (0.19-0.32)	0.23±0.03 (0.18-0.29)	**<0.001**	0.25±0.03 (0.18-0.32)

Table 3. Morphometric measurements of the trapezoid line

Measurements	Right (n=39)	Left (n=38)	p	General (n=77)
Medio-lateral dimension of the trapezoid line (mm)	17.29±2.80 (12.01-23.41)	16.08±2.54 (10.48-20.45)	0.051	16.69±2.73 (10.48-23.41)
Antero-posterior dimension of trapezoid line (mm)	9.82±1.87 (4.86-13.68)	9.39±1.73 (5.98-13.24)	0.292	9.61±1.80 (4.86-13.68)
Distance between the clavicle acromial end and the center of the trapezoid line (mm)	18.66±2.41 (14.13-25.30)	17.62±3.09 (11.93-25.28)	0.101	18.15±2.80 (11.93-25.30)
Distance from clavicle acromial end to trapezoid line/clavicle length	0.13±0.02 (0.11-0.17)	0.13±0.02 (0.09-0.16)	0.150	0.13±0.02 (0.09-0.17)
Distance between the center of the conoid tubercle and the center of the trapezoid line (mm)	18.58±3.05 (13.32-27.48)	18.82±3.20 (10.06-25.60)	0.738	18.70±3.11 (10.06-27.48)

There was a significant moderate and positive correlation between the medio-lateral dimension of the conoid tubercle and the medio-lateral dimension of the trapezoid line (r=0.447, p<0.001). While no significant correlation was found between the supero-inferior dimension of the conoid tubercle and the antero-posterior dimension of the trapezoid line (r=0.125, p=0.278).

DISCUSSION
Acromioclavicular joint injuries commonly affect young athletes and are often caused by direct trauma to the lateral aspect of the shoulder or acromion process with the arm in adduction (6). Acromioclavicular joint injuries can also be caused by falling on an outstretched hand or elbow (13). More than 60 surgical procedures have been identified for treating acromioclavicular joint injuries, and their application is supported by hundreds of biomechanical and anatomical investigations (14). Anatomical reconstruction of the coracoclavicular ligaments has become popular in recent years due to successful clinical outcomes. With this technique, the residual stumps of the ruptured ligaments are punctured, and synthetic materials or grafts are inserted through them to restore the coracoclavicular ligaments as distinct anatomical structures (15).

Traditionally, in the anatomical reconstruction technique, trapezoid and conoid tunnels are created 25 and 45 mm medial to the lateral edge of the clavicle, respectively (6,16). After some failures were reported with this technique, it was suggested that clavicular tunnels should be placed according to the "tunnel ratio". This ratio is calculated by dividing the distance from the lateral edge of the clavicle to the center of the conoid tubercle/trapezoid line by the total clavicular length (1). In this surgical technique, it has been reported that using a ratio of 0.20-0.25 for the conoid tunnel and a ratio of 0.13-0.16 for the trapezoid tunnel provides higher survival (17). Clavicular tunnels placed outside of these ratios have been related to the failure of this technique (17,18). Anatomical reconstruction by creating clavicular tunnels requires accurate knowledge of the distances and ratios of the conoid tubercle and trapezoid line, and therefore, in this study, the morphometry of the conoid tubercle and trapezoid line was evaluated in detail.

Clavicle Length: The clavicle length was measured as 150 mm by Boehm et al. (19), 141.3 mm by Chahla et al. (20), 139.9±9.4 mm by Xue et al. (21) on 172 cadaver shoulders, 149.4±10.3 mm by Bernat et al. (22), 149±9.1 mm by Rios et al. (1), 148.57±12.63 mm by Ominde et al. (23) on 180 human dry clavicles, 156.87±9.75 mm on males

and 145.79±7.95 mm on females by King et al. (24). In the present study, the clavicle length between the sternal and acromial ends was measured as 138.37±10.69 mm and no difference was found between sides. The clavicle length found in the present study was in accordance with the previous studies (Table 4).

Supero-Inferior Thickness of Distal Clavicle: The thickness of the distal clavicle is crucial to predict how much graft will be in the clavicle tunnels and to design a more appropriate interference screw for anatomical reconstruction technique. The supero-inferior thickness of the distal clavicle was found to be 11.4±1.6 mm by Rios et al. (1), 10.09±2.36 mm by Ominde et al. (23), and 10.31 mm by Daruwalla et al. (25). King et al. (24) examined 418 clavicles and measured the clavicle height at the middle of the acromial third as 10.56±1.96 mm on males and 9.74±1.65 mm on females. In the present study, the supero-inferior thickness at the midpoint between the conoid tubercle and trapezoid line was measured as 9.08±1.69 mm, which was consistent with the literature (Table 4). When determining the graft length and tension, it is needed for approximately 1 cm of the graft to be positioned within the distal clavicle tunnel.

Antero-Posterior Width of Distal Clavicle: The lateral aspect of the distal clavicle is relatively narrow and rectangular in shape. Renfree et al. (26) evaluated 41 clavicles and measured the antero-posterior width of the distal clavicle as 26.7±2.7 mm in males and 21.5±2.7 mm in females. Rios et al. (1) analyzed 120 human dry clavicles and measured the antero-posterior thickness as 19.2±2.8 mm. Daruwalla et al. (25) evaluated 27 human clavicles and measured the acromial width as 21.24 mm on the left and 21.91 mm on the right side. King et al. (24) examined 418 clavicles using CT imaging and found the clavicle width at the middle of the acromial third to be 18.26±3.04 mm in males and 15.14±2.53 mm in females. Antero-posterior width of the distal clavicle was measured as 17.70±2.37 in the present study, and thus this result was convenient with the studies performed by Rios et al. (1) and King et al. (24). Our result was narrower than the studies done by Daruwalla et al. (25) and Renfree et al. (26). Differences in distal clavicle width measurements across studies may be due to differences in geographical regions and measurements methods.

Conoid Tubercle: The conoid tubercle is the prominent eminence placed on the lateral part of the clavicle inferior aspect. It serves as an attachment point for the conoid ligament and is situated between the trapezoid line and the subclavius muscle groove (5). Morphometric features of the conoid

tubercle are important for the anatomical coracoclavicular reconstruction. Takase (27) dissected 40 shoulders of 20 cadavers and measured the sagittal (medio-lateral) dimension of the conoid ligament footprint as 17.4 mm and the coronal (antero-posterior) dimension of the conoid ligament footprint as 5.4 mm. Harris et al. (28) dissected 24 shoulder specimens and measured the width of the conoid ligament footprint as 20.6±3.6 mm. Xue et al. (21) performed a dissection on 172 shoulders and measured the medio-lateral dimension of the conoid ligament as 13.1±2.2 mm, and antero-posterior dimension 6.0±1.4 mm. Rios et al. (1) dissected 19 fresh-frozen cadaveric shoulders and measured the width of the conoid ligament footprint as 25.3±4.9 mm. In the present study, the medio-lateral dimension of the conoid tubercle was measured as 17.17±3.58, similar to the studies of Xue et al. (21), Takase (27), and Harris et al. (28). Our result was lower than Rios et al. (1)'s study. This difference may be due to the difference in geographical regions and measurement methods. Cadaveric studies, of course, give more precise results in the measurements of ligaments, while only the footprints of the ligaments can be measured in human dry bone studies. Therefore, we only measured the footprints of the ligaments in the present study and this is a limitation. In the present study, the supero-inferior dimension of the conoid tubercle was found to be 7.59±1.38 mm in accordance with previous studies (Table 5).

The origins of the coracoclavicular ligaments with respect to the distal end of the clavicle are crucial for successful anatomical reconstruction of the coracoclavicular ligaments. The distance from the clavicle acromial end to the center of the conoid tubercle has been examined by several authors. This distance was found to be 35.0±5.9 mm by Rios et al. (1), 35.7±3.4 mm by Xue et al. (21), 39.52±5.93 mm by Ominde et al. (23), and 36.6±0.9 mm by Zhu et al. (29). The ratio calculated by dividing the distance from the clavicle lateral edge to the conoid tubercle by the length of the clavicle was found 0.24 by Rios et al. (1), 0.25 by Xue et al. (21), and 0.27 by Ominde et al. (23). In the present study, this distance was measured as 34.43±5.41 mm and the ratio was found to be 0.25±0.03, similar to the previous studies (Table 5). According to the measurements of the present study, for making reconstruction of the conoid ligament in as an anatomical position as possible, the conoid tunnel on the clavicle should be created 34 mm medial from the acromial end of the clavicle and at a ratio of 0.25.

Trapezoid Line: The trapezoid line is the narrow ridge found on the lateral part of the inferior face of the clavicle. It serves as an attachment point for the trapezoid ligament and extends anterolaterally from the conoid tubercle (5). Morphometric properties of the trapezoid line are important in performing successful anatomical reconstruction. Medio-lateral dimension of the trapezoid ligament was found to be 11.8±1.0 mm by Rios et al. (1), 14.7±2.0 mm by Xue et al. (21), 18.5 mm by Takase (27), and 21.7±4.0 mm by Harris et al. (28). In the present study, medio-lateral dimension of the trapezoid line was measured as 16.69±2.73 mm, similar to the studies of Xue et al. (21) and Takase (27). Our result was wider than Rios et al. (1)'s study and narrower than the study of Harris et al. (28). This discrepancy might result from different measurement techniques and conducting studies in different geographic locations. Antero-posterior dimension of the trapezoid ligament was found to be 8.2±2.5 mm by Xue et al. (21), and 15.4 mm by Takase (27). In the present study, the antero-posterior dimension of the trapezoid line was found to be 9.61±1.80 mm (Table 6) in accordance with the study of Xue et al. (21).

Accurate knowledge of the trapezoid ligament attachment sites is required for successful anatomical coracoclavicular ligament reconstruction. The distance between the clavicle acromial end and the center of the trapezoid line was found to be 24.9±3.8 mm on dry clavicles and 25.9±3.9 mm on cadaveric shoulders by Rios et al. (1), 21.8±2.7 mm by Xue et al. (21), 17.96±3.42 mm by Ominde et al. (23), and 21.7±1.1 mm by Zhu et al. (29). In the present study, this distance was measured as 18.15±2.80 mm, similar to the previous studies (Table 6). Our result was lower than the study of Rios et al. (1). The ratio calculated by dividing the distance from the clavicle acromial end to the trapezoid line by the length of the clavicle was found to be 0.17 by Rios et al. (1), 0.15 by Xue et al. (21), and 0.12 by Ominde et al. (23). The ratio was found to be 0.13±0.02 in the present study in accordance with the previous studies. According to the measurements of the present study, for making reconstruction of the trapezoid ligament in as an anatomical position as possible, the trapezoid tunnel on the clavicle should be created 18 mm medial from the acromial end of the clavicle and at a ratio of 0.13.

Table 4. Length, thickness, and width of the clavicles in previous studies

	n	Method	Clavicle length (mm)	Supero-inferior thickness of the distal clavicle (mm)	Antero-posterior width of the distal clavicle (mm)
Rios et al. (1)	120	Dry clavicles	149.0±9.1	11.4±1.6	19.2±2.8
Boehm et al. (19)	36	Cadaver shoulder	150	-	-
Chahla et al. (20)	10	Fresh-frozen shoulder	141.3	-	-
Xue et al. (21)	172	Cadaver shoulder	139.9±9.4	-	-
Bernat et al. (22)	68	Cadaver shoulder	149.4±10.3	-	-
Ominde et al. (23)	180	Dry clavicles	148.57±12.63	10.09±2.36	-
King et al. (24)	101 male 108 female	Computed tomography	156.87±9.75 145.79±7.95	10.56±1.96 9.74±1.65	18.26±3.04 15.14±2.53
Daruwalla et al. (25)	27	Cadaver clavicles	-	10.31	21.58
Renfree et al. (26)	41	Cadaver clavicles	-	-	24.1±2.7
Present study	77	Dry clavicles	138.37±10.69	9.08±1.69	17.70±2.37

Table 5. Measurements of the conoid tubercle in previous studies

	n	Method	Medio-lateral dimension of the conoid tubercle (mm)	Supero-inferior dimension of the conoid tubercle (mm)	Distance between the clavicle acromial end and the center of the conoid tubercle (mm)	Distance from acromial end to conoid/clavicle length
Rios et al. (1)	19	Cadaver shoulder	25.3±4.9	-	35.0±5.9	0.24±0.03
Xue et al. (21)	172	Cadaver shoulder	13.1±2.2	6.0±1.4	35.7±3.4	0.25
Ominde et al. (23)	180	Dry clavicles	-	-	39.52±5.93	0.27
Takase (27)	40	Cadaver shoulder	17.4	5.4	-	-
Harris et al. (28)	24	Cadaver shoulder	20.6±3.6	-	-	-
Zhu et al. (29)	40	Cadaver shoulder	-	-	36.6±0.9	-
Present study	77	Dry clavicles	17.17±3.58	7.59±1.38	34.43±5.41	0.25±0.03

Table 6. Measurements of the trapezoid line in previous studies

	n	Method	Medio-lateral dimension of the trapezoid line (mm)	Antero-posterior dimension of the trapezoid line (mm)	Distance between the clavicle acromial end and the center of the trapezoid line (mm)	Distance from acromial end to trapezoid/clavicle length
Rios et al. (1)	120	Dry clavicles	-	-	24.9±3.8	0.17±0.03
	19	Cadaver shoulder	11.8±1.0	-	25.9±3.9	0.17±0.02
Xue et al. (21)	172	Cadaver shoulder	14.7±2.0	8.2±2.5	21.8±2.7	0.15
Ominde et al. (23)	180	Dry clavicles	-	-	17.96±3.42	0.12
Takase (27)	40	Cadaver shoulder	18.5	15.4	-	-
Harris et al. (28)	24	Cadaver shoulder	21.7±4.0	-	-	-
Zhu et al. (29)	40	Cadaver shoulder	-	-	21.7±1.1	-
Present study	77	Dry clavicles	16.69±2.73	9.61±1.80	18.15±2.80	0.13±0.02

There is limited knowledge in the literature about the distance between the conoid tubercle and the trapezoid line. Chahla et al. (20) dissected 10 fresh-frozen cadaveric shoulders and measured the distance between the centers of the trapezoid and conoid ligament attachments as 16.2 mm. In the present study, the distance between the center of the conoid tubercle and the center of the trapezoid line was found to be 18.70±3.11 in accordance with the study of Chahla et al. (20). According to the present study, there should be a distance of 18 mm between the conoid and trapezoid tunnels to make an anatomical reconstruction.

Study Limitations

The present study has some limitations inherent to a human dry bone design. Since the present study was performed on dry bone, measurements were taken from clavicles devoid of soft tissue, making it difficult to know exactly where the ligament was attached. Consequently, the footprints of ligaments would not be entirely precise in comparison to cadaveric research. The anatomical structures on the human dry clavicles may have been eroded because they are also used in student education. The other limitation is that this study was conducted with bones of unknown age and sex. Therefore, the effects of age and sex on the measured parameters could not be evaluated. Finally, this sample from a south-Mediterranean population may not be generalized. Further studies performed on cadavers and radiologic images should be planned for evaluating these sex, age, and geographical differences in distal clavicle morphometry.

CONCLUSION

Morphometric features of the distal clavicle are significant for anatomical reconstruction of the coracoclavicular ligament. According to our measurements, the conoid tunnel should be created 34 mm medial from the lateral edge and at a ratio of 0.25. The trapezoid tunnel should be created 18 mm medial from the lateral edge and at a ratio of 0.13 to achieve a successful anatomical reconstruction of the coracoclavicular ligaments. The distance between the tunnels to be created for the conoid and trapezoid ligaments should be 18 mm. The measurements obtained in this study can be used as a guide for coracoclavicular ligament reconstruction.

REFERENCES

1. Rios CG, Arciero RA, Mazzocca AD. Anatomy of the clavicle and coracoid process for reconstruction of the coracoclavicular ligaments. Am J Sports Med. 2007;35(5):811-7.
2. Berthold DP, Muench LN, Dyrna F, Mazzocca AD, Garvin P, Voss A, et al. Current concepts in acromioclavicular joint (AC) instability - a proposed treatment algorithm for acute and chronic AC-joint surgery. BMC Musculoskelet Disord. 2022;23(1):1078.
3. Lim YW. Triple endobuttton technique in acromioclavicular joint reduction and reconstruction. Ann Acad Med Singap. 2008;37(4):294-9.
4. Bishop JY, Kaeding C. Treatment of the acute traumatic acromioclavicular separation. Sports Med Arthrosc Rev. 2006;14(4):237-45.
5. Standring S. Gray's anatomy e-book: the anatomical basis of clinical practice, 42nd ed. Elsevier Health Sciences; 2021.
6. Mazzocca AD, Arciero RA, Bicos J. Evaluation and treatment of acromioclavicular joint injuries. Am J Sports Med. 2007;35(2):316-29.
7. Marchese RM, Black AC, Bordoni B. Anatomy, shoulder and upper limb, coracoclavicular joint (coracoclavicular ligament). In: StatPearls [Internet]. Treasure Island (FL): StatPearls Publishing; 2025.
8. Moatshe G, Kruckeberg BM, Chahla J, Godin JA, Cinque ME, Provencher MT, et al. Acromioclavicular and coracoclavicular ligament reconstruction for acromioclavicular joint instability: a systematic review of clinical and radiographic outcomes. Arthroscopy. 2018;34(6):1979-95.e8.
9. Panarello NM, Colantonio DF, Harrington CJ, Feeley SM, Bandarra TD, Dickens JF, et al. Coracoid or clavicle fractures associated with coracoclavicular ligament reconstruction. Am J Sports Med. 2021;49(12):3218-25.
10. Cartaya MA, Vargas JM. Use of the pectoralis minor and coracoacromial ligament for a biplanar coracoclavicular and acromioclavicular reconstruction: A cadaveric feasibility study. J Exp Orthop. 2024;11(4):e70032.
11. Kocadal O, Yüksel K, Güven M. Evaluation of the clavicular tunnel placement on coracoclavicular ligament reconstruction for acromioclavicular dislocations: a finite element analysis. Int Orthop. 2018;42(8):1891-6.
12. Celik H, Chauhan A, Flores-Hernandez C, Dorthe E, D'Lima D, Hoenecke H. Sagittal orientation of coracoclavicular ligament reconstruction affects the stability of surgical repair. J Shoulder Elbow Surg. 2020;29(9):1901-11.
13. Sirin E, Aydin N, Mert Topkar O. Acromioclavicular joint injuries: diagnosis, classification and ligamentoplasty procedures. EFORT Open Rev. 2018;3(7):426-33.
14. Frank RM, Cotter EJ, Leroux TS, Romeo AA. Acromioclavicular joint injuries: evidence-based treatment. J Am Acad Orthop Surg. 2019;27(17):e775-88.
15. Takase K, Yamamoto K. Changes in surgical procedures for acromioclavicular joint dislocation over the past 30 years. Orthopedics. 2013;36(10):e1277-82.
16. Mazzocca AD, Santangelo SA, Johnson ST, Rios CG, Dumonski ML, Arciero RA. A biomechanical evaluation of an anatomical coracoclavicular ligament reconstruction. Am J Sports Med. 2006;34(2):236-46.
17. Eisenstein ED, Lanzi JT, Waterman BR, Bader JM, Pallis MP. Medialized clavicular bone tunnel position predicts failure after anatomic coracoclavicular ligament reconstruction in young, active male patients. Am J Sports Med. 2016;44(10):2682-9.
18. Cook JB, Shaha JS, Rowles DJ, Bottoni CR, Shaha SH, Tokish JM. Clavicular bone tunnel malposition leads to early failures in coracoclavicular ligament reconstructions. Am J Sports Med. 2013;41(1):142-8.
19. Boehm TD, Kirschner S, Fischer A, Gohlke F. The relation of the coracoclavicular ligament insertion to the acromioclavicular joint A cadaver study of relevance to lateral clavicle resection. Acta Orthopaedica Scandinavica. 2003;74(6):718-21.
20. Chahla J, Marchetti DC, Moatshe G, Ferrari MB, Sanchez G, Brady AW, et al. Quantitative assessment of the coracoacromial and the coracoclavicular ligaments with 3-dimensional mapping of the coracoid process anatomy: a cadaveric study of surgically relevant structures. Arthroscopy. 2018;34(5):1403-11.
21. Xue C, Song LJ, Zhang M, Zheng TS, Fang JH, Li X. Coracoclavicular ligament attachment regions of the Chinese population: a quantitative anatomic study. Anat Sci Int. 2013;88(4):189-94.
22. Bernat A, Huysmans T, Van Glabbeek F, Sijbers J, Gielen J, Van Tongel A. The anatomy of the clavicle: a three-dimensional cadaveric study. Clin Anat. 2014;27(5):712-23.
23. Ominde BS, Awori KO, Olabu BO, Ogeng'o JA. Anatomical measurements of the distal clavicle in a Kenyan population. Anat J Afr. 2015;4(1):450-6.
24. King PR, Scheepers S, Ikram A. Anatomy of the clavicle and its medullary canal: a computed tomography study. Eur J Orthop Surg Traumatol. 2014;24(1):37-42.
25. Daruwalla ZJ, Courtis P, Fitzpatrick C, Fitzpatrick D, Mullett H. Anatomic variation of the clavicle: A novel three-dimensional study. Clin Anat. 2010;23(2):199-209.
26. Renfree KJ, Riley MK, Wheeler D, Hentz JG, Wright TW. Ligamentous anatomy of the distal clavicle. J Shoulder Elbow Surg. 2003;12(4):355-9.
27. Takase K. The coracoclavicular ligaments: an anatomic study. Surg Radiol Anat. 2010;32(7):683-8.
28. Harris RI, Vu DH, Sonnabend DH, Goldberg JA, Walsh WR. Anatomic variance of the coracoclavicular ligaments. J Shoulder Elbow Surg. 2001;10(6):585-8.
29. Zhu NF, Rui BY, Zhang YL, Chen YF. Anatomic study of coracoclavicular ligaments for reconstruction of acromioclavicular joint dislocations. J Orthop Sci. 2016;21(6):749-52.

The Investigation of Electrodiagnostic Findings in Patients with Nerve Injury Due to Earthquake: Single Centre Experience

Deprem Nedeni ile Sinir Hasarı Olan Hastaların Elektrodiagnostik Bulgularının İncelenmesi: Tek Merkez Deneyimi

Dilara MERMİ DİBEK[1]
0000-0001-9963-9450
Şule DEVECİ[2]
0000-0002-3863-9171
Azize Esra GÜRSOY[2]
0000-0002-8103-0927

[1]Department of Neurology and Clinical Neurophysiology, University of Health Sciences Başakşehir Çam and Sakura City Hospital, İstanbul, Türkiye

[2]Department of Neurology, University of Health Sciences Başakşehir Çam and Sakura City Hospital, İstanbul, Türkiye

Corresponding Author
Sorumlu Yazar
Dilara MERMİ DİBEK
dilara_mermi@hotmail.com

ABSTRACT

Aim: This study aimed to evaluate neuromuscular damage in the patients affected by the earthquakes that struck Kahramanmaraş, Türkiye.
Material and Methods: Patients referred to the electrodiagnostic (EDx) laboratory between February and August 2023, who were trapped under rubble, were included in this study. Demographic data, clinical information (renal failure, serum creatine kinase level, and time spent under the rubble), and EDx results were analyzed.
Results: Thirty-seven patients were included, while three patients with normal nerve conduction studies were excluded. Two (5.9%) of the 34 patients exhibited neurogenic and myogenic changes on EDx performed on days 24 and 25 post-trauma. In the remaining patients, neurogenic changes were observed, with 18 (52.9%) having peripheral nerve injury, 10 (29.4%) having plexopathy, 1 (2.9%) showing root involvement, and 5 (14.7%) of those with peripheral nerve injury presenting with complex involvement. Complete axonal damage was unrelated to the duration spent under the rubble (p=0.294). The presence of regeneration motor unit action potentials (MUAPs) was found statistically significantly related to the timing of the electromyography (EMG) performed (p=0.003), with the earliest regeneration findings observed on day 35. No statistically significant difference was found in the time spent under the rubble according to the regeneration presence (p=0.129).
Conclusion: This study shows that earthquake injuries primarily result in multiple peripheral nerve injuries. The regeneration MUAP occurrence was not related to the duration spent under the rubble. In addition, myogenic and neurogenic MUAPs may appear on EMG in neurogenic injuries caused by compartment syndrome.
Keywords: Earthquake; electromyography; myogenic; neurogenic; peripheral nerve injury.

ÖZ

Amaç: Bu çalışmanın amacı, Kahramanmaraş, Türkiye'de meydana gelen depremlerden etkilenen hastalarda nöromüsküler hasarın değerlendirmektir.
Gereç ve Yöntemler: Bu çalışmaya, Şubat ve Ağustos 2023 tarihleri arasında elektronöromiyografi (ENMG) laboratuvarına yönlendirilen ve enkaz altında kalmış olan hastalar dahil edilmiştir. Demografik veriler, klinik bilgiler (böbrek yetmezliği, serum kreatin kinaz düzeyi ve enkaz altında geçirilen süre) ve ENMG sonuçları analiz edilmiştir.
Bulgular: Otuz yedi hasta çalışmaya dahil edilirken, sinir iletim çalışmaları normal olan üç hasta çalışma dışı bırakıldı. Travma sonrası 24. ve 25. günlerde yapılan ENMG'de 34 hastanın ikisinde (%5,9) nörojenik ve miyojenik değişiklikler görüldü. Geri kalan hastalarda ise nörojenik değişiklikler gözlenmiş olup, 18 (%52,9)'inde periferik sinir hasarı, 10 (%29,4)'unda pleksopati, 1 (%2,9)'inde kök tutulumu ve periferik sinir hasarı olanların 5 (%14,7)'inde kompleks tutulum izlendi. Tam aksonal hasarın enkaz altında geçirilen süre ile ilişkisi bulunmadı (p=0,294). Rejenerasyon motor ünitesi aksiyon potansiyellerinin (MUAPs) varlığının yapılan elektromiyografi (EMG) zamanlaması ile istatistiksel olarak anlamlı ilişkili olduğu (p=0,003) ve en erken rejenerasyon bulgularının 35. günde gözlendiği bulundu. Rejenerasyon varlığına göre enkaz altında geçen sürede istatistiksel olarak anlamlı bir fark bulunmadı (p=0,129).
Sonuç: Bu çalışma, deprem yaralanmalarının öncelikle çoklu periferik sinir yaralanmalarına neden olduğunu göstermektedir. Rejenerasyon MUAP oluşumu enkaz altında geçirilen süre ile ilişkili değildir. Ek olarak, kompartıman sendromunun neden olduğu nörojenik yaralanmalarda EMG'de miyojenik ve nörojenik MUAP'lar görülebilir.
Anahtar kelimeler: Deprem; elektromiyografi; miyojenik; nörojenik; periferik sinir hasarı.

INTRODUCTION

On February 6, 2023, two main earthquakes with magnitudes of 7.8 and 7.6, respectively, occurred nine hours apart in the Kahramanmaraş region of southeastern Turkey, according to the Kandilli Observatory and Earthquake Research Institute (1). Besides the two largest earthquakes, several other earthquakes with magnitudes between 4.0 and 6.6 occurred throughout the day. Too many people were trapped under the rubble. Crush syndrome, loss of extremities, or paralysis occurred due to the entrapment of limbs or other parts of the body.

The electrodiagnostic studies (EDx), which contain motor and sensory nerve conduction studies (NCSs) and needle electromyography (EMG) examination, are one of the important tools to diagnose nerve injury. In addition, it gives information about lesion localization, severity of nerve injury, and occurrence of regeneration according to the special time spaces (2). If the axonal loss or Wallerian degeneration has not occurred, the compound muscle action potential (CMAP) should be normal. The amplitude of the CMAP occurred by distal stimulation will start to fall approximately at day three and reach the lowest level approximately at day nine, and it will disappear by complete axon loss, however the actual time course depends on the length of the distal nerve segment between the lesion and the muscle (3). Wallerian degeneration in sensory fibers has occurred about 11 days post-injury, which is longer than motor NCSs due to the earlier failure of neuromuscular junction transmission (4). The spontaneous activity in EMG, which includes fibrillation potentials (FPs) and positive sharp waves (PSWs) are occurs according to the length between the injury and the distal nerve stump. If it is short, the FPs develop in only 10-14 days; if it is longer, 3-4 weeks are required for the development of FPs and PSWs (5). The motor unit action potentials (MUAPs) are not recorded in the complete axonal loss, while reduced or discrete recruitment with normal MUAPs morphology are recorded in the incomplete axonal loss at the beginning, and are followed by the increased percentage of polyphasy, prolonged duration, and increased amplitude of MUAPs (6). The regeneration occurs along the distal nerve segment at a rate of about 1 mm/day (7). The timing of EDx is decided by considering these pathophysiological and electrophysiological points. The studies reported that the peripheral nerve injuries are the most frequent damage due to an earthquake (8-10).

This study aimed to document findings of patients with nerve injury who were referred to EDx laboratories.

MATERIAL AND METHODS

Patients and Procedures

Ethics committee approval was obtained from the clinical research ethics committee of Başakşehir Çam and Sakura City Hospital (dated 24.05.2023, and numbered 200).

EDx findings were evaluated in patients who had been trapped under rubble following the earthquake and were referred between February and August 2023, with inclusion limited to those demonstrating pathological EDx results. Patients with a history of polyneuropathy, rheumatic disease, alcohol consumption, cervical and lumbar radiculopathy, hereditary pressure-sensitive neuropathy, myopathy, or any other traumatic sequelae were excluded from the study. Sensory and motor NCSs, along with concentric needle electrode (CNE) findings, were collected. Sensory NCSs were performed antidromically, and the peak-to-peak amplitude was considered. Sensory conduction velocity was evaluated based on baseline distal latency. Both extremities were evaluated, and the normal value was determined based on the contralateral extremity if it was unaffected. If both sides were affected, Shapiro's normal value was used as the reference (11). The EDx examination was performed by two different physicians (DMD, ŞD) using three distinct devices [Keypoint (Dantec, Denmark), Natus (Nicolet Viking Quest, Synergy), and Cadwell (Sierra Summit)] in the EMG laboratory of the Neurology Clinic at Başakşehir Çam and Sakura City Hospital.

The EDx protocols were determined based on the condition of the extremities. The EMG findings first evaluated the localization of nerve damage. Lesions were classified as root, plexus, or peripheral nerve injuries. Peripheral nerve damage was further classified as mononeuropathy or multiple peripheral neuropathy. The frequency of affected peripheral nerves was also noted.

The duration of time spent under the rubble, serum creatine kinase (CK) levels, history of renal failure, and presence of fasciotomy history were noted. Patients under the age of 18 years were considered a pediatric age group.

Statistical Analysis

IBM SPSS version 26 was used for the statistical analysis. Descriptive statistics were conducted to examine the frequency distribution of nerve injuries. The Shapiro-Wilk test was used for normality assumption for age, time of EMG performed after trauma, time lying under rubble, and serum CK level. Due to the non-normal distribution, the median, interquartile range (IQR, Q3-Q1), and [min, max] were presented. The Mann-Whitney U test was used to compare numerical variables that did not show a normal distribution, while Fisher's exact test was used to analyze categorical data. Statistical significance was considered as a p-value of <0.05.

RESULTS

Of the 2,170 patients affected by the earthquake who applied to the Başakşehir Çam and Sakura City Hospital, 37 (1.71%) were referred to the EDx laboratory. Three patients had normal NCSs and were excluded. Median age of the remaining 34 patients was 25 (range, 6-76) years. Eleven (32.4%) of the patients were in the pediatric age group, and 23 (67.6%) of the patients were in the adult age group (Table 1).

Regarding the localization of the damage, 52.9% (n=18) of patients had peripheral nerve injury, 29.4% (n=10) of patients had plexopathy, 2.9% (n=1) had root involvement, in addition to complex involvement of the peripheral nerve, plexus, and root in 14.7% (n=5). Peripheral nerve injuries were classified as mononeuropathy in 39.1% (n=9) and as multiple nerve injury in 60.9% (n=14). The most affected peripheral nerve was the fibular nerve (40.9%, n=9), followed by the tibial nerve (36.4%, n=8), ulnar nerve (27.3%, n=6), radial nerve (27.3%, n=6), and median nerve. (22.7%, n=5), sciatic nerve (18.2%, n=4), femoral nerve (4.5%, n=1), and musculocutaneous nerves (4.5%, n=1), respectively.

Table 1. Demographical and electromyographical results

	n*	Median (Q1-Q3) [min-max]
Age (year)	34	25 (15-43) [6-76]
Time of EMG after trauma (day)	34	47 (25-70) [8-180]
The time lying under rubble (hour)	32	22 (8-75) [4-144]
Serum CK level (IU/L)	28	279.5 (36-432) [11-10215]
Gender, n (%)		
Female	34	20 (58.8)
Male		14 (41.2)
Age group, n (%)		
Pediatric, <18 years	34	11 (32.4)
Adult, >18 years		23 (67.6)
Motor NCS, n (%)		
Partial	34	14 (41.2)
No response		20 (58.8)
Sensory NCS, n (%)		
Normal		1 (2.9)
Partial	34	10 (29.4)
No response		23 (67.6)
CNE-spontaneous, n (%)		
Normal	33	1 (3.0)
Denervation potentials (PSW, FPs)		32 (97.0)
CNE-denervation scale, n (%)		
1+		0 (0.0)
2+	25	6 (24.0)
3+		19 (76.0)
CNE-MUAPs, n (%)		
Neurogenic	34	32 (94.1)
Myogenic and neurogenic		2 (5.9)
With Regeneration, n (%)	29	17 (58.6)
CNE-recruitment pattern, n (%)		
No activity	32	28 (84.8)
Decreased		4 (12.2)
Distribution of nerve damage, n (%)		
Upper Extremity	34	11 (32.4)
Lower Extremity		23 (67.6)
Fasciotomy, n (%)	34	22 (64.7)
Kidney Failure, n (%)	24	8 (33.3)

*: number of patients the statistics were calculated, Q1-Q3: 25th-75th percentile, EMG: electromyography, CK: creatine kinase, NCS: nerve conduction studies, CNE: concentric needle electrode, PSW: positive sharp waves, FPs: fibrillation potentials, MUAPs: motor unit action potentials

Two (5.9%) of 34 exhibited neurogenic and myogenic changes in EMG that was performed on days 24 and 25 of trauma. These two patients also had acute kidney failure and elevated CK levels, which are 23000 and 111000 IU/L, respectively. Myogenic changes were found in only two patients with a history of renal failure. However, renal failure was not statistically significantly related to either myogenic MUAPs (100% vs 0.0%, p=0.101) or elevated CK levels (21.5 vs 13.96, p=0.212). Additionally, myogenic MUAPs were not statistically significantly related to a history of fasciotomy (0.0% vs 100%, p=0.212).

The results of motor and sensory NCVs and EMG findings, as well as whether fasciotomy was performed and whether kidney dysfunction was present, were summarized in Table 1.

Distal total axonal damage was more prominent in the lower extremities (75.0% vs 25.0%, p=0.033) compared to the upper extremities. Complete axonal injury was not statistically significantly related to the duration of time spent under the rubble (12.10 vs 16.75, p=0.294).

The presence of regeneration MUAPs was related to the timing of EDx performed (18.94 vs 9.42, p=0.003). The earliest day for the presence of regeneration was day 35. Presence of regeneration MUAPs was not differed to the duration time of underlying the rubble, localization of the damage in upper or lower extremities, presence of renal failure, and severity of axonal damage (16.07 vs 11.42, p=0.129; 77.8 vs 50.0%, p=0.234; 25.0% vs 75.0%, p=0.133; 100% vs 52.0%, p=0.121, respectively).

The pediatric and adult age groups did not differ in terms of damage to the upper or lower extremities. Although regeneration of MUAPs was higher in the pediatric group compared to the adult group, this difference was not statistically significant (87.5% vs. 47.6%, p=0.060).

DISCUSSION

The results of the study demonstrated early post-earthquake neuromuscular damage. We primarily found neurogenic changes due to peripheral nerve damage on EDx in earthquake survivors. Complete axonal degeneration was more prominent in the lower extremities compared to the upper extremities, and the most affected nerve was the fibular nerve. The fibular nerve may be more prone to damage than other nerves due to its anatomical pathway. On the other hand, one patient had demyelination of the ulnar nerve at the elbow, possibly due to an inability to protect the extremity's position. According to the latest studies on nerve injury resulting from earthquakes, peripheral nerve injury is the most frequent type of damage, which confirms the study results (8-10).

The regeneration MUAPs were recorded in 17 (58.6%) patients, and was observed on day 35, which is the earliest time in the study group. The severity of axonal damage, the presence of kidney comorbidities, and the time spent under the rubble did not relate to the presence of regeneration MUAPs. The timing of regeneration depends on nerve length, with regeneration speed known to be approximately 1 mm/day, and the earliest time is 30 days for evaluating regeneration MUAPs, which is supported by our results. The significance of regenerative MUAPs lies in predicting that clinical improvement may begin earlier than 2-3 months (12). Regeneration was observed at a higher percentage in the pediatric age group compared to the adult group (87.5% vs. 47.6%, respectively). However, this difference was not statistically significant. These results are similar to those reported after the Marmara Earthquake (8). In the present study, only 9% of the pediatric age group was referred for EDx laboratories before the 35th day post-trauma, whereas 39% of the adult age group was referred within the same period. The higher percentage of regeneration in the pediatric group may be related to the later referral of pediatric patients, as physicians may avoid performing EMG on younger patients compared to adults. Another reason may be the shorter nerve length in pediatric patients compared to adult patients.

Two patients in this study had concomitant myogenic and neurogenic changes. Other studies have not mentioned myogenic changes in earthquake survivors. EMG examinations were performed on the 24th-25th days after being trapped, which is early for observing regenerative MUAPs in the two patients who exhibited myogenic

changes. The myogenic changes may be due to muscle fiber damage or necrosis caused by insufficient blood supply as a result of high compartmental pressure (13,14). The extremities of these two patients were enlarged, with thin, tense, and swollen skin; unfortunately, we did not have the opportunity to measure the pressure in the affected compartments. These two patients had spent eight hours under the rubble, exhibited high CK levels, and required hemodialysis due to rhabdomyolysis. Although other patients whose EMG findings showed only neurogenic changes had a history of fasciotomy, these two patients with myogenic changes did not require fasciotomy during their follow-up. Although it is difficult to draw definitive conclusions from these two cases alone, we speculate that the presence of both myogenic and neurogenic changes does not necessarily indicate a need for fasciotomy or a poor prognosis for all patients.

The study has several limitations. Firstly, we included all patients referred to the EDx laboratory, but some data were missing due to the retrospective analysis. Secondly, our case series was relatively small. Thirdly, some muscles could not be evaluated due to the extensive damage in those areas. Another limitation is that follow-up EMG could not be performed because most patients moved to other cities after their treatment.

CONCLUSION
The present study demonstrates that peripheral nerve injury is the most common cause of axonal degeneration following earthquake trauma. Another result is that both myogenic and neurogenic MUAP changes can occur in patients with neuronal damage who experience rhabdomyolysis. Furthermore, regeneration MUAPs can develop regardless of the duration spent under the rubble.

REFERENCES
1. Hussain E, Kalaycıoğlu S, Milliner CWD, Çakır Z. Preconditioning the 2023 Kahramanmaraş (Türkiye) earthquake disaster. Nat Rev Earth Environ. 2023;4(5):287-9.
2. Robinson LR. Traumatic injury to peripheral nerves. Muscle Nerve. 2022;66(6):661-70.
3. Chaudhry V, Cornblath DR. Wallerian degeneration in human nerves: serial electrophysiological studies. Muscle Nerve. 1992;15(6): 687-93.
4. Ferrante MA. The assessment and management of peripheral nerve trauma. Curr Treat Options Neurol. 2018;20(7):25.
5. Thesleff S. Trophic functions of the neuron. II. Denervation and regulation of muscle. Physiological effects of denervation of muscle. Ann N Y Acad Sci. 1974;228(0):89-104.
6. Dorfman LJ. Quantitative clinical electrophysiology in the evaluation of nerve injury and regeneration. Muscle Nerve. 1990;13(9):822-8.
7. Sunderland S. The anatomy and physiology of nerve injury. Muscle Nerve. 1990;13(9):771-84.
8. Uzun N, Savrun FK, Kiziltan ME. Electrophysiologic evaluation of peripheral nerve injuries in children following the Marmara earthquake. J Child Neurol. 2005;20(3):207-12.
9. Uzun N, Tanriverdi T, Savrun FK, Kiziltan ME, Sahin R, Hanimoglu H, et al. Traumatic peripheral nerve injuries: demographic and electrophysiologic findings of 802 patients from a developing country. J Clin Neuromuscul Dis. 2006;7(3):97-103.
10. Gesoglu Demir T, Ethemoplu KB. Clinical, etiological, and electrophysiological characteristics of patients with peripheral nerve damage caused by the February 6 earthquake in Türkiye. Turk J Neurol. 2024;30(3):141-8.
11. Preston DC, Shapiro BE. Electromyography and neuromuscular disorders. 4th ed. Appendix: nerve conduction studies: normal adult values, pediatric values. Amsterdam: Elsevier; 2020. p.763.
12. Oh SJ. Electromyographic studies in peripheral nerve injuries. South Med J. 1976;69(2):177-82.
13. Myers RR, Mizisin AP, Powell HC, Lampert PW. Reduced nerve blood flow in hexachlorophene neuropathy: relationship to elevated endoneurial fluid pressure. J Neuropathol Exp Neurol. 1982;41(4):391-9.
14. Broadhurst PK, Robinson LR. Compartment syndrome: Neuromuscular complications and electrodiagnosis. Muscle Nerve. 2020;62(3):300-8.

Performance Assessment of the Concepta Automated ANA Detection System in Routine Clinical Samples

Concepta Otomatik ANA Tespit Sisteminin Rutin Klinik Örneklerde Performans Değerlendirmesi

Mehmet Akif DURMUŞ
0000-0002-3637-6451
Ayşe Nur CEYLAN
0000-0002-0049-6873
Kübra EVREN
0000-0002-2512-470X

Department of Medical Microbiology, Başakşehir Çam ve Sakura City Hospital, İstanbul, Türkiye

ABSTRACT

Aim: Indirect immunofluorescence (IIF) on HEp-2 cells is the standard method for detecting anti-nuclear antibodies (ANA) due to its high sensitivity. Recently, several artificial intelligence-supported automated immunofluorescence systems have been developed to improve standardization and efficiency in ANA detection using the IIF method. This study aimed to evaluate the performance of the Concepta automated immunofluorescence system in routine clinical settings for ANA testing using the IIF method.

Material and Methods: A total of 1000 patient serum samples were analyzed using the Concepta automated system after preparation with the iPRO processor. The results were compared to manual evaluations conducted by two expert clinicians to assess the system's agreement, sensitivity, specificity, and accuracy in pattern recognition.

Results: The Concepta system demonstrated an overall agreement of 98.11% with manual evaluations for positive and negative discrimination, corresponding to a κ value of 0.958. The sensitivity and specificity were found to be 99.08% and 97.61%, respectively, with positive and negative predictive values of 87.96% and 99.83%. High concordance rates were observed for homogeneous (95.7%), centromere (92.3%), and nucleolar (92.1%) patterns, while lower rates were noted for speckled (60%) and cytoplasmic (44.4%) patterns.

Conclusion: The Concepta automated system demonstrated very high accuracy in ANA positive and negative discrimination, comparable to other automated systems. Despite some limitations in recognizing dense fine speckled and mixed patterns, it proved particularly effective in distinguishing between positive and negative results. These findings suggest that the Concepta system is a promising new alternative in the field of ANA testing.

Keywords: Autoantibodies; antinuclear autoantibodies; immunofluorescence microscopy.

ÖZ

Amaç: Anti-nükleer antikorların (ANA) tanısında HEp-2 hücrelerinin kullanıldığı indirekt immünofloresans (IIF) testi, yüksek duyarlılığı nedeniyle standart yöntemdir. Son yıllarda, IIF yöntemi ile ANA tespitinde standardizasyonu ve verimliliği artırmak amacıyla yapay zeka destekli birçok otomatik immünofloresans sistemi geliştirilmiştir. Bu çalışmanın amacı, otomatik immünofloresans sistemi olan Concepta'nın, IIF yöntemi kullanılarak ANA testinde rutin klinik ortamlardaki performansını değerlendirmektir.

Gereç ve Yöntemler: iPRO işlemcisiyle hazırlanan toplam 1000 hasta serum örneği, Concepta otomatik sistemi kullanılarak analiz edildi. Sonuçlar, iki uzman klinisyen tarafından yapılan manuel değerlendirmelerle karşılaştırılarak sistemin uyumu, duyarlılığı, özgüllüğü ve patern tanımlama doğruluğu değerlendirildi.

Bulgular: Concepta sistemi, pozitif ve negatif ayrımda manuel değerlendirmelerle %98,11 genel uyum gösterdi ve κ değeri 0,958 olarak hesaplandı. Duyarlılık ve özgüllük sırasıyla %99,08 ve %97,61 olarak belirlenirken, pozitif prediktif değerleri ve negatif prediktif değerleri %87,96 ve %99,83 bulundu. Homojen (%95,7), sentromer (%92,3) ve nükleoler (%92,1) paternlerde yüksek uyum oranları gözlemlenirken, benekli (%60) ve sitoplazmik (%44,4) paternlerde uyum daha düşüktü.

Sonuç: Concepta otomatik sistemi, ANA pozitif ve negatif ayrımında diğer otomatik sistemlerle kıyaslanabilir oldukça yüksek bir doğruluk oranı sergiledi. Concepta sisteminin yoğun ince benekli ve mix paternlerin tanınmasında bazı sınırlılıkları bulunsa da özellikle pozitif ve negatif sonuçlar arasında ayrım yapmada gösterdiği başarı dikkat çekmektedir. Bu sonuçlar, Concepta sisteminin ANA testi alanında umut verici yeni bir alternatif olduğunu göstermektedir.

Anahtar kelimeler: Otoantikorlar; antinükleer antikor testi; immünfloressan mikroskobi.

INTRODUCTION

Autoimmune diseases can occur through various mechanisms. One of these mechanisms is the production of autoantibodies, by which the immune system attacks an individual's structural antigens and creates a pathological response (1). Autoantibodies that target nuclear and cytoplasmic antigens, commonly known as anti-nuclear antibodies (ANA), are crucial diagnostic markers for systemic autoimmune rheumatic diseases. These diseases include systemic lupus erythematosus, rheumatoid arthritis, systemic sclerosis, Sjögren's syndrome, idiopathic inflammatory myopathies, and systemic vasculitis (2,3).

Indirect immunofluorescence (IIF) on HEp-2 cells remains the favored approach for ANA screening. The remarkable sensitivity of ANA assessment using IIF enables the detection of over 50 antibodies. Consequently, this method is an indispensable tool for identifying systemic autoantibodies during the initial stages of diagnostic procedures (4).

In the ANA test, 30 different classes have been defined based on image differences (5). The International Consensus on Anti-nuclear Antibody Patterns has a web portal (www.anapatterns.org) that includes the classification and image examples (6). Furthermore, the variability of IIF is significantly influenced by biological factors (such as sample preparation, antigen expression, and disease heterogeneity) and non-biological factors (including laboratory procedures, observer subjectivity, and CAD system algorithms), which poses a challenge to the standardization of IIF (7,8). The results may differ when specialized physicians evaluate IIF images. The specialist physician can examine the image with manual microscopes, but commercial automated products that include a decision support system in their structure can also perform image analysis in their structure (3). Advancements in technology have led to the development of automated IIF systems. These systems utilize artificial intelligence to process and recognize digitized fluorescent images automatically. Using a standardized approach, patterns are classified to facilitate computer-aided diagnosis, including automatic positive and negative discrimination and pattern interpretation. In these systems, high-resolution digital images captured using precision cameras and integrated automatic microscopes are analyzed by computer-aided systems. Numerous automated systems are currently available (9). Computer-aided systems and artificial intelligence are becoming increasingly present in our lives. In the IIF evaluation, automated systems are becoming increasingly crucial in immunology laboratories.

We evaluated the performance of a system that is an automatic system recently used in Türkiye. In this context, this study analyzed the performance of the automated system in ANA IIF testing. The evaluation focused on the ability of the systems to distinguish between positive and negative results and to identify various anti-nuclear antibody patterns.

To achieve this goal, we studied 1000 routine patient samples that were sent to the laboratory and evaluated the results. To evaluate the performance of automated systems in real life, we planned the study on routine patients, not on a predefined patient group.

MATERIAL AND METHODS

Between November 2023 and February 2024, 1000 serum samples that were sent to the laboratory to analyze ANA patterns using IIF were studied. For ANA detection, iPRO (BioSystems, Barcelona, Spain) was used for sample preparation, and Concepta (BioSystems, San Giovanni Valdarno, Italy) for automated evaluation. iPRO is a fully automated IIF processor. Samples are loaded to the processor with racks. The system will scan barcodes automatically. Test assignments can be programmed manually or sent by the laboratory information system. According to the programmed worklist, necessary dilutions are prepared automatically, samples can be unloaded from the device, and another group of samples can be loaded. At the session's end, laboratory professionals must pick the slides up, dispense mounting medium, and close coverslips. After closing the coverslips, slides are placed in the Concepta automated microscope and evaluation device. Concepta is an automated in vitro diagnostic system that reads, displays, and archives slides containing IIF assays from patient serum or plasma samples. The system provides positive/uncertain/negative results for the HEp-2 test that must be confirmed by expert laboratory personnel or physicians and provides aid for pattern identification through the automatic recognition of the HEp-2 patterns: Homogeneous, speckled, centromere, nuclear dots, nucleolar, cytoplasmic, and cytoplasmic AMA-like. Concepta only identifies a single pattern. In mixed patterns, it identifies only one pattern. Although it provides a value based on fluorescence intensity, it cannot determine the titer based on this intensity.

All samples finalized with Concepta were evaluated by two experienced experts separately on the system screen. Internal quality controls, both positive and negative, were performed in each study. In addition, our laboratory participates in two external quality assurance programs (Institute for Quality Assurance Lübeck and UK NEQAS). This research was approved by the Ethics Committee of Başakşehir Çam and Sakura City Hospital with approval date/number: 2024-62.

Statistical Analysis

IBM SPSS version 27 statistical program for Mac was used for statistical evaluation, and descriptive information was shown using number and percentage distributions. The percentages of agreement and κ coefficients were calculated to determine the agreement between the automated system and the manual expert evaluation.

RESULTS

A total of 1000 serum samples sent to the immunology laboratory for routine ANA testing were analyzed. 47 samples were excluded from the study due to repetition, dilution requirements, or inter-observer variability in pattern identification during manual evaluation.

Of the 953 samples analyzed by the expert physicians, 326 were positive, and 627 were negative. The percentage of agreement between Concepta and the expert assessment in the positive-negative discrimination is 98%, indicating a near-perfect match (Table 1).

Concepta's analytical sensitivity and specificity were 99.08% and 97.61%, respectively, while the positive and negative predictive values were 87.96% and 99.83%, respectively (Table 2). Of the 326 positive samples, 29 had

Table 1. Compatibility between Concepta and expert assessment

		Concepta		Total	Agreement (%)	κ value (95% CI)
		Positive (%)	Negative (%)			
Expert	**Positive**	323	3	326 (34.21)	323/326 (99.08)	
	Negative	15	612	627 (65.79)	612/627 (97.61)	0.958 (0.939-0.977)
	Total	338 (35.47)	615 (64.53)	953	935/953 (98.11)	

Table 2. Performance parameters of Concepta

Test	Sensitivity (95% CI)	Specificity (95% CI)	PPV (95% CI)	NPV (95% CI)
Concepta	99.08 (97.33-99.81)	97.61 (96.08-98.65)	87.96 (81.59-92.34)	99.83 (99.49-99.95)

PPV: positive predictive value, NPV: negative predictive value, CI: confidence interval

more than one pattern. The compatibility results of the 326 positive sample results were shown in Table 3.

Concepta identifies seven patterns (homogeneous, speckled, centromere, nuclear dots, nucleolar, cytoplasmic, and cytoplasmic AMA-like) but not dense fine speckled and nuclear membrane. It identified 52 of 63 samples with dense fine speckled as homogeneous (Figure 1).

Among the patterns that Concepta can identify, the largest group it fails to recognize is the speckled pattern. Among the 100 specimens that specialists identified as speckled, Concepta correctly classified 60, while 40 were misclassified.

DISCUSSION

Initially, the ANA test was primarily requested by rheumatologists. Due to its association with various diseases, the ANA test is in increasing demand from physicians of different specialties, going beyond rheumatology (10). Studies conducted with groups diagnosed with autoimmune diseases do not adequately reflect daily laboratory practices. When these groups are selected and studied, a group with higher ANA positivity is selected compared to the routine patient group. At the same time, ANA positivity in this group will be at higher titers than in the routine patient group. Since ANA can also be found in healthy individuals, this often leads to uncertain results. Studies involving routine patient groups are likely to yield more uncertain results. Consequently, research conducted with routine patient samples more accurately reflects actual laboratory conditions. 47 samples were excluded (duplicate samples, requiring dilution, and samples where two physicians identified different patterns during manual assessment). There may be differences in judgment between the experts, so samples where both experts disagreed were not evaluated (11). Among the studies on ANA IIF, there were no data on the Concepta system. However, our study revealed a 98.11% agreement between Concepta and expert assessment, with a close to perfect

Table 3. Agreement between expert evaluation and Concepta in pattern identification

Pattern	Expert (n)	Concepta (n)	Concordance rate (%)
Cytoplasmic reticular/AMA like	12	8	66.7
Homogeneous	47	45	95.7
Speckled	100	60	60
Nucleolare	38	35	92.1
Nuclear dots	5	3	60
Nuclear membrane	3	0	-
Dense fine speckled	63	0	-
Centromere	13	12	92.3
Cytoplasmic	9	4	44.4
Multiple patterns	29	0	-
Other	7		
Total	326	167	
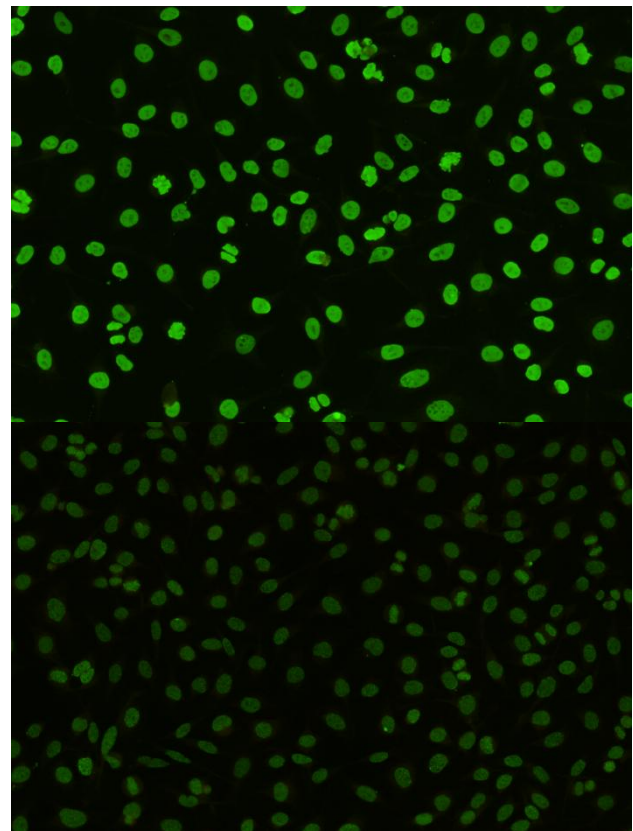
Figure 1. BioSystems ANA IIF pattern image examples, **A)** homogeneous, **B)** dense fine speckled

match (κ value 0.958). In 3 studies conducted with different commercial automated systems, the κ value was found to be 0.97, 0.932, and 0.860 (12-14). These findings are significant as they present a new alternative to automated systems.

The sensitivity and specificity of Concepta were 99.08% and 97.61%, respectively. In a study by Loock et al (15) in which two different automated systems were evaluated with routine samples coming to the laboratory, sensitivity was satisfying (89%/87% for Aklides/Helios), and the specificity was relatively low (59%/54% for Aklides/Helios). In two different studies with another automated system, EUROPattern, analytical sensitivity and specificity varied, with sensitivity between 94.3% and 98.95% and specificity between 88.2% and 98.4% (12-14). In another study with two different automated systems, Nova View/Helios's sensitivity was 96.7%/95.8%, and its specificity was 91%/93.5% (16).

When the pattern identification results are analyzed, Concepta and conventional IIF pattern recognition results match 51.2% (167/326) of the samples. Concepta could identify homogeneous, speckled, centromere, nuclear dots, nucleolar, cytoplasmic, and cytoplasmic AMA-like patterns. However, it struggled with mixed patterns as it could only provide a single result, leading to incomplete classifications. The Concepta identification algorithm does not include the dense fine speckled pattern. When the unidentified specimens were analyzed, it was found that the majority belonged to the dense fine speckled pattern. In particular, Concepta was identified as homogeneous in 52 out of 63 dense fine speckled samples. One sample was classified as nucleolar, two as negative, and two as speckled. The remaining six specimens could not be identified. Out of 1,000 patient samples processed by the device, experts identified 326 positive cases. The Concepta classification algorithm identifies various patterns, including homogeneous, speckled, centromere, nuclear dots, nucleolar, cytoplasmic, and cytoplasmic AMA-like patterns (Table 4). Concepta was unable to identify 112 samples due to various patterns such as dense fine speckled, nuclear membrane, and mixed patterns. As a result, it could only identify 224 out of the 326 positive samples. When its success in these patterns was analyzed, it was found that it correctly identified 167 out of 224 samples. Concepta concordance rates differed across pattern types in the following sequence: homogeneous (95.7%), centromere (92.3%), nucleolar (92.1%), cytoplasmic reticular /AMA-like (66.7%), nuclear dot (60%), speckled (60%),

and cytoplasmic (44.4%). As no study was conducted with Concepta, no comparison could be made.

In the study by Park et al. (13), the EUROPattern concordance rates varied between different pattern types in the following order: cytoplasmic and nuclear dot (100%), centromere (87.5%), speckled (79.3%), homogeneous (62.5%), nucleolar (60.0%), nuclear membrane and mitotic (0.0%) patterns. van Beers et al. (11) found the relative sensitivity as homogenous (93.6%), speckled (87.3%), nucleolar (91.9%), centromere (93.8%), nuclear spots (80.0%), nuclear membrane (100%), and cytoplasmic (86.4%). Another study observed correct pattern recognition in 94.6% of sera with a single pattern. The effectiveness of automated recognition for various patterns differed (12): cytoplasmic pattern, nucleolar pattern (100%), speckled pattern (97.2%), homogeneous pattern (91.6%), nuclear dots pattern (75%), centromeres pattern (60.7%). Our study's Concepta results demonstrated higher concordance rates for centromere, homogeneous, and nucleolar patterns than others. However, lower concordance rates were observed for cytoplasmic, nuclear dot, and speckled patterns. Concepta identified only 60 out of 100 speckled patterns correctly.

Among the 40 specimens that Concepta failed to identify, 24 were incorrectly classified, while 16 could not be evaluated at all. Other studies have also shown that identifying the speckled pattern is complex (17-20). Therefore, low identification rates in speckled can be considered normal.

There are automated systems that only distinguish between positive and negative results, as well as systems that can identify various patterns. The number and types of patterns recognized by these systems differ (Table 4). Pattern recognition algorithms may experience difficulties in identification as the number of patterns they can recognize increases. Homogeneous, speckled, and dense fine speckled patterns share similarities, making them challenging to distinguish, particularly for AI-enabled systems (15,21). An algorithm designed to identify only homogeneous and speckled patterns will classify homogeneous patterns more accurately, as dense fine speckles cannot be easily confused with them. However, as our study shows, this algorithm may mistakenly classify dense fine speckled patterns as homogeneous. Therefore, it is advisable to evaluate each system based on its unique characteristics and limitations.

The present study was conducted using routine patient samples rather than samples from patients with autoimmune rheumatologic diseases. ANA positivity is more

Table 4. Patterns identified by automated systems*

System	Patterns
EUROPattern	Homogeneous, speckled, dense fine speckled, nucleolar, centromere, nuclear dots, nuclear membrane, cytoplasmic reticular / AMA like and cytoplasmic
NOVA View	Homogeneous, speckled, fine speckled, coarse speckled, dense fine speckled centromere, nucleolar and nuclear dots
Helios	Homogeneous, speckled, centromere, nuclear membrane, nuclear dots, nucleolar, and cytoplasmic
Zenit G-Sight	Homogeneous, nucleolar, speckled, centromere, and mitochondrial patterns
Aklides	Homogeneous, speckled, nucleolar, centromere, nuclear dots, and cytoplasmic
Image Navigator	Positive/negative (no pattern distinction)
Concepta	Homogeneous, speckled, nucleolar, centromere, nuclear dots, cytoplasmic reticular / AMA like and cytoplasmic

* Adapted from Bizzaro et al. (3) and Tebo AE (22)

clearly observed in studies that focus on patient groups with these autoimmune conditions. The design of our study, which involves routine patient groups, may influence the performance of the device due to the presence of more intermediate values.

CONCLUSION

This study highlights the performance and limitations of the Concepta automated system in the detection and pattern recognition of ANA using IIF. The system demonstrated high sensitivity and specificity in distinguishing between positive and negative results, achieving a 98.1% agreement with expert evaluations. Concepta's inability to identify the dense fine speckled pattern we frequently encounter can be considered a disadvantage. However, its pattern recognition capability was limited, especially for homogeneous, speckled, centromere, nuclear dots, nucleolar, cytoplasmic, and cytoplasmic AMA-like patterns. Concepta, presented as a new alternative among automated systems, is an important tool for its success in distinguishing both positive and negative results.

REFERENCES

1. Pisetsky DS. Pathogenesis of autoimmune disease. Nat Rev Nephrol. 2023;19(8):509-24.
2. Tebo AE. Recent approaches to optimize laboratory assessment of antinuclear antibodies. Clin Vaccine Immunol. 2017;24(12):e00270-17.
3. Bizzaro N, Antico A, Platzgummer S, Tonutti E, Bassetti D, Pesente F, et al. Automated antinuclear immunofluorescence antibody screening: A comparative study of six computer-aided diagnostic systems. Autoimmun Rev. 2014;13(3):292-8.
4. Kavanaugh A, Tomar R, Reveille J, Solomon DH, Homburger HA. Guidelines for clinical use of the antinuclear antibody test and tests for specific autoantibodies to nuclear antigens. American College of Pathologists. Arch Pathol Lab Med. 2000;124(1):71-81.
5. Damoiseaux J, Andrade LEC, Carballo OG, Conrad K, Francescantonio PLC, Fritzler MJ, et al. Clinical relevance of HEp-2 indirect immunofluorescent patterns: the International Consensus on ANA patterns (ICAP) perspective. Ann Rheum Dis. 2019;78(7):879-89.
6. Andrade LEC, Klotz W, Herold M, Musset L, Damoiseaux J, Infantino M, et al. Reflecting on a decade of the international consensus on ANA patterns (ICAP): Accomplishments and challenges from the perspective of the 7th ICAP workshop. Autoimmun Rev. 2024;23(9):103608.
7. Infantino M, Meacci F, Grossi V, Manfredi M, Benucci M, Merone M, et al. The burden of the variability introduced by the HEp-2 assay kit and the CAD system in ANA indirect immunofluorescence test. Immunol Res. 2017;65(1):345-54.
8. Cinquanta L, Bizzaro N, Pesce G. Standardization and quality assessment under the perspective of automated computer-assisted HEp-2 immunofluorescence assay systems. Front Immunol. 2021;12:638863.
9. Kim J, Lee W, Kim GT, Kim HS, Ock S, Kim IS, et al. Diagnostic utility of automated indirect immunofluorescence compared to manual indirect immunofluorescence for anti-nuclear antibodies in patients with systemic rheumatic diseases: A systematic review and meta-analysis. Semin Arthritis Rheum. 2019;48(4):728-35.
10. Mahler M, Meroni PL, Bossuyt X, Fritzler MJ. Current concepts and future directions for the assessment of autoantibodies to cellular antigens referred to as anti-nuclear antibodies. J Immunol Res. 2014;2014:315179.
11. van Beers JJBC, Hahn M, Fraune J, Mallet K, Krause C, Hormann W, et al. Performance analysis of automated evaluation of antinuclear antibody indirect immunofluorescent tests in a routine setting. Auto Immun Highlights. 2018;9(1):8.
12. Li Z, Han R, Yan Z, Li L, Feng Z. Antinuclear antibodies detection: A comparative study between automated recognition and conventional visual interpretation. J Clin Lab Anal. 2019;33(1):e22619.
13. Park Y, Kim SY, Kwon GC, Koo SH, Kang ES, Kim J. Automated versus conventional microscopic interpretation of antinuclear antibody indirect immunofluorescence test. Ann Clin Lab Sci. 2019;49(1):127-33.
14. Yoo IY, Oh JW, Cha HS, Koh EM, Kang ES. Performance of an automated fluorescence antinuclear antibody image analyzer. Ann Lab Med. 2017;37(3):240-7.
15. Loock CD, Egerer K, Feist E, Burmester GR. Automated evaluation of ANA under real-life conditions. RMD Open. 2017;3(1):e000409.
16. Daves M, Blecken J, Matthias T, Frey A, Perkmann V, Dall´ Acqua A, et al. New automated indirect immunofluorescent antinuclear antibody testing compares well with established manual immunofluorescent screening and titration for antinuclear antibody on HEp-2 cells. Immunol Res. 2017;65(1):370-4.
17. Durmuş MA, Kömeç S, Gülmez A. Artificial intelligence applications for immunology laboratory: image analysis and classification study of IIF photos.

Immunol Res. 2024;72(6):1277-87.

18. Hobson P, Lovell BC, Percannella G, Vento M, Wiliem A. Classifying anti-nuclear antibodies HEp-2 images: A benchmarking platform. 22nd International Conference on Pattern Recognition. 2014. p.3233-8.

19. Hobson P, Lovell BC, Percannella G, Vento M, Wiliem A. Benchmarking human epithelial type 2 interphase cells classification methods on a very large dataset. Artif Intell Med. 2015;65(3):239-50.

20. Boral B, Togay A. Automatic classification of antinuclear antibody patterns with machine learning. Cureus. 2023;15(9):e45008.

21. Won DIL. Measurements of endpoint titers based on the fluorescence intensity trend in anti-nuclear antibody testing. Lab Med. 2020;51(5):469-77.

22. Tebo AE. Recent Approaches to optimize laboratory assessment of antinuclear antibodies. Clin Vaccine Immunol. 2017;24(12):e00270-17.

Association of Hepatitis B Virus Polymerase/Surface Gene Overlap Mutations Developed in Nucleos(t)id Analogue Treatments of Chronic Hepatitis B with Hepatocellular Carcinoma

Kronik Hepatit B'nin Nükleoz(t)id Analoğu Tedavilerinde Gelişen Hepatit B Virüsü Polimeraz/Yüzey Geni Çakışma Mutasyonlarının Hepatosellüler Karsinom ile İlişkisi

Seda EREM BASMAZ[1]
[ID] *0000-0002-1734-872X*
Sadettin HÜLAGÜ[2]
[ID] *0000-0001-6659-1286*
Murat SAYAN[3,4]
[ID] *0000-0002-4374-7193*
Yeşim Saliha GÜRBÜZ[5]
[ID] *0000-0002-1201-1968*

[1]Endocrinology and Metabolic Diseases Clinic, Kocaeli City Hospital, Kocaeli, Türkiye

[2]Grand National Assembly of Türkiye, Türkiye Büyük Millet Meclisi, Ankara, Türkiye

[3]Clinical Laboratory, PCR Unit, Kocaeli University, Kocaeli, Türkiye

[4]DESAM Research Institute, Near East University, Nicosia, Northern Cyprus

[5]Department of Medical Pathology, İstinye University Faculty of Medicine, İstanbul, Türkiye

ABSTRACT

Aim: Nucleos(t)id analogs (NA) used in hepatitis B virus (HBV) treatment may cause rtA181T and sW172* mutations. sW172* increases progression to hepatocellular carcinoma (HCC). This study aimed to reveal the rtA181T/sW172* mutation in HCC patients on the background of chronic hepatitis B (CHB) to determine its association with NA.

Material and Methods: A total of 90 CHB patients, 42 patients with HCC (DNA of 4 patients could not be analyzed), and 48 patients without HCC as the control group, were included in this study. Patients in the control group were divided into two groups, those who received NA treatment (n=21) and those who did not (n=21). Drug resistance analysis was performed by DNA sequencing.

Results: Among the 42 patients with HCC, the median age was 63 (range, 37-81) years, and the median HBV DNA level was 6.0×10^6 (range, $30-1.14 \times 10^8$) IU/ml. In the 48 patients included as controls, the median age and HBV DNA level were 46 (range, 20-75) years and 1.41×10^7 (range, $80-1.70 \times 10^8$) IU/ml in the treatment-naive patients, and 36 (range, 21-50) years and 7.6×10^6 (range, $15.9 \times 10^2 - 5.1 \times 10^7$) IU/ml in the NA-treated patients, respectively. sW172* mutation, which causes rtA181T mutation to occur, was identified in only 2 (5.3%) patients in the study group with HCC.

Conclusion: Association between HCC and rtA181T/sW172* mutation suggests that HCC may develop in patients under NA treatment. The rtA181T/sW172* mutation should be screened in patients receiving treatment, and when detected, they should be closely monitored for HCC development.

Keywords: Hepatocellular carcinoma; hepatitis B virus; drug resistance; nucleos(t)id analog.

ÖZ

Amaç: Hepatit B virüsü (HBV) tedavisinde kullanılan nükleoz(t)id analogları (NA), rtA181T ve sW172* mutasyonlarına neden olabilir. sW172* hepatosellüler karsinoma (hepatocellular carcinoma, HCC) ilerlemesini artırır. Bu çalışmanın amacı, kronik hepatit B (chronic hepatitis B, CHB) zemininde HCC hastalarında rtA181T/sW172* mutasyonunu ortaya koyarak NA kullanımı ile ilişkisini belirlemektir.

Gereç ve Yöntemler: Bu çalışmaya, 42 HCC'li hasta (4 hastanın DNA'sı analiz edilemedi) ve kontrol grubu olarak 48 HCC'siz hasta olmak üzere toplam 90 CHB hastası dahil edildi. Kontrol grubundaki hastalar, NA tedavisi alanlar (n=21) ve almayanlar (n=27) olmak üzere iki gruba ayrıldı. İlaç direnci analizi DNA sekanslama yöntemi ile gerçekleştirildi.

Bulgular: HCC'li 42 hastada, ortanca yaş 63 (aralık, 37-81) yıl ve ortanca HBV DNA düzeyi 6.0×10^6 (aralık, $30-1.14 \times 10^8$) IU/ml idi. Çalışmaya kontrol olarak dahil edilen 48 hastada, ortanca yaş ve HBV DNA düzeyi, sırasıyla, tedavi naif hastalarda 46 (aralık, 20-75) yıl ve 1.41×10^7 (aralık, $80-1.70 \times 10^8$) IU/ml ve NA tedavisi alan hastalarda 36 (aralık, 21-50) yıl ve 7.6×10^6 (aralık, $15.9 \times 10^2 - 5.1 \times 10^7$) IU/ml idi. Çalışma grubundaki HCC'li hastaların sadece 2'sinde (%5,3), rtA181T mutasyonunun ortaya çıkmasına neden olan sW172* mutasyonu tespit edildi.

Sonuç: HCC ile rtA181T/sW172* arasındaki ilişki, NA tedavisi alan hastalarda HCC gelişebileceğini düşündürmektedir. Tedavi alan hastalarda rtA181T/sW172* mutasyonu taranmalı ve tespit edildiğinde hastalar HCC gelişimi açısından yakın takip edilmelidir.

Anahtar kelimeler: Hepatosellüler karsinom; hepatit B virüsü; ilaç direnci; nükleoz(t)id analoğu.

INTRODUCTION

Hepatocellular carcinoma (HCC) is one of the most common hepatic malignancies and the sixth most common cancer worldwide (1). Hepatitis B virus (HBV) is a risk factor for HCC. 20-30% of adults with chronic hepatitis B (CHB) will develop cirrhosis and/or HCC (2). The molecular processes underlying HCC development are complex and various, either independent of liver disease etiology or etiology-related. The reciprocal interlinkage among non-viral and viral risk factors, the damaged cellular microenvironment, the dysregulation of the immune system, and the alteration of gut-liver-axis are known to participate in liver cancer development and progression (3). HBV genome, due to its ability to integrate into the host, can cause genomic instability, disrupting normal regulatory mechanisms (4).

HBV genome is a circular, double-stranded DNA virus that contains four readable gene regions (ORFs). Gene regions encode envelope (pre-S/S/S), core (pre-core/core), pol, and X protein. Pre-S/S/S region synthesizes L, M, and S surface glycoproteins. The pre-core/core region encodes nucleocapsid core protein and synthesizes HBeAg. The pol gene encodes a DNA polymerase, which is reverse transcriptase (RT) (5). HBx protein is a multifunctional regulator, and X protein plays an essential role in the progression of HCC (6).

X protein modulates cellular transcription, protein degradation, proliferation, and apoptotic signaling pathways; it does not directly bind to DNA but affects cells by altering protein-protein interactions and cytoplasmic signaling pathways (7).

Nucleos(t)id analog (NA) used in CHB treatment causes point mutations. These mutations may cause drug resistance (8). Drug resistance is classified into two groups as primary resistance and compensatory mutations. Primary drug resistance mutations mainly lead to non-responsiveness, and compensatory mutations repair replication ability due to the circular structure of HBV pol and S gene overlap (9). This overlapping (pol/S) leads to changes in the region encoding HBsAg protein in primary/compensatory drug resistance mutations. According to findings obtained in recent years, it leads to the formation of potential vaccine escape mutations, namely antiviral drug-associated potential vaccine escape mutation (ADAPVEM) (10).

Lamivudine (LMV) and adefovir (ADV) are safe and inexpensive for long-term use in the treatment of CHB. For this reason, it is used widely and for a long time. Resistance to these drugs develops as a result of long-term use (11). Due to the circular structure of HBV, gene loci overlap each other. As a result of this overlap, point mutations occur. The main one is rtA181T (major drug resistance mutation) on the pol gene, causing sW172* mutation on the S gene (9). The stop codon (sW172*) mutation causes large pieces from the C-terminal hydrophobic area to be cut off and these pieces to accumulate in the cell. L, M surface proteins accumulating within the cell cause stress in the endoplasmic reticulum, leading to progression to HCC (12).

The goal of this study was to indicate the presence of the rtA181T/sW172* mutation in patients who developed HCC at the CHB level and reveal the relationship of these mutations with NA use.

MATERIAL AND METHODS

Forty-two patients over 18 years with HCC and who were admitted to the Gastroenterology Department of the Kocaeli University Faculty of Medicine between 2012 and 2014 were included in the study. Patients were diagnosed by the combination of serologic markers, imaging techniques, and/or biopsy. Serum from 19 patients and biopsy material from 23 patients were used. HBV, hepatitis C virus (HCV), human immunodeficiency virus (HIV), hepatitis D virus (HDV) markers, and HBV DNA were analyzed. Patients with positive HBV DNA levels were included (n=38). Biopsy materials constituting the other part of the study group were obtained from the Pathology Department of the Kocaeli University Faculty of Medicine. As the control group, 48 patients with CHB were divided into two groups as treatment naive (n=27) and patients receiving NA treatment (n=21). The study was conducted with the decision of the Kocaeli University Clinical Research Ethics Committee (2012/67).

Patient history was obtained, including their age, gender, smoking and alcohol use, as well as whether they were receiving antiviral treatment and the duration of the treatment. The presence and staging of cirrhosis were assessed, and the classification of HCC was determined based on clinical conditions and imaging methods. A 5 cc blood sample was collected and serum was separated by centrifugation and stored at -20 ºC. Patient files with pathologic materials were scanned, and information regarding age, gender, alcohol use, antiviral treatment, cirrhosis status, HCC staging, and clinical status was examined. Serum and pathology materials were analyzed using the HBV DNA sequencing method.

Hepatitis B Virus DNA Isolation

HBV DNA was isolated on the QIAsymphony SP magnetic particle isolation platform (QIAGEN GmbH, Hilden, Germany). Paraffin block sections were analyzed using the DNA spin column isolation technique (DNA MiniElute, QIAGEN GmbH, Hilden, Germany).

Real-Time Polymerase Chain Reaction

HBV DNA was analyzed by real-time polymerase chain reaction (PCR) using an RGQ kit on the Rotor-GENE platform (QIAGEN GmbH, Hilden, Germany) (13). HBV genotype detection, all known primary/compensatory NA resistance mutations, S gene (HBsAg protein; amino acids 111 to 227) mutations overlapping with pol gene were analyzed by sequencing HBV pol gene (RT region, amino acids 80 to 250), removal of paraffin with xylol (14). HBV DNA was isolated from the serum sample (Anatolia Geneworks, Bosphore® Viral DNA Extraction Spin Kit, and Magnesia® 16 Magnetic Bead Extraction System, İstanbul, Türkiye). For HBV pol gene (742 bp) amplification, forward (F:5'-tcgtggtggacttctctctcaatt-3'), reverse (R:5'-cgttgacagacttccaatcaat-3') primers were used. PCR conditions were pre-denaturation at 95 °C for 10 minutes, followed by 35 cycles of 95 °C for 45 seconds, 60 °C for 45 seconds, and 72 °C for 45 seconds. PCR products were purified with a High Pure PCR Product Purification Kit (Roche Diagnostics, Germany). Phire Hot Start DNA polymerase (Finnzymes Oy, Finland) was used in the sequencing protocol. Sequencing was performed on the ABI PRISM 3130 (Applied Biosystems Inc, USA) platform using BigDye Terminator v3.1 Cycle Sequencing Kit (Amersham Pharmacia Biotech Inc, USA), 36 cm

capillary and POP-7 TM polymer (Applied Biosystems Inc, USA) according to manufacturer's recommendations. PCR protocol used for direct sequencing was 35 cycles of 95 °C for 20 seconds, 50 °C for 25 seconds, and 60 °C for 2 minutes. Electropherograms were obtained using Vector NTI v5.1 (InforMax, Invitrogen, Life Science Software, USA). Sequences were analyzed in the Geno2pheno Drug Resistance program (Center of Advanced European Studies and Research, Germany).

The Geno2pheno program compares unknown nucleic acid sequences in FASTA format with reference sequences found in the database. After comparison, 80th, 84th, 85th, 91st, 169th, 173rd, 180th, 181st, 184th, 191st, 194th, 202nd, 204th, 214th, 215th, 233rd, 236th-238th, and 250th amino acid positions in HBV pol gene RT coil were analyzed for primary drug resistance and compensatory mutations. In addition, 121st, 135th, 137th, 139th-149th, 151st-153rd, 155th-157th, 161st, 164th, 172nd, 173rd, 175th, 176th, 182nd, and 193rd-196th amino acid positions in the S gene region overlapping with the HBV RT strand were analyzed for mutations (15).

Statistical Analysis
For statistical analysis, IBM SPSS version 20.0 was used. Following the normal distribution assumption, the student t test was used to compare groups as a parametric test, and the Mann-Whitney U test was used as a non-parametric one. Chi-square test was used to analyze categorical data. A p-value of <0.05 was considered statistically significant.

RESULTS
A total of 90 patients were divided into three groups. Patients with HCC (n=42) were included in the study group, and patients with CHB without HCC (n=48) were included in the control group. The control group was further divided into two groups as those receiving NA treatment (n=21) and those not receiving (n=27). Diagnosis of HCC was made by biopsy in 23 patients by combining alpha fetoprotein (AFP) value and HCC typical appearance in 2 imaging modalities in 19 patients. HBV DNA sequencing analysis could be performed in 38 (90.5%) patients in the study group. The majority of patients in the study groups were male, the mean age was higher in the HCC group compared to other groups (Table 1). When the HbeAg status of these patients was compared, no significant difference was found (p=0.478). Patients did not have superinfection/co-infection.

Information on AFP values, the presence of cirrhosis, and the alcohol intake status of patients with HCC was shown in Table 1. The majority of patients with cirrhosis and HCC were found to be C in Child-Pugh staging.

Table 1. Demographic information of the patients included in the study

	Study Group (n=42)	No Treatment (n=27)	NA Treatment (n=21)
Gender, n (%)			
Male	38 (90.5)	17 (63.0)	14 (66.7)
Female	4 (9.5)	10 (37.0)	7 (33.3)
Age (years), median (range)	63 (37 - 81)	46 (20 - 75)	36 (21 - 50)
AST (U/L), median (range)	142 (20 - 968)	41 (18 - 41)	135 (11 - 1042)
ALT (U/L), median (range)	179 (20 - 1021)	48 (18 - 48)	182 (17 - 1315)
HBeAg[*1] (+), n (%)	10 (25.0)	3 (11.1)	6 (28.6)
HBV DNA (IU/ml), median (range)	6.0×10^6 (30 - 1.14×10^8)	1.41×10^7 (80 - 1.70×10^8)	7.6×10^6 (15.9×10^2 - 5.1×10^7)
HBV genotype[*2] (D), n (%)	38 (100)	27 (100)	21 (100)
HBV sub genotype[*2], n (%)			
D1	35 (92.1)	26 (96.3)	17 (81.0)
D2	-	1 (3.7)	2 (9.5)
D3	3 (7.9)	-	2 (9.5)
AFP (ng/ml), median range	20025 (1-521300)	-	-
Cirrhosis[*3] (+), n (%)	32 (82.1)	-	-
Child-Pugh Staging, n (%)			
A	3 (9.4)		
B	9 (28.1)	-	-
C	20 (62.5)		
Treatment[*4], n (%)	18 (42.9)	-	21 (100)
Treatment[*4], n (%)			
LAM	11 (61.0)		12 (57.1)
ADV	1 (5.6)		5 (23.8)
LdT	1 (5.6)		1 (4.8)
ETV	1 (5.6)	-	3 (14.3)
LAM+ADV	2 (11.1)		-
LAM+TDF	2 (11.1)		-
Duration (month), median (range)			
LAM	43 (1 - 96)	-	26 (12 - 48)
ADV	32 (12 - 60)	-	20 (8 - 36)
LdT	1	-	9
ETV	12	-	18 (12 - 24)
TDF	90 (84 - 96)	-	-

NA: nucleos(t)id analog, AST: aspartate aminotransferase, ALT: alanine aminotransferase, HBeAg: hepatitis B e antigen, HBV: hepatitis B virus, DNA: deoxyribonucleic acid, AFP: alpha fetoprotein, LAM: lamivudine, ADV: adefovir; LdT: telbivudine; ETV: entecavir; TDF: tenofovir, [*1]: no information on HBeAg status in two patients, [*2]: HBV DNA sequencing analysis could be performed in 38 patients, [*3]: no information on cirrhosis status in three patients, [*4]: no information on medication use in three patients

Patients were classified according to drug use. The HBV pol gene region was analyzed for drug resistance mutations in the study and the control group. Primary drug resistance, partial drug resistance, and compensatory mutations were analyzed. Primary drug resistance mutations (rtM204I/V, rtA181T, rtA184V, rtT184A/S) were detected in the study group and the NA control group, and were frequently associated with NA. No primary drug resistance mutations were detected in the treatment-naive control group.

Mutations causing primary drug resistance (rtM204I, rtA181T, rtA184V, rtT184S) were detected in 8/38 (21.1%) of the HCC group. In the control group, drug resistance mutations (rtM204I, rtM204V, rtT184A) were detected in 6/21 (28.6%) of the NA-treated group. No primary drug resistance was found in the treatment-naive group. When the groups were compared in terms of the primary drug resistance, no significant difference was found (p=0.833). In the control group, partial drug resistance mutations were associated with NA. In contrast to primary drug resistance mutations, partial resistance mutations were found in the treatment-naive control group. Replication capacity restoring, viral load increasing mutations, and compensatory mutations (L91I, Q215H/S, Q149K) were detected in the study and control groups (Table 2).

The potential of oral antivirals used in the treatment of CHB to create vaccine escape mutations (ADAPVEM) was analyzed (Table 3). While no ADAPVEM patterns were detected in the treatment-naive control group, ADAPVEM patterns were detected in the study group and the control group under NA treatment. While sS143L, sW196L, and sW172* were detected in the study group, sI195M and W196L patterns were detected in the control group under treatment. The sW172* ADAPVEM detected in the study group is also the mutation that causes HBsAg to accumulate in the cell after truncation (Table 3). The W172* development rate between patients in the study group and the control group was not statistically significant (p=0.192). When the duration of drug use in both groups (HCC and NA treatment groups) was compared, no statistically significant difference was found between them (p=128 for LAM, p=0.252 for ADV).

DISCUSSION

Global distribution of HCC depends on regions, incidence rate, gender, age, and etiology (16). The prevalence of HBV RT mutations prior to treatment varies. The ratio of HCC incidence in the non-cirrhotic and cirrhotic stages in HBV-related liver disease is 0.3-3.23% (17). These controversial mutations depend on geographic factors, HBV genotypes, HBeAg serostatus, HBV viral loads, and disease progression (18).

The median age of 42 HCC patients included in the present study was found to be higher compared to the control group. Studies have reported that 80-90% of patients with HCC have cirrhosis. A cohort study conducted in Italy showed that patients with stages B and C, according to Child-Pugh staging, had a higher risk of developing HCC compared to stage A (19). In the present study, the rate of cirrhosis in patients with HCC was similarly high (82.1%). When HCC patients with cirrhosis, a high proportion of patients were found to be in the Child C stage (62.5%).

Studies have shown that basal loads of HBV DNA are important in progression to HCC (20). In the present study,

Table 2. HBV polymerase gene mutations and drug resistance status in study and control groups

Mutation Pattern	Study Group* (n=42)	No Treatment (n=27)	NA Treatment (n=21)
Primary Drug Resistance, n (%)			
M204I	4 (10.5)	-	3 (14.3)
M204V	-	-	2 (9.5)
A181T	2 (5.3)	-	-
A184V	1 (2.6)	-	-
T184A	-	-	1 (4.8)
T184S	1 (2.6)	-	-
Partial Drug Resistance, n (%)			
A194S	1 (2.6)	-	-
A194X	-	1 (3.7)	-
C233F	1 (2.6)	-	-
P236T	1 (2.6)	-	-
L180M	1 (2.6)	-	5 (23.8)
Compensatory Mutation, n (%)			
L91I	2 (5.3)	-	4 (19.1)
Q215H/S	9 (23.7)	-	5 (23.8)
Q149K	1 (2.6)	1 (3.7)	3 (14.3)

HBV: hepatitis B virus, NA: nucleos(t)id analog, *: HBV DNA sequencing analysis could be performed in 38 patients

Table 3. Potential vaccine escape mutations associated with oral antivirals in the study and control groups

Mutation Pattern	Study Group* (n=42)	No Treatment (n=27)	NA Treatment (n=21)
ADAPVEM, n (%)			
I195M	-	-	2 (9.5)
S143L	3 (7.9)	-	-
W196L	4 (10.5)	-	3 (14.3)
W172*	2 (5.3)	-	-

NA: nucleos(t)id analog, ADAPVEM: antiviral drug-associated potential vaccine escape mutation, *: HBV DNA sequencing analysis could be performed in 38 patients

the median HBV DNA load was found to be higher in the treatment-naive group. This finding may be due to the suppression of HBV DNA loads after antiviral drug use in the study group and the group receiving NA.

The long-term use of NA therapy can result in drug resistance, which can lead to treatment failure (21). It has been shown that primary drug resistance developed in CHB treatment increases the risk of HCC (8). One study reported that HCC developed in 8 of 141 HCC patients with sL21*, sW156*, and sW172* mutations. This study may be important in showing that HCC develops after the use of LAM (8,20).

In another study conducted in South Korea between January 2004 and December 2012, it was reported that the risk of HCC development increased in patients who developed drug resistance. Cumulative risk of HCC development in cirrhotic patients who developed drug resistance in years 1, 2, 3, and 5 was found to be 3.93%, 5.55%, 6.71%, and 9.02% (22).

In a study involving 1948 CHB patients, 917 patients were found to have a drug-resistance gene mutation in the RT region (47.07%). HBV-related cirrhosis rate and HBV DNA load were higher in the group with drug resistance

than in the group without mutation. In patients with drug resistance, 53 gene mutation patterns were found. Among these patterns, rtL180M+rtM204V+rtS202G (9.70%) was the most dominant pattern. Five types of drug resistance were detected, the highest being LAM+Ldt (21.25%). Among 18 regions associated with LAM, ADV, ETV, and Ldt resistance in HBV RT regions, 14 regions were found to be mutated, and the most common mutation regions were rtL180M, rtM204V, rtM204, and rtS202G (23).

In the present study, mutations causing primary drug resistance (rtM204I, rtA181T, rtA184V, rtT184S) were identified in 8/38 (21.1%) of HCC patients. Mutations causing drug resistance (rtM204I, rtM204V, rtT184A) were identified in 6/21 (28.6%) of the group receiving NA. When groups using NA were compared, no statistically significant difference was found in terms of prevalence of primary resistance. However, the A181T mutation was identified in the HCC patient group (2/38, 5.3%), which was not found in the NA-treated control group. In HCC patients with the A181T mutation, the W172* mutation in the S gene. The median duration of LAM and ADV treatments, which are known to be responsible for the development of the rtA181T mutation, was 43 and 32 months in the HCC patient group and 26 and 20 months in the NA-treated group. The rate of W172* development between the study and control group was not statistically significant. When the duration of drug use was compared in HCC and NA groups, the difference was not statistically significant. Development of the A181T mutation may be independent of the duration of LAM and ADV use. This data shows that HBsAg escape mutations with epidemiologic and clinical significance can develop due to NA.

In another study, 100 patients who had been undergoing NA therapy for one year or more were included. 84 patients that could be sequenced with HBV pol gene HBV, 53 (63.09%) were males and 31 (36.91%) were females, and the mean age was 47±14.99 (range, 20-67) years. Primary/secondary drug mutations (rtM204I/V, rtI169S, rtL180M, rtT184L, rtA194V, rtM204I/rtL91I, rtQ149K, rtQ215H/S, rtN238D) were detected in 38 (45.2%) of the patients. Because of the HBV pol/S gene overlapping, in 27 patients immune-selected amino acid substitutions (sI110L, sT127P, sS114A, sT123A), in nine patients HBIg selected escape mutants (sP120R, sT123N, sE164D, sY134F, sQ129H, sT118A, sP127K), in seven patients vaccine escape mutants (sT126I, sP120S, sG145A, sS193L), and in one patient misdiagnosis of HBsAg (sT131I) were detected. In addition, ADAPVEM in 13 (15.4%) patients (20).

In a study, 6 types of ADAPVEM (sE164D, sI195M, sW196L, sW172L, sL175F, s176V) were identified in 10/94 (10.6%) patients (24). In another study, seven different ADAPVEM (rtM204V/sI195M, rtM204I/sW196S, rtM204I/sW196L, rtV173L/sE164D, rtA181T/sW172*, rtA181T/sW172L, and rtA181V/sL173F) mutations were found in 46/442 (10.4%). In this study, the rate of ADAPVEM in NA-treated and treatment-naive patients was found to be 44/186 (23.7%) and 2/256 (0.78%), respectively, and was reported statistically significant (24). The present study identified four different ADAPVEM. While 7/38 (18.4%) ADAPVEM were detected in the study group (sS143L, sW196L, sW172*), 5/21 (23.8%) were detected in the NA-treated control group (sW196L, sI195M). No ADAPVEM was found in the treatment naive control group. As in similar studies, ADAPVEM was observed only in NA-treated patients in this study. These findings suggest that NA treatment plays a role in the occurrence of ADAPVEM. sW172* causes accumulation of HBsAg in hepatocytes was detected only in 2/38 (5.3%) patients in the HCC group. In these patients, HBsAg accumulation in hepatocytes may be effective in HCC progression.

In another study, it was reported that drug resistance was detected in 36/198 (18.2%) of patients in whom NA was initiated in 320 decompensated cirrhotic patients. Among these patients, HCC was detected in 5 patients who did not respond to salvage therapy, and it was reported that the rtA181T mutation was associated with salvage therapy failure. However, since S gene analysis was not performed in this study, it was not stated whether the rtA181T leads to sW172*. However, according to the study, NA drug resistance plays a role in the cumulative incidence of HCC (24). Results of both studies indicate that patients should be followed up in the long term.

Major limitations of this study include a relatively small sample size, lack of follow-up from the initiation of the treatment, and lack of timing of HCC diagnosis.

CONCLUSION
The rtM204I, rtA181T, rtA184V, and rtT184S mutations causing primary drug resistance were found in 21.1% of HCC patients. In the control group, rtM204I, rtM204V, and rtT184A mutations were found in 28.6% of patients receiving NA. The relationship between HCC development and the rtA181T/sW172* mutation duo in CHB patients under NA treatment may be assessed in a larger study group with longer patient follow-up for more certain findings.

REFERENCES

1. Fidan E, Fidan S, Merev E, Kazaz N. The relationship between albumin-bilirubin grade and survival in hepatocelluler carcinoma patients treated with sorefanib. Nijer J Clin Pract. 2022;25(2):173-7.

2. Kumar R. Review on hepatitis B virus precore/core promoter mutations and their correlation with genotypes and liver disease severity. World J Hepatol. 2022;27(4):708-18.

3. Stella L, Santopaolo F, Gasbarrini A, Pompili M, Ponziani FR. Viral hepatitis and hepatocellular carcinoma: From molecular pathways to the role of clinical surveillance and antiviral treatment. World J Gastroenterol. 2022;28(21):2251-81.

4. Perisetti A, Goyal H, Yendala R, Thandassery RB, Giorgakis E. Non-cirrhotic hepatocellular carcinoma in chronic viral hepatitis: Current insights and advancements. World J Gastroenterol. 2021;27(24):3466-82.

5. Fang ZL, Sabin CA, Dong BQ, Ge LY, Wei SC, Chen QY, et al. HBV A1762T, G1764A mutations are a valuable biomarker for identifying a subset of male HBsAg carriers at extremely high risk of hepatocellular carcinoma: a prospective study. Am J Gastroenterol. 2008;103(9):2254-62.

6. Motavaf M, Safari S, Saffari Jourshari M, Alavian SM. Hepatitis B virus-induced hepatocellular carcinoma: the role of the virus X protein. Acta Virol. 2013;57(4):389-96.

7. Bouchard MJ, Schneider RJ. The enigmatic X gene of hepatitis B virus. J Virol. 2004;78(23):12725-34.

8. Warner N, Locarnini S. Can antiviral therapy for chronic hepatitis B enhance the progression to hepatocellular carcinoma? Antivir Ther. 2009(14):139-42.

9. Locarnini S. Primary resistance, multidrug resistance, and cross-resistance pathways in HBV as a consequence of treatment failure. Hepatol Int. 2008;2(2):147-51.

10. Sheldon J, Rodès B, Zoulim F, Bartholomeusz A, Soriano V. Mutations affecting the replication capacity of the hepatitis B virus. J Viral Hepat. 2006;13(7):427-34.

11. Lai MW, Yeh CT. The oncogenic potential of hepatitis B virus rtA181T/surface truncation mutant. Antivir Ther. 2008;13(7):875-9.

12. Qi X, Xiong S, Yang H, Miller M, Delaney WE 4th. In vitro susceptibility of adefovir-associated hepatitis B virus polymerase mutations to other antiviral agents. Antivir Ther. 2007;12(3):355-62.

13. Kim JH, Jung YK, Joo MK, Kim JH, Yim HJ, Park JJ, et al. Hepatitis B viral surface mutations in patients with adefovir resistant chronic hepatitis B with A181T/V polymerase mutations. J Korean Med Sci. 2010;25(2):257-64.

14. Bock CT, Tillmann HL, Torresi J, Klempnauer J, Locarnini S, Manns MP, et al. Selection of hepatitis B virus polymerase mutants with enhanced replication by lamivudine treatment after liver transplantation. Gastroenterology 2002;122(2):264-73.

15. Avellón A, Echevarria JM. Frequency of hepatitis B virus 'a' determinant variants in unselected Spanish chronic carriers. J Med Virol. 2006;78(1):24-36.

16. Bracco C, Gallarate M, Badinella Martini M, Magnino C, D'Agnano S, Canta R, et al. Epidemiology, therapy and outcome of hepatocellular carcinoma between 2010 and 2019 in Piedmont, Italy. World J Gastrointest Oncol. 2024;16(3):761-72.

17. Tarao K, Nozaki A, Ikeda T, Sato A, Komatsu H, Komatsu T, et al. Real impact of liver cirrhosis on the development of hepatocellular carcinoma in various liver diseases-meta-analytic assessment. Cancer Med. 2019;8(3):1054-65.

18. Choi YM, Lee SY, Kim BJ. Naturally occurring hepatitis B virus reverse transcriptase mutations related to potential antiviral drug resistance and liver disease progression. World J Gastroenterol. 2018;24(16):1708-24.

19. Bolondi L, Sofia S, Siringo S, Gaiani S, Casali A, Zironi G, et al. Surveillance programme of cirrhotic patients for early diagnosis and treatment of hepatocellular carcinoma: a cost effectiveness analysis. Gut. 2001;48(2):251-9.

20. Kırdar S, Yaşa MH, Sayan M, Aydın N. HBV pol/S gene mutations in chronic hepatitis B patients receiving nucleoside/nucleotide analogues treatment. Mikrobiyol Bul. 2019;53(2):144-55. Turkish.

21. Yeh CT, Shen CH, Tai DI, Chu CM, Liaw YF. Identification and characterization of a prevalent hepatitis B virus X protein mutant in Taiwanese patients with hepatocellular carcinoma. Oncogene. 2000;19(46):5213-20.

22. Jun CH, Hong HJ, Chung MW, Park SY, Cho SB, Park CH, et al. Risk factors for hepatocellular carcinoma in patients with drug-resistant chronic hepatitis B. World J Gastroenterol. 2013;19(40):6834-41.

23. Bian CR, Li JJ, Song YW, Song LJ, Zhao J, Dong RM, et al. Analysis of characteristics of drug resistance gene mutation in HBV RT region of hepatitis B infected patients. Zhonghua Yu Fang Yi Xue Za Zhi. 2023;57(6):868-76. Chinese.

24. Zhang ZH, Wu CC, Chen XW, Li X, Li J, Lu MJ. Genetic variations of hepatitis B virus and its significance for pathogenesis. World J Gastroenterol. 2016;22(1):126-44.

Evaluation of Vitamin D and Hematological Parameters in Pediatric Non-Scarring Alopecias

Pediatrik Non-Skatrisyel Alopesilerde Vitamin D ve Hematolojik Parametrelerin Değerlendirilmesi

Betül ŞEREFLİCAN
0000-0001-9947-7690
Merve DİLCAN
0000-0001-9870-4767
Mualla POLAT
0000-0001-9226-5134

Department of Dermatology, Bolu Abant İzzet Baysal University Faculty of Medicine, Bolu, Türkiye

ABSTRACT

Aim: Vitamin D is an important factor for the hair follicle cycle. Alopecia areata (AA), androgenetic alopecia (AGA), and telogen effluvium (TE) are the most common forms of non-scarring alopecia. This study aimed to define vitamin D levels and hemogram parameters in children and adolescents with non-cicatricial alopecia.

Material and Methods: A total of 157 patients under the age of 18 and diagnosed with AA, AGA, and TE were included in this retrospective study. Vitamin D levels, and neutrophil/lymphocyte (neu/lym) and platelet/lymphocyte (plt/lym) ratios were evaluated. Vitamin D levels were examined in four different groups according to the admission period as autumn, winter, spring, and summer.

Results: Of the patients, 30 were diagnosed with AA, 11 with AGA, and 116 with TE. Vitamin D deficiency was detected in 128 of 153 patients, of whom vitamin D levels were examined, insufficiency in 20, and sufficiency in 5. There was no statistically significant difference in vitamin D levels between groups (p=0.114). Also, no statistically significant difference was found between the groups in terms of vitamin D deficiency and insufficiency (p=0.403). Vitamin D levels were significantly higher in males than in females (p<0.001), and in autumn than in winter (p=0.043). The ratio of neu/lym in patients with TE was significantly higher than the patients in the AA group (p=0.005).

Conclusion: Vitamin D deficiency was seen in a very high percentage of all non-cicatricial alopecia. Neu/lym ratio may be a more appropriate inflammatory marker for patients with TE than the other nonscarring alopecia.

Keywords: Alopecia; alopecia areata; androgenetic alopecia; vitamin D.

ÖZ

Amaç: D vitamini saç folikülü döngüsü için önemli bir faktördür. Alopesi areata (AA), androgenetik alopesi (AGA) ve telogen effluvium (TE) skarsız alopesilerin en sık görülen formlarıdır. Bu çalışmada non-skatrisyel alopesisi olan çocuk ve adölesanlarda D vitamini düzeylerinin ve hemogram parametrelerininin belirlenmesi amaçlanmıştır.

Gereç ve Yöntemler: Bu geriye dönük çalışmaya AA, AGA ve TE tanısı almış ve 18 yaş altı olan toplam 157 hasta dahil edildi. D vitamini düzeyleri ile nötrofil/lenfosit (neu/lym) ve platelet/lenfosit (plt/lym) oranları değerlendirildi. D vitamini düzeyleri başvuru dönemine göre sonbahar, kış, ilkbahar ve yaz olmak üzere dört farklı grupta incelendi.

Bulgular: Tüm hastaların 30'u AA, 11'i AGA ve 116'sı TE tanısı aldı. D vitamini düzeylerine bakılmış olan 153 hastanın 128'inde D vitamini eksikliği, 20'sinde yetersizlik, 5'inde ise yeterlilik saptandı. Gruplar arasında D vitamini düzeyleri açısından istatistiksel olarak anlamlı bir farklılık yoktu (p=0,114). Ayrıca, gruplar arasında D vitamini eksikliği ve yetersizliği açısından da istatistiksel olarak anlamlı bir fark bulunmadı (p=0,403). D vitamini düzeyleri erkeklerde kadınlara göre (p<0,001) ve sonbaharda kışa göre (p=0,043) anlamlı olarak daha yüksekti. Neu/lym oranı, TE hastalarında AA grubundaki hastalara göre anlamlı olarak daha yüksekti (p=0,005).

Sonuç: Tüm non-skatrisyel alopesilerin çok yüksek bir yüzdesinde D vitamini eksikliği görüldü. Neu/lym oranı TE'li hastalar için diğer non-skatrisyel alopesilerden daha uygun bir inflamatuar belirteç olabilir.

Anahtar kelimeler: Alopesi; alopesi areata; androgenetik alopesi; D vitamini.

Corresponding Author
Sorumlu Yazar
Betül ŞEREFLİCAN
ozbetul@yahoo.com

INTRODUCTION

Hair loss is a clinical condition that is frequently seen in dermatology clinics and affects the quality of life of patients. There are two major categories of hair loss: scarring alopecia and non-scarring alopecia. Alopecia areata (AA), androgenetic alopecia (AGA), and telogen effluvium (TE) exemplify the three most common patterns of non-scarring alopecia (1,2).

Vitamin D is a fat resolvable vitamin and plays a considerable role in bone metabolism, adjustment of the immune system, keratinocyte differentiation, and hair follicle cycle. Vitamin D is generated in the skin and involved in the etiopathogenesis of various diseases, including hair loss (3).

Low vitamin D levels have been shown in patients with non-cicatricial alopecia in several studies (4). However, there are not enough studies in the pediatric age group to understand the effects of vitamin D on non-cicatricial alopecia in childhood.

Neutrophils (neu), lymphocytes (lym), and platelets (plt) play a role in the inflammatory response of the body, and their levels vary depending on the severity of systemic inflammation. Recent studies have shown that the plt/lym and neu/lym ratios can be used as new inflammatory parameters associated with many inflammatory diseases, cardiovascular system diseases, and malignancies (5). AA, AGA, and TE may result from inflammatory conditions (6-8).

The objective of this study was to investigate the levels of vitamin D in patients with AA, AGA, and TE, as well as to evaluate the plt/lym and neu/lym ratios in these patient groups.

MATERIAL AND METHODS

The study included patients under the age of 18 who were referred to the dermatology outpatient clinic of Bolu Abant İzzet Baysal University İzzet Baysal Training and Research Hospital between January 2012 and December 2019 and were diagnosed with AA, AGA, and TE.

In this retrospective study, laboratory information of the patients was evaluated based on their first admission to the dermatology outpatient clinic. Vitamin D levels, plt, lym, and neu counts in the complete blood examination were recorded based on the laboratory values of the patients. Vitamin D values were examined in four different groups according to the admission period: autumn, winter, spring, and summer.

Following the Endocrine Society Clinical Practice Guideline, serum 25 (OH) vitamin D levels ≥30 ng/ml

were considered adequate, levels of 20-29 ng/ml indicate vitamin D insufficiency, and levels below 20 ng/ml indicate vitamin D deficiency (9).

The study was approved by the Bolu Abant İzzet Baysal University Faculty of Medicine Ethics Committee with the decision dated 19.12.2023 and numbered 2023/459.

Statistical Analysis

R v.4.3.0 software was used in statistical analyses. Prior to undertaking any statistical analysis, the Shapiro-Wilk test was employed to ascertain whether the data exhibited a normal distribution. For variables not showing normal distribution, median, 25th-75th percentiles, minimum, and maximum were used as descriptive statistics. Comparison between groups was made with the Kruskal-Wallis test. Mann-Whitney U test with Bonferroni correction was utilized as a post-hoc test to detect the significantly different groups. Cross-tabulations containing absolute frequencies were created for categorical variables, and a chi-squared test was used for statistical analysis, but Fisher's exact test was used where the expected count was less than 5 in a cell. A p-value of <0.05 was determined as the statistical significance level.

RESULTS

Data for 157 patients were obtained. The median age of all patients was 15 (range, 1-17) years. Of the patients, 129 were female and 28 were male. There were 17 females and 13 males in patients with AA, 3 females and 8 males in patients with AGA, and 109 females and 7 males in patients with TE. The details for demographic data and hemogram values according to patient groups were presented in Table 1.

The distribution of plt/lym and neu/lym ratios according to patient groups was shown in Table 1. No significant difference was found in the plt/lym ratios between the groups (p=0.271). A significant difference was observed in neu/lym ratios between the patient groups (p=0.006). The ratio of neu/lym in patients with TE was found to be significantly higher than in the AA group (p=0.005) according to the post hoc test results.

Vitamin D levels were examined in 153 patients, of whom 127 were female and 26 were male. Among them, 29 patients were diagnosed with AA, 10 with AGA, and 114 with TE. While 57 of these patients applied in the autumn, 34 in the winter, 26 in the spring, and 36 in the summer. Vitamin D deficiency was detected in 128 of these patients, insufficiency in 20 patients, and sufficiency in 5 patients. The median vitamin D levels of the patients were

Table 1. Demographic data and hemogram values according to patient groups

	AA (n=30)	AGA (n=11)	TE (n=116)	p
Age (years)	9.5 (5-15) [1-17][a]	16 (15-17) [12-17][b]	16 (14-17) [2-17][b]	**<0.001**
Plt (K/uL)	299 (252-358) [118-573]	254 (225-268) [178-306]	270 (234-318) [162-415]	0.060
Lym (K/uL)	2.5 (2.0-3.4) [1.1-8.7]	2.2 (2.0-3.0) [1.9-3.3]	2.3 (1.9-2.8) [1.0-6.0]	0.227
Neu (K/uL)	3.6 (2.8-4.3) [1.8-8.0]	3.8 (3.2-5.2) [2.7-6.8]	4.2 (3.5-5.5) [1.3-10.3]	0.087
Plt/Lym	115.3 (88.9-146.8) [31.2-301.9]	104.6 (77.6-127.6) [68.6-145.6]	120.4 (95.0-144.6) [38.7-240.9]	0.271
Neu/Lym	1.4 (1.0-1.7) [0.4-4.0][a]	1.7 (1.5-2.0) [1.0-3.0][b]	1.9 (1.3-2.6) [0.4-5.5][b]	**0.006**

AA: alopecia areata, AGA: androgenetic alopecia, TE: telogen effluvium, Plt: platelet, Lym: lymphocyte, Neu: neutrophil, values not sharing a common superscript within each row are significantly different as determined by Bonferroni corrected Mann-Whitney U test, values were presented as median (25th-75th percentile) [minimum-maximum]

found to be 13.4 (range, 4.1-29.2) ng/ml in AA patients, while 15.9 (range, 6.3-25.1) ng/ml in AGA patients, and 11.3 (range, 3.1-35.3) ng/ml in TE patients (Figure 1). No significant difference was observed in vitamin D levels between the groups (p=0.114).

Median vitamin D levels were found significantly higher in males at 17.6 (range, 7.7-29.2) ng/ml, compared to females at 10.5 (range, 3.1-35.3) ng/ml (p<0.001).

The vitamin D levels of the patient groups according to seasons were presented in Table 2. Vitamin D levels showed a significant difference across seasons (p=0.043). Post hoc test with Bonferroni correction showed that vitamin D levels in autumn were significantly higher than those observed in winter.
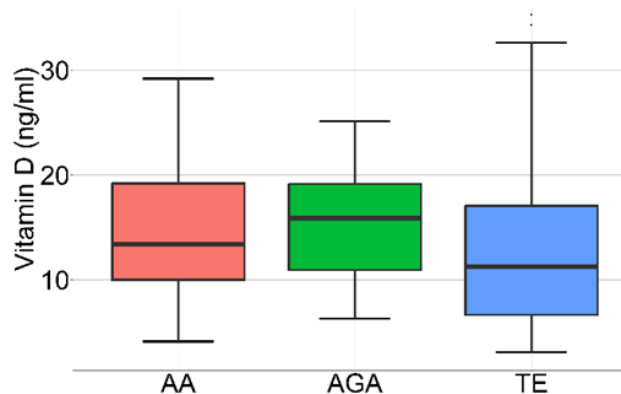

Figure 1. Vitamin D levels in patient groups

Table 2. The vitamin D levels according to the seasons[*]

	Autumn (n=57)	Winter (n=34)	Spring (n=26)	Summer (n=36)	p
VitD (ng/ml)	13.9 (9.3-18.6) [3.1-32.6][a]	9.6 (5.5-14.2) [3.3-31.9][b]	11.3 (6.3-18.2) [4.1-29.2][ab]	10.7 (6.9-19.2) [3.4-35.3][ab]	0.043

VitD: vitamin D, *: vitamin D levels were examined in 153 patients, values not sharing a common superscript within each row are significantly different as determined by Bonferroni corrected Mann-Whitney U test, values were presented as median (25th-75th percentile) [minimum-maximum]

The distribution of vitamin D status according to patient groups was as indicated in Table 3. There was no significant difference between the groups in terms of vitamin D deficiency and insufficiency (p=0.403).

The distribution of patient groups according to the season of admission to the hospital was presented in Table 4. No statistically significant difference was found between the patient groups according to the seasons admitted to the hospital (p=0.582).

Table 3. Vitamin D status according to patient groups

	AA (n=29)	AGA (n=10)	TE (n=114)	p
VitD, n (%)				
Deficiency	23 (79.3%)	9 (90.0%)	96 (84.2%)	
Insufficient	6 (20.7%)	1 (10.0%)	13 (11.4%)	0.403
Sufficient	0 (0.0%)	0 (0.0%)	5 (4.4%)	

VitD: vitamin D, AA: alopecia areata, AGA: androgenetic alopecia, TE: telogen effluvium, *: vitamin D levels were examined in 153 patients

DISCUSSION

Vitamin D levels were shown to be linked to different dermatological diseases, such as atopic dermatitis, psoriasis, vitiligo, and systemic sclerosis (10).

In the study of Gade et al. (11), significant systemic inflammation and vitamin D deficiency were found in patients with AA compared to healthy controls. In the study of Bhat et al. (12), levels of 25(OH)D were lower in AA patients than in the controls. A few studies have failed to identify a significant association between AA and vitamin D (13,14). In a meta-analysis by Liu et al. (15) on 1585 AA patients, a deficiency of serum 25(OH)D level was found. So a relationship between vitamin D and AA can be mentioned (16). In the present study, 79.3% of patients with AA exhibited vitamin D deficiency, with no patients demonstrating sufficient vitamin D levels within this patient group.

Although there are studies examining the relationship between AA and vitamin D levels in adults, there are few studies examining this relationship in the pediatric patient group.

In pediatric AA cases evaluated by Siddappe et al. (17) and Kundak et al. (18), 25(OH)D levels were determined to be lower, and vitamin D deficiency incidence was higher than the controls. In the study conducted by Lim et al. (19), to determine the predictors of vitamin D insufficiency in child and adolescent AA patients, insufficiency was found in 60.4%, and deficiency was found in 38.2% of the patients.

Table 4. Patient groups by seasons

	AA (n=30)	AGA (n=11)	TE (n=116)	p
Season, n (%)				
Autumn	7 (23.3%)	4 (36.4%)	47 (40.5%)	
Spring	8 (26.7%)	2 (18.2%)	17 (14.7%)	
Summer	7 (23.3%)	3 (27.3%)	28 (24.1%)	0.582
Winter	8 (26.7%)	2 (18.2%)	24 (20.7%)	

AA: alopecia areata, AGA: androgenetic alopecia, TE: telogen effluvium

In the study of Unal et al. (20), lower serum 25(OH)D levels in the pediatric AA patients than the controls were detected, but there was no significant difference.

The present study represents low vitamin D levels in AA in the pediatric age group, parallel to the few studies conducted on pediatric AA patients in the literature.

In the study of Tran et al. (21), AA patients had a significantly lower mean vitamin D level than the other alopecias, including cicatricial and noncicatricial. In the study of Öner et al. (22), vitamin D levels in nonscarring alopecia, including AA, TE, and AGA in the pediatric age group and adults, were evaluated. The mean vitamin D levels in all groups indicate vitamin D deficiency. The incidence of patients with vitamin D deficiency was higher in the TE group. In the present study, there was no significant difference in median vitamin D levels between the patient groups.

AGA in pediatric patients is rarely reported in the literature (23). In one study by Losoya-Jaquez et al. (24), 145 AGA patients in the pediatric age group were analyzed, and vitamin D deficiency was found in 84% of the patients. In the present study, vitamin D deficiency was detected in 90% of the patients in a smaller group.

There are studies in the literature showing low levels of vitamin D regarding TE, as well as studies stating the opposite (25-27). In a study conducted on pediatric TE patients, it was reported that the vitamin D deficiency seen in this group of patients was similar to the general pediatric population (28).

The study of Conic et al. (3) evaluated the prevalence of vitamin D deficiency in scarring and nonscarring alopecia. They found vitamin D deficiency in 64.8% of all the patients. TE patients were 3.7 times more likely to have severe vitamin D deficiency than those with AA.

In a recent meta-analysis assessing serum 25(OH)D levels in non-scarring alopecia, decreased serum 25(OH)D levels and increased incidence of vitamin D deficiency were found (4). So, we can say that although there are a few opposite results, in general, low vitamin D levels can be expected in non-cicatricial alopecia.

In the study of Lim et al. (19), children and adolescents with AA showed significantly increased odds of vitamin D insufficiency in the non-summer season. In a meta-analysis by Chen et al. (4) examining non-scarring alopecia in all age groups, there is a study in which vitamin D deficiency was observed in AA patients, particularly in winter and autumn, and one study in which deficiency was observed in almost all seasons. In the present study, vitamin D levels in patients were found to be higher in autumn than in winter. This result can be explained as the result of exposure to sunlight throughout summer and continuing sun exposure in autumn.

Neu/lym ratio and plt/lym ratio are strong predictors of inflammation used in a great deal of diseases (29). However, there are few studies investigating the relationship of these markers with hair diseases. In two studies examining neu/lym ratio and plt/lym ratio in patients with AA and control groups, no significant difference was found (30,31). In one study, the plt/lym ratio was higher in patients with AA than in controls, but there was no difference in the neu/lym ratio (32). In the study of El-Taweel et al. (33), neu/lym and plt/lym ratios were found to be significantly higher in AGA patients compared to controls. To our knowledge, there was no study in patients with TE regarding the relationship with these inflammatory markers.

In the study of Öner et al. (22), the number of patients with the highest differences in all laboratory parameters, including vitamin D, vitamin B12, ferritin, hemoglobin deficiency, and thyroid dysfunction, was observed in TE compared to AA and AGA. In the present study, the neu/lym ratio was highest in the TE group, and the ratio of neu/lym in patients with TE was significantly higher than that of patients in AA, but there was no difference in the plt/lym ratios between patient groups.

Limitations of this study were that a control group could not be formed as there was no homogeneous distribution in the groups, the study was conducted in one center, and the relatively small number of patients.

CONCLUSION
Vitamin D deficiency was seen in a very high percentage of all non-cicatricial alopecia in our study. But no subgroup stands out in terms of low vitamin D levels. Neu/lym ratio is one of the constantly used markers to determine inflammation in many diseases, including dermatological ones. It can be considered that the neu/lym ratio may be a more appropriate inflammatory marker for patients with TE than other nonscarring alopecias. Multicenter studies conducted with control groups will contribute more objective results.

REFERENCES
1. Mounsey AL, Reed SW. Diagnosing and treating hair loss. Am Fam Physician. 2009;80(4):356-62.
2. Almohanna HM, Ahmed AA, Tsatalis JP, Tosti A. The role of vitamins and minerals in hair loss: a review. Dermatol Ther (Heidelb). 2019;9(1):51-70.
3. Conic RRZ, Piliang M, Bergfeld W, Atanaskova-Mesinkovska N. Vitamin D status in scarring and nonscarring alopecia. J Am Acad Dermatol. 2021;85(2):478-80.
4. Chen Y, Dong X, Wang Y, Li Y, Xiong L, Li L. Serum 25 hydroxyvitamin D in non-scarring alopecia: A systematic review and meta-analysis. J Cosmet Dermatol. 2024;23(4):1131-40.
5. Wang Q, Ma J, Jiang Z, Ming L. Prognostic value of neutrophil-to-lymphocyte ratio and platelet-to-lymphocyte ratio in acute pulmonary embolism: a systematic review and meta-analysis. Int Angiol. 2018;37(1):4-11.
6. Trüeb RM. Telogen effluvium: Is there a need for a new classification? Skin Appendage Disord. 2016;2(1-2):39-44.
7. Peyravian N, Deo S, Daunert S, Jimenez JJ. The inflammatory aspect of male and female pattern hair loss. J Inflamm Res. 2020;13:879-81.

8. Zhang B, Zhao Y, Cai Z, Caulloo S, McElwee KJ, Li Y, et al. Early-stage alopecia areata is associated with inflammation in the upper dermis and damage to the hair follicle infundibulum. Australas J Dermatol. 2013;54(3):184-91.

9. Holick MF, Binkley NC, Bischoff-Ferrari HA, Gordon CM, Hanley DA, Heaney RP, et al. Evaluation, treatment, and prevention of vitamin D deficiency: an Endocrine Society clinical practice guideline. J Clin Endocrinol Metab. 2011;96(7):1911-30.

10. Kechichian E, Ezzedine K. Vitamin D and the skin: An update for dermatologists. Am J Clin Dermatol. 2018;19(2):223-35.

11. Gade VKV, Mony A, Munisamy M, Chandrashekar L, Rajappa M. An investigation of vitamin D status in alopecia areata. Clin Exp Med. 2018;18(4):577-84.

12. Bhat YJ, Latif I, Malik R, Hassan I, Sheikh G, Lone KS, et al. Vitamin D level in alopecia areata. Indian J Dermatol. 2017;62(4):407-10.

13. Oğrum A, Boyraz N, Karataş Toğral A, Karasatı S, Ekşioğlu HM. Evaluation of 25 hydroxy vitamin D3 levels in patients with alopecia areata. Turk Arch Dermatol Venereol. 2015;49(1):50-3. Turkish.

14. Thompson JM, Li T, Park MK, Qureshi AA, Cho E. Estimated serum vitamin D status, vitamin D intake, and risk of incident alopecia areata among US women. Arch Dermatol Res. 2016;308(9):671-6.

15. Liu Y, Li J, Liang G, Cheng C, Li Y, Wu X. Association of alopecia areata with vitamin D and calcium levels: A systematic review and meta-analysis. Dermatol Ther (Heidelb). 2020;10(5):967-83.

16. Lin X, Meng X, Song Z. Vitamin D and alopecia areata: possible roles in pathogenesis and potential implications for therapy. Am J Transl Res. 2019;11(9):5285-5300.

17. Siddappa H, Kumar YHK, Neladimmanahally V. Evaluation of vitamin D in pediatric alopecia areata: a case-control study of thirty patients in a tertiary care hospital. Indian J Paediatr Dermatol. 2019;20(1):32-5.

18. Kundak S, Kutlu A. Serum 25-hydroxy-vitamin D and vitamin B12 levels in childhood alopesia areata. J Dr Behcet Uz Child Hosp. 2021;11(1):101-7.

19. Lim RK, Castelo-Soccio L, Putterman E, Qureshi AA, Cho E. Predictors of vitamin D insufficiency in children and adolescents with alopecia areata. Cureus. 2022;14(3):e22934.

20. Unal M, Gonulalan G. Serum vitamin D level is related to disease severity in pediatric alopecia areata. J Cosmet Dermatol. 2018;17(1):101-4.

21. Tran PT, Chen A, Yi L, Goh C. Vitamin D levels in alopecia areata and other alopecias: A retrospective case-control study at a single institution. Int J Trichology. 2022;14(5):175-7.

22. Öner Ü, Akdeniz N. Nonscarring scalp alopecia: Which laboratory analysis should we perform on whom? Turk J Med Sci. 2022;52(1):188-94.

23. Gomes TF, Soares RO. Pediatric androgenetic alopecia: an updated review. J Dtsch Dermatol Ges. 2023;21(1):19-25.

24. Losoya-Jaquez MR, Lopez Yañez-Blanco A, Armendariz-Barragan Y, Aguilar-Figueroa NG, Rudnicka L, Sanchez-Dueñas LE. Androgenetic alopecia in children and adolescents: From trichoscopy to therapy. Skin Appendage Disord. 2024;10(2):123-8.

25. Rasheed H, Mahgoub D, Hegazy R, El-Komy M, Abdel Hay R, Hamid MA, et al. Serum ferritin and vitamin D in female hair loss: Do they play a role? Skin Pharmacol. Physiol. 2013;26(2):101-7.

26. Nayak, K, Garg A, Mithra P, Manjrekar P. Serum vitamin D3 levels and diffuse hair fall among the student population in South India: A case-control study. Int J Trichology. 2016;8(4):160-4.

27. Karadag AS, Ertugrul DT, Tutal E, Akin KO. The role of anemia and vitamin D levels in acute and chronic telogen effluvium. Turk J Med Sci. 2011;41(5): 827-33.

28. Chen V, Strazzulla L, Asbeck SM, Bellodi Schmidt F. Etiology, management, and outcomes of pediatric telogen effluvium: A single-center study in the United States. Pediatr Dermatol. 2023;40(1):120-4.

29. Işıktaş Sayılar E, Çelik S, İnce ME, Ergün İ. The post-transplant neutrophil-to-lymphocyte ratio and platelet-to-lymphocyte ratio in relation to graft function among renal transplant recipients. Duzce Med J. 2020;22(3):212-7.

30. İslamoğlu ZGK, Demirbaş A. Evaluation of complete blood cell and inflammatory parameters in patients with alopecia areata: Their association with disease severity. J Cosmet Dermatol. 2020;19(5):1239-45.

31. Dere G, Gündoğdu M. Investigation of the relationship between alopecia areata and inflammatory blood parameters. J Cosmet Dermatol. 2021;20(12):4048-51.

32. Aksoy Sarac G, Acar O, Nayır T, Hararcı Yıldırım P, Dinçer Rota D. The use of new hematological markers in the diagnosis of alopecia areata. Dermatol Pract Concept. 2023;13(2):e2023118.

33. El-Taweel A, Mustafa A, Abd El-Halim W, Roshdy A. Blood indices in patients with androgenetic alopecia. Benha J Appl Sci. 2020;5(5):269-72.

The Distribution of Hereditary Risk Factors in Patients with Pulmonary Thromboembolism without Identifiable Acquired Risk Factors

Tanımlanabilir Edinsel Risk Faktörleri Olmayan Pulmoner Tromboembolizmli Hastalarda Kalıtsal Risk Faktörlerinin Dağılımı

Savaş GEGİN[1]
0000-0001-7362-8710
Taner KARAKAYA[2]
0000-0002-3437-5324
Esra ARSLAN AKSU[3]
0000-0003-0448-1801
Burcu ÖZDEMİR[1]
0000-0003-4678-7729
Levent ÖZDEMİR[3]
0000-0002-3478-5454
Ahmet Cemal PAZARLI[4]
0000-0002-7094-837X

[1]Department of Chest Diseases, Samsun Education and Research Hospital, Samsun, Türkiye

[2]Department of Medical Genetics, Samsun University Faculty of Medicine, Samsun, Türkiye

[3]Department of Chest Diseases, Samsun University Faculty of Medicine, Samsun, Türkiye

[4]Department of Pulmonary Diseases, Tokat Gaziosmanpaşa University Faculty of Medicine, Tokat, Türkiye

ABSTRACT

Aim: This study aimed to investigate the distribution of hereditary risk factors in patients with pulmonary thromboembolism (PTE) who have no acquired risk factors and to explore the relationship between genetic factors and the early mortality risk of embolism.

Material and Methods: Data from 295 patients diagnosed with PTE were examined retrospectively. Of these, 44 patients who had no acquired risk factors and were screened for hereditary risk factors, including factor V Leiden (FVL), prothrombin (PT) G20210A, methylenetetrahydrofolate reductase (MTHFR) C677T, MTHFR A1298C, plasminogen activator inhibitor (PAI) 4G/5G, factor XIII, antithrombin (AT) III, protein C, protein S, and activated protein C resistance (APCR), were included in the study.

Results: Of the patients, 14 (31.8%) were female and 30 (68.2%) were male, with a mean age of 46.5±17.3 years. Among the hereditary risk factors, the most common homozygous mutations were MTHFR A1298C (n=10, 22.7%), PAI 4G/5G (n=9, 20.5%), and FVL (n=5, 11.4%), while the most common heterozygous mutations were PAI 4G/5G (n=26, 59.1%), MTHFR A1298C (n=19, 43.2%), and MTHFR C677T (n=16, 36.4%). The heterozygous MTHFR A1298C mutation was detected in 10 (52.6%) patients with a history of recurrent PTE.

Conclusion: This study highlights the presence of genetic mutations such as PAI 4G/5G, MTHFR A1298C, MTHFR C677T, FVL, factor XIII, and PT G20210A in patients with PTE. The results show a high prevalence of genetic causes, especially in patients under 50 years of age with no acquired risk factors, no history of recurrent PTE or thrombophilia in any family member.

Keywords: Pulmonary thromboembolism; acquired risk factors; hereditary risk factors.

ÖZ

Amaç: Bu çalışmada edinilmiş risk faktörü olmayan pulmoner tromboemboli (PTE) hastalarında kalıtsal risk faktörlerinin dağılımının araştırılması ve genetik faktörler ile emboli kaynaklı erken mortalite riski arasındaki ilişkinin araştırılması amaçlanmıştır.

Gereç ve Yöntemler: PTE tanısı almış 295 hastanın verileri geriye dönük olarak incelendi. Bunlardan edinilmiş risk faktörü olmayan ve faktör V Leiden (FVL), protrombin (PT) G20210A, metilentetrahidrofolat redüktaz (MTHFR) C677T, MTHFR A1298C, plazminojen aktivatör inhibitörü (PAI) 4G/5G, faktör XIII, antitrombin (AT) III, protein C, protein S ve aktive protein C direnci (APCR) dahil olmak üzere kalıtsal risk faktörleri açısından taranan 44 hasta çalışmaya dahil edildi.

Bulgular: Hastaların 14'ü (%31,8) kadın ve 30'u (%68,2) erkek olup, yaş ortalaması 46,5±17,3 yıl idi. Kalıtsal risk faktörleri arasında en sık görülen homozigot mutasyonlar MTHFR A1298C (n=10, %22,7), PAI 4G/5G (n=9, %20,5) ve FVL (n=5, %11,4) iken, en sık görülen heterozigot mutasyonlar PAI 4G/5G (n=26, %59,1), MTHFR A1298C (n=19, %43,2) ve MTHFR C677T (n=16, %36,4) idi. Tekrarlayan PTE öyküsü olan 10 (%52,6) hastada heterozigot MTHFR A1298C mutasyonu tespit edildi.

Sonuç: Bu çalışma, PTE'li hastalarda PAI 4G/5G, MTHFR A1298C, MTHFR C677T, FVL, faktör XIII ve PT G20210A gibi genetik mutasyonların varlığını vurgulamaktadır. Sonuçlar, özellikle edinilmiş risk faktörü olmayan, tekrarlayan PTE öyküsü olmayan veya herhangi bir aile üyesinde trombofili olmayan 50 yaş altı hastalarda genetik nedenlerin yüksek prevalansta olduğunu göstermektedir.

Anahtar kelimeler: Pulmoner tromboemboli; edinilmiş risk faktörleri; kalıtsal risk faktörleri.

Corresponding Author
Sorumlu Yazar
Ahmet Cemal PAZARLI
dracp60@gmail.com

INTRODUCTION

Pulmonary thromboembolism (PTE) has a multifactorial pathogenesis and, with its increasing incidence and decreasing mortality rate, is currently a common cause of cardiovascular mortality. It typically presents as a complication of deep vein thrombosis (DVT). In addition to acquired factors such as, active cancer, advanced age, major trauma, surgery, pregnancy, and immobilization, genetic factors like factor V Leiden (FVL), prothrombin (PT) G20210A, antithrombin (AT) III, protein C, and protein S deficiencies play a significant role in the development of PTE (1). The coexistence of multiple prothrombotic disorders increases the risk of developing PTE, both in the presence and absence of acquired risk factors (2). Although the true prevalence of hereditary factors in the development of PTE is not clearly known, studies have shown that the rate of thrombophilia detection varies between 10%-50%, depending on the characteristics of the selected population. In studies conducted in Türkiye on hereditary thrombophilia, the frequency of thrombophilia was found to be 15.1% in healthy populations, while it was 41.6% in patients with PTE. Frequently, commonly identified mutations include FVL, PT G20210A, factor VIII elevation, AT III, protein C, and protein S deficiency (3). Understanding the distribution of hereditary thrombophilias in PTE patients and their impact on the disease plays a crucial role in disease management, risk classification, and determining personalized treatment options. Therefore, it is recommended to investigate hereditary thrombophilia in patients under 50 years old who develop PTE without acquired risk factors, patients who develop PTE for the first time with a family history of PTE or thrombophilia, those with a history of recurrent PTE, patients with PTE in atypical locations, those with a history of warfarin-induced skin necrosis, patients with unexplained multiple miscarriages, those with a history of neonatal thrombosis, and young patients with arterial ischemia caused by paradoxical embolism (right-to-left shunt) (4).

This study aimed to investigate the distribution of hereditary risk factors in patients with PTE without identifiable acquired risk factors and to explore the relationship between genetic factors and the risk of PTE.

MATERIALS AND METHODS

The data of 295 patients diagnosed with PTE through pulmonary angiography or ventilation-perfusion scintigraphy at Samsun Education and Research Hospital Chest Diseases Clinic between July 2021 and July 2024 were retrospectively analyzed. Genetic screening for hereditary risk factors was performed in 51 patients who had no acquired risk factors and for whom genetic testing was recommended according to the PTE diagnosis and treatment consensus report (3). The data of 7 patients were unavailable, thus, 44 patients were included in the study. Screening for hereditary risk factors was conducted in patients under 50 years of age who developed PTE without acquired risk factors (n=24), patients with a history of recurrent PTE (n=19), and patients with a family history of PTE or thrombophilia who developed PTE for the first time (n=1). Patients with incomplete data were excluded from the study (n=7).

Demographic data, comorbid conditions, PTE risk status, and hereditary risk factors of the patients were recorded. Acquired risk factors were questioned as advanced age, nephrotic syndrome, obesity, long-term travel, major surgery (pelvic abdominal), immobility due to sitting (e.g. prolonged car or air travel), cancer, congestive heart failure, myocardial infarction, stroke, oral contraceptive use, hormone replacement therapy, chemotherapy, central venous catheter, spinal cord injury, polycythemia vera, pregnancy/puerperium, and trauma. PTE risk classification was performed according to the 2019 European Society of Cardiology (ESC) Guidelines (5), categorizing patients into low, intermediate (intermediate-low, intermediate-high), and high risk groups (Figure 1). The hereditary risk factors examined included FVL, PT G20210A, methylenetetrahydrofolate reductase (MTHFR) C677T, MTHFR A1298C, plasminogen activator inhibitor (PAI) 4G/5G, factor XIII, AT III, protein C, protein S, and activated protein C resistance (APCR).

The levels of protein C, protein S, and AT III were measured after the acute phase of pulmonary embolism. The levels of protein C and protein S were measured two weeks after discontinuing warfarin treatment, while the levels of AT III were measured 48 hours after the initiation or discontinuation of low-molecular-weight heparin/heparin therapy (3).

Ethical approval for the study was obtained from the Samsun University Non-Interventional Clinical Research Ethics Committee (Date: 10.07.2024, No: 2024/13/7).

Statistical Analysis

All data were analyzed using the IBM SPSS v.23 for Windows program. Frequencies and percentages of categorical variables, as well as means and standard deviations of numerical variables, were calculated. The assumption of normal distribution was made using the Kolmogorov-Smirnov test.

Early mortality risk		Indicators of risk			
		Haemodynamic instability[a]	Clinical parameters of PE severity and/or comorbidity: PESI class III–V or sPESI ≥1	RV dysfunction on TTE or CTPA[b]	Elevated cardiac troponin levels[c]
High		+	[+][d]	+	[+]
Intermediate	Intermediate-high	–	+[e]	+	+
	Intermediate-low	–	+[e]	One [or none] positive	
Low		–	–	–	Assessment optional; if assessed, negative

Figure 1. Pulmonary thromboembolism risk classification

RESULTS

Of the 44 patients included in the study, 14 (31.8%) were female and 30 (68.2%) were male, with a mean age of 46.5±17.3 years. Comorbidity was detected in 28 (63.6%) of the patients. The most common comorbidities were DVT (n=16, 36.4%) and hypertension (n=8, 18.2%). Nineteen patients (43.2%) were classified as low-risk, while 6 (13.6%) were classified as high-risk (Table 1).

The most common homozygous mutations among the hereditary risk factors were MTHFR A1298C (n=10, 22.7%), PAI 4G/5G (n=9, 20.5%), and FVL (n=5, 11.4%), while the most common heterozygous mutations were PAI 4G/5G (n=26, 59.1%), MTHFR A1298C (n=19, 43.2%), and MTHFR C677T (n=16, 36.4%). The distribution of mutations was shown in Table 2 and Figure 2.

In PTE patients under 50 years old without acquired risk factors, the most common heterozygous mutation identified was PAI 4G/5G (n=17, 70.8%), while in patients with a history of recurrent PTE, the most common heterozygous mutation was MTHFR A1298C (n=10, 52.6%, Table 3).

Protein C and protein S levels were assessed in 26 patients, while AT III and APCR were assessed in 16 patients. The mean AT III level was 103.3±20.2%, with one

patient having a low level of 78%. The mean protein S level was 80.2±40.6%, and it was found to be low in 4 patients. The mean protein C level was 102.2±26.3%, and it was found to be low in 2 patients. The mean APCR was 0.88±0.1. APCR deficiency was not observed (Table 4).

In PTE patients with low risk, the most common mutations were MTHFR A1298C and PAI 4G/5G (n=15, 78.9%). The most common mutation was PAI 4G/5G both in intermediate-low risk patients (n=11, 91.7%) and in intermediate-high risk patients (n=5, 71.4%), while MTHFR A1298C (n=5, 83.3%) was the most common mutation in high-risk patients (Table 5).

Table 1. Demographic features (n=44)

Age (years), mean±SD	
Overall	46.5±17.3
Female	56.7±18.7
Male	41.8±14.7
Gender, n (%)	
Female	14 (31.8)
Male	30 (68.2)
Comorbidity and Risk Factors, n (%)	
Deep vein thrombosis	16 (36.4)
Hypertension	8 (18.2)
Ischemic heart disease	4 (9.1)
Diabetes	3 (6.8)
COPD	3 (6.8)
Asthma	2 (4.5)
Cerebrovascular disease	1 (2.3)
Pulmonary Thromboembolism Risk, n (%)	
Low Risk	19 (43.2)
Intermediate Risk	19 (43.2)
intermediate-low risk	12 (27.3)
intermediate-high risk	7 (15.9)
High Risk	6 (13.6)

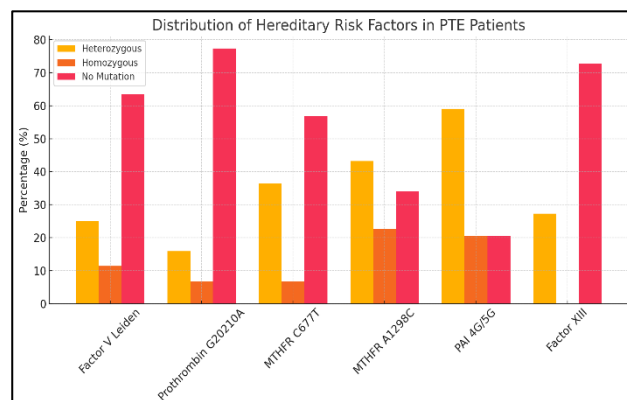SD: standard deviation, COPD: chronic obstructive pulmonary disease

Table 2. Distribution of hereditary risk factors (n=44)

Factor V Leiden, n (%)	
Heterozygous	11 (25.0)
Homozygous	5 (11.4)
No mutation	28 (63.6)
Prothrombin G20210A, n (%)	
Heterozygous	7 (15.9)
Homozygous	3 (6.8)
No mutation	34 (77.3)
MTHFR C677T, n (%)	
Heterozygous	16 (36.4)
Homozygous	3 (6.8)
No mutation	25 (56.8)
MTHFR A1298C, n (%)	
Heterozygous	19 (43.2)
Homozygous	10 (22.7)
No mutation	15 (34.1)
PAI 4G/5G, n (%)	
Heterozygous	26 (59.1)
Homozygous	9 (20.5)
No mutation	9 (20.5)
Factor XIII, n (%)	
Heterozygous	12 (27.3)
Homozygous	0 (0.0)
No mutation	32 (72.7)

MTHFR: methylenetetrahydrofolate reductase, PAI: plasminogen activator inhibitor

Table 3. Distribution of mutations according to clinical features

	Age <50 Years (n=24)	Recurrent PTE (n=19)	Familial PTE (n=1)
Factor V Leiden, n (%)			
Homozygous	1 (4.2)	4 (21.1)	0 (0.0)
Heterozygous	8 (33.3)	3 (15.8)	0 (0.0)
Prothrombin G20210A, n (%)			
Homozygous	0 (0.0)	3 (15.8)	0 (0.0)
Heterozygous	5 (20.8)	2 (10.5)	0 (0.0)
MTHFR C677T, n (%)			
Homozygous	8 (33.3)	1 (5.3)	0 (0.0)
Heterozygous	2 (8.3)	8 (42.1)	0 (0.0)
MTHFR A1298C, n (%)			
Homozygous	5 (20.8)	4 (21.1)	0 (0.0)
Heterozygous	9 (37.5)	10 (52.6)	0 (0.0)
PAI 4G/5G, n (%)			
Homozygous	4 (16.7)	4 (21.1)	1 (100)
Heterozygous	17 (70.8)	9 (47.4)	0 (0.0)
Factor XIII, n (%)			
Homozygous	0 (0.0)	0 (0.0)	0 (0.0)
Heterozygous	8 (33.3)	4 (21.1)	0 (0.0)

MTHFR: methylenetetrahydrofolate reductase, PAI: plasminogen activator inhibitor, PTE: pulmonary thromboembolism

Figure 2. Distribution of hereditary risk factors in patients

DISCUSSION

As a result of this study, a significant number of hereditary risk factors were identified in PTE patients without acquired risk factors. In particular, homozygous mutations were found as follows: MTHFR A1298C in 10 (22.7%) patients, PAI 4G/5G in 9 (20.5%) patients, FVL in 5 (11.4%) patients, and PT G20210A in 3 (6.8%) patients; while heterozygous mutations were most commonly observed in PAI 4G/5G (n=26, 59.1%), MTHFR A1298C (n=19, 43.2%), MTHFR C677T (n=16, 36.4%), Factor XIII (n=12, 27.3%), FVL (n=11, 25%), and PT G20210A (n=7, 15.9%). In the present study, the causes of hereditary thrombophilia were detected in 4 (15%) patients with protein S deficiency and 2 (7.6%) patients with protein C deficiency. Furthermore, it has been reported that genetic polymorphisms such as MTHFR (C677T, A1298C), FVL, and PT G20210A are considered risk factors for thromboembolism. However, certain genetic mutations like F13 V34L polymorphism may provide a protective role against thrombosis (6).

Many studies have been conducted on hereditary risk factors in patients with PTE. Rossi et al. (7) found that different types of hereditary thrombophilia significantly affected the incidence of symptomatic PTE, with AT III deficiency increasing the PTE risk when combined with the PT G20210A gene mutation, while it decreased the risk when combined with FVL. Similarly, Turan et al. (4) observed a high prevalence of genetic mutations such as FVL and protein S deficiency in patients with recurrent pulmonary embolism episodes, emphasizing the need for comprehensive screening of at-risk populations to conduct

careful genetic testing. Komsa-Penkova et al. (8) highlighted that hereditary thrombophilias, such as FVL and PT G20210A, make individuals more susceptible to developing pulmonary embolism. Similarly, Brandimarti et al. (9) demonstrated the presence of multiple genetic mutations involved in the development of pulmonary embolism by examining thrombophilia-related specific genes in the post-mortem tissues of individuals who died from PTE.

Many studies with varying results have been conducted using retrospective and case-control designs to determine the frequency of genetic risk factors in identifying etiological causes. Most of these studies focused on screening for genetic risk factors in patients with acquired risk factors. In the present study, however, genetic risk factors were screened in patients with PTE who did not have identified acquired risk factors.

In the study by Turan et al. (4) evaluating hereditary thrombophilias in patients with PTE, FVL was identified in 19.1% of patients (18% heterozygous, 1.1% homozygous); PT G20210A in 3.4% (all heterozygous); MTHFR C677T in 58.4% (51.7% heterozygous, 6.7% homozygous); MTHFR A1298C in 53.3% (52.8% heterozygous, 0.9% homozygous); AT III deficiency in 1.1%; protein C deficiency in 5.7%; protein S deficiency in 13.6%; and APCR in 34.2%. In the study by Gurgey et al. (10) investigating FVL and PT G20210A mutations in 146 patients with thrombosis, FVL was identified in 30.8% of patients (26% heterozygous, 4.8% homozygous), PT G20210A in 6.8% (all heterozygous), and both FVL and PT G20210A mutations in 4.1% of patients. In the study by Kalkanlı et al. (11) evaluating FVL mutations in 61 patients with venous thrombosis, the FVL mutation was identified in 24.6% of patients (22.9% heterozygous, 1.6% homozygous). Results of the present study demonstrated, as observed in previous studies, that these mutations have a high prevalence. Notably, FVL and PT G20210A homozygous mutations were detected at a higher rate compared to the studies by Turan et al. (4), Gurgey et al. (10), and Kalkanlı et al. (11), whereas heterozygous mutations were identified at rates similar to those reported.

Table 4. Hereditary thrombophilia blood level

Hereditary Thrombophilia	Available
Protein C Deficiency, n (%) (n=26)	2 (7.6)
Protein S Deficiency, n (%) (n=26)	4 (15.0)
AT III Deficiency, n (%) (n=16)	1 (6.3)
APCR, n (%) (n=16)	0 (0.0)

AT: antithrombin, APCR: activated protein C resistance

Table 5. Distribution of mutations according to pulmonary thromboembolism risk

	Low (n=19)	Intermediate-Low (n=12)	Intermediate-High (n=7)	High (n=6)
Factor V Leiden, n (%)				
Homozygous	3 (15.8)	2 (16.7)	0 (0.0)	0 (0.0)
Heterozygous	4 (21.1)	3 (25.0)	2 (28.6)	2 (33.3)
Prothrombin G20210A, n (%)				
Homozygous	1 (5.3)	2 (16.7)	0 (0.0)	0 (0.0)
Heterozygous	2 (10.5)	3 (25.0)	2 (28.6)	0 (0.0)
MTHFR C677T, n (%)				
Homozygous	2 (10.5)	0 (0.0)	1 (14.3)	0 (0.0)
Heterozygous	6 (31.6)	6 (50)	2 (28.6)	2 (33.3)
MTHFR A1298C, n (%)				
Homozygous	3 (15.8)	3 (25.0)	2 (28.6)	2 (33.3)
Heterozygous	12 (63.2)	2 (16.7)	2 (28.6)	3 (50.0)
PAI 4G/5G, n (%)				
Homozygous	5 (26.3)	2 (16.7)	1 (14.3)	1 (16.7)
Heterozygous	10 (52.6)	9 (75.0)	4 (57.1)	3 (50.0)
Factor XIII, n (%)				
Homozygous	0 (0.0)	0 (0.0)	0 (0.0)	0 (0.0)
Heterozygous	7 (36.8)	2 (16.7)	1 (14.3)	2 (33.3)

MTHFR: methylenetetrahydrofolate reductase, PAI: plasminogen activator inhibitor, PTE: pulmonary thromboembolism

In their case-control study, Kupeli et al. (12) evaluated genetic risk factors for PTE in the Turkish population, including 80 PTE patients and 104 healthy individuals, and found no association between the presence or absence of acquired risk factors and genetic risk factors. Heterozygous FVL (14.2%), heterozygous PT G20210A mutation (15.2%), and homozygous MTHFR C677T (23.8%) were significantly higher among the patients. In a subgroup analysis comparing patients with and without acquired risk factors, the homozygous MTHFR C677T gene mutation (46.3%) was significantly higher in those without acquired risk factors, while the PAI 4G/5G gene mutation was high in both groups. In a case-control study by Oguzulgen et al. (13) with 143 PTE patients and 200 controls, it was found that the FVL mutation was significantly higher in the patient group (21%) compared to the control group (7.7%). However, no significant differences were observed between the patient and control groups for PT G20210A and PAI 4G/5G, leading to the conclusion that PAI is not a risk factor for PTE. In the subgroup analysis of 33 patients without acquired risk factors, no FVL or PT G20210A mutations were detected; in this subgroup, PAI was detected in 45.5% of patients, compared to 51.5% in the control group. In a case-control study conducted by Okumus et al. (14) with 191 PTE patients and 191 controls, FVL and protein C deficiency were found to be significantly higher in PTE patients compared to the control group, while no significant differences were found regarding protein S, AT activities, homocysteine levels, and PT G20210A mutations. In a case-control study conducted by Dölek et al. (15) with 270 DVT patients and 114 controls, FVL (DVT: 28.3%, control: 3.5%) and PT G20210A (DVT: 8.6%, control: 1.8%) were significantly higher in patients compared to the control group. Although MTHFR C677T (DVT: 49.8%, control: 39.5%) and MTHFR A1298C (DVT: 63.2%, control: 56.1%) gene mutations were higher in both groups, no significant difference was observed. In another case-control study conducted by Erkekol et al. (16) with 64 PTE patients and 64 controls, the FVL mutation was significantly higher in the patient group (26.9%), while no significant difference was observed for the PT G20210A mutation between the two groups. In the present study, heterozygous mutations of FVL, PT G20210A, MTHFR, and PAI 4G/5G were found at a high rate, similar to the case-control studies. However, unlike other studies, homozygous mutations, except for Factor XIII, were detected at a higher rate. This suggests that excluding acquired risk factors in this study to create a more isolated group for assessing genetic risk factors may have contributed to this difference, and that homozygous mutations, in addition to heterozygous mutations, could increase the risk of PTE.

In the literature review, no studies were found regarding the frequency of genetic risk factors stratified by the early mortality risk level of PTE. In Oguzulgen et al.'s (13) study, no acquired risk factors were found in 7 out of 32 high-risk patients, and genetic analysis in these patients revealed FVL in 6 cases and PT G20210A in 2 cases. In this study, unlike others, genetic risk factors were also evaluated based on the early mortality risk level of PTE. No correlation was observed between pulmonary embolism risk classes of 2019 ESC Guidelines and genetic factors. In low-risk patients, homozygous PAI 4G/5G was found in 26.3%, and heterozygous MTHFR A1298C was found in 63.2%. In intermediate-low risk patients, homozygous MTHFR A1298C was found in 25%, and heterozygous PAI 4G/5G was found in 75%. In intermediate-high risk patients, homozygous MTHFR A1298C was detected, and heterozygous PAI 4G/5G was found in 57.1%. In high-risk patients, homozygous MTHFR A1298C was found in 33.3%, and heterozygous PAI 4G/5G was found in 50%. It was thought that the reason why homozygous mutation was less common than homozygous mutation in high-risk patients was that the synergistic effect of heterozygous mutations was unknown.

The limitations of the study include a small sample size, a single-center and retrospective design, and the lack of a case-control design. Additionally, not all genetic factors were fully evaluated in PTE, and protein C, protein S, AT III, and APCR were not tested in all patients. This may have affected the results, preventing a full representation of the true picture. Another limitation is the failure to assess the combined effects of multiple genetic mutations or their interactions with acquired risk factors.

CONCLUSION

This study highlights the presence of genetic mutations such as PAI 4G/5G, MTHFR A1298C, MTHFR C677T, FVL, Factor XIII, and PT G20210A in patients with PTE. The results show a high prevalence of genetic causes, especially in patients under 50 years of age with no acquired risk factors, no history of recurrent PTE or thrombophilia in any family member. Future studies that integrate genetic screening into clinical practice, involve larger sample sizes in multicenter research, include a broader range of genetic tests, and examine the combined effects of multiple genetic mutations or their interactions with acquired risk factors could help identify high-risk individuals, facilitate targeted prevention measures, reduce disease incidence, and improve patient outcomes.

REFERENCES

1. Nizankowska-Mogilnicka E, Adamek L, Grzanka P, Domagala TB, Sanak M, Krzanowski M, et al. Genetic polymorphisms associated with acute pulmonary embolism and deep venous thrombosis. Eur Respir J. 2003;21(1):25-30.

2. Hodeib H, Youssef A, Allam AA, Selim A, Tawfik MA, Abosamak MF, et al. Genetic risk profiling associated with recurrent unprovoked venous thromboembolism. Genes (Basel). 2021;12(6):874.

3. Arseven O, Bingöl Z, Öngen HG, Uzun O, Okumuş NG, editors. Turkish Thoracic Society pulmonary thromboembolism diagnosis and treatment consensus report. Ankara: Optimus Publishing; 2021. Turkish.

4. Turan O, Ündar B, Günay T, Akkoçlu A. Investigation of inherited thrombophilias in patients with pulmonary embolism. Blood Coagul Fibrinolysis. 2013;24(2):140-9.

5. Konstantinides SV, Meyer G, Becattini C, Bueno H, Geersing GJ, Harjola VP, et al. 2019 ESC Guidelines for the diagnosis and management of acute pulmonary embolism developed in collaboration with the European Respiratory Society (ERS). Eur Heart J. 2020;41(4):543-603.

6. Şimşek F, Ceylan M, Bilge N. The relationship between etiology and genetic polymorphism in adults with cerebral venous thrombosis. Duzce Med J. 2019;21(3):166-71. Turkish.

7. Rossi E, Za T, Ciminello A, Leone G, Stefano V. The risk of symptomatic pulmonary embolism due to proximal deep venous thrombosis differs in patients with different types of inherited thrombophilia. Thromb Haemost. 2008;99(6):1030-4.

8. Komsa-Penkova R, Tonchev PT, Kovacheva KS, Georgieva GB, Ivanov YY, Ivanov PD, et al. Predisposition to thrombophilia and hypofibrinolysis in pulmonary embolism: analysis of inherited factors. J Biomed Clin Res. 2013;6(2):73-81.

9. Brandimarti F, Alessandrini F, Pesaresi M, Catalani C, De Angelis L, Galeazzi R, et al. Investigation on genetic thrombophilic factors in FFPE autopsy tissue from subjects who died from pulmonary embolism. Int J Legal Med. 2017;131(2):447-58.

10. Gurgey A, Haznedaroglu IC, Egesel T, Buyukasik Y, Ozcebe OI, Sayinalp N, et al. Two common genetic thrombotic risk factors: factor V Leiden and prothrombin G20210A in adult Turkish patients with thrombosis. Am J Hematol. 2001;67(2):107-11.

11. Kalkanli S, Ayyildiz O, Tiftik N, Batun S, Isikdogan A, Ince H, et al. E. Factor V Leiden mutation in venous thrombosis in southeast Turkey. Angiology. 2006;57(2):193-6.

12. Kupeli E, Verdi H, Simsek A, Atac FB, Eyuboglu FO. Genetic mutations in Turkish population with pulmonary embolism and deep venous thrombosis. Clin Appl Thromb Hemost. 2011;17(6):E87-94.

13. Oguzulgen IK, Yilmaz E, Demirtas S, Erkekol FO, Ekim N, Demir N, et al. The role of plasminogen activator inhibitor-1 polymorphism, factor-V-Leiden, and prothrombin-20210 mutations in pulmonary thromboembolism. Clin Appl Thromb Hemost. 2009;15(1):73-7.

14. Okumus G, Kiyan E, Arseven O, Tabak L, Diz-Kucukkaya R, Unlucerci Y, et al. Hereditary thrombophilic risk factors and venous thromboembolism in Istanbul, Turkey: the role in different clinical manifestations of venous thromboembolism. Clin Appl Thromb Hemost. 2008;14(2):168-73.

15. Dölek B, Eraslan S, Eroğlu S, Kesim BE, Ulutin T, Yalçıner A, et al. Molecular analysis of factor V Leiden, factor V Hong Kong, factor II G20210A, methylenetetrahydrofolate reductase C677T, and A1298C mutations related to Turkish thrombosis patients. Clin Appl Thromb Hemost. 2007;13(4):435-8.

16. Erkekol FO, Ulu A, Numanoglu N, Akar N. High plasma levels of factor VIII: an important risk factor for isolated pulmonary embolism. Respirology. 2006;11(1):70-4.

Evaluation of Osteoarticular Involvement Associated with Brucellosis in Children

Çocukluk Çağı Brusellozuna İlişkin Osteoartiküler Tutulumun Değerlendirilmesi

Tuğba Nur KUTLU BEŞEREN[1]
0000-0003-4583-0860
Hayrunnisa BEKİS BOZKURT[2]
0000-0001-8642-4872
Müferet ERGÜVEN[3]
0000-0002-3255-1208
Zafer BIÇAKCI[4]
0000-0002-1321-4708

[1]Department of Pediatrics, Kafkas University Faculty of Medicine, Kars, Türkiye

[2]Division of Pediatric Allergy and Immunology, Department of Pediatrics, Ümraniye Training and Research Hospital, İstanbul, Türkiye

[3]Division of Pediatric Rheumatology, Department of Pediatrics, Düzce University Faculty of Medicine, Düzce, Türkiye

[4]Division of Pediatric Hematology, Department of Pediatrics, Atatürk University Faculty of Medicine, Erzurum, Türkiye

ABSTRACT

Aim: Brucellosis is a significant public health problem with high morbidity. Its most frequent complication is osteoarticular involvement. The study aimed to evaluate the relationship of osteoarticular involvement with clinical features and prognosis in children with brucellosis.

Material and Methods: This retrospective study included pediatric patients between the ages of 1 and 18 years who were hospitalized and diagnosed with brucellosis between 2015 and 2020, and were regularly followed up. and all their findings and osteoarticular involvement data within the last two years were recorded. Clinical features, laboratory findings, osteoarticular involvement, and relapse rates of the patients were evaluated.

Results: A total of 80 patients were included study. During the follow-up period, relapse developed in 14 (17.5%) patients. The most commonly affected joints were right (40%, n=32) and left (26.3%, n=21) hips, then right (27.5%, n=22) and left (23.8%, n=19) knees. Shoulder joint involvement rates and C-reactive protein (CRP), erythrocyte sedimentation rate (ESR), alanine transaminase (ALT), and aspartate aminotransferase (AST) levels were statistically significantly higher in the relapse group (p=0.016, p=0.003, p=0.001, p<0.001, p<0.001, respectively). There was no significant difference in demographic characteristics, clinical features, and treatment responses of the patients between age groups, except weakness and sweating complaints that were high among older children (p=0.036).

Conclusion: High admission ALT, AST, CRP, and ESR levels in brucellosis cases with osteoarticular involvement and the presence of shoulder joint involvement, albeit rarely, can be a warning sign in terms of relapse. Patients should be closely followed up in terms of brucellosis complications.

Keywords: Brucellosis; osteoarthritis; sacroiliac joint; shoulder joint; relapse.

ÖZ

Amaç: Bruselloz, yüksek morbiditeye sahip önemli bir halk sağlığı sorunudur. En sık görülen komplikasyonu osteoartiküler tutulumdur. Bu çalışmanın amacı, bruselloz tanılı çocuklarda osteoartiküler tutulumun klinik özellikler ve prognoz ile ilişkisini değerlendirmektir.

Gereç ve Yöntemler: Geriye dönük bu çalışmaya, 2015 ve 2020 yılları arasında bruselloz tanısıyla hastaneye yatırılan ve düzenli takipleri yapılan 1 ile 18 yaş aralığındaki pediatrik hastalar dahil edildi. Son iki yıldaki tüm bulguları ve osteoartiküler tutulum verileri kaydedildi. Hastaların klinik özellikleri, laboratuvar bulguları, osteoartiküler tutulum ve nüks oranları değerlendirildi.

Bulgular: Çalışmaya toplam 80 hasta dahil edildi. Takip süresinde hastaların 14 (%17,5) hastada relaps gelişti. En sık etkilenen eklemler sağ (%40, n=32) ve sol (%26,3, n=21) kalçalar, ardından sağ (%27,5, n=22) ve sol (%23,8, n=19) dizlerdi. Omuz eklem tutulum oranları ile C-reaktif protein (CRP), eritrosit sedimantasyon hızı (ESH), alanin transaminaz (ALT) ve aspartat aminotransferaz (AST) düzeyleri relaps grubunda istatistiksel olarak anlamlı şekilde daha yüksekti (sırasıyla p=0,016, p=0,003, p=0,001, p<0,001, p<0,001). Sadece yaşı büyük çocuklarda daha yüksek olan güçsüzlük ve terleme şikayetleri dışında (p=0,036), hastaların demografik özellikleri, klinik özellikleri ve tedavi yanıtları bakımından yaş grupları arasında anlamlı bir farklılık yoktu.

Sonuç: Osteoartiküler tutulumu olan bruselloz olgularında yüksek başvuru ALT, AST, CRP ve ESR düzeyleri ve nadir de olsa omuz eklem tutulumunun varlığı relaps açısından uyarıcı olabilir. Hastalar bruselloz komplikasyonları açısından yakından takip edilmelidir.

Anahtar kelimeler: Bruselloz; osteoartrit; sakroiliak eklem; omuz eklemi; relaps.

Corresponding Author
Sorumlu Yazar
Hayrunnisa BEKİS BOZKURT
hayrunisabekis@hotmail.com

INTRODUCTION

Brucellosis is a zoonotic disease caused by gram-negative *Brucella* species bacteria (1). Its incidence rate varies between 0.3-100/100.000 and from region to region, and the incidence rate of osteoarticular involvement varies between 10-85% all around the world (2). This disease is more frequently seen in developing countries, infects humans through direct contact with infected animals, inhalation, and consumption of non-pasteurized milk or dairy products, and leads to severe problems, especially in children (1-3). It is endemic in certain regions of Türkiye (3). The disease affects mostly hematological, gastrointestinal, cardiorespiratory, and musculoskeletal systems (1,4). It has a low mortality, but delayed or inappropriate/inadequate treatment increases its morbidity risk (4,5). This disease puts patients at risk in terms of severe complications and relapse (5).

The most frequent complication seen in brucellosis is osteoarticular involvement, which can cause severe morbidity (6,7). Osteoarticular brucellosis covers arthritis, tenosynovitis, bursitis, sacroiliitis, spondylitis, and osteomyelitis. Detailed physical examination and history are necessary for correct diagnosis and treatment management in order not to overlook cases of brucellosis with osteoarticular involvement. Data on the effect of joint involvement sites on the rate of relapse are limited.

The study aimed to evaluate osteoarticular involvement in cases with brucellosis, along with patient characteristics and in line with the literature, and to reveal its relationship with the clinical features and the prognosis in terms of demonstrating their quality of life.

MATERIAL AND METHODS

Eighty cases between the ages of 1 and 18 years who were hospitalized and diagnosed with brucellosis in the pediatric clinic of our hospital between 2015 and 2020 were regularly followed up, and all their findings and osteoarticular involvement data within the last two years were recorded. Those having joint dysplasia, arthritis, chronic arthritis, and trauma before the diagnosis were excluded from the study.

A form was developed to record the patients' age, gender, admission duration, complaints, intra-family infection, physical examination findings, and detailed joint findings, as well as admission whole blood count, acute phase reactants (erythrocyte sedimentation rate (ESR), C-reactive protein (CRP) value), liver function tests, serum creatinine values, *Brucella* standard tube agglutination test, Coombs test, blood culture results, if any, radiological examination results, if any, and all information covering treatment approaches, duration, and results. An increase in the *Brucella* tube agglutination test values of the patients within six months of the follow-up and/or the development of clinical findings (any of them: fever, hepatomegaly, splenomegaly, weakness, and/or arthralgia or arthritis) was defined as relapse.

In addition to clinical symptoms and findings, brucellosis was diagnosed when the *Brucella* standard tube agglutination test was positive (1/160 titer), or there was at least a four-fold increase in the titer in serum samples collected with an interval of 2-3 weeks, and/or *Brucella* spp. bacteria developed in the blood or sterile body fluid culture. If the patient's complaints lasted less than 2 months, it was considered acute, if between 2 months and 1 year, it was considered subacute, and if it continued for more than 1 year, it was considered chronic brucellosis (5,6). All cases were examined with abdominal ultrasonography (USG). Osteoarticular involvement means arthralgia and arthritis. For determining arthritis, in addition to arthralgia, movement limitation, increased interarticular fluid, and edema were evaluated. Only leg pain or joint pain was not evaluated as joint involvement. Joint USG was performed on patients for whom clinical osteoarticular involvement was detected. Abdominal USG was performed on every patient with brucellosis diagnosis admitted to the service in order to screen for the presence of hepatosplenomegaly that could not be detected during examination. Joint USG was performed on all patients. Magnetic resonance imaging (MRI) was performed on only 3 patients. The standard treatment approach in children older than 8 years is a combination of doxycycline with rifampin and/or gentamicin. Doxycycline is not used in children younger than 8 years because it causes discoloration of the teeth. In this age group, gentamicin, streptomycin, or rifampicin treatments are added to trimethoprim-sulfamethoxazole treatment (5,6).

Patients were divided into three groups according to their ages as 1-5 years, 6-11 years, and ≥12 years. Patients who did not show complete clinical recovery within 4 weeks, and especially those with slow regression of joint findings, were considered to have a partial response. All results were recorded from patient files.

The study was approved by the local ethics committee of the Kafkas University (26.02.2020, 06/22).

Statistical Analysis

The data was evaluated using the IBM SPSS v.26.0 software. The Shapiro-Wilk and Kolmogorov-Smirnov normality tests were used to determine the distribution patterns of the variables. Continuous data are presented as mean and standard deviation, or median, accompanied by the interquartile range, minimum-maximum values. The Mann-Whitney U test and Student's t-test were used for comparisons between two groups of continuous variables, and the Kruskal-Wallis test and One-Way ANOVA tests were used for comparisons between more than two groups, respectively. The chi-squared test, Fisher's exact test, and Fisher-Freeman-Halton test were used to analyze categorical variables. Statistical significance will be accepted at the level of $p < 0.05$.

RESULTS

Of the 80 patients with osteoarticular involvement included in the study, 54 (67.5%) were male and 26 (32.5%) were female. The median age was 12 (range, 1-17) years. 52.5% (n=42) of the cases were admitted in the summer, and 95% (n=76) of the patients had a history of livestock/domestic transmission, while 70% (n=56) had a history of raw milk/dairy products consumption.

All patients had arthralgia. While 57.5% (n=46) of the patients were admitted with monoarthritis/arthralgia, 42.5% (n=34) presented with at least 2 joint involvements. Weakness and sweating complaints were significantly higher in older children (p=0.036). Among the most frequently involved joints, the right hip was involved by 40% (n=32), the left hip by 26.3% (n=21), the right knee

by 27.5% (n=22), and the left knee by 23.8% (n=19). 93.7% (n=75) of the patients presented with an acute clinic, while 6.3% (n=5) had a subacute clinic. Rose Bengal and agglutination test positivity was 93.8% (n=75) and 96.3% (n=77), respectively, and the growth rate in blood/joint aspirate culture was 6.3% (n=5). Demographic and clinical characteristics of the patients were presented in Table 1.

Blood cultures were taken from 42 patients, but positivity was detected in 3 patients. Joint fluid cultures were taken from 2 patients, and positivity was detected. Kx result information could not be accessed from the file or the system. The file contained information that a growth signal was received.

Relapse developed in 14 (17.5%) patients within six months. Septic arthritis developed only in two patients, a 13-year-old female and a 14-year-old male. Response to non-complication treatment was taken, and they recovered. No headache was seen in patients with relapse, while there were 19 (28.8%) patients with headache in those without (p=0.003). ESR (p=0.001), CRP (p=0.003), ALT (p<0.001), and AST (p<0.001) values at admission were found statistically significantly higher in the relapse group. There was no other significant difference between the patients with and without relapse (Table 2).

The rate of sacroiliac joint was higher in the relapse group, but the difference was not at the level of statistical significance (p=0.068). On the other hand, shoulder joint involvement both for left and right shoulders was found significantly higher in the patients with relapse (p=0.016). No other significant difference was found in joint involvement sites between the patients with and without relapse (Table 3).

DISCUSSION

In the present study, relapse developed in 14 out of the 80 children diagnosed with brucellosis, accompanied by active osteoarticular involvement. The most frequent involvement was the hip, and the upper extremity joints were rarely involved. Admission ALT, AST, CRP, and ESR values were higher, and shoulder joint involvement was more frequent in the patients with relapse.

Table 1. Demographic characteristics, clinical features, and treatment responses of the patients

	1-5 years (n=9)	6-11 years (n=23)	12-18 years (n=48)	p	Total (n=80)
Gender, n (%)					
Male	5 (55.6)	14 (60.9)	35 (72.9)	0.430	54 (67.5)
Female	4 (44.4)	9 (39.1)	13 (27.1)		26 (32.5)
Follow-up period (months)	28.33±12.91	21.98±2.49	22.55±1.81	0.941	22.28±1.37
Admission Season, n (%)					
Spring	3 (33.3)	2 (8.7)	6 (12.5)		11 (13.8)
Summer	4 (44.4)	10 (43.5)	28 (58.3)		42 (52.5)
Autumn	1 (11.1)	4 (17.4)	7 (14.6)	0.427	12 (15.0)
Winter	1 (11.1)	7 (30.4)	7 (14.6)		15 (18.8)
Livestock/Domestic Transmission, n (%)	8 (88.9)	21 (91.3)	47 (97.9)	0.199	76 (95.0)
Raw Milk/Dairy Product Consumption, n (%)	4 (44.4)	15 (65.2)	37 (77.1)	0.123	56 (70.0)
Fever, n (%)	8 (88.9)	17 (73.9)	38 (79.2)	0.723	63 (78.8)
Weakness/Sweating, n (%)	0 (0.0)	7 (30.4)	21 (43.8)	**0.036**	28 (35.0)
Stomachache, n (%)	3 (33.3)	4 (17.4)	7 (14.6)	0.360	14 (17.5)
Headache, n (%)	5 (55.6)	4 (17.4)	10 (20.8)	0.056	19 (23.8)
Joint Involvement, n (%)					
Monoarthritis/arthralgia	8 (89.9)	12 (52.2)	26 (54.2)	0.128	46 (57.5)
Polyarthritis/arthralgia	1 (11.1)	11 (47.8)	22 (45.8)		34 (42.5)
Joint Involvement, n (%)					
Monoarthritis/arthralgia	8 (88.9)	12 (52.2)	26 (54.2)		46 (57.5)
2	1 (11.1)	7 (30.4)	14 (29.2)	0.791	22 (27.5)
3	0 (0.0)	2 (8.7)	4 (8.3)		6 (7.5)
>4	0 (0.0)	2 (8.7)	4 (8.3)		6 (7.5)
Hepatosplenomegaly, n (%)	1 (11.1)	4 (17.4)	10 (20.8)	0.919	15 (18.9)
Neurological Involvement, n (%)	0 (0.0)	0 (0.0)	2 (4.2)	>0.999	2 (2.5)
Rose Bengal (+), n (%)	8 (88.9)	22 (95.6)	45 (93.7)	0.632	75 (93.8)
Agglutination test (+), n (%)	9 (100)	22 (95.6)	46 (95.8)	>0.999	77 (96.3)
Blood/Joint Aspirate Culture (+), n (%)	1 (11.1)	1 (4.3)	3 (6.3)	0.632	5 (6.3)
Treatment, n (%)					
TMP-STX + Genta	9 (100)	10 (43.5)	-	-	19 (23.8)
Dox + RIF + Genta	-	13 (56.5)	48 (100)		61 (76.2)
Treatment Response, n (%)					
Full Response	7 (10.6)	20 (30.3)	39 (59.1)	0.756	66 (82.5)
Partial Response	2 (14.3)	3 (21.4)	9 (64.3)		14 (17.5)

TMP-STX: trimethoprim sulfamethoxazole, Genta: gentamicin, Dox: doxycycline, RIF: rifampicin, patients who did not show complete clinical recovery within 4 weeks, and especially those with slow regression of joint findings, were considered to have a partial response

Table 2. Evaluation of patients with and without relapse in terms of demographic characteristics and laboratory results at admission

	Relapse (+) (n=14)	Relapse (-) (n=66)	p
Age Group, n (%)			
1-5 years	2 (14.3)	7 (10.6)	
6-11 years	3 (21.4)	20 (30.3)	0.756
12-18 years	9 (64.3)	39 (59.1)	
Gender, n (%)			
Male	9 (64.3)	45 (68.2)	0.763
Female	5 (35.7)	21 (31.8)	
Admission Season, n (%)			
Spring	3 (21.4)	8 (12.1)	
Summer	9 (64.3)	33 (50.0)	0.435
Autumn	1 (7.1)	11 (16.7)	
Winter	1 (7.1)	14 (21.2)	
Fever, n (%)	12 (85.7)	51 (77.3)	0.722
Weakness/Sweating, n (%)	7 (50.0)	21 (31.8)	0.226
Stomachache, n (%)	0 (0.0)	14 (21.2)	0.114
Headache, n (%)	0 (0.0)	19 (28.8)	**0.033**
Joint Involvement, n (%)			
Monoarthritis/arthralgia	9 (64.3)	37 (56.1)	0.572
Polyarthritis/arthralgia	5 (35.7)	29 (43.9)	
Joint Involvement, n (%)			
Monoarthritis/arthralgia	9 (64.3)	37 (56.1)	
2	3 (21.4)	19 (28.8)	0.954
3	1 (7.1)	5 (7.6)	
>4	1 (7.1)	5 (7.6)	
Hepatosplenomegaly, n (%)	3 (21.4)	12 (18.2)	0.720
Neurological Involvement, n (%)	1 (7.1)	1 (1.7)	0.321
WBC (/mm3)	6.1 (5.5-6.8) [3.3-8.2]	6.5 (5.1-7.9) [3.2-13.5]	0.449
Hb (g/dL)	13.2 (12-14) [10-15.6]	13.3 (12-14) [8.3-16.7]	0.819
PLT (/mm3)	263.5 (242-324) [192-414]	282.5 (230-358) [170-473]	0.767
ESR (mm/hour)	25 (14-39) [4-67]	8 (5-20) [2-37]	**0.001**
CRP (mg/dL)	1.3 (0.1-3.7) [0.04-8.9]	0.3 (0.1-0.9) [0.01-4.85]	**0.003**
ALT (U/L)	131 (60-226) [29-388]	30 (22-56) [11-141]	**<0.001**
AST (U/L)	96 (78-119) [21-382]	25 (15-51) [10-211]	**<0.001**
Urea (mg/dL)	22.92±6.56	24.04±6.75	0.574
Creatinine (mg/dL)	0.54±0.19	0.57±0.16	0.563

WBC: white blood cell, Hb: hemoglobin, PLT: platelet, ESR: erythrocyte sedimentation rate, CRP: C-reactive protein, ALT: alanine transaminase, AST: aspartate aminotransferase, descriptive statistics for numerical variables were presented as median (25th-75th percentile) [minimum-maximum] or mean±standard deviation

Table 3. Evaluating the relationship between the osteoarticular involvement site and relapse

	Relapse (+) (n=14)	Relapse (-) (n=66)	p	Total (n=80)
Right Hip, n (%)	7 (50.0)	25 (37.9)	0.400	32 (40.0)
Left Hip, n (%)	3 (21.4)	18 (27.3)	0.751	21 (26.3)
Right Knee, n (%)	2 (14.3)	20 (30.3)	0.328	22 (27.5)
Left Knee, n (%)	3 (21.4)	16 (24.2)	>0.999	19 (23.8)
Right Ankle, n (%)	0 (0.0)	9 (13.6)	0.348	9 (11.3)
Left Ankle, n (%)	0 (0.0)	7 (10.6)	0.344	7 (8.8)
Sacroiliac Joint, n (%)	4 (28.6)	6 (9.1)	0.068	10 (12.5)
Right Shoulder, n (%)	3 (21.4)	1 (1.5)	**0.016**	4 (5.0)
Left Shoulder, n (%)	3 (21.4)	1 (1.5)	**0.016**	4 (5.0)
Right Elbow, n (%)	1 (7.1)	1 (1.5)	0.321	2 (2.5)
Left Elbow, n (%)	0 (0.0)	6 (9.1)	0.584	6 (7.5)
Right Wrist, n (%)	1 (7.1)	5 (7.6)	>0.999	6 (7.5)
Left Wrist, n (%)	2 (14.3)	3 (4.5)	0.209	5 (6.3)

Various studies conducted on Brucella reported that the highest risk factor for the disease was non-pasteurized dairy products, especially cheese (2,8-10). Likewise, in the present study, the patients had a history of direct raw milk/dairy products consumption by 70% (n=56) and livestock/domestic transmission by 95% (n=76).

The clinical course can be acute, subacute, and chronic. The disease can sometimes display subclinical and localized infection symptoms (9). 93.8% of the complaints of patients in the present study developed acutely. The main clinical symptoms seen in children with brucellosis are fever, loss of appetite, weight loss, diffuse muscle, joint pain, headache, stomachache, and night sweats (3,9,10). The main complaints of the patients in this study were fever, arthralgia, weakness and sweating, headache, and stomachache, which were compatible with the literature.

In the laboratory, the gold standard for diagnosis is culture positivity, but it is highly difficult to detect. The culture positivity rate in studies is around 3-36% (5,11,12). Therefore, when serological tests are not helpful for diagnosis, producing microorganisms in blood, bone marrow, or other infected tissue cultures and joint aspiration material can help with diagnosis (11). In the present study, blood/joint fluid culture positivity was determined in 6.3% (n=5) of the patients. In the whole blood count, we can find some clues. Mild leukocytosis is expected in the whole blood count in the presence of brucellosis with osteoarticular involvement (5). The related studies revealed a distinct increase in acute-phase reactants, especially in the inflammation period (13,14). In the present study, acute phase reactants as well as ALT and AST values were distinctively higher than the admission laboratory values of the patients with relapse. In their study, Bozukluhan et al. (15) found that serum ALT and AST values were significantly higher in brucellosis cases compared to healthy controls. It is known that ALT and AST values increase in case of inflammation in the liver (15,16). Higher values in patients with relapse can indicate that subclinical inflammation will continue.

The involvement mostly manifests itself in the joints as arthritis. The incidence rate of this involvement varies between 10-85% all around the world. In another study, Brucella arthritis incidence was reported to vary between 10% and 56% (8,17). It was compatible with the literature. The most frequently involved joints are large joints such as the knee, hip, ankle, and sacroiliac joints. It is rarely seen in the upper extremities (4,6,7,18). Joint involvements determined in the present study are compatible with the literature. Arthritis is generally in the form of monoarthritis or asymmetrical peripheral oligoarthritis (6,7). Likewise, monoarthritis/arthralgia percentage (57.5%) was higher than in polyarthritis patients in the present study. 42.5% of the cases had involvement in more than one joint. Brucella arthritis generally does not cause destruction or permanent functional disorder. Response to treatment is good, and relapse is rarely seen. Joint symptoms did not repeat in patients with relapse in the present study (2,17,19).

In brucellosis cases who did not develop complications, relapse rates ranged between 3.6-4.5%, while high relapse rates were reported (10.6-21%) in cases with focal and osteoarticular involvements (20,21). In the present study, the relapse rate of the patients with osteoarticular involvement was 17.5% (n=14), which was slightly higher compared to the literature. This situation can be explained by the fact that 95% of the patients in the present study were engaged in livestock, as well as high risks of interfamily and recurrent infections.

Among joint involvements in adult brucellosis cases, sacroiliitis is the most frequently seen clinical form, and its incidence rate has been reported to vary between 8-20% by numerous studies. Sacroiliac involvement has been reported in 10-60% of the cases with arthritis (2,22,23). Sacroiliitis is mostly unilateral and seen in young patients in an acute disease course. Sacroiliac involvement is more rarely seen in young children. Some studies have reported mostly knee and hip localization (8,24). In the present study, the sacroiliac involvement rate was 12.5%. This high rate might have been because the majority of the patients were 12-18 years old. In line with the literature, the highest involvements were observed in the hip and knee joints.

A previous study reported that peripheral involvement rates were detected in the sternoclavicular joint (4.5%), wrist (2.4%), elbow (1.07%), and shoulder (0.6%) (25). Shoulder involvement, right and left elbow involvement, and right and left wrist involvement were slightly higher in the present study compared to other studies. In addition, relapse rates of shoulder joint involvement were higher. There are studies in the literature reporting that the presence of osteoarticular involvement is associated with relapse (26); however, data on which joint involvement is limited.

Nervous system involvement is a serious complication that is seen at rates of 2.6-14.4% in adults and 1-2.2% in children (25,26). Neurological complications include such as meningitis, meningoencephalitis, cranial nerve involvement, and radiculitis (27). Mortality of these complications is low, but the probability of sequela is high. In the present study, 2.5% of the patients were diagnosed with meningoencephalitis, and they recovered without sequela.

The limitation of the study was that the first relapse group was small. Second, joint MRI could not be performed on every patient. The patients were followed up for approximately 22 months, but long-term results of 5-10 years could not be evaluated. The strength of the study was that it was conducted in childhood and produced hypotheses about the relationship between the location of joint involvement and relapse.

CONCLUSION

High admission ALT, AST, CRP, and ESR levels in brucellosis cases with osteoarticular involvement and the presence of shoulder joint involvement, albeit rarely, can be a warning sign in terms of relapse. Therefore, these patients should be followed more carefully, maybe they should receive the treatment at the maximum dose and frequency, and if possible, they should be treated as hospitalized, which may be a suggestion to reduce relapse rates. However, for all these, new studies need to be planned regarding the duration and type of treatment. There is a need for further studies with larger populations. Patients should be closely monitored in terms of complications.

Ethics Committee Approval: The study was approved by the Ethics Committee of Kafkas University Faculty of Medicine (26.02.2020, 22).

Conflict of Interest: None declared by the authors.

Financial Disclosure: None declared by the authors.

Acknowledgments: None declared by the authors.

Author Contributions: Idea/Concept: TNKB, ME; Design: TNKB, HBB; Data Collection/Processing: HBB, ME, ZB; Analysis/Interpretation: HBB; Literature Review: TNKB; Drafting/Writing: TNKB, HBB, ME; Critical Review: ME.

All authors were working at Kafkas University during the study period and were appointed to a different city, which reflects their current place of employment.

REFERENCES

1. Kaman A, Öz FN, Fettah A, Durmuş SY, Teke TA, Tanır G. Clinicoepidemiological findings of childhood brucellosis in a tertiary care center in Central Anatolia: with the emphasis of hematological findings. Turk J Pediatr. 2022;64(1):10-8.
2. Savion N, Guzner N, Hashavya S, Reif S, Ohana Sarna Cahan L. Brucellosis in pediatric populations: An 11-year cohort study. Isr Med Assoc J. 2023;25(8):542-6.
3. Tanir G, Tufekci SB, Tuygun N. Presentation, complications, and treatment outcome of brucellosis in Turkish children. Pediatr Int. 2009;51(1):114-9.
4. Buzgan T, Karahocagil MK, Irmak H, Baran AI, Karsen H, Evirgen O, et al. Clinical manifestations and complications in 1028 cases of brucellosis: a retrospective evaluation and review of the literature. Int J Infect Dis. 2010;14(6):e469-78.
5. Bukhari EE. Pediatric brucellosis. An update review for the new millennium. Saudi Med J. 2018;39(4):336-41.
6. Bosilkovski M, Zezoski M, Siskova D, Miskova S, Kotevska V, Labacevski N. Clinical characteristics of human brucellosis in patients with various monoarticular involvements. Clin Rheumatol. 2016;35(10):2579-84.
7. Khateeb MI, Araj GF, Majeed SA, Lulu AR. Brucella arthritis: A study of 96 cases in Kuwait. Ann Rheum Dis. 1990;49(12):994-8.
8. Geyik MF, Gür A, Nas K, Çevik R, Saraç J, Dikici B, et al. Musculoskeletal involvement in brucellosis in different age groups: A study of 195 cases. Swiss Med Wkly. 2002;132(7-8):98-104.
9. Dutta D, Sen A, Gupta D, Kuila P, Chatterjee D, Sanyal S, et al. Childhood brucellosis in Eastern India. Indian J Pediatr. 2018;85(4):266-71.
10. Wang W, Wang Z, Jia K, Tang J, Wang L. Clinical and laboratory characteristics of childhood brucellosis in high-risk area of Western China. Jpn J Infect Dis. 2022;75(2):127-32.
11. Criado MD, MacHain UB, Rey LV, Antón MP, Loza SM, Alcobendas Rueda RM, et al. Evaluation of diagnostic tests in pediatric brucellosis. Eur J Pediatr. 2019;178(11):1707-8.

12. Kara SS, Cayir Y. Predictors of blood culture positivity in pediatric brucellosis. J Coll Physicians Surg Pak. 2019;29(7):665-70.
13. Pourakbari B, Abdolsalehi M, Mahmoudi S, Banar M, Masoumpour F, Mamishi S. Epidemiologic, clinical, and laboratory characteristics of childhood brucellosis: A study in an Iranian children's referral hospital. Wien Med Wochenschr. 2019;169(9-10):232-9.
14. Parlak M, Akbayram S, Doğan M, Tuncer O, Bayram Y, Ceylan N, et al. Clinical manifestations and laboratory findings of 496 children with brucellosis in Van, Turkey. Pediatr Int. 2015;57(4):586-9.
15. Bozukluhan K, Merhan O, Celebi O, Buyuk F, Ogun M, Gokce G. Levels of certain biochemical and oxidative stress parameters in cattle with Brucellosis. J Hellenic Vet Med Soc. 2017;68(3):285-90.
16. Albayrak A, Albayrak F. Hepatic granulomas associated with brucellosis: Hepatic granulomas and brucellosis. Hepat Mon. 2011;11(1):1-2.
17. Çiftdoğan DY, Aslan S. Osteoarticular involvement of brucellosis in pediatric patients: Clinical and laboratory characteristics. Turk J Pediatr. 2020;62(2):199-207.
18. Turan H, Serefhanoglu K, Karadeli E, Togan T, Arslan H. Osteoarticular involvement among 202 brucellosis cases identified in Central Anatolia region of Turkey. Intern Med. 2011;50(5):421-8.
19. Zamani A, Kooraki S, Mohazab RA, Zamani N, Matloob R, Hayatbakhsh MR, et al. Epidemiological and clinical features of Brucella arthritis in 24 children. Ann Saudi Med. 2011;31(3):270-3.
20. Bosilkovski M, Kirova-Urosevic V, Cekovska Z, Labacevski N, Cvetanovska M, Rangelov G, et al. Osteoarticular involvement in childhood brucellosis: Experience with 133 cases in an endemic region. Pediatr Infect Dis J. 2013;32(8):815-9.
21. Hashemi SH, Keramat F, Ranjbar M, Mamani M, Farzam A, Jamal-Omidi S. Osteoarticular complications of brucellosis in Hamedan, an endemic area in the west of Iran. Int J Infect Dis. 2007;11(6):496-500.
22. Turan Ozden H, Togan T. Osteoarticular involvement among brucellosis cases in Konya city. Cukurova Med J. 2015;40(3):483-94. Turkish.
23. Ebrahimpour S, Bayani M, Moulana Z, Hasanjani Roushan MR. Skeletal complications of brucellosis: A study of 464 cases in Babol, Iran. Caspian J Intern Med. 2017;8(1):44-8.
24. Özger HS, Karaşahin Ö, Yildiz Y, Dizbay M. Osteoarticular involvement and inadequate treatment of brucellosis are related to relapse. Mediterr J Infect Microb Antimicrob. 2020;9(1):1.
25. Hendaus MA, Qaqish RM, Alhammadi AH. Neurobrucellosis in children. Asian Pac J Trop Biomed. 2015;5(2):158-61.
26. Akbayram S, Dogan M, Peker E, Bektas MS, Caksen H, Karahocagil M. Evaluation of children with neurobrucellosis. Bratisl Lek Listy. 2012;113(7):424-30.
27. Su XW, Feng WY, Li JL, Song RX, Wu RH, Zhu H. Brucella meningoencephalitis in children with status epilepticus: A case report and literature review. China Trop Med. 2023;23(3):319-22.

Tracheobronchial Foreign Body Aspirations for Children

Çocuklarda Trakeobronşiyal Yabancı Cisim Aspirasyonları

Leyla Nesrin ACAR[1]
0009-0001-8920-7416
Seray HAZER[1]
0000-0003-1474-5591
Göktürk FINDIK[2]
0000-0002-8861-7608
Pınar BIÇAKÇIOĞLU[1]
0000-0002-7058-6508
Selim Şakir Erkmen GÜLHAN[1]
0000-0002-1143-9655

[1]Department of Thoracic Surgery, Atatürk Sanatorium Training and Research Hospital, Ankara, Türkiye

[2]Department of Thoracic Surgery, Dr. Abdurrahman Yurtaslan Ankara Oncology Training and Research Hospital, Ankara, Türkiye

ABSTRACT

Aim: Tracheobronchial foreign body aspiration (FBA) is a leading cause of accidental injury and sudden death in childhood. This study aimed to categorize pediatric patients under the age of 16 years with tracheobronchial FBA into distinct age groups, compare gender distribution, assess clinical and radiological findings, characterize the types of aspirated foreign body (FB), and evaluate preventive measures to reduce the incidence of FBA.

Material and Methods: This retrospective study included patients under the age of 16 years who were evaluated for suspected tracheobronchial FBA between 2010 and 2019. The patients were categorized into four age groups: ≤3 years, 4-7 years, 8-10 years, and >10 years.

Results: Among the 132 patients included, 80 (60.6%) were male, and 52 (39.4%) were female. The FBA was found to be significantly (p=0.003) most prevalent among males aged ≤3 years (72.7%, n=32) and among females aged >10 years (59.2%, n=29). The type of aspirated FB significantly varied by age group, with dried nuts being the most aspirated in children ≤3 years (50.0%, n=22), stationery items in the 8-10 years (47.1%, n=8), and headscarf needles in the >10-year (36.7%, n=18) groups (p<0.001).

Conclusion: The type of aspirated FBs varies according to age and cultural factors. The severity of FBA-related complications depends on the size, shape, and location of the aspirated object, as well as the patient's age, duration of aspiration, and degree of airway obstruction. Enhancing public awareness, facilitating early diagnosis, and ensuring prompt treatment are crucial for minimizing FBA-related complications and mortality.

Keywords: Foreign body; tracheobronchial aspiration; bronchoscopy; child.

ÖZ

Amaç: Trakeobronşiyal yabancı cisim aspirasyonu (YCA), çocukluk çağında kazara yaralanmaların ve ani ölümlerin önde gelen nedenidir. Bu çalışmada, trakeobronşiyal YCA olan 16 yaş altı çocukların farklı yaş gruplarına göre kategorize edilmesi, cinsiyet dağılımının, klinik ve radyolojik bulguların, aspire edilen yabancı cisim (YC) tiplerinin karşılaştırılarak YCA insidansının azaltılması için koruyucu önlemlerin değerlendirilmesi amaçlanmıştır.

Gereç ve Yöntemler: Bu geriye dönük çalışmaya 2010 ve 2019 yılları arasında trakeobronşiyal YCA şüphesi ile değerlendirilen 16 yaşından küçük hastalar dahil edilmiştir. Hastalar dört yaş grubuna ayrılmıştır: ≤3 yaş, 4-7 yaş, 8-10 yaş ve >10 yaş.

Bulgular: Çalışmaya dahil edilen 132 hastadan 80'i (%60,6) erkek ve 52'si (%39,4) kadındı. YCA'nın, ≤3 yaş erkeklerde (%72,7; n=32) ve >10 yaş kadınlarda (%59,2; n=29) anlamlı olarak en yaygın olduğu bulundu (p=0,003). Aspire edilen YB tipleri yaş grubuna göre anlamlı bir şekilde değişiyordu; kuru yemişler ≤3 yaş çocuklarda (%50,0; n=22), kırtasiye malzemeleri 8-10 yaş grubunda (%47,1; n=8) ve başörtüsü iğneleri ise >10 yaş grubunda (%36,7; n=18) en çok aspire edildi (p<0,001).

Sonuç: Aspire edilen YC türleri yaş grubuna ve kültürel faktörlere göre değişmektedir. YCA ile ilişkili komplikasyonların şiddeti, aspire edilen cismin büyüklüğüne, şekline ve lokalizasyonuna, ayrıca hastanın yaşına, aspirasyon süresine ve hava yolu tıkanıklığının derecesine bağlıdır. Kamuoyunun farkındalığını artırmak, erken tanıyı kolaylaştırmak ve hızlı tedaviyi sağlamak, YCA ile ilişkili komplikasyonları ve mortaliteyi en aza indirmek için çok önemlidir.

Anahtar kelimeler: Yabancı cisim; trakreobronşiyal aspirasyon; bronkoskopi; çocuk.

INTRODUCTION

Tracheobronchial foreign body aspiration (FBA) is most commonly observed in pediatric populations and constitutes a medical emergency necessitating prompt diagnosis and intervention. The severity of FBA-related complications depends on the size, shape, and location of the aspirated object, as well as the patient's age, duration of aspiration, and degree of airway obstruction. In severe cases, FBA can result in life-threatening complications and even death (1-3). In the United States, 160 children under the age of 14 died due to FBA in 2000, and it accounts for 7% of deaths in children under the age of 3 (2-5).

The type of foreign body (FB) aspirated varies according to age, geographic region, dietary habits, seasonal factors, and socioeconomic conditions. Studies have shown that in children under 3 years of age, the most frequently aspirated FBs are nuts and seeds, such as hazelnuts, peanuts, and roasted chickpeas (1,6,7). In Muslim societies like Türkiye, headscarf needle aspiration is a significant concern in girls aged 10 years and older (8). The primary treatment for FBA in children is rigid bronchoscopy, while fiberoptic bronchoscopy (FOB) may be used in selected cases (9). Delayed diagnosis and treatment can lead to recurrent lung infections, irreversible atelectasis, and bronchiectasis, potentially necessitating lung resection (1,5). Moreover, hypoxic-ischemic encephalopathy has been reported due to prolonged airway obstruction (10). Therefore, early diagnosis and intervention are critical to prevent serious complications and fatalities (1,2,10).

Aspirated FBs differ by age group. Children under 3 years commonly aspirate nuts and food particles, preschool-aged children often aspirate toy parts, school-aged children frequently aspirate stationery items such as pen caps and springs, and adolescent girls (≥10 years old) are at high risk for headscarf needle aspiration (1,8,11).

This study aimed to categorize pediatric patients under 16 years of age with FBA into distinct age groups, compare gender distribution, characterize the FB types, assess clinical presentations and radiological findings, and identify preventive strategies to reduce FBA-related morbidity and mortality.

MATERIAL AND METHODS

This retrospective study analyzed 291 patients evaluated for suspected tracheobronchial FBA between 2010 and 2019 in our clinic. Among these, 151 patients (51.9%) were below 16 years. Nineteen (12.6%) patients in whom FBs could not be detected during clinical and radiological evaluations were excluded from the study.

A total of 132 patients (87.4%) under the age of 16 with confirmed FBA were included in the study. The patients were categorized into four age groups: ≤3 years, 4-7 years, 8-10 years, and >10 years.

The differences between the groups were analyzed in terms of gender, presenting symptoms, physical examination findings, radiological findings, time from aspiration to hospital admission, FB type, localization, treatment approach, and procedural complications. The time to hospital admission was defined as the interval between the aspiration event or the onset of symptoms and the patient's presentation to the hospital.

For all patients, posteroanterior chest radiographs were obtained during inspiration. In cases where the initial radiographic findings were normal, additional expiratory or lateral radiographic images were taken to enhance diagnostic accuracy.

Bronchoscopy Treatment Protocol

The treatment approach was determined based on patient history, physical examination, and radiological findings. In cases where radiological evaluation did not confirm the presence of an FB, but anamnesis and/or physical examination suggested aspiration, the families were informed about the potential risks, and further evaluation was conducted. For patients with severe dyspnea due to tracheobronchial FB obstruction, rigid bronchoscopy was performed under general anesthesia (GA) in an emergency setting. In other cases, prior to bronchoscopy, the following laboratory tests were conducted: complete blood count, comprehensive biochemical analysis, coagulation tests, and blood group determination. Bronchoscopy was performed after a minimum 5-hour fasting period. FOB was used as an adjunctive treatment in cases where the FB was located in the distal airways or the upper lobe bronchus and could not be accessed using rigid bronchoscopy. Surgical intervention was performed for cases in which the FB could not be removed despite all endoscopic attempts. A comprehensive evaluation of the central airway, including both bronchial systems, was performed to rule out bilateral FBA. Following rigid bronchoscopy under GA, patients were monitored in the intensive care unit for 2 hours. For cases in which bronchoscopy lasted longer than 20 minutes, oxygen therapy via mask, nebulized steam therapy, and steroid treatment were administered. A post-procedural chest X-ray was routinely performed following bronchoscopy.

Ethical approval for this study was obtained from the Keçiören Training and Research Hospital Clinical Research Ethics Committee (09.03.2021, 2249).

Statistical Analysis

Statistical analyses were performed using IBM SPSS Statistics for Windows, Version 25.0 (IBM Corp., Armonk, NY, USA). Descriptive statistics for the variables in the study were expressed as numbers and percentages. Chi-square or Fisher's exact test was calculated to determine the relationships between categorical variables. A p-value of <0.05 was considered statistically significant.

RESULTS

Among the 132 patients included in the study, 80 (60.6%) were male and 52 (39.4%) were female. The mean age of the patients was 8.4±5.5 (range, 1-16) years. When analyzed by age groups, males predominantly belonged in the ≤3-year-old group, whereas females were predominantly in the >10-year-old group, with a statistically significant difference (p=0.003).

The largest proportion of patients (37.1%, n=49) belonged to the >10-year-old group, followed by the ≤3-year-old group (33.3%, n =44).

The majority (64.4%, 85) of the patients across all age groups were admitted within the first 24 hours following aspiration. However, in the ≤3-year-old group, seven patients had no history of aspiration, and they were referred to our clinic by the pediatrics department due to chronic cough and suspected FBA. All remaining patients had a confirmed history of aspiration.

The most frequently reported symptoms in patients were cough (70.5%, n=93) and shortness of breath (40.2%, n=53). However, no statistically significant difference was observed between the age groups (p=0.141 and p=0.723, respectively). Additional symptoms included cyanosis and vomiting, which were more common in the ≤3-year-old group, while chronic infection and shortness of breath were more frequently observed in the >10-year-old group. No statistically significant relationship was observed. However, wheezing was found to be significantly more frequent in the ≤3 years age group (p=0.032). Physical examination findings were generally unremarkable; however, diminished breath sounds were the second most common finding in the ≤3-year-old group (p=0.069). Chest X-rays were normal in 59 (44.7%) patients, whereas FBs were directly visualized in 28 (21.2%) patients. When evaluated according to age groups, FBs were detected most frequently in the >10 age group. A statistically significant relationship was observed between chest X-ray findings and age groups (p<0.001, Table 1, Figure 1).

Bronchoscopy was performed as an emergency procedure in 29 (22.0%) patients due to severe respiratory distress, while in the remaining cases, the procedure was conducted under elective conditions. Under GA, rigid bronchoscopy was performed in 104 (78.8%) cases, while FOB with local anesthesia and sedation was performed in 28 (21.2%) cases.

In terms of FB localization, 88 (66.7%) cases had FBs in the right bronchial system, 34 (25.8%) cases had FBs in the left bronchial system, 10 (7.5%) cases in the trachea, and 56 (42.4%) cases in the lower lobes (Table 1).

The FBs were most frequently located in the main bronchus in the ≤3-year-old group, while they were most commonly found in the lower lobes in the >10-year-old group. No statistical significance was found in FB localization between age groups (p=0.138).

Table 1. Patient characteristics according to age groups

	≤3 years (n=44)	4-7 years (n=22)	8-10 years (n=17)	>10 years (n=49)	p
Gender, n (%)					
Female	12 (27.3)	8 (36.4)	3 (17.6)	29 (59.2)	**0.003**
Male	32 (72.7)	14 (63.6)	14 (82.4)	20 (40.8)	
Admission Time, n (%)					
0-24 h	25 (56.8)	14 (63.6)	15 (88.2)	31 (63.3)	
<7 day	11 (25.0)	4 (18.2)	1 (5.9)	9 (18.4)	0.506
>7 day	8 (18.2)	4 (18.2)	1 (5.9)	9 (18.4)	
Symptoms, n (%)					
Cough, n (%)	29 (65.9)	12 (54.5)	14 (82.4)	38 (77.6)	0.141
Shortness of breath, n (%)	16 (36.4)	11 (50.0)	6 (35.3)	20 (40.8)	0.723
Wheezing, n (%)	5 (11.4)	0 (0.0)	1 (5.9)	0 (0.0)	**0.032**
Cyanosis, n (%)	7 (15.9)	3 (13.6)	0 (0.0)	3 (6.1)	0.184
Chronic infection, n (%)	3 (6.8)	2 (9.1)	0 (0.0)	5 (10.2)	0.684
Vomiting, n (%)	5 (11.4)	1 (4.5)	1 (5.9)	2 (4.1)	0.594
Physical Examination, n (%)					
Normal	18 (40.9)	13 (59.1)	12 (70.6)	34 (69.4)	
Ral/ronkus	11 (25.0)	3 (13.6)	2 (11.8)	8 (16.3)	0.069
Diminished breath sounds	13 (29.5)	3 (13.6)	2 (11.8)	3 (6.1)	
Stridor	2 (4.5)	3 (13.6)	1 (5.9)	4 (8.2)	
Chest X-ray, n (%)					
Normal	22 (50.0)	12 (54.5)	4 (23.5)	21 (42.9)	
Foreign body	0 (0.0)	3 (13.6)	7 (41.2)	18 (36.7)	
Obstructive emphysema of the lung	9 (20.5)	2 (9.1)	1 (5.9)	0 (0.0)	**<0.001**
Atelectasis	9 (20.5)	2 (9.1)	3 (17.6)	1 (2.0)	
Consolidation	4 (9.1)	3 (13.6)	2 (11.8)	9 (18.4)	
Side, n (%)					
Right	29 (65.9)	12 (54.5)	13 (76.5)	34 (69.4)	
Left	14 (31.8)	7 (31.8)	3 (17.6)	10 (20.4)	0.391
Trachea	1 (2.3)	3 (13.6)	1 (5.9)	5 (10.2)	
Location, n (%)					
Trachea	1 (2.3)	3 (13.6)	1 (5.9)	5 (10.2)	
Main bronchus	20 (45.5)	6 (27.3)	5 (29.4)	10 (20.4)	
Upper bronchus	2 (4.5)	0 (0.0)	0 (0.0)	2 (4.1)	0.138
Intermediate bronchus	4 (9.1)	1 (4.5)	4 (23.5)	12 (24.5)	
Lower bronchus	17 (38.6)	12 (54.5)	7 (41.2)	20 (40.8)	
Foreign Body, n (%)					
Dried nuts	22 (50.0)	7 (31.8)	5 (29.4)	5 (10.2)	
Food scraps	7 (15.9)	5 (22.7)	1 (5.9)	10 (20.4)	
Headscarf needle	0 (0.0)	2 (9.1)	2 (11.8)	18 (36.7)	**<0.001**
Toys	14 (31.8)	3 (13.6)	1 (5.9)	0 (0.0)	
Stationery items	1 (2.3)	5 (22.7)	8 (47.1)	16 (32.7)	

The type of aspirated FBs significantly varied by age group (p<0.001). The most frequently aspirated objects were dried nuts for ≤3 years, stationery items were the most commonly aspirated objects in 8-10 years, and the most frequently aspirated object was the headscarf needle for >10 years (Table 1, Figure 2).

In two cases where headscarf needles were lodged in the distal bronchial system and could not be removed via rigid bronchoscopy, bronchotomy with posterolateral thoracotomy was performed for FB extraction.

Post-bronchoscopy complications included bronchospasm in 8 (6.1%) cases, laryngeal edema in 14 (10.6%) cases, and desaturation in 21 (15.9%) cases. These patients were treated with steroids, anti-inflammatory agents, bronchodilators, and oxygen therapy. Following the procedure, 107 (81.1%) patients were discharged on the same day, 23 (17.4%) patients were discharged 1 day post-procedure, and 2 (1.5%) patients who underwent thoracotomy were discharged on postoperative day 5. No mortality was recorded during the study period.

DISCUSSION

The FBA can be a life-threatening condition in children, necessitating immediate diagnosis and intervention. The incidence of FBA is significantly higher (53-92.1%) in children <3 years of age (1,5,7,10,12). Additionally, in Muslim countries, a distinct pattern is observed among adolescent females, where the aspiration of headscarf needles is particularly common, with a median age of 14 years (8). The high incidence of FBA in young children is attributed to several factors, including their natural tendency to explore objects with their mouths, the absence of molar teeth, which makes chewing difficult and results in food being held in the mouth, and the increased risk of aspiration during crying or laughing. Other contributing factors include playing with age-inappropriate toys, consumption of unsuitable foods, and inadequate parental supervision due to unawareness or lack of education (1,13-16). Interestingly, our study differs from previous reports as we identified a significantly higher incidence of FBA in children >10 years of age compared to those <3 years. We hypothesize that this discrepancy may be due to the referral patterns in our healthcare system. As our institution is a thoracic surgery clinic, younger children are more frequently referred to the pediatric surgery clinic, potentially leading to an underrepresentation of this age group in our dataset.

The male predominance in FBA is well-documented in the literature, with rates ranging from 63-65% for males and 34-36% for females (1,3,5). In our study, the distribution was 60.6% male and 39.4% female, aligning with these findings. While the male-to-female ratio was higher in younger age groups, we observed a reverse trend in children >10 years. This reversal is likely due to the high prevalence of headscarf needle aspiration among adolescent females, a practice by Muslim women in Türkiye, who use these needles to secure their headscarves.

The timing of admission following aspiration varies, with most cases presenting within the first 24 hours (10-50%), while 22-57.6% seek medical attention within the first week, and 3.9-20% present after 1 week (9,17-19). Our study is consistent with the literature, as the majority of all patients were admitted within the first 24 hours.
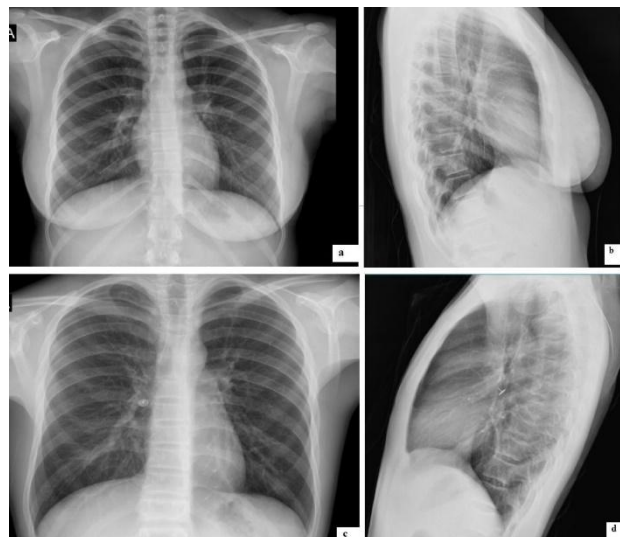

Figure 1. a) A 12-year-old female patient, chest X-ray plain shows a headscarf needle in the right lower lobe bronchus, **b)** the lateral chest X-ray; **c)** A 9-year-old male patient, chest X-ray plain shows a thumbtack right intermediate bronchus, **d)** the lateral chest X-ray

Figure 2. Some of the tracheobronchial foreign bodies

The clinical presentation of FBA depends on several factors, including the elapsed time since aspiration, the size and location of the FB, and the degree of airway obstruction. The classic triad of FBA symptoms includes a sudden-onset cough, shortness of breath, and wheezing with decreased unilateral breath sounds. These findings are crucial for early diagnosis (7,15,20). In our study, cough was the most frequently reported symptom across all age groups.

Although physical examination findings are often unremarkable, decreased breath sounds are commonly observed in young children due to airway obstruction (1,5). Our results are consistent with those of previous reports, as decreased breath sounds were the most common physical examination finding in our study group.

In all suspected cases, radiological imaging is essential to determine the localization of the FB. The primary imaging modalities include anteroposterior and lateral chest X-rays

and thoracic computed tomography. In cases where the FB is radiopaque, it can be easily visualized on imaging studies. However, radiolucent FBs may not be directly detectable, and instead, secondary changes such as atelectasis, emphysema, or pneumonia may indicate aspiration (5,21). It is crucial to perform lateral chest X-rays, as radiopaque objects positioned behind mediastinal structures may not be visible on anteroposterior imaging. However, it is important to note that 24-30% of FBs may not cause significant radiological changes, leading to false-negative results (21-23). The sensitivity and specificity of radiological evaluations have been reported as 62-77% and 57-74%, respectively (24,25). Therefore, normal chest X-rays do not rule out FBA, and in cases of persistent clinical suspicion, bronchoscopy should be performed (21,22). In our study, radiological findings were normal in most cases, aligning with previous literature. However, the radiopaque headscarf needle could be detected in radiological imaging.

A detailed patient history is a cornerstone in diagnosing FBA. However, young children are highly active, and aspiration events often occur outside of parental supervision, leading to unreported or unnoticed incidents. Consequently, clinical findings are more critical than radiology or history-taking in young children, and bronchoscopy should be performed in suspected cases, even in the absence of a definitive history (26,27).

Bronchoscopy remains the gold standard for both diagnosis and treatment of FBA (27). Rigid bronchoscopy is preferred in pediatric patients due to its wide lumen, ability to accommodate large forceps, and simultaneous ventilation capability (2,28). However, some studies advocate for FOB, as it does not require GA and allows for better access to the upper lobe and small-diameter bronchi (29,30). In our study, rigid bronchoscopy under GA was performed in 104 (78.8%) cases, while FOB was utilized in 28 (21.2%) cases where the FB was located in the distal airways or upper lobes. Negative bronchoscopy rate varies 10-37.7% in the literature (11,18,27,29). Considering the potential complications of undiagnosed FBA, such as lung infections, abscesses, and bronchiectasis, this rate is considered acceptable. In our study, the negative bronchoscopy rate was 12.6%, consistent with prior research.

Surgical removal of FBs via thoracotomy may be necessary in cases where the FB is peripherally located and cannot be extracted through endoscopy. Kaptanoğlu et al. (8,31) reported the need for thoracotomy and bronchotomy in 1 out of 63 cases and 2 out of 121 cases involving headscarf needle aspiration. Similarly, in a large cohort of 1,035 cases, Hasdıraz et al. (32) performed thoracotomy in six cases, including lobectomy in four cases due to distal FB localization. In our study, two out of 18 patients with aspirated headscarf needles required thoracotomy and bronchotomy, and the FBs were successfully removed.

FBs are most commonly detected in the right bronchus, as it is shorter, wider, and more vertical, resembling the trachea (33). However, in children, the left main bronchus is anatomically closer to the right main bronchus, which can result in a more balanced distribution of FBs (2). In previous studies, FB localization rates were reported as 34% in the trachea, 34-51% in the right bronchial system, and 15-53% in the left bronchial system (5,29,34,35). Our findings were consistent, with the majority of FBs detected in the right bronchial system.

The type of FB aspirated is influenced by cultural and dietary habits. Young children (<3 years) most commonly aspirate nuts and seeds, whereas school-aged (8-10 years) children frequently aspirate stationery items, pen caps, springs, and fasteners (1,3,6). In Muslim countries like Türkiye, adolescent girls commonly aspirate headscarf needles due to their habit of holding them in their mouths while adjusting their headscarves (8,30,36). In our study, dried nuts were the most frequently aspirated objects in the ≤3-year-old group, stationery items in school-aged children (8-10 years), and headscarf needles in children >10 years. Notably, four children <10 years of age aspirated headscarf needles while their mothers were tying their headscarves.

Complications associated with FBA or removal occur in 1-14.6% of cases. Failure to remove FBs may result in bronchospasm, hypoxia, laryngeal edema, pneumomediastinum, and pneumothorax (5,7,10,37). Most critically, hypoxic-ischemic encephalopathy can be fatal (3-5,10). Liang et al. (38), in their series of 2000 cases, reported 15 fatalities, seven of which were due to acute obstructive asphyxia during aspiration, while the remaining eight resulted from chronic asphyxia and respiratory circulatory failure. In our study, some cases developed bronchospasm, laryngeal edema, and desaturation following bronchoscopy; however, all responded to medical treatment, and no mortality was observed.

This study has certain limitations. It is a single-center, retrospective study conducted at a single hospital.

CONCLUSION

Delayed diagnosis of FBA increases the risk of severe complications, including recurrent lung infections, lung abscess, and bronchiectasis. In some cases, thoracotomy may be required to remove the FB, and lung resection may become necessary due to irreversible lung damage. Therefore, we emphasize the critical importance of prevention, early diagnosis, and timely intervention in cases of FBA.

To reduce the risk of aspiration, children under the age of 3 should be fed in accordance with their developmental stage, and foods with a high risk of aspiration should be provided in safe, child-friendly forms. Small objects should be kept out of children's reach, and toys should be selected based on their durability and safety features. Additionally, warning labels regarding choking hazards should be placed on toys. Educational programs should be developed, particularly targeting parents, to increase awareness and prevention. School-age children and teachers should also be informed about the risks and preventive measures.

Considering the significant Muslim population worldwide, headscarf needle aspiration presents a serious health concern. We recommend that headscarf needles be designed with larger heads to prevent accidental aspiration. Women should exercise caution while using headscarf needles and should avoid holding them in their mouths while wearing a headscarf.

A detailed history of FBA should be meticulously obtained. In cases with a history or suspicion of aspiration, bronchoscopy should be performed promptly under appropriate conditions to facilitate early diagnosis and treatment.

Ethics Committee Approval: The study was approved by the Clinical Research Ethics Committee of Keçiören Training and Research Hospital (09.03.2021, 2249).

Conflict of Interest: None declared by the authors.

Financial Disclosure: None declared by the authors.

Acknowledgments: None declared by the authors.

Author Contributions: Idea/Concept: LNA, SH, SŞEG; Design: LNA, SH; Data Collection/Processing: LNA; Analysis/Interpretation: LNA, SH, GF, PB; Literature Review: LNA, GF, PB, SŞEG; Drafting/Writing: LNA, SH, GF, PB; Critical Review: SŞEG.

REFERENCES

1. Gang W, Zhengxia P, Hongbo L, Yonggang L, Jiangtao D, Shengde W, et al. Diagnosis and treatment of tracheobronchial foreign bodies in 1024 children. J Pediatr Surg. 2012;47(11):2004-10.
2. Dorterler ME, Kocaman OH, Gunendi T, Boleken ME. A single-center experience of pediatric foreign-body aspiration: A retrospective 4-year case series. Lung India. 2019;36(3):202-6.
3. Pietraś A, Markiewicz M, Mielnik-Niedzielska G. Rigid bronchoscopy in foreign body aspiration diagnosis and treatment in children. Children (Basel). 2021;8(12):1206.
4. From the Centers for Disease Control and Prevention. Nonfatal choking-related episodes among children--United States, 2001. JAMA. 2002;288(19):2400-2.
5. Oncel M, Sunam GS, Ceran S. Tracheobronchial aspiration of foreign bodies and rigid bronchoscopy in children. Pediatr Int. 2012;54(4):532-5.
6. Zur KB, Litman RS. Pediatric airway foreign body retrieval: surgical and anesthetic perspective. Pediatr Anaesth. 2009;19(Suppl 1):109-17.
7. Jaswal A, Jana U, Maiti PK. Tracheo-bronchial foreign bodies: a retrospective study and review of literature. Indian J Otolaryngol Head Neck Surg. 2014;66(Suppl 1):156-60.
8. Kaptanoglu M, Dogan K, Onen A, Kunt N. Turban pin aspiration; a potential risk for young Islamic girls. Int J Pediatr Otorhinolaryngol. 1999;48(2):131-5.
9. Bodart E, Gilbert A, Thimmesch M. Removal of an unusual bronchial foreign body: rigid or flexible bronchoscopy? Acta Clin Belg. 2014;69(2):125-6.
10. Ding L, Su S, Chen C, Yao H, Xiao L. Tracheobronchial foreign bodies in children: experience from 1,328 patients in China. Front Pediatr. 2022;10:873182.
11. Bakal Ü, Keleş E, Saraç M, Karlidağ T, Kaygusuz İ, Kazez A. A study of foreign body aspiration in children. J Craniofac Surg. 2016;27(4):e358-63.
12. Midulla F, Guidi R, Barbato A, Capocaccia P, Forenza N, Marseglia G, et al. Foreign body aspiration in children. Pediatr Int. 2005;47(6):663-8.
13. Ozdemir C, Uzun I, Sam B. Childhood foreign body aspiration in Istanbul, Turkey. Forensic Sci Int. 2005;153(2-3):136-41.
14. Samarei R. Survey of foreign body aspiration in airways and lungs. Glob J Health Sci. 2014;6(7):130-5.
15. Mallick MS. Tracheobronchial foreign body aspiration in children: A continuing diagnostic challenge. Afr J Paediatr Surg. 2014;11(3):225-8.
16. Bayraktar S, Tanyeri Bayraktar B, Çalışkan B, Ziyade S, Elevli M. Pneumothorax and subcutaneous emphysema due to foreign body aspiration. Duzce Med J. 2016;18(2):77-8. Turkish.
17. Cevizci MN. Our bronchoscopy results in suspected tracheobronchial foreign body aspiration in children. Balikesir Med J. 2020;4(1):32-9. Turkish.
18. Yıldırım M, Doğusoy I, Okay T, Yaşaroğlu M, Demirbağ H, Aydemir B, et al. Tracheobronchial foreign bodies. Turkish J Thorac Cardiovasc Surg 2003;11(4):228-31. Turkish.
19. Mu L, He P, Sun D. Inhalation of foreign bodies in Chinese children: a review of 400 cases. Laryngoscope. 1991;101(6 Pt 1):657-60.
20. AlRabiah AA, Alaithan TM, Alaithan A, Alsaeri AS, Alenazi FM, Ageeli FA, et al. Knowledge and awareness of the first aid management of foreign body aspiration in children among the general population: a cross-sectional study in Saudi Arabia. Cureus. 2024;16(9):e68841.
21. Gürsu S, Sırmalı M, Gezer S, Fındık G, Türüt H, Aydın E, et al. Tracheobronchial foreign body aspirations in adults. Turkish J Thorac Cardiovasc Surg. 2006;14(1):38-41. Turkish.
22. Erikci V, Karacay S, Arikan A. Foreign body aspiration: A four-year experience. Ulus Travma Acil Cerrahi Derg. 2003;9(1):45-9.
23. İlçe Z. Tracheobronchial foreign body aspiration in children. Kocaeli Med J. 2012;1(2):47-54. Turkish.
24. Sersar SI, Rizk WH, Bilal M, El Diasty MM, Eltantawy TA, Abdelhakam BB, et al. Inhaled foreign bodies: presentation, management and value of history and plain chest radiography in delayed presentation. Otolaryngol Head Neck Surg. 2006;134(1):92-9.
25. Heyer CM, Bollmeier ME, Rossler L, Nuesslein TG, Stephan V, Bauer TT, et al. Evaluation of clinical, radiologic, and laboratory prebronchoscopy findings in children with suspected foreign body aspiration. J Pediatr Surg. 2006;41(11):1882-8.
26. Antón-Pacheco JL, Martín-Alelú R, López M, Morante R, Merino-Mateo L, Barrero S, et al. Foreign body aspiration in children: Treatment timing and related complications. Int J Pediatr Otorhinolaryngol. 2021;144:110690.
27. Kısacık E, Gülhan E, Sırmalı M, Sarıca E, Türüt H, Karasu S, et al. Tracheobronchial foreign body aspirations: Retrospective analysis of 261 cases. Solunum Hast. 2004;15(2):86-91. Turkish.
28. Kaptanoğlu M, Kunt T, Kunt N, Doğan K, Markuz Ş. Foreign body inhalation (review of 119 cases. Turkish J Thorac Cardiovasc Surg. 1995;3(1):78-81. Turkish.
29. Korlacki W, Korecka K, Dzielicki J. Foreign body aspiration in children: diagnostic and therapeutic role of bronchoscopy. Pediatr Surg Int. 2011;27(8):833-7.
30. Gencer M, Ceylan E, Koksal N. Extraction of pins from the airway with flexible bronchoscopy. Respiration. 2007;74(6):674-9.

31. Kaptanoglu M, Nadir A, Dogan K, Sahin E. The heterodox nature of "Turban Pins" in foreign body aspiration; the central Anatolian experience. Int J Pediatr Otorhinolaryngol. 2007;71(4):553-8.

32. Hasdiraz L, Oguzkaya F, Bilgin M, Bicer C. Complications of bronchoscopy for foreign body removal: experience in 1,035 cases. Ann Saudi Med. 2006;26(4):283-7.

33. Panda SS, Bajpai M, Singh A, Baidya DK, Jana M. Foreign body in the bronchus in children: 22 years experience in a tertiary care paediatric centre. Afr J Paediatr Surg. 2014;11(3):252-5.

34. Parida P, Nirmal N, Gopalakrishnan S, Saxena SK. Factors predicting early diagnosis of pediatric laryngotracheobronchial foreign bodies. Otolaryngol Pol. 2015;69(6):45-52.

35. Darrin DH, Holinger LD. Foreign body of the larynx, trachea and bronchi. In: Bluestone CD, Stool S, Kenna MA, editors. Pediatric Otolaryngology. 1st ed. Philadelphia:WB Saunders; 1995. p.1390-8.

36. Dayıoğlu E, Rahimi M, Toker A, Akaslan İ, Barlas S, Tireli E, et al. Intrabronchial foreign bodies: complications of turban needles. Turkish J Thorac Cardiovasc Surg. 1995;3(1):82-5. Turkish.

37. Sezer HF, Eliçora A, Topçu S. Foreign body aspirations with rigid bronchoscopy and esophagoscopy in children. Turk Gogus Kalp Damar Cerrahisi Derg. 2024;32(Suppl 1):S55-9.

38. Liang J, Hu J, Chang H, Gao Y, Luo H, Wang Z, et al. Tracheobronchial foreign bodies in children - a retrospective study of 2,000 cases in Northwestern China. Ther Clin Risk Manag. 2015;11:1291-5.

Evaluation of the Effects of Acute Cisplatin Administration on Testicular and Ovarian Tissue in Rats

Sıçanlarda Akut Sisplatin Uygulamasının Testis ve Yumurtalık Dokusundaki Etkilerinin Değerlendirilmesi

Betül YALÇIN[1]
0000-0003-1176-8843
Kübra Tuğçe KALKAN[2]
0000-0001-7461-277X
Sedat ÇARKIT[3]
0000-0002-0747-2209
Özge CENGİZ MAT[4]
0000-0003-4638-6116
Gözde Özge ÖNDER[4,5]
0000-0002-0515-9286
Arzu YAY[4,5]
0000-0002-0541-8372

[1]Department of Histology and Embryology, Adıyaman University Faculty of Medicine, Adıyaman, Türkiye

[2]Department of Histology and Embryology, Kırşehir Ahi Evran University Faculty of Medicine, Kırşehir, Türkiye

[3]Department of General Surgery, Erciyes University Faculty of Medicine, Kayseri, Türkiye

[4]Department of Histology and Embryology, Erciyes University Faculty of Medicine, Kayseri, Türkiye

[5]Genome and Stem Cell Center, GENKOK, Erciyes University, Kayseri, Türkiye

Corresponding Author
Sorumlu Yazar
Betül YALÇIN
by-by-2005@hotmail.com

ABSTRACT

Aim: Cisplatin, one of the effective chemotherapeutics in cancer treatment, has the potential to affect the testis and ovary, leading to permanent or temporary infertility. This study aimed to determine the acute effects of cisplatin on testis and ovary histology and to investigate whether it induces any changes in immunohistochemical cyclooxygenase-2 (COX2), nuclear factor kappa B p65 (NFκB-p65), and heat-shock protein 70 (HSP70) levels.

Material and Methods: The study was planned as four groups: male control, male cisplatin, female control, and female cisplatin. The cisplatin group rats were administered with 7 mg/kg cisplatin, and all rats were sacrificed 24 hours later. Hematoxylin-eosin and Masson's trichrome stains were applied to testis and ovary tissues to examine their histopathological structure, and an immunohistochemistry staining protocol was applied to determine immunostaining intensity of COX2, NFκB-p65, and HSP70.

Results: In the cisplatin group, a decrease in seminiferous tubule epithelium, an elevation in fibrotic response in the interstitial area, and a notable reduction in Johnson testicular biopsy score (p<0.001) were seen in the testis. In the ovary, atretic follicles (p=0.006) and luteal structures within the cortex, as well as vascular congestion (p=0.001), edema (p=0.001), and fibrotic areas within the medulla, were evident. These alterations resulted in a statistically significant increase in ovarian histoscores, except for leukocyte infiltration (p=0.322). In both tissues, cisplatin significantly increased the immunostaining intensity of COX2, NFκB-p65, and HSP70 compared to the control group.

Conclusion: Acute cisplatin administration can induce tissue damage and pro-inflammatory response in the testis and ovary.

Keywords: Cisplatin; testis; ovary; cyclooxygenase-2; NF-kappa B p65; heat-shock protein 70.

ÖZ

Amaç: Kanser tedavisinde etkili kemoterapötiklerden biri olan sisplatin, testis ve overi etkileyerek kalıcı veya geçici infertiliteye yol açma potansiyeline sahiptir. Bu çalışma, sisplatinin testis ve over histolojisi üzerindeki akut etkilerini belirlemeyi ve immünohistokimyasal siklooksijenaz-2 (COX2), nükleer faktör kappa B p65 (NFκB-p65) ve ısı-şok protein 70 (HSP70) düzeylerinde herhangi bir değişikliğe neden olup olmadığını araştırmayı amaçlamıştır.

Gereç ve Yöntemler: Çalışma dört grup olarak planlandı: erkek kontrol, erkek sisplatin, dişi kontrol ve dişi sisplatin. Sisplatin grubu sıçanlara 7 mg/kg sisplatin uygulandı ve tüm sıçanlar 24 saat sonra sakrifiye edildi. Testis ve over dokularına histopatolojik yapılarını incelemek amacıyla hematoksilen-eozin ve Masson trikrom boyaları uygulandı ve COX2, NFκB-p65 ve HSP70'in immün boyama yoğunluğunu belirlemek amacıyla immünohistokimya boyama protokolü uygulandı.

Bulgular: Sisplatin grubunda, testiste seminifer tübül epitelinde azalma, interstisyel alanda fibrotik yanıtta artış ve Johnson testiküler biyopsi skorunda kayda değer bir azalma (p<0,001) görüldü. Overde, kortekste atretik foliküller (p=0,006) ve luteal yapılar yanı sıra medullada vasküler konjesyon (p=0,001), ödem (p=0,001) ve fibrotik alanlar belirgindi. Bu değişiklikler, lökosit infiltrasyonu (p=0,322) dışında, over histoskorlamasında istatistiksel olarak anlamlı bir artışla sonuçlandı. Her iki dokuda da, sisplatin, kontrol grubuna kıyasla COX2, NFκB-p65 ve HSP70 immün boyanma yoğunluğunu önemli ölçüde artırdı.

Sonuç: Akut sisplatin uygulaması, testiste ve overde doku hasarına ve proinflamatuar yanıta yol açabilir.

Anahtar kelimeler: Sisplatin; testis; over; siklooksijenaz-2; NF-kappa B p65; ısı-şok protein 70.

INTRODUCTION

Since obtaining Food and Drug Administration approval in 1978, cisplatin has been utilized as the first chemotherapy drug to contain heavy metal compounds due to its platinum content. It has been employed both as a monotherapy and in combination with other antineoplastic agents (1,2). The cytotoxic effects of this drug are mediated by its ability to bind to DNA, leading to cell cycle arrest and DNA damage, which in turn activate apoptosis (3,4). Cisplatin has the potential to impact the physiological functions of various systems by inducing toxicity in both healthy and tumor cells (5). Furthermore, the toxicity of cisplatin, which may have adverse effects on numerous organs, including the reproductive system (6), restricts its use in treating various types of solid tumors. Due to the presence of cells with elevated mitotic activity, the testis and ovary are particularly susceptible to chemotherapeutic agents (7,8).

Heat shock proteins are molecules induced in response to a variety of physiological and environmental stimuli, including inflammatory processes. These molecules, which also function as molecular chaperones, contribute to the protection of cells by recognizing misfolded and mutated proteins (9-11). One of these molecules, heat-shock protein 70 (HSP70), is capable of fulfilling anti-apoptotic, anti-inflammatory, and antioxidant functions based on its intracellular and extracellular localization (12). The HSP70 protein has the capacity to inhibit the activity of nuclear factor kappa B (NFκB), which in turn reduces the expression of tumor necrosis factor alpha (TNF-α) and interleukin-6 (IL-6), thus attenuating inflammatory responses in various cell types (13).

The transcription factor NFκB serves a regulatory function in immune responses, stimulating the activity of cyclooxygenase-2 (COX2) and iNOS enzymes and the release of proinflammatory mediators. This molecule has been demonstrated to be sensitive to the effects of oxidative stress (14). Moreover, abnormalities in the NFκB signaling pathway have been linked to a range of pathological disorders, including various inflammatory diseases and malignancies. Accordingly, the inhibition of NFκB may facilitate an effective strategy for the alleviation of ovarian damage. One of the inflammatory agents encoded by the NFκB gene, COX2, has been demonstrated to enhance cytokine production concomitant with reactive oxygen species (ROS) production in normal tissues (15,16).

The objective of this study was to ascertain the impact of cisplatin on the histology of rat testicular and ovarian tissue, as well as on the immunoreactivity of COX2, NFκB p65 (NFκB-p65), and HSP70.

MATERIAL AND METHODS

Animal Care

Approval for the utilization of twelve male and twelve female adult Wistar albino rats sourced from the Erciyes University Experimental Animal Application and Research Centre was obtained from the Animal Experiment Local Ethics Committee of the Erciyes University (dated 06.03.2024, and numbered 24/056). The rats had a 12-hour light/dark cycle, were kept in hygienic cages at 22-24°C, and were fed commercial pellets and water in accordance with their preferences.

Experimental Design

The experiment was composed of four groups, with a total of twenty-four animals, as detailed below: Control male group: The rats were not subjected to any treatment. Cisplatin male group: A single dose (7 mg/kg) of cisplatin was administered intraperitoneally (17). Control female group: The rats were not subjected to any treatment. Cisplatin female group: A single dose of (7 mg/kg) cisplatin was administered intraperitoneally (18).

Twenty-four hours after cisplatin administration, all animals were euthanized using a xylazine (10 mg/kg) and ketamine (60 mg/kg) combination as general anesthetic agents. Testicular and ovarian tissues were promptly subjected to a 10% formaldehyde solution for subsequent histopathological and immunohistochemical examination.

Histopathological Examination

Following a fixation period of 72 hours in formaldehyde, a histological follow-up procedure was conducted. After the completion of the dehydration, transparency, and paraffin blocking processes, respectively, 5 µm-thick sections were obtained. For the purpose of enabling examination under a light microscope, the tissue sections underwent staining with hematoxylin and eosin (H&E) and Masson's trichrome (MT).

The degree of testicular damage was quantified using the Johnsen testicular biopsy score (JTBS). Histological evaluations of seminiferous tubules according to the JTBS and identification were given in Table 1 (19). Accordingly, X indicates normal spermatogenesis, IX indicates multiple spermatozoa with irregularities in the germinal epithelium, VIII indicates a small number of spermatozoa, VII-II indicates maturation arrest, and a score of I indicates the complete absence of cells in the seminiferous tubules (20). In order to detect ovarian damage, twenty non-overlapping fields were randomly selected for analysis at 40x magnification, and the mean values for each group were subsequently evaluated. Ovarian scoring was conducted in accordance with the criteria for hemorrhage, edema, follicular degeneration, vascular congestion, and leukocyte infiltration. In order to assess the severity of the histopathological damage in the ovarian tissue section, a scoring system that adopted the specified criteria was employed, with scores ranging from 0 to 3 (21-23).

Immunohistochemistry Analysis

The testis and ovary sections on polylysine-coated slides underwent immunohistochemical staining for COX2, NFκB-p65, and HSP70 by the avidin-biotin peroxidase method. The paraffin removal process, utilizing xylene, rehydration with a series of progressively lower alcohol concentrations, and subsequent rinsing with distilled water, was completed in that order. The sections for antigen retrieval were incubated with citrate buffer solution in a 95°C microwave for 10 min, followed by incubation in the same solution and duration at room temperature. After washing in PBS, they were incubated with 3% hydrogen peroxide for 12 minutes to eliminate endogenous peroxidase activation. Following exposure to the ultra V block component of the immunostaining kit, primary antibodies were applied to the sections overnight at 4°C. The biotinylated secondary antibody solution and the peroxidase-conjugated streptavidin solution, both provided in the kit, were incubated for 10 minutes each. Three times, PBS washing was conducted at the conclusion

Table 1. Qualitative histological assessments of the seminiferous tubules according to the Johnsen testicular biopsy score

Score	Identification of histological findings
1	There are no cellular structures within the tubules.
2	Sertoli cells are present in the absence of germ cells.
3	Among the germ cells, only spermatogonia are available.
4	Only a few spermatocytes are present.
5	The presence of several or many spermatocytes in the absence of spermatozoa and spermatids.
6	The presence of a few spermatids in the absence of spermatozoa.
7	The presence of many spermatids in the absence of spermatozoa.
8	Only a few spermatozoa are present.
9	The presence of many spermatozoa and germinal epithelial debris in the tubular lumen.
10	There are numerous spermatozoa resulting from spermatogenesis and tubules with regular germinal epithelium and lumen.

of each chemical treatment. The sections were subjected to chromogen staining with diaminobenzidine and core staining with Mayer hematoxylin. Subsequent to the application of distilled water, a series of progressively higher alcohol concentrations and xylenes were employed to impregnate the sections with entellan. In order to ascertain the degree of immunostaining for COX2, NFκB-p65, and HSP70 in the testis and ovary, ten distinct areas from each rat in the experimental group were evaluated using the ImageJ software program.

Statistical Analysis
The normality of the histopathological scoring and immunohistochemical measurements of the ovarian and testicular tissues was established through the utilization of both the Shapiro-Wilk and Kolmogorov-Smirnov tests. Non-normally distributed immunostaining data were evaluated using the Mann-Whitney U test, and as descriptive statistics, the median with interquartile range, and minimum-maximum were presented. The data analysis, conducted with the aid of the GraphPad Prism 9 program (San Diego, CA), was accepted as statistically significant if the p-value was less than 0.05.

RESULTS
Histopathological Results
In HE-stained sections, the testicular tissue of control group rats was observed to comprise seminiferous tubules and interstitial connective tissue. The seminiferous tubule epithelium displayed a normal testicular architecture, comprising cells of the spermatogenic series at varying developmental stages. These cells were observed to be located from the basement membrane to the lumen, with spermatozoa present in the lumen. In the acute cisplatin-treated rats, a reduction in the number of spermatozoa was observed within the lumen of some tubules, with the absence of spermatozoa noted in others. Furthermore, the seminiferous tubule epithelium was observed to be disorganized, with a tendency to shed into the lumen (Figure 1).

The assessment of MT-stained sections was undertaken with the objective of determining the presence of fibrotic changes in the testicular tissue. The control group testes exhibited no alterations in the capsule thickness or the area of connective tissue within the tubules. In the group treated with cisplatin, an increase in fibrotic tissue was observed, notably in the vessel walls within the connective tissues, when compared to the control group (Figure 1A).

In terms of JTBS score, a notable decrease was discerned in the cisplatin group in comparison to the control group, with a statistical significance (p<0.001, Table 2). The JTBS findings, together with the related images representing the histology of the experimental groups, were presented in Figure 1B.

Table 2. Comparison of JTBS between the groups

	Control	Cisplatin	p
JTBS	10 (8-10) [7-10]	5 (4-5) [1-9]	**<0.001**

JTBS: Johnsen testicular biopsy score, descriptive statistics were presented as median (25th-75th percentile) [minimum-maximum]
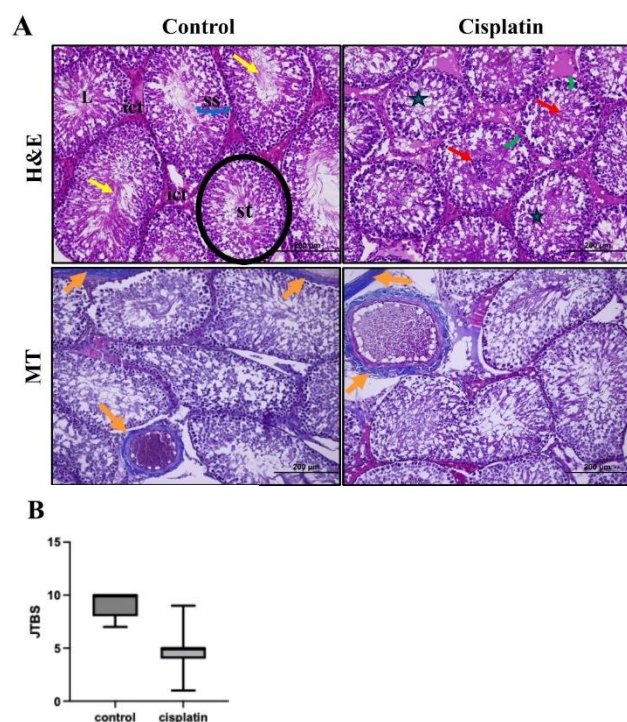
Figure 1. A) HE and MT stained testicular sections, and **B)** JTBS of experimental groups

HE: hematoxylin-eosin staining, 200x, MT: Masson's trichrome staining, 200x, JTBS: Johnsen testicular biopsy score, seminiferous tubules (st, encircled by black circle), lumen (L), interstitial connective tissue (ict), spermatogenic series (ss, blue bracket), sperm (yellow arrow), shedding of spermatogenic cells (red arrow), reduction of the quantity of spermatozoa (star), decreased seminiferous tubule epithelial thickness (green bracket), fibrosis (orange arrow)

In HE-stained sections, the ovarian tissue of the control group appeared healthy, with its medulla and cortex containing follicles at different stages of development. In the cisplatin-treated group, the cortex exhibited a prevalence of corpus luteum and follicles with impaired structure. In this group, the scores of vascular congestion (p=0.001), hemorrhage (p<0.001), edema (p=0.001), and follicular degeneration (p=0.006), except for the leukocyte infiltration (p=0.322), were significantly elevated in comparison to the control group (Figure 2, Table 3).

MT-stained ovarian sections of the cisplatin group exhibited blue-stained fibrotic structures extending from the medulla of the ovarian tissue to the cortex. These fibrotic structures were not present in the control group (Figure 2A).

Immunohistochemical Analysis

After acute cisplatin-induced testicular and ovarian toxicity, immunohistochemical staining was performed on testicular and ovarian sections to determine the immunoreactivity of COX2, NFκB-p65, and HSP70 proteins (Table 4). In the cisplatin groups, there was a notable enhancement in COX2, NFκB-p65, and HSP70 immunostaining intensity in both the testis (p<0.001, p=0.049, p<0.001) and ovary (p=0.045, p=0.005, p=0.010) when compared to the control group (Figures 3 and 4).

DISCUSSION

In the cisplatin-administered group, deterioration in the structure of the epithelial cells of the seminiferous tubules was observed, along with a reduction in the number of spermatozoa. Administration of cisplatin resulted in an increase in the immunoreactivity of COX2, NFκB-p65, and HSP70 in the testicular tissue. Similar to these results, in ovarian tissue, the administration of cisplatin was demonstrated to result in the occurrence of histopathological alterations, including the presence of hemorrhage, edema, follicular degeneration, and vascular congestion. Furthermore, an increase in the immunostaining intensities of both COX2 and NFκB-p65, as well as HSP70, was observed in the ovary of this group. The findings indicated that acute dose cisplatin induced damage to testicular and ovarian tissue, accompanied by a notable increase in COX2, NFκB-p65, and HSP70 immunostaining intensity.

On the 7th day of the 14-day experimental period, the cisplatin administration at a dose of 7 mg/kg/day was observed to induce irregularities in the spermatogenic series, a reduction in germinal cells, and a shrinkage of cells in interstitial areas within the testicular tissue (24). Four days after 7 mg/kg cisplatin administration in the present study resulted in tubule degeneration and a reduction in germinal cells, accompanied by a decrease in

Table 3. Comparison of ovarian scoring results

	Control	**Cisplatin**	**p**
Vascular congestion	0 (0-0.5) [0-1]	2 (0.5-2) [0-3]	**0.001**
Hemorrhage	0 (0-0) [0-1]	2 (1-3) [0-3]	**<0.001**
Leukocyte infiltration	0 (0-0) [0-1]	0 (0-1) [0-1]	0.322
Edema	0 (0-0) [0-1]	1 (1-2) [0-2]	**0.001**
Follicular degeneration	0 (0-1) [0-1]	1 (0.5-2) [0-3]	**0.006**

descriptive statistics were presented as median (25th-75th percentile) [minimum-maximum]
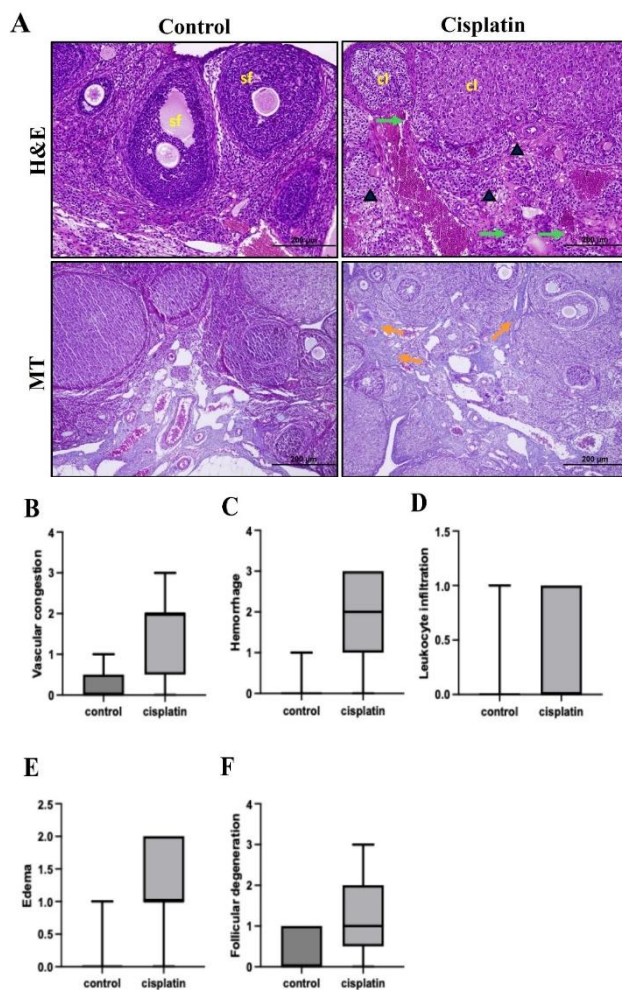
Figure 2. A) HE and MT stained ovarian sections, and **B)** vascular congestion, **C)** hemorrhage, **D)** leukocyte infiltration, **E)** edema, **F)** follicular degeneration scores

HE: hematoxylin-eosin staining, 200x, MT: Masson's trichrome staining, 200x, secondary follicle (sf), corpora lutea (cl), vascular congestion (green arrow), edema (arrowhead), fibrosis (orange arrow)

Table 4. Analysis of immunostaining intensity for COX2, NFκB-p65, and HSP70 in testis and ovarian tissue

		Control	**Cisplatin**	**p**
Testis	**COX2**	92.10 (89.56-92.10) [81.15-102.5]	94.39 (90.08-102.7) [84.08-127.4]	**<0.001**
	NFκB-p65	89.92 (86.67-94.61) [73.56-109.1]	91.19 (87.45-97.67) [81.99-148.1]	**0.049**
	HSP70	93.82 (91.01-95.95) [84.87-99.88]	99.27 (94.22-102.9) [84.87-158.5]	**<0.001**
Ovary	**COX2**	90.72 (86.06-94.91) [80.33-99.02]	92.19 (88.79-98.67) [81.20-140.8]	**0.045**
	NFκB-p65	86.11 (83.98-88.69) [75.44-97.86]	89.95 (86.65-93.66) [74.13-98.30]	**0.005**
	HSP70	91.19 (88.59-93.61) [80.62-99.52]	92.88 (90.03-96.28) [85.81-99.87]	**0.010**

COX2: cyclooxygenase-2, NFκB: nuclear factor kappa B, HSP70: heat-shock protein 70, descriptive statistics were presented as median (25th-75th percentile) [minimum-maximum]
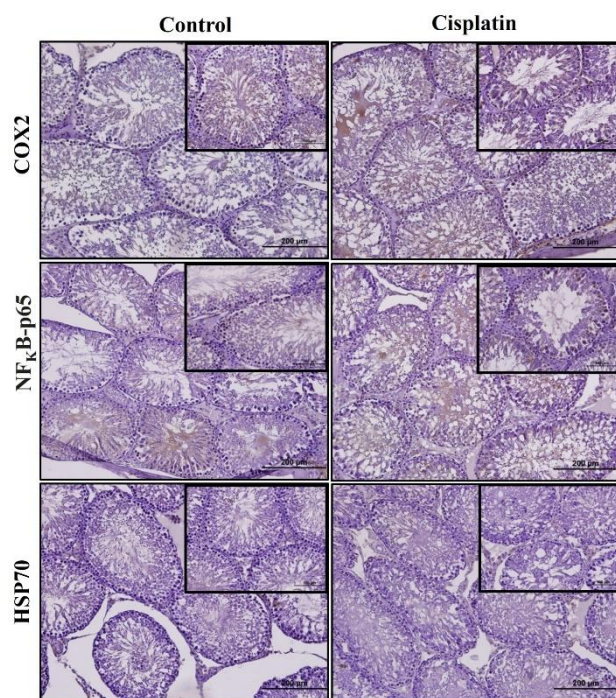
Figure 3. The immunoreactivity of COX2, NFκB-p65, and HSP70 in rat testicular tissue sections

COX2: cyclooxygenase-2, NFκB: nuclear factor kappa B, HSP70: heat-shock protein 70, larger images are x20, 200x, and upper left images are x40, 400x
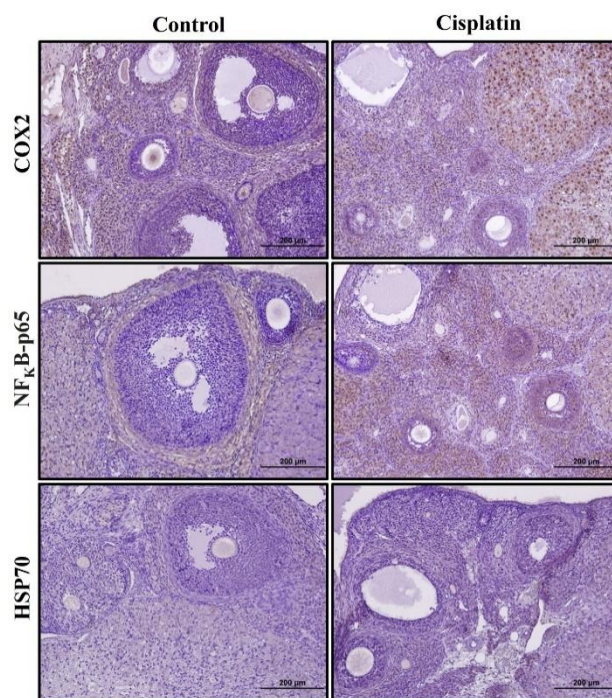

Figure 4. The immunoreactivity of COX2, NFκB-p65, and HSP70 in rat ovarian tissue sections

COX2: cyclooxygenase-2, NFκB: nuclear factor kappa B, HSP70: heat-shock protein 70, x20 magnification 200x

the thickness of the germinal epithelium (25). The histological findings demonstrated the presence of desquamation and disorganization of germinal cells, along with degenerative changes in these cells, thereby corroborating the deterioration in sperm quality in cisplatin-administered rats (24). In MT-stained testis, the presence of capsule thickening was discernible on days 7 and 14, while the emergence of perivascular fibrosis could only be observed on day 14 (26). The ovarian damage induced by cisplatin was comparable to the findings of the study in which 2.5 mg/kg cisplatin was administered once a day for 14 days. However, the severity of the damage was more pronounced in comparison to the 7 mg/kg dose employed in this study. The observed effect was thought to be related to both the increased dosage of cisplatin administered and the longer duration of exposure (21). In an investigation of the role of cisplatin treatment administered on the 21st day of a 28-day experiment on ovarian follicle reserve, a reduction in primary follicles and secondary follicles was observed, accompanied by an increase in damaged follicles and luteal structures (18). Furthermore, it has been reported that the fertility capacity of rats may be diminished as a consequence of cisplatin-induced ovarian morphological degeneration and a reduction in serum anti-müllerian hormone (AMH) levels (27). Seven days following cisplatin administration, an increased deposition of collagen was evident in both the tunica albuginea located beneath the surface epithelium and the stroma encircling the follicles (23). The outcomes of previous research studies corroborated the histopathological alterations associated with cisplatin on both the testis and ovary revealed in the present investigation.

In order to prevent cisplatin-induced reproductive toxicity, it is of great importance to inhibit the NFκB, oxidative stress, and inflammatory pathways (28). The overexpression of the NFκB-p65 protein has been shown to stimulate the expression of proinflammatory cytokines, particularly interleukin-1 beta (IL-1β) and TNF-α. These cytokines have been demonstrated to induce testicular inflammation (29). In the testis, a significant positive immunostaining was observed within the cytoplasm of both interstitial and spermatogenic cells three days following the administration of cisplatin (24). A study demonstrated that the administration of cisplatin on the 7th day of a 14-day experimental period resulted in an increase in TNF-α and NFκB-p65 protein levels in testicular tissue, as evidenced by western blot analysis (20). In the ovary, according to the carried out studies, the levels of the pro-inflammatory cytokines NFκB, IL-1β, IL-6, TNF-α, COX2, and iNOS were all significantly elevated (18,21).

HSP70 is observed to be present in low quantities within the cytoplasm under any conditions (30,11). In the presence of stress, this molecule is increased in the nucleus (30), thereby ensuring the survival of the cell (31). The overproduction of HSP70 was found to suppress the LPS-stimulated augmentation of TNF-α and IL-6 generation by impeding the activation of IκBα and the nuclear translocation of NFκB-p65 in rats (32). Heat shock proteins are crucial for the process of spermatogenesis and for maintaining cellular integrity against external insults, including heat, chemicals, and radiation (33). The expression of HSP70 in the testis of adult rats is influenced by fluctuations in temperature, with elevated levels of protein expression observed in response to temperature changes (34). A notable elevation in HSP70 immunoreactivity was observed in the germinal epithelium and testicular interstitial tissue within experimental injury groups subjected to ecstasy-induced injury. Moreover, it

was reported that there was a significant increase in HSP70 immunoreactivity in spermatogonia, primary spermatocytes, spermatids, Sertoli, and Leydig cells in response to the increased dose of ecstasy compared to the control group (35). The findings of the present study also demonstrated that cisplatin administration led to an increased HSP70 immunostaining intensity in spermatogenic cells and the interstitial tissue. Similarly, under conditions of excessive cellular stress induced by ecstasy, the increased expression of heat shock proteins in spermatogenic cells and the interstitial tissue has been found to exert cytoprotective effects and prevent apoptosis (33,35). Ovarian damage and its severity have been reported to be associated with increased serum HSP70 (36). In cases where premature ovarian failure has been experimentally induced by cyclophosphamide, there has been a notable elevation in the concentration of HSP70, and it is widely accepted that this is related to inflammatory factors (37).

CONCLUSION

The present study provided evidence to support the damage caused by cisplatin in both testicular and ovarian tissue by histopathological evaluations conducted 24 hours after acute cisplatin administration. In testicular and ovarian tissues, an elevation in the immunostaining intensity of COX2, NFκB-p65, and HSP70 was revealed by immunohistochemical analysis. It is recommended that new studies be designed to elucidate the mechanisms underlying the damage, with particular emphasis on the role of the immune response in the reproductive organs following cisplatin administration at varying doses and durations.

Author Contributions: Idea/Concept: BY, AY; Design: BY, AY; Data Collection/Processing: BY, KTK, ÖCM; Analysis/Interpretation: SÇ, ÖCM, GÖÖ; Literature Review: BY, KTK, SÇ; Drafting/Writing: BY, SÇ, ÖCM, GÖÖ; Critical Review: BY, KTK, GÖÖ, AY.

REFERENCES

1. Mezencev R. Interactions of cisplatin with non-DNA targets and their influence on anticancer activity and drug toxicity: the complex world of the platinum complex. Curr Cancer Drug Targets. 2015;14(9):794-816.
2. Ghosh S. Cisplatin: The first metal based anticancer drug. Bioorg Chem. 2019;88:102925.
3. Aldossary SA. Review on pharmacology of cisplatin: clinical use, toxicity and mechanism of resistance of cisplatin. Biomed Pharmacol J. 2019;12(1):7-15.
4. Qari M, Harakeh S, Akefe IO, Saber SH, Al-Raddadi R, Abd Elmageed ZY, et al. Pomegranate nanoparticle mitigates cisplatin-induced testicular toxicity and improves cisplatin anti-cancer efficacy in Ehrlich carcinoma model. J King Saud Univ Sci. 2023;35(4):102631.
5. Khan R, Khan AQ, Qamar W, Lateef A, Tahir M, Rehman MU, et al. Chrysin protects against cisplatin-induced colon. toxicity via amelioration of oxidative stress and apoptosis: probable role of p38MAPK and p53. Toxicol Appl Pharmacol. 2012;258(3):315-29.
6. Negm WA, El-Kadem AH, Hussein IA, Alqahtani MJ. The mechanistic perspective of bilobetin protective effects against cisplatin-induced testicular toxicity: Role of Nrf-2/Keap-1 signaling, inflammation, and apoptosis. Biomedicines. 2022;10(5):1134.
7. Ghobadi E, Moloudizargari M, Asghari MH, Abdollahi M. The mechanisms of cyclophosphamide-induced testicular toxicity and the protective agents. Expert Opin Drug Metab Toxicol. 2017;13(5):525-36.
8. Lopes F, Tholeti P, Adiga SK, Anderson RA, Mitchell RT, Spears N. Chemotherapy induced damage to spermatogonial stem cells in prepubertal mouse in vitro impairs long-term spermatogenesis. Toxicol Rep. 2020;8:114-23.
9. Ince S, Ozer M, Kadioglu BG, Kuzucu M, Ozkaraca M, Gezer A, et al. The effect of taxifolin on oxidative ovarian damage and reproductive dysfunctions induced by antipsychotic drugs in female rats. J Obstet Gynaecol Res. 2021;47(6):2140-8.
10. Liman N. Heat shock proteins (HSP)-60, -70, -90, and 105 display variable spatial and temporal immunolocalization patterns in the involuting rat uterus. Anim Reprod. 2017;14(4):1072-86.
11. Schmitt E, Gehrmann M, Brunet M, Multhoff G, Garrido C. Intracellular and extracellular functions of heat shock proteins: repercussions in cancer therapy. J Leukoc Biol. 2007;81(1):15-27.
12. Lavie L, Dyugovskaya L, Golan-Shany O, Lavie P. Heat-shock protein 70: expression in monocytes of patients with sleep apnoea and association with oxidative stress and tumour necrosis factor-alpha. J Sleep Res. 2010;19(1 Pt 2):139-47.
13. Suemasu S, Tanaka K, Namba T, Ishihara T, Katsu T, Fujimoto M, et al. A role for HSP70 in protecting against indomethacin-induced gastric lesions. J Biol Chem. 2009;284(29):19705-15.
14. Benzer F, Kandemir FM, Kucukler S, Comaklı S, Caglayan C. Chemoprotective effects of curcumin on doxorubicin-induced nephrotoxicity in Wistar rats: by modulating inflammatory cytokines, apoptosis, oxidative stress, and oxidative DNA damage. Arch Physiol Biochem. 2018;124(5):448-57.
15. Elshawi OE, Nabeel AI. Modulatory effect of a new benzopyran derivative via COX-2 blocking and down regulation of NF-κB against γ-radiation induced-intestinal inflammation. J Photochem Photobiol B. 2019;192:90-6.

16. Hassan MH, Ghobara M, Abd-Allah GM. Modulator effects of meloxicam against doxorubicin-induced nephrotoxicity in mice. J Biochem Mol Toxicol. 2014;28(8):337-46.

17. Sahu BD, Rentam KK, Putcha UK, Kuncha M, Vegi GM, Sistla R. Carnosic acid attenuates renal injury in an experimental model of rat cisplatin-induced nephrotoxicity. Food Chem Toxicol. 2011;49(12):3090-7.

18. Ibrahim MA, Albahlol IA, Wani FA, Abd-Eltawab Tammam A, Kelleni MT, Sayeed MU, et al. Resveratrol protects against cisplatin-induced ovarian and uterine toxicity in female rats by attenuating oxidative stress, inflammation and apoptosis. Chem Biol Interact. 2021;338:109402.

19. Johnson L, Petty CS, Neaves WB. The relationship of biopsy evaluation and testicular measurement to over-all daily sperm production in human testes. Fertil Steril 1980;34(1):36-40.

20. Alqahtani MJ, Negm WA, Saad HM, Salem EA, Hussein IA, Ibrahim HA. Fenofibrate and Diosmetin in a rat model of testicular toxicity: New insight on their protective mechanism through PPAR-α/NRF-2/HO-1 signaling pathway. Biomed Pharmacother. 2023;165:115095.

21. Dinc K, Ozyurt R, Coban TA, Yazici GN, Suleyman Z, Yavuzer B, et al. The effect of carvacrol on the proinflammatory cytokines, histology, and fertility outcome of cisplatin-related ovarian change in a rat model. Taiwan J Obstet Gynecol. 2023;62(2):256-63.

22. Ayazoglu Demir E, Mentese A, Livaoglu A, Turkmen Alemdar N, Demir S. Ameliorative effect of gallic acid on cisplatin-induced ovarian toxicity in rats. Drug Chem Toxicol. 2023;46(1):97-103.

23. Al-Shahat A, Hulail MAE, Soliman NMM, Khamis T, Fericean LM, Arisha AH, et al. Melatonin mitigates cisplatin-induced ovarian dysfunction via altering steroidogenesis, inflammation, apoptosis, oxidative stress, and PTEN/PI3K/Akt/mTOR/AMPK signaling pathway in female rats. Pharmaceutics. 2022;14(12):2769.

24. Othman EM, Habib HA, Zahran ME, Amin A, Heeba GH. Mechanistic protective effect of cilostazol in cisplatin-induced testicular damage via regulation of oxidative stress and TNF-α/NF-κB/caspase-3 pathways. Int J Mol Sci. 2023;24(16):12651.

25. Ashtari A, Niazvand F, Chamkouri N, Mohammadi A, Karami AB. The ameliorative effects of Alpinia officinarum rhizome hydroalcoholic extract on cisplatin-induced testicular toxicity in rats. JBRA Assist Reprod. 2023;27(1):41-8.

26. Hokmabadi A, Ranjbar E, Alipour F, Ebrahimzadeh-Bideskan A, Afshari JT, Rezaei MM, et al. Protective effect of dental pulp stem cells' conditioned medium against cisplatin-induced testicular damage in rats. Toxicology. 2024;504:153788.

27. Demir EA. Syringic acid alleviates cisplatin-induced ovarian injury through modulating endoplasmic reticulum stress, inflammation and Nrf2 pathway. J Trace Elem Med Biol. 2024;82:127356.

28. Chtourou Y, Aouey B, Kebieche M, Fetoui H. Protective role of naringin against cisplatin induced oxidative stress, inflammatory response and apoptosis in rat striatum via suppressing ROS-mediated NF-κB and P53 signaling pathways. Chem Biol Interact. 2015;239:76-86.

29. Jarosz M, Olbert M, Wyszogrodzka G, Młyniec K, Librowski T. Antioxidant and anti-inflammatory effects of zinc. Zinc-dependent NF-κB signaling. Inflammopharmacology. 2017;25(1):11-24.

30. Song J, Hong H, Ko JI, Park EJ, Park SM, Son SY, et al. Structure and nuclear transport mechanism of Hsp70 nuclear transporter, Hikeshi. BioDesign. 2015;3(3):117-22.

31. Kandil B, Kurtdede N, Bayraktaroglu AG. Immunohistochemical localization and expression of heat shock proteins (HSP27, HSP60, HSP70, and HSP90) during the oestrous cycle, pregnancy, and lactation in rat ovaries. Acta Histochem. 2024;126(3):152157.

32. Dokladny K, Lobb R, Wharton W, Ma TY, Moseley PL. LPS-induced cytokine levels are repressed by elevated expression of HSP70 in rats: possible role of NF-kappaB. Cell Stress Chaperones. 2010;15(2):153-63.

33. Rockett JC, Mapp FL, Garges JB, Luft JC, Mori C, Dix DJ. Effects of hyperthermia on spermatogenesis, apoptosis, gene expression, and fertility in adult male mice. Biol Reprod. 2001;65(1):229-39.

34. Park SH, Park K, Park YI. Effects of temperature change on heat shock protein 70 expression in rat testes. Korean J Urol. 2003;44(2):186-91.

35. Mobaraki F, Seghatoleslam M, Fazel A, Ebrahimzadeh-Bideskan A. Effects of MDMA (ecstasy) on apoptosis and heat shock protein (HSP70) expression in adult rat testis. Toxicol Mech Methods. 2018;28(3):219-29.

36. Narayansingh RM, Senchyna M, Vijayan MM, Carlson JC. Expression of prostaglandin G/H synthase (PGHS) and heat shock protein-70 (HSP-70) in the corpus luteum (CL) of prostaglandin F2 alpha-treated immature superovulated rats. Can J Physiol Pharmacol. 2004;82(6):363-71.

37. Wu G, Hu X, Ding J, Yang J. Abnormal expression of HSP70 may contribute to PCOS pathology. J Ovarian Res. 2019;12(1):74.

Treatment of Subcutaneous Sarcoidosis with Hydroxychloroquine in a Hepatitis B Carrier Patient: A Case Report

Hepatit B Taşıyıcısı Bir Hastada Subkutan Sarkoidozun Hidroksiklorokin ile Tedavisi: Olgu Sunumu

Tuna SEZER[1]
0000-0002-6861-2869
Mualla POLAT[1]
0000-0001-9226-5134
Yasin Hakan KANDİL[1]
0009-0004-5072-3124
Selma ERDOĞAN DÜZCÜ[2]
0000-0001-6768-1275

[1]Department of Dermatology, Bolu Abant İzzet Baysal University Faculty of Medicine, Bolu, Türkiye

[2]Department of Pathology, Bolu Abant İzzet Baysal University Faculty of Medicine, Bolu, Türkiye

ABSTRACT

Sarcoidosis is a disorder of unknown etiology affecting many systems and characterized by non-caseating granulomas. Subcutaneous sarcoidosis is the rarest form of specific lesions in cutaneous sarcoidosis. It occurs more frequently in the fourth decade of life and is more common in females than in males. Multiple asymptomatic to slightly painful, firm, mobile, round to oval, skin-colored, or erythematous nodules frequently occur in a bilateral and asymmetric pattern on the extremities. In the differential diagnosis, other diseases presenting with subcutaneous nodules should be excluded. Here, a case of subcutaneous sarcoidosis in a 51-year-old female hepatitis B carrier patient who partially responded to topical steroid treatment and was successfully treated with hydroxychloroquine was presented. In subcutaneous sarcoidosis, patients should be evaluated for systemic involvement. Hydroxychloroquine should be considered among the treatment options.
Keywords: Sarcoidosis; subcutaneous; hydroxychloroquine.

ÖZ

Sarkoidoz, etiyolojisi tam olarak bilinmeyen, birçok sistemi tutan, non-kazeifiye granülomlarla karakterize bir hastalıktır. Deri sarkoidozunda spesifik lezyonların en nadir görülen formu subkutan sarkoidozdur. Subkutan sarkoidoz genellikle yaşamın dördüncü dekadında daha sık görülür ve kadınlarda erkeklerden daha yaygındır. Çoğunlukla ekstremitelerde, bilateral ve asimetrik bir şekilde yerleşen, çoklu asemptomatikten hafif ağrılıya kadar değişebilen, sert, hareketli, yuvarlak ila oval, deri renginde veya eritemli nodüller şeklinde görülür. Ayırıcı tanıda subkutan nodül ile seyreden diğer hastalıklar dışlanmalıdır. Bu çalışmada, topikal steroid tedavisine kısmen yanıt veren ve hidroksiklorokin ile başarılı bir şekilde tedavi edilen, hepatit B taşıyıcısı olan 51 yaşında bir kadın hastada görülen bir subkutan sarkoidoz olgusu sunulmaktadır. Subkutan sarkoidozda hastalar sistemik tutulum açısından da değerlendirilmelidir. Tedavi seçenekleri arasında hidroksiklorokin düşünülmelidir.
Anahtar kelimeler: Sarkoidoz; subkutan; hidroksiklorokin.

Corresponding Author
Sorumlu Yazar
Tuna SEZER
tunasezer@yahoo.com

INTRODUCTION

Sarcoidosis, with skin involvement as the second most common manifestation after pulmonary involvement, can present with different morphologies and has been referred to as the "great imitator" (1,2). Subcutaneous sarcoidosis, also known as Darier-Rousy sarcoidosis, is a rare form of cutaneous sarcoidosis. The incidence of subcutaneous sarcoidosis increases in the 4th decade of life and it is more common in

females (1,2). In the treatment of cutaneous sarcoidosis, the extent of lesions and systemic involvement are important and treatment plans should be created accordingly (3).

This case report aimed to present a case of subcutaneous sarcoidosis in a hepatitis B carrier patient who partially responded to topical steroid treatment and was successfully treated with hydroxychloroquine.

CASE REPORT

A 51-year-old female patient applied to our clinic with a complaint of painless swelling in her arms for approximately 1.5 years. Lesions initially appeared as small nodules on both arms and gradually enlarged over time. The patient had a history of hepatitis B carrier status and cholecystectomy. Dermatological examination revealed numerous painless, firm, erythematous subcutaneous nodules ranging from 1 to 3 cm in diameter on the extensor surfaces of both arms (Figure 1).

In the histopathological examination, hyperkeratosis, hypergranulosis, and acanthosis were observed in the epidermis; epithelioid histiocytes, multinucleated giant cells, and granuloma structures consisting of lymphocytes and intense inflammation were observed in the deep dermis and subcutaneous fatty tissue; and no staining with Ziehl-Neelsen or periodic acid-Schiff was observed (Figure 2). The patient was diagnosed with subcutaneous sarcoidosis and referred to the pulmonology and ophthalmology departments for examinations of systemic involvement. A chest X-ray revealed hilar fullness (Figure 3), while thorax computed tomography detected millimetric nodules and hilar lymph nodes consistent with sarcoidosis. Serum angiotensin-converting enzyme and calcium levels were normal, as were the results of liver function tests, blood counts, thyroid function tests, and sedimentation rate. Anti-streptolysin O was negative and no ocular pathology was detected. HBsAg, anti-HBe, HBV-DNA, and anti-HBc IgG (+) were present. Due to the patient's status as a carrier of hepatitis B, clobetasol 17-propionate was started instead of systemic corticosteroids. A partial response was achieved after 2 months of treatment. Since the patient's ophthalmological examination and laboratory tests were normal, hydroxychloroquine 400 mg/day was initiated. After 5 months, the lesions disappeared completely.

DISCUSSION

Sarcoidosis is a systemic disease affecting the lungs, skin, lymph nodes, and eyes. Skin involvement is seen in about 25% of sarcoidosis patients. The etiology remains unknown, but a combination of genetic predisposition and environmental factors are thought to play a role. The disease typically begins before the age of 50 and is more common in females, with an estimated prevalence of 2.17-160 per 100,000 population (2-4).

Skin lesions in sarcoidosis, which are referred to as the "great imitator" and present in different clinical forms, are categorized as specific or nonspecific. Subcutaneous sarcoidosis entails specific skin lesions and constitutes the least common lesion type of that category. These lesions range from 0.5 to 2 cm in size, can vary in number, and are firm, mobile, erythematous, violaceous, skin-colored, or hyperpigmented. They are asymptomatic or mildly painful

Figure 1. A) Firm, erythematous subcutaneous nodules on right forearm, **B)** Closer view of picture A
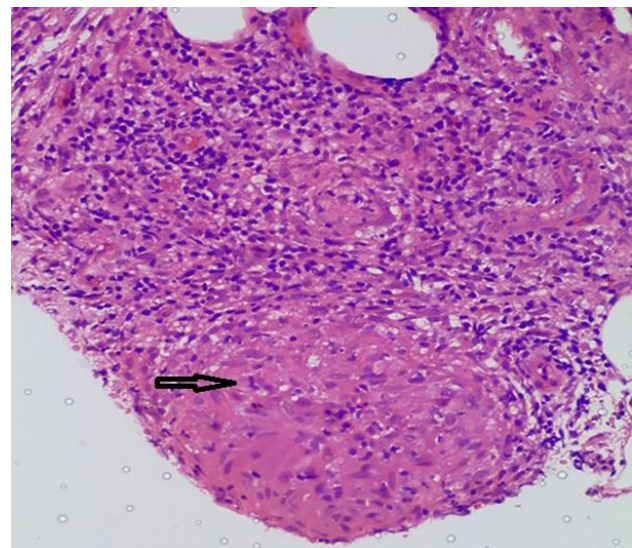
Figure 2. Epithelioid histiocytes and granuloma structures in the deep dermis and subcutaneous fatty tissue (black arrow)

Figure 3. Bilateral hilar lymphadenopathy

and typically bilateral and asymmetrically located on the extremities. Differential diagnoses include lipomas, cysts, subcutaneous granuloma annulare, foreign body granulomas, lupus profundus, and cutaneous manifestations of lymphoproliferative malignancies (1,2,5).

The typical histopathological finding for sarcoidosis is non-caseating granuloma (naked granuloma) consisting of epithelioid cells and multinuclear giant cells (3). Three major criteria are required to diagnose sarcoidosis: sufficient clinical findings, demonstration of non-caseating granulomas in one or more tissue samples, and exclusion of other granulomatous diseases (6).

Systemic involvement may occur in subcutaneous sarcoidosis, and bilateral hilar lymphadenopathy was most frequently reported in a previous case series. Uveitis, parotitis, arthritis, mucositis, dactylitis, neurological and renal involvement, and hepatosplenomegaly occur in about 15% of patients, in descending order of frequency There have also been reports of subcutaneous sarcoidosis cases with systemic involvement (5,7). Our patient was also examined for systemic involvement and millimetric nodules were detected in the lungs along with bilateral hilar lymphadenopathy.

In cutaneous sarcoidosis, treatment should be planned according to the extent of the disease, its severity, and its impact on quality of life. Topical steroids, topical calcineurin inhibitors, or intralesional steroids are preferred for localized lesions. If the disease is widespread, slowly progressing, stable, or persistent localized disease, tetracycline or antimalarials can be added to topical treatments. For cosmetically disfiguring, rapidly progressive, or refractory cutaneous sarcoidosis, combination immunosuppressive therapy (topical steroids plus systemic steroids), JAK inhibitors, methotrexate, infliximab, or adalimumab may be used (3). A case of sarcoidosis accompanied by Hepatitis C infection and treated with adalimumab has been reported in the literature (8).

In a retrospective multicentric study by Cohen et al. (4), the use of hydroxychloroquine combined with topical steroids was recommended as the first step in the treatment of cutaneous sarcoidosis. Marchetti et al. (9) treated two cases of subcutaneous sarcoidosis with hydroxychloroquine and proposed it as a first-line treatment option for patients for whom steroids are contraindicated. Youn et al. (10) also treated a patient with subcutaneous sarcoidosis with hydroxychloroquine at 400 mg/day for 5 months and reported improvement in the lesions. Since our patient was a hepatitis B carrier, systemic steroid treatment was not given. Our patient, who did not benefit from topical steroids, received hydroxychloroquine at 400 mg/day and all lesions had healed after 5 months.

In cases of subcutaneous sarcoidosis, patients should be investigated for systemic involvement. As in our case, hydroxychloroquine should be considered among the treatment options.

REFERENCES

1. Koneti J, Cherukuri SP, Gadde S, Kalluru R, Chikatimalla R, Dasaradhan T. Sarcoidosis and its dermatological manifestations: A narrative review. Cureus. 2022;14(8):e28053.
2. Sève P, Pacheco Y, Durupt F, Jamilloux Y, Gerfaud-Valentin M, Isaac S, et al. Sarcoidosis: A clinical overview from symptoms to diagnosis. Cells. 2021;10(4):766.
3. Ezeh N, Caplan A, Rosenbach M, Imadojemu S. Cutaneous sarcoidosis. Dermatol Clin. 2023;41(3):455-70.
4. Cohen E, Lheure C, Ingen-Housz-Oro S, Hotz C, Bettuzzi T, Chasset F, et al. Which first-line treatment for cutaneous sarcoidosis? A retrospective study of 120 patients. Eur J Dermatol. 2023;33(6):680-5.
5. Lopez-Sundh AE, Maestre-Orozco T, Gonzalez-Vela MC, Fernandez-Ayala M. Subcutaneous sarcoidosis: A case series of 19 patients. J Postgrad Med. 2021;67(3):154-7.
6. Crouser ED, Maier LA, Wilson KC, Bonham CA, Morgenthau AS, Patterson KC, et al. Diagnosis and detection of sarcoidosis. An official American Thoracic Society clinical practice guideline. Am J Respir Crit Care Med. 2020;201(8):e26-e51.
7. Dalle Vedove C, Colato C, Girolomoni G. Subcutaneous sarcoidosis: report of two cases and review of the literature. Clin Rheumatol. 2011;30(8):1123-8.
8. Juratli HA, Hertl M, Gualtieri B. Sarcoidosis with concomitant hepatitis C infection treated successfully with adalimumab. J Dtsch Dermatol Ges. 2019;17(9):936-8.
9. Marchetti M, Baker MG, Noland MM. Treatment of subcutaneous sarcoidosis with hydroxychloroquine: report of 2 cases. Dermatol Online J. 2014;20(1):21250.
10. Youn P, Francis RJ, Preston H, Lake F. Subcutaneous sarcoidosis (Darier-Roussy sarcoidosis) with extensive disease on positron emission tomography: A case report and review of the literature. Respirol Case Rep. 2022;10(5):e0949.

Management of Prosthesis Embolization into Left Ventricle after Transcatheter Aortic Valve Implantation: A Case Report

Transkateter Aort Kapak İmplantasyonu Sonrası Sol Ventriküle Protez Embolizasyonunun Yönetimi: Bir Olgu Sunumu

Osman Fehmi BEYAZAL
0000-0001-6211-0676
Hasan TEZCAN
0009-0008-4745-6757
Mehmed YANARTAŞ
0000-0001-7780-3950
Nihan KAYALAR
0000-0002-1220-7071
Süleyman YAZICI
0000-0001-6346-9664

Department of Cardiovascular Surgery, Başakşehir Çam and Sakura City Hospital, İstanbul, Türkiye

ABSTRACT

Transcatheter aortic valve implantation is recommended in advanced aortic stenosis, in elderly patients who are not suitable for surgery. Valve embolization is one of the most important complications that is life-threatening. A 61-year-old male patient was being followed up with a complaint of shortness of breath. He had a history of coronary artery bypass graft operation. Transthoracic echocardiography revealed severe aortic stenosis. Transfemoral transcatheter aortic valve implantation was performed, but while the balloon passed through the valve, the valve embolized the ventricle. The patient was then taken into operation. The native aortic valve was resected, the valve embolized into the ventricle was cut and removed, and surgical aortic valve replacement was performed. Endovascular methods can be preferred in suitable patients, but in cases where they fail, urgent open-heart surgery is required. One of the most important points is that the guidewire should not be removed when embolization.
Keywords: Transcatheter aortic valve implantation; aortic stenosis; prosthesis embolization.

ÖZ

İleri aort darlığında, cerrahiye uygun olmayan yaşlı hastalarda transkateter aort kapak implantasyonu önerilmektedir. Kapak embolizasyonu hayatı tehdit eden en önemli komplikasyonlardan biridir. 61 yaşında erkek hasta nefes darlığı şikayetiyle takip ediliyordu. Koroner arter baypas greft operasyonu öyküsü vardı. Transtorasik ekokardiyografide ciddi aort darlığı saptandı. Hastaya transfemoral transkateter aort kapak implantasyonu yapıldı, ancak balon kapaktan geçerken kapak ventrikülü embolize oldu. Hasta daha sonra operasyona alındı. Doğal aort kapağı rezeke edildi, ventriküle embolize olan kapak kesilerek çıkarıldı ve cerrahi aort kapak replasmanı yapıldı. Uygun hastalarda endovasküler yöntemler tercih edilebilir ancak başarısız olunduğu durumlarda acil açık kalp ameliyatı gerekir. En önemli noktalardan biri embolizasyon sırasında kılavuz telin çıkarılmamasıdır.
Anahtar kelimeler: Transkateter aort kapak implantasyonu; aort stenozu; protez embolizasyonu.

INTRODUCTION

According to the European Society of Cardiology (ESC) and the European Association for Cardio-Thoracic Surgery (EACTS) guidelines, transcatheter aortic valve implantation (TAVI) is recommended in advanced aortic stenosis (AS), elderly patients, in patients with high-risk (Society of Thoracic Surgeons-Predicted Risk of Mortality (STS-PROM)/European System for Cardiac Operative Risk Evaluation (EuroSCORE) II >8%) or who are not suitable for surgery (Class I) (1). Successful results have been reported in suitable patients, but many serious complications may occur, such as vascular problems, aortic root, valve, heart rhythm

problems, paravalvular leak, ischemic complications, and valve embolization (2). Although many of the complications can be managed with interventions, when endovascular interventions are insufficient, especially in cases such as valve embolization, these patients, who are already in the high-risk group for surgical aortic valve replacement (SAVR), may need to undergo urgent surgery.

In this case, a patient who underwent TAVI due to symptomatic severe AS, who was operated on under emergency conditions after ventricular embolization of the valve was presented, and the points that should be taken into consideration during the operation management.

CASE REPORT

A 61-year-old (81 kg) male patient was being followed up with a complaint of shortness of breath for 3 months. He had a history of hypertension, and diabetes mellitus (DM), a coronary artery bypass graft (CABG) operation performed 20 years ago, and a history of percutaneous coronary intervention (PCI) 2 years ago. Transthoracic echocardiography (TTE) revealed severe AS (max/mean gradient: 75/43 mmHg, aortic valve area: 0.89 cm^2), moderate aortic regurgitation (AR) and ejection fraction (EF) was 55%. The aortic annulus measured was 22 mm. Coronary computed tomographic angiography (CTA) revealed that the bypass grafts and the stent placed in the left circumflex artery were patent. Due to CABG history, DM, and comorbidities, the STS score, expected operative mortality was 1.7%, and estimated morbidity and mortality was 11.2%. The patient was evaluated multidisciplinary by the heart team, in terms of surgery, TAVI, and sutureless valve options, and it was decided to perform TAVI because the surgery was high risk due to the patient's comorbidities, previous heart surgery, poor general condition, and the high STS score.

He was operated on by the cardiology clinic for this purpose. Firstly, two Perclose ProGlide™ systems (Abbott Vascular, CA, USA) were placed in the right femoral artery, a sheath was placed in the left femoral artery and jugular vein, and a temporary pace was placed over the right jugular vein. Subsequently, Myval transcatheter heart valve 27 mm (Meril Life Sciences Pvt. Ltd., Vapi, India) was implanted. As moderate paravalvular AR was detected after the procedure, a balloon was planned. However, while the balloon was being passed through the valve, it was observed that the valve embolized the ventricle (Figure 1). The patient was hemodynamically stable but was referred to us for emergency surgery. Due to the position of the valve in the ventricle, in order to prevent it from moving and closing the left ventricular outflow tract (LVOT) and causing sudden hemodynamic deterioration, the guidewire holding the valve was not removed and was left in place. The patient was taken into operation under emergency conditions. An incision was made in the right axillary region, an 8 mm Dacron graft was placed in the axillary artery and arterial cannulation was performed. A venous cannula was placed percutaneously into the left femoral vein. Then re-sternotomy was performed. After the adhesions were removed, a second venous cannula was placed in the superior vena cava and selective venous cannulation was performed. The left internal mammary artery (LIMA) and other saphenous

vein grafts were carefully located and confirmed to be patent. After LIMA flow was stopped, the heart was arrested by giving intermittent antegrade and continuous retrograde cardioplegia, and then aortotomy was performed. Native aortic valve leaflets were observed to be calcified. The valve falling into the ventricle and the support wire holding this valve were seen (Figure 2). Native aortic valve leaflets were resected and the supporting wire was cut and separated from the valve. The valve, which fell into the left ventricle and was over the LVOT, could not be removed in one piece because it was stuck in the surrounding tissues due to the cobalt alloy frame. The valve stuck in the left ventricle was removed in 3 pieces with wire cutters and scissors (Figure 3). Then, a 23 mm Dafodil™ pericardial bioprosthesis (Meril Life Sciences Pvt. Ltd., India) valve was implanted. Cross
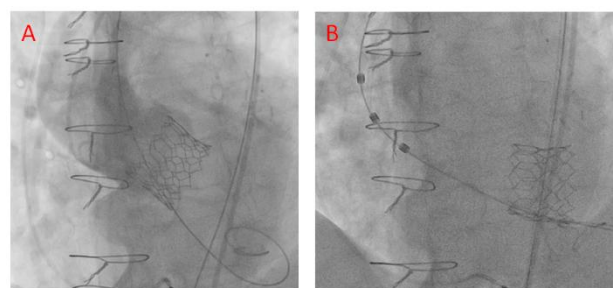

Figure 1. A) Fluoroscopic image of the transcatheter aortic valve implantation valve after placement, **B)** fluoroscopic image of the valve after it is embolized into the ventricle while the balloon is passed through the valve
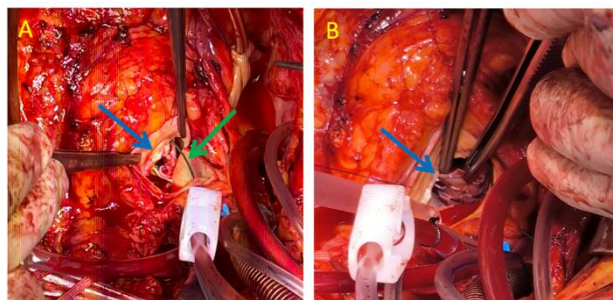

Figure 2. A) After aortotomy, the guidewire holding the valve in place (green arrow), and the calcified native aortic valve (blue arrow), **B)** the transcatheter aortic valve implantation valve embolized into the ventricle after the native aortic valve was resected (blue arrow)

Figure 3. Image of the transcatheter aortic valve implantation valve, which was not removed in one piece and had to be cut off

clamp time (XCL) was 123 min and cardiopulmonary bypass (CPB) time was 230 min. After the operation, a total of 700 ml was drained and a total of 2 U of erythrocyte suspension was given. In the TTE performed in the first postoperative week, EF was 55% and no pathology was detected in the aortic valve. The patient was taken to the service on the 3rd postoperative day and discharged with Asa + Warfarin on the 8th postoperative day without any complications.

DISCUSSION

With the development of technology, TAVI is an extremely important treatment option for severe AS patients, especially in patients with a high risk of surgery, and has found its place in the guidelines with a Class I recommendation (1). However, this procedure has its own important complications. Valve embolization is one of the most important complications that is life-threatening and requires urgent intervention. In the study conducted by Thomas et al. (3) with SAPIEN Aortic Bioprosthesis, the embolization rate was reported as 0.3%. In a cohort study by Frumkin et al. (4) with 3757 patients, valve embolization and migration were seen in 1.44%. The transfemoral approach has been associated with a higher ventricular embolization rate compared to the transapical approach (5). Reasons such as suboptimal positioning, incorrect measurement of the annulus, inadequate aortic valve calcifications, insufficient support in subvalvular structures, ventricular pacing error, complex annulus or aortic valve structure, septal hypertrophy, incomplete or late inflation of the balloon may lead to embolization (5-7).

Embolization may be towards the aorta or, more rarely, into the ventricle. During valve placement, aortic embolization is attempted to be prevented by reducing contractility with rapid ventricular pacing. However, embolization of the valve into the aorta may be better tolerated than embolization into the ventricle. The issue that needs to be taken into consideration is maintaining the wire position. With this, the rotation of the valve can be prevented and blood flow is not blocked. The most important point to pay attention to is maintaining the guidewire position. With this, the rotation of the valve can be prevented and blood flow is not blocked. The valve can be snared or repositioned with a partially inflated balloon into a stable position in the more distal aorta (8). However, if valve stability cannot be achieved, surgery is required.

Left ventricular embolization is less common and in many cases, the valve requires surgical removal. In this case, one of the most important points is to keep the guidewire on the valve. A released valve may obstruct the LVOT and cause sudden hemodynamic compromise, leading to an arrest. We also applied this in our case. After the valve was embolized into the ventricle, we took the patient to the operating table and started the operation, without changing the position of the existing guide wire and femoral catheter. After undergoing CPB and placing the XCL, we performed an aortotomy and saw the guidewire inside the aorta. After perfusion was achieved by CPB, we cut and separated the guidewire and then removed the cover.

Another option after ventricular embolization is the placement of a second valve. In the report of Tiroch et al. (9), a second prosthesis was implanted and fixed the first prosthesis within the annulus. In the case series of Otalvaro et al. (10)

with left ventricle embolization, a second transcatheter prosthesis was implanted and then the first embolizing valve was removed and the operation was completed without the need to use SAVR and XCL. Astarci et al. (11), in a patient who developed left ventricle embolization after transapical TAVI, removed the valve using the same access route and then implanted a second transcatheter valve. For this, femoral CPB and induced ventricular fibrillation may be helpful (10). In addition, after the second valve implantation, the anatomical location of this valve is also important. It should be kept in mind that a thrombus may develop in this valve in addition to the first valve. Care should be taken to ensure that this second valve does not cover the branches of the aorta. In addition, care should be taken in terms of possible aortic dissection after these repeated interventions. The valve can also be removed via the left atrium, but it should not be forgotten that mitral valve damage may occur. In the case report of Seecherran et al. (12), after LVOT embolization, balloon-assisted recapture and subsequent successful implantation of the valve across the aortic annulus without significant hemodynamic compromise or surgical intervention have been reported.

In our case, it was not possible to move the valve using the endovascular method. Since the valve could not be guided back to its original position, we decided to remove it. However, we decided to perform a re-sternotomy because he had a previous CABG history, and his grafts were patent. Even after the native aortic valve was resected, we could not remove the TAVI valve from where it was embolized into the ventricle. Therefore, we had to cut the valve off. In patients with a high risk of sternotomy, the valve can be removed with thoracotomy and femoral CPB and a second TAVI valve can be re-implanted. However, in difficult cases like this, removing the valve may not be easy. If the valve cannot be removed after thoracotomy, it may be necessary to return to sternotomy again. Therefore, in addition to deciding on the operation, it is also important to decide how the operation will be performed. In particular, mobilization of the embolized valve should be evaluated fluoroscopically. If it is thought that it will be easy to remove, thoracotomy can be performed in appropriate anatomical localization. However, in complex cases, sternotomy, which is the gold standard, will be life-saving in these patients. SAVR can also be performed after sternotomy.

Although embolization after TAVI can be managed effectively, each repeated intervention increases mortality and morbidity for these patients who are already in the high-risk group. More important than dealing with this complication is preventing it. We think that these complications can be reduced with appropriate measurement, appropriate positioning, appropriate ventricular pacing, and correct patient selection. However, when it occurs, we think that this case report will guide physicians in the management of this complication, which is rare in the literature.

CONCLUSION

Valve embolization to the ventricle after TAVI is a rare but life-threatening complication that requires urgent intervention. Endovascular methods can be preferred in suitable patients with a rapid strategy, but in cases where

they fail, urgent open heart surgery is required. In patients with a history of cardiac surgery, the first valve can be removed by thoracotomy and a second valve can be placed, but it may also be necessary to remove the valve by sternotomy. Appropriate patient selection is important in this regard. One of the most important points is that the guidewire should not be removed when embolization occurs.

Informed Consent: Written informed consent was obtained from the patient for publication and accompanying images.

Conflict of Interest: None declared by the authors.

Financial Disclosure: None declared by the authors.

Acknowledgments: None declared by the authors.

Author Contributions: Idea/Concept: OFB, SY; Design: OFB; Data Collection/Processing: OFB, HT, MY, NK; Analysis/Interpretation: HT, MY, NK; Literature Review: OFB; Drafting/Writing: OFB, HT, SY; Critical Review: MY, NK, SY.

REFERENCES

1. Vahanian A, Beyersdorf F, Praz F, Milojevic M, Baldus S, Bauersachs J, et al. 2021 ESC/EACTS Guidelines for the management of valvular heart disease. Eur Heart J. 2022;43(7):561-632.
2. Vallabhajosyula P, Bavaria JE. Transcatheter aortic valve implantation: complications and management. J Heart Valve Dis. 2011;20(5):499-509.
3. Thomas M, Schymik G, Walther T, Himbert D, Lefèvre T, Treede H, et al. Thirty-day results of the SAPIEN aortic Bioprosthesis European Outcome (SOURCE) Registry: A European registry of transcatheter aortic valve implantation using the Edwards SAPIEN valve. Circulation. 2010;122(1):62-9.
4. Frumkin D, Pietron M, Kind A, Brand A, Knebel F, Laule M, et al. Valve embolization during transcatheter aortic valve implantation: Incidence, risk factors and follow-up by computed tomography. Front Cardiovasc Med. 2022;9:928740.
5. Makkar RR, Jilaihawi H, Chakravarty T, Fontana GP, Kapadia S, Babaliaros V, et al. Determinants and outcomes of acute transcatheter valve-in-valve therapy or embolization: a study of multiple valve implants in the U.S. PARTNER trial (Placement of AoRTic TraNscathetER Valve Trial Edwards SAPIEN Transcatheter Heart Valve). J Am Coll Cardiol. 2013;62(5):418-30.
6. Cuttone F, Ivascau C, Grollier G, Massetti M. Distal embolization of Edwards SAPIEN prosthesis during transcatheter aortic valve implantation. G Chir. 2013;34(9-10):275-7.
7. Gul M, Erkanli K, Erol MK, Bakir I. Ventricular embolization of Edwards SAPIEN prosthesis following transcatheter aortic valve implantation. J Invasive Cardiol. 2012;24(10):537-8.
8. Masson JB, Kovac J, Schuler G, Ye J, Cheung A, Kapadia S, et al. Transcatheter aortic valve implantation: review of the nature, management, and avoidance of procedural complications. JACC Cardiovasc Interv. 2009;2(9):811-20.
9. Tiroch K, Schleiting H, Karpettas N, Schmitz E, Vetter HO, Seyfarth M, et al. How should I treat dislocation of a TAVI SAPIEN prosthesis into the left ventricle? EuroIntervention. 2015;10(11):1370-2.
10. Otalvaro L, Damluji A, Alfonso CE, Williams DB, Heldman AW. Management of transcatheter aortic valve embolization into the left ventricle. J Card Surg. 2015;30(4):360-3.
11. Astarci P, Desiron Q, Glineur D, El Khoury G. Transapical explantation of an embolized transcatheter valve. Interact Cardiovasc Thorac Surg. 2011;13(1):1-2.
12. Seecheran N, Ittleman F, Dauerman H. Left ventricular outflow tract embolization and balloon assisted recapture of a SAPIEN XT prosthesis during transcatheter aortic valve replacement. Catheter Cardiovasc Interv. 2016;88(3):E89-92.

Tetralogy of Fallot, Absent Vena Cava Superior, Persistent Left Vena Cava Superior, and Interrupted Vena Cava Inferior: A Case of Struggle in Open Heart Surgery

Fallot Tetralojisi, Vena Cava Süperior Yokluğu, Persistan Sol Vena Cava Süperior ve Kesintili Vena Cava İnferior: Açık Kalp Cerrahisindeki Güçlük Üzerine Bir Olgu

Hande İŞTAR
ⓘ *0000-0002-7150-0171*
Buğra HARMANDAR
ⓘ *0000-0002-7487-1779*

Department of Cardiovascular Surgery, Muğla Sıtkı Koçman University Faculty of Medicine, Muğla, Türkiye

ABSTRACT

Interruption of vena cava inferior (VCI) is extremely rare, in occurrence in isolation or association with asplenia or polysplenia syndromes. In this abnormality, the infrahepatic segment of the VCI is absent, by representing the inadequacy of fusion of subcardinal embryological parts of the VCI. It is compensated by an azygos or hemiazygos vein that continues on the posterior wall of the thoracic cavity. In this case report, a case of incidentally diagnosed interrupted VCI in a patient diagnosed with tetralogy of Fallot (TOF), major aortopulmonary collateral artery (MAPCA), right arcus aorta, absence of right vena cava superior (VCS), and persistent left vena cava superior (PLVCS), and its successful surgical treatment was presented. If the hepatic vein confluence is of adequate size, the cannulation for cardiopulmonary bypass circuit through the hepatic vein confluence is safe in case of interrupted VCI.
Keywords: Superior vena cava; inferior vena cava; persistent left vena cava superior; tetralogy of Fallot.

ÖZ

Kesintili vena kava inferior (vena cava inferior, VCI), izole olarak ya da aspleni veya polispleni sendromlarıyla birlikte meydana gelmesiyle, oldukça nadir olarak görülür. Bu anomalide, vitellin ve subkardinal embriyolojik VCI'nın füzyonundaki yetersizlik nedeniyle, VCI'nın infrahepatik segmenti gelişmemiştir. Bu durum, torasik boşluğun posterior duvarında devam eden azygos ya da hemiazygos veni tarafından kompanze edilir. Bu olgu sunumunda, Fallot tetralojisi (tetralogy of Fallot, TOF), majör aortikpulmoner kollateral arter (major aortopulmonary collateral artery, MAPCA), sağ arkus aorta, sağ vena kava süperior (vena cava superior, VCS) yokluğu ve persistan sol vena kava süperior (persistent left vena cava superior, PLVCS) tanısı olan bir hastada tesadüfen teşhis edilen kesintili VCI vakası ve başarılı cerrahi tedavisi sunulmuştur. Hepatik ven konflüensi yeterli büyüklükteyse, kesintili VCI durumunda hepatik ven konflüensinden açık kalp cerrahisi dolaşımı için kanülasyon güvenlidir.
Anahtar kelimeler: Superior vena kava; inferior vena kava; persistan sol vena kava süperior; Fallot tetralojisi.

Corresponding Author
Sorumlu Yazar
Hande İŞTAR
hande13@msn.com

INTRODUCTION

Congenital heart surgery is challenging by nature. Different intra and extra cardiac abnormalities may be in close relation in the same patient, and it may be difficult to choose which abnormality is of the greatest importance and the priority for surgical treatment. For example, cyanotic and abnormal systemic venous return can present together. In isolation, interrupted vena cava inferior (VCI) is very rare and a compensatory azygos or hemiazygos vein continuity is present. Interrupted VCI and

azygos or hemiazygos continuity are present in occurrence with 0.6-2% of people with congenital heart diseases, <0.3% in isolation in normal people (1). It is associated in the literature with tetralogy of Fallot (TOF), truncus arteriosus, absence of the pulmonary artery, atrioventricular septal defect, pulmonary valvular stenosis, pulmonary atresia, interrupted aortic arch, atrial septal defect, coarctation of aorta, pulmonary venous stenosis, common atrium, common atrioventricular valve, and double outlet right ventricle (2-4). Here we share our experience of the surgical correction of TOF, major aortopulmonary collateral artery (MAPCA) in association with interrupted VCI, absence of vena cava superior (VCS), right arcus aorta, and persistent left vena cava superior (PLVCS).

CASE REPORT
A 2-year-old female, 10 kg in weight, patient was admitted to our center due to cyanosis with a room air saturation of 78%. She was diagnosed on echocardiography with features of TOF and a MAPCA arising from the ascending aorta. A PLVCS was enlarged; however, the right VCS was not well determined. The right aortic arch and an interrupted VCI were present. On catheterization, the exact anatomy was determined and an interrupted VCI was seen (Figures 1A, and 1B). The McGoon ratio was measured as 2.18 due to well-developed right and left pulmonary arteries. We decided total correction for the TOF and MAPCA pathologies in light of the adequate McGoon ratio and low room air saturation. Informed consent was taken from the patient's relatives.

Following median sternotomy, we observed that the hypoplastic main pulmonary artery was situated to the left side of the aorta. The right aortic arch and a well-developed PLVCS were present. Right-sided VCS was not observed and the innominate vein course was through the coronary sinus. Instead of an appropriate entrance of the VCI, we observed an enlarged confluence made by multiple hepatic veins with a central course and a central entrance to the right atrium (Figure 1C). After systemic heparinization, aortic and PLVCS cannulations were performed as usual. MAPCA division was performed. Following cardiopulmonary bypass (CPB) establishment, cannulation of the hepatic vein confluence was performed.

Systemic hypothermia (32° C) and Custodiol cardioplegia delivered via the antegrade route were used. Through the right atriotomy and atrial septectomy, a sump cannula was inserted in the left atrium. Another sump cannula was used for the aspiration of blood coming from the innominate vein through the coronary sinus. Venous return to the reservoir of the CBP machine was safe and adequate in spite of the unusual venous source due to the challenging anatomy. Ventricular septal defect closure was performed using a Gore-Tex graft. The muscle resection was performed to resolve the right ventricular outflow tract. The main pulmonary artery was opened longitudinally. We observed a bicuspid pulmonary valve. Glutaraldehyde-treated autologous pericardium was fashioned to the main pulmonary artery in an extended manner, cross annularly to obtain an enlargement for the right ventricular outflow. The atrial septum was repaired and weaning from CPB was performed as usual. Following decannulation of the hepatic vein confluence, we did not observe any stenosis. The postoperative course was uneventful. The patient was discharged on the 10th day postoperatively. Throughout the hospitalization, we did not observe any abnormal liver test results or hepatomegaly. No rhythm disturbance occurred postoperatively.

DISCUSSION
Interrupted VCI and azygos or hemiazygos venous continuity occurs in 0.6 to 2% of people with congenital heart diseases. It occurs <0.3% in isolation in normal people (1). Interrupted VCI and azygos or hemiazygos continuity at the level of the liver frequently presents in patients in addition to heterotaxy syndrome, who exhibit left isomerism of the atrial appendage, i.e. polysplenia syndrome. Chen et al. (4) performed a study of imaging of interrupted VCI and concluded that 96.4% of the cohort had left atrial isomerism. Splenic abnormalities were common and 11.8% had a normal cardiac structure; however, 30 of the 34 patients had a simple to severe degree of congenital heart disease. The most frequently associated congenital heart diseases were pulmonary stenosis or atresia and double outlet right ventricle, in ratio of 70.6% and 61.8% of patients, respectively (4). 44.1% of cohort studies showed that sinus bradycardia can occur in
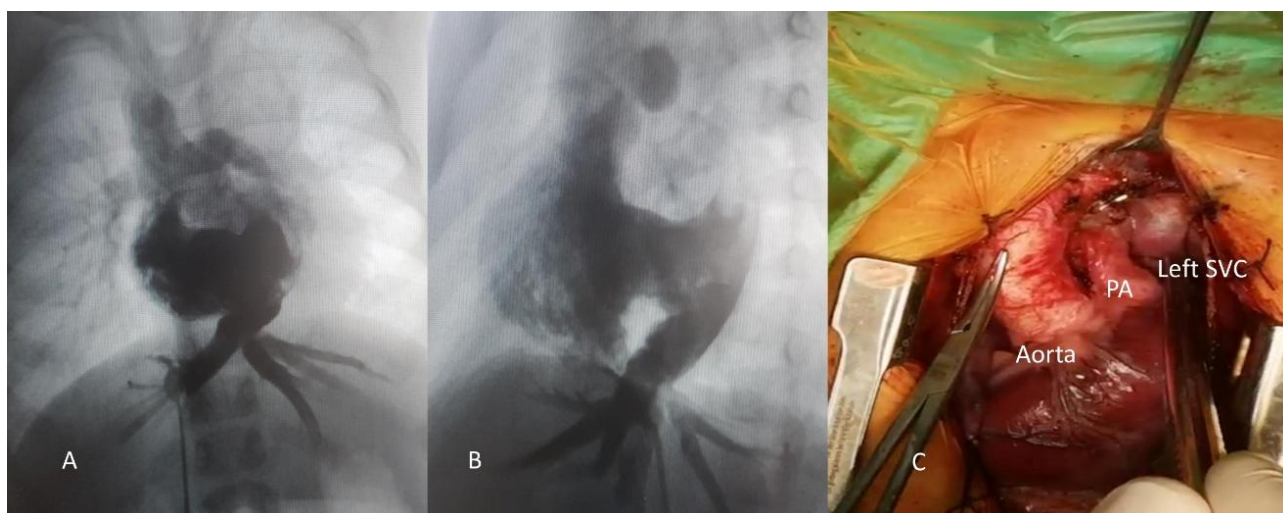

Figure 1. A, B) Angiographic view of hepatic vein confluence, **C)** intraoperative view of persistent left vena cava superior (PLVCS)

the long-term outcome. In the literature, five types of interrupted VCI have been described (5), and the most common type is interruption of the hepatic segment (4). As a result, to maintain the antegrade flow in intrauterine life, some venous anastomosis between right supracardinal and right subcardinal veins persist. They result in azygos and hemiazygous continuations (4). Due to their strong associations, an interrupted VCI should warn us of the presence of additional congenital heart diseases.

Before planning a cardiac intervention via the femoral vein or cardiac surgery in a patient with an interrupted VCI, preoperative awareness is important. Particularly in open heart surgery, while inserting the venous cannula into the VCS and VCI for CPB, two adequately sized veins are required. In the case of interrupted VCI, hepatic vein confluences have to be cannulated instead. Snaring hepatic veins after cannulation and inadequate drainage may therefore result in postoperative elevated hepatic enzymes and hepatomegaly. Moreover, in cases of intracardiac surgical repair, it is not adequate to only snare the VCS. To obtain a good exposure, it should be performed by direct sucking of the hepatic veins besides hypothermia with low flows, moreover the total circulatory arrest (6).

To complete the single ventricle type repair, it is necessary to redirect the VCI drainage into the right pulmonary artery. However, if an interrupted VCI is present and azygos or hemiazygos continuity drain the flow to the brachiocephalic vein, the Kawashima operation (consisting of end-to-side anastomosis of the VCS and the azygos or hemiazygos continuation and the confluent pulmonary artery, and division or ligation of the pulmonary artery trunk) is required. Except for hepatocardiac venous and coronary sinus flow, the total venous return drains directly into the pulmonary artery, bypassing the right-sided heart, i.e., right ventricle and right atrium (7).

TOF can present with other venous return abnormalities. Shah et al. (8) presented a case report that both the VCS were absent and only the VCI and ambiguous innominate vein were draining the systemic venous flow into the cardiac cavity. In our case, the surprising intraoperative discovery of the absence of both VCS made the TOF total repair difficult while cannulation before CPB. However, after cannulation of the VCI and the ambiguous innominate vein, also with total circulatory arrest, TOF total correction became possible (8).

Even though isolated interrupted VCIs are asymptomatic in the general population, there have been some case reports of lower limb oedema, pelvic vein or pulmonary thrombosis, and deep venous thrombosis as severe symptoms (9,10).

CONCLUSION
Our case was challenging due to an absent right VCS, interrupted VCI, PLVCS, and well-developed hepatic vein confluence when we performed venous cannulation before repairing the TOF and MAPCA. The hepatic vein drainage was fortunately adequate in the CPB period. We did not observe a serious hepatic dysfunction postoperatively. We believe this association is the first to be published in the literature. Further investigations are crucial.

REFERENCES
1. Zafar SI, Halim A, Khalid W, Shafique M, Nasir H. Two cases of interrupted inferior vena cava with azygos / hemiazygos continuation. J Coll Physicians Surg Pak. 2022;32(8):S101-3.
2. Bista B, Ferris J, Na N, Krishnam M, Urgun D. Unilateral absence of pulmonary artery and azygous continuation of interrupted inferior vena cava. Radiol Case Rep. 2020;15(6):688-90.
3. Bansal N, Ghosh R, Sankhyan LK, Chatterjee S, Chatterjee S, Bose S. Left isomerism with bilateral superior vena cava, interrupted inferior vena cava and tetralogy of Fallot. Ann Pediatr Cardiol. 2020;13(4):364-7.
4. Chen SJ, Wu MH, Wang JK. Clinical implications of congenital interruption of inferior vena cava. J Formos Med Assoc. 2022;121(10):1938-44.
5. Abu-Hilal LH, Barghouthi DI, AbuKeshek T, Tamimi H, Khatib H, Dayeh AH. Interrupted inferior vena cava syndrome discovered incidentally after minimally invasive mitral valve repair in a 31-year-old female patient: A case report. Int J Surg Case Rep. 2023;109:108621.
6. Pillai JB, Kpodonu J, Yu C, Borger MA. Heterotaxy syndrome with azygous continuation-causing pseudo Budd-Chiari syndrome after cardiopulmonary bypass. Ann Thorac Surg. 2006;81(5):1890-2.
7. Kawashima Y, Kitamura S, Matsuda H, Shimazaki Y, Nakano S, Hirose H. Total cavopulmonary shunt operation in complex cardiac anomalies: A new operation. J Thorac Cardiovasc Surg. 1984;87(1):74-81.
8. Shah TR, Hiremath CS, Diwakar A, Soman Rema KM. Absent superior vena cava in tetralogy of Fallot. Ann Card Anaesth. 2018;21(2):205-7.
9. Cheung CKM, Law MF, Wong KT, Tam MTK, Chow KM. Massive pulmonary embolism in a patient with polysplenia syndrome and interrupted inferior vena cava with azygous continuation. Arch Med Sci. 2018;14(1):251-3.
10. Koc Z, Oguzkurt L. Interruption or congenital stenosis of the inferior vena cava: prevalence, imaging, and clinical findings. Eur J Radiol. 2007;62(2):257-66.

A Case of Prenatally Diagnosed Arthrogryposis Multiplex Congenita

Prenatal Tanı Alan Artrogripozis Multipleks Konjenita Olgusu

Şenay Bengin ERTEM¹
0000-0002-7237-6061
Süreyya SARIDAŞ DEMİR²
0000-0002-4051-3703
Mustafa REŞORLU¹
0000-0002-2941-8879
Seda ATMACA KILIN³
0009-0001-5918-9704

¹Department of Radiology, Çanakkale Onsekiz Mart University Faculty of Medicine, Çanakkale, Türkiye

²Obstetrics and Gynecology Specialist, Private Practice, Çanakkale, Türkiye

³Department of Radiology, Akdeniz University Faculty of Medicine, Antalya, Türkiye

ABSTRACT

Arthrogryposis multiplex congenita (AMC) is a clinical entity characterized by reduced fetal movements (fetal akinesia), fetal growth restriction (FGR), joint contractures (arthrogryposis), facial anomalies, lung developmental delay (pulmonary hypoplasia), and other developmental abnormalities. It is accepted that this condition is a description of a group of abnormalities resulting from reduced fetal movements rather than a true diagnosis or a specific syndrome. In many arthrogryposis cases, the etiology has not yet been determined. Prenatal diagnosis of AMC is critical for providing adequate counseling to families. When a fetus with multiple congenital contractures is detected on prenatal ultrasound (US), management of the pregnant woman should be undertaken by a multidisciplinary team. In this report, a case of AMC detected in the prenatal period, together with US and fetal magnetic resonance imaging (MRI) findings, was presented.
Keywords: Fetal akinesia; arthrogryposis multiplex congenita; prenatal ultrasound; fetal magnetic resonance imaging.

ÖZ

Artrogripozis multipleks konjenita (AMK), fetal hareketlerde azalma (fetal akinezi), fetal büyüme kısıtlaması (FBK), çoklu eklem kontraktürleri (artrogripozis), yüz anomalileri, akciğerlerde gelişimsel bozukluklar (pulmoner hipoplazi) ve diğer gelişimsel anormalliklerle karakterize bir klinik tablodur. Bu durumun gerçek bir tanı veya spesifik bir sendrom olmadığı, daha ziyade fetal hareketlerde azalma sonucu oluşan bir grup anormalliğin tanımı olduğu genel olarak kabul edilmektedir. Birçok artrogripozis vakasında etiyoloji henüz belirlenememiştir. Ailelere yeterli danışmanlık sağlamak için AMC'nin prenatal tanısı kritik öneme sahiptir. Prenatal ultrasonda (US) multipl konjenital kontraktürleri olan bir fetüs tespit edildiğinde, gebe kadının yönetimi multidisipliner bir ekip tarafından yapılmalıdır. Bu yazıda, prenatal dönemde tespit edilen bir AMK vakası, US ve fetal manyetik rezonans görüntüleme (MRG) bulgularıyla birlikte sunulmuştur.
Anahtar kelimeler: Fetal akinezi; artrogripozis multipleks konjenita; doğum öncesi ultrason; fetal manyetik rezonans görüntüleme.

Corresponding Author
Sorumlu Yazar
Şenay Bengin ERTEM
benginertem@gmail.com

INTRODUCTION

For normal fetal functional development, intrauterine fetal movements are necessary (1). Normal fetal breathing, swallowing, facial muscle movements, and amniotic fluid volume are necessary for normal lung development, extremities, and facial configuration. The absence or reduction of these movements is responsible for lung hypoplasia, polyhydramnios, limb contractures, and facial abnormalities (2).

The severity and prognosis of fetal joint contractures may vary depending on the degree of involvement and underlying cause (3,4). Of these, talipes equinovarus (TEV) is the most common and mildest. Adduction, supination, and varus deformities were observed in the ankle. Unilateral or bilateral, TEV is usually an isolated anomaly and has a good outcome with orthopedic treatment (5,6). The second most common and severe form, arthrogryposis multiplex congenita (AMC), is observed with joint contractures in more than one body region. The lower and upper extremities are most commonly involved, while contractures are less frequently observed only in the upper extremities. The least common but most severe form is the fetal akinesia deformity sequence (FADS), also known as the Pena-Shokeir syndrome. This is the lethal form of AMC, often accompanied by lung hypoplasia, polyhydramnios, flattened facial features, and fetal growth restriction (7).

It is accepted that this condition describes a group of abnormalities resulting from reduced fetal movements rather than a true diagnosis or a specific syndrome (8). This report aimed to present a case of AMC detected during the second-trimester screening ultrasound (US), together with ultrasound and fetal magnetic resonance imaging (MRI) findings.

CASE REPORT

A 27-year-old primigravida woman, 23 +4 gestational weeks, was referred to our clinic for a second-trimester screening US. She had no known disease in her history, no consanguinity with her husband, and antenatal screening test results were normal. In the US, mild ventriculomegaly in the cranium (atrial diameter approximately 11 mm), increased thickness in the nuchal fold (approximately 0.77 mm), open mouth on the fetal face, flexion contractures in the bilateral elbow joints (Figure 1a), extension contractures in the bilateral knee joints (Figure 1b), and dorsiflexion contractures in the ankle joints (Figure 1c) were observed.

No fetal swallowing or movement of the fetal extremities was observed during the examination. The amniotic fluid index (AFI) was 26 cm (polyhydramnios). However, a gastric pouch was also observed. No micrognathia or thoracic hypoplasia was observed. Due to the multiple anomalies observed in the US, fetal MRI was performed. Fetal MRI confirmed the US findings, but did not provide any additional findings (Figure 2).

Perinatology evaluation, genetic examination, and family counseling were recommended for the case with suspected AMC.

After perinatology evaluation, the patient was diagnosed with AMC and did not want to continue the pregnancy, and the pregnancy was terminated (Figure 3).

No genetic mutation was detected in the L1CAM whole gene sequence analysis performed on fetal material. Informed consent was taken from the patient's relatives.

DISCUSSION

Decreased intrauterine fetal movement is thought to lead to AMC (9,10). An alternative hypothesis is that atypical tissue modeling causes muscle hypercontractility during development, leading to restricted movement and joint
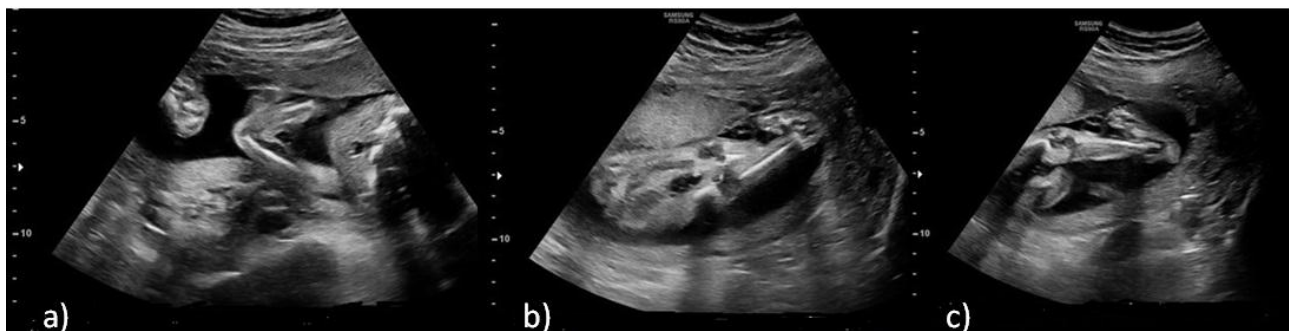

Figure 1. Ultrasonographic findings of the fetus with arthrogryposis multiplex congenita; **a)** flexion contractures in bilateral elbow joints, **b)** extension contractures in knee joints, and **c)** dorsiflexion contractures in ankle joints
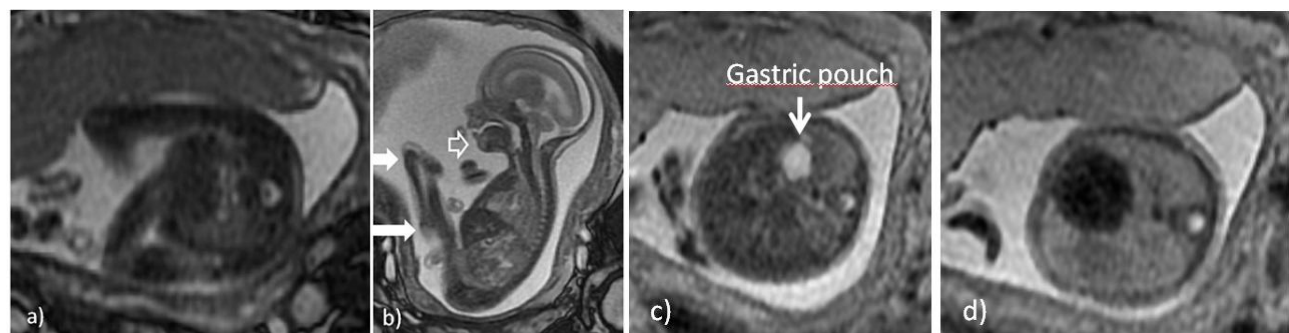

Figure 2. Findings of fetal magnetic resonance imaging; **a)** Axial 2D FIESTA weighted image shows flexion contractures in bilateral elbow joints, **b)** Coronal 2D FIESTA weighted image shows extension contractures in bilateral knee joints and dorsiflexion contractures in ankle joints (white arrow), open mouth (white open arrow) and polyhydramnios, **c)** Axial T2 weighted image shows normal gastric pouch, **d)** Axial T2 weighted image shows normal thorax

contraction (11). Arthrogryposis may be accompanied by a number of syndromes (Pena-Shokeir syndrome, multiple pterygium syndrome, Fowler syndrome, and Freeman-Sheldon syndrome). It has also been observed as a clinical feature in more than 400 specific disorders, such as genetic disorders affecting fetal neurological and musculoskeletal development (12). Although chromosomal abnormalities, mitochondrial diseases, and more than 320 single-gene diseases have been described as etiologies in many arthrogryposis cases in the literature, the exact etiology has not yet been determined (13). As reported in the literature, no specific disorder was detected in our case to explain the exact cause.

Prenatal first and second trimester US, fetal MRI, and genetic tests are used for diagnosis.

Arthrogryposis multiplex congenita can be detected using US in the first trimester (14,15). Decreased movements, increased nuchal translucency, cystic hygroma, and hydrops fetalis are the first-trimester findings (16). However, it is usually diagnosed in the early second trimester (17). The majority of prenatally diagnosed AMC cases are detected by US in the second or third trimester. Common findings include decreased fetal movement, clenched hands, joint contractures, abnormal extension or flexion of the extremities, and polyhydramnios. Other findings include fetal growth retardation (FGR), brain malformations, cleft lip palate, retrognathia/micrognathia, cardiomegaly, diaphragmatic hernia, absent fetal gastric pouch, gastroschisis, short umbilical cord, fetal hydrops, and fetal musculoskeletal disorders. In some cases, intrauterine fetal death may occur (3). We performed a second-trimester screening US in our case. Mild ventriculomegaly, increased nuchal fold thickness, open mouth on the face, flexion contractures in the bilateral elbow joints, extension contractures in the bilateral knee joints, dorsiflexion contractures in the ankle joints, and polyhydramnios. We also did not observe fetal swallowing or movement of the fetal extremities during the examination.

Fetal MRI has been used as an adjunct to US imaging since 1983 (18). Magnetic resonance imaging is particularly useful for the evaluation of brain malformations and thoracic hypoplasia (19). However, fetal MRI is not as widely available as US, is more expensive, and requires specialized expertise for interpretation, limiting its use in prenatal diagnosis of AMC (3). In our case, we performed fetal MRI. Fetal MRI confirmed the US findings, but did not provide any additional findings.

Genetic testing is one of the most important steps in the prenatal diagnosis of AMC and decision-making for families. For this purpose, invasive tests such as chorionic villus sampling or amniocentesis should be offered (3).

Genetic analysis is not always performed before birth; sometimes, it can be postponed until after birth at the request of the families (3). Whole-exome sequencing (WES) and whole-genome sequencing (WGS) are the most comprehensive testing options (3). In our case, L1CAM WGS was performed on fetal material after the termination of pregnancy. However, no genetic mutations have been identified.

Despite advanced imaging, AMC remains a complex prenatal diagnosis without a single etiology in many instances. When AMC is detected on prenatal US, families

Figure 3. Image of the fetus after termination

should receive comprehensive support from a multidisciplinary team. This team typically includes specialists in perinatology, radiology, genetics, neonatology, pediatric neurology, pediatric orthopedics, and mental health counseling. Clear communication regarding findings, prognosis, and options is essential during this process (3). We recommend perinatology evaluation, genetic examination, and family counseling for this case.

CONCLUSION

Prenatal diagnosis of AMC is critical for providing adequate counseling to families. Prenatal first and second trimester US, fetal MRI, and genetic testing are used for diagnosis. When a fetus with multiple congenital contractures is detected on prenatal US, management of the pregnant woman should be undertaken by a multidisciplinary team.

REFERENCES

1. Parlakgümüş HA, Tarım E, Küçükgöz Ü. Fetal akinesia/hypokinesia deformation sequence (FADS): two and three dimentional ultrasound presentation. Turkiye Klinikleri J Gynecol Obst. 2008;18(5):336-9.

2. Takada E, Koyama N, Ogawa Y, Itoyama S, Takashima S. Neuropathology of infant with Pena-Shokeir I syndrome. Pediatr Neurol. 1994;10(3):241-3.

3. Lowry RB, Sibbald B, Bedard T, Hall JG. Prevalence of multiple congenital contractures including arthrogryposis multiplex congenita in Alberta, Canada, and a strategy for classification and coding. Birth Defects Res A Clin Mol Teratol. 2010;88(12):1057-61.

4. Sharon-Weiner M, Sukenik-Halevy R, Tepper R, Fishman A, Biron-Shental T, Markovitch O. Diagnostic accuracy, work-up, and outcomes of pregnancies with clubfoot detected by prenatal sonography. Prenat Diagn. 2017;37(8):754-763.

5. Canto MJ, Cano S, Palau J, Ojeda F. Prenatal diagnosis of clubfoot in low-risk population: associated anomalies and long-term outcome. Prenat Diagn. 2008;28(4):343-6.

6. Lauson S, Alvarez C, Patel MS, Langlois S. Outcome of prenatally diagnosed isolated clubfoot. Ultrasound Obstet Gynecol. 2010;35(6):708-14.

7. Tjon JK, Tan-Sindhunata MB, Bugiani M, Witbreuk MMEH, van der Sluijs JA, Weiss MM, et al. Care pathway for foetal joint contractures, foetal akinesia deformation sequence, and arthrogryposis multiplex congenita. Fetal Diagn Ther. 2021;48(11-12):829-39.

8. Niles KM, Blaser S, Shannon P, Chitayat D. Fetal arthrogryposis multiplex congenita/fetal akinesia deformation sequence (FADS)-Aetiology, diagnosis and management. Prenat Diagn. 2019;39(9):720-31.

9. DeMyer W, Baird I. Mortality and skeletal malformations from amniocentesis and oligohydromnios in rats: cleft palata, clubfoot, microstomia and adactyly. Teratology. 1969;2(1):33-7.

10. Moessinger AC. Fetal akinesia deformation sequence: an animal model. Pediatrics. 1983;72(6):857-63.

11. Coste B, Houge G, Murray MF, Stitziel N, Bandell M, Giovanni MA, et al. Gain-of-function mutations in the mechanically activated ion channel PIEZO2 cause a subtype of distal arthrogryposis. Proc Natl Acad Sci USA. 2013;110(12): 4667-72.

12. Hall JG. Arthrogryposis (multiple congenital contractures): diagnostic approach to etiology, classification, genetics and general principles. Eur J Med Genet. 2014;57(8):464-72.

13. Beecroft SJ, Lombard M, Mowat D, McLean C, Cairns A, Davis M, et al. Genetics of neuromuscular fetal akinesia in the genomics era. J Med Genet. 2018;55(8):505-14.

14. Adam S, Coetzee M, Honey EM. Pena-Shokeir syndrome: current management strategies and palliative care. Appl Clin Genet. 2018;11:111-20.

15. Busack B, Ott CE, Henrich W, Verlohren S. Prognostic significance of prenatal ultrasound in fetal arthrogryposis multiplex congenita. Arch Gynecol Obstet 2021;303(4):943-53.

16. Shafqat G, Fatima K, Hanif F. Foetal Akinesia deformation sequence: a rare lethal entity. J Pak Med Assoc. 2023;73(11):2266-8.

17. Muller LM, de Jong G. Prenatal ultrasonographic features of the Pena-Shokeir I syndrome and trisomy 18 syndrome. Am J Med Genet. 1986;25(1):119-29.

18. Smith FW, Adam AH, Phillips WD. NMR imaging in pregnancy. Lancet. 1983;1(8314-5):61-2.

19. Prayer D, Brugger PC. Investigation of normal organ development with fetal MRI. Eur Radiol. 2007;17(10):2458-71.

Delayed Onset Anton-Babinski Syndrome following Post-Hypoxic Cortical Injury: A Case Report

Post-Hipoksik Kortikal Hasar Sonrası Gelişen Gecikmiş Anton-Babinski Sendromu: Olgu Sunumu

Özlem ÖNDER
0000-0002-7133-9808
Şahin IŞIK
0000-0001-6375-3673

Department of Neurology, Near East University Faculty of Medicine, Nicosia, Northern Cyprus

ABSTRACT

Delayed post-hypoxic cortical blindness is a rare but clinically significant condition that can manifest days or weeks following a hypoxic event, such as cardiac arrest. During these events, the brain is deprived of oxygen and glucose, leading to selective vulnerability in metabolically active regions, particularly the occipital lobes. Although initial resuscitation may restore spontaneous circulation, secondary injury mechanisms can contribute to delayed and progressive neurological damage. Here, a case of Anton-Babinski syndrome manifesting as sudden cortical blindness and profound anosognosia following successful cardiopulmonary resuscitation was reported. Despite undeniable visual loss confirmed by bilateral occipital ischemia on neuroimaging, the patient insisted she could see and provided confabulatory descriptions, highlighting a rare and intriguing complication of post-hypoxic injury. This case provides a unique perspective to the limited literature on Anton-Babinski syndrome, highlighting the critical importance of early recognition and comprehensive evaluation in uncovering rare and elusive post-hypoxic complications.
Keywords: Cardiac arrest; hypoxia; cortical blindness; cerebral ischemia; hypoxic-ischemic encephalopathy; ischemia-reperfusion injury; Anton-Babinski syndrome.

ÖZ

Gecikmiş post-hipoksik kortikal körlük, kardiyak arrest gibi hipoksik olayları takiben günler veya haftalar sonra ortaya çıkabilen nadir ancak klinik olarak önemli bir durumdur. Bu tür olaylar sırasında beyin, oksijen ve glukozdan yoksun kalır ve özellikle metabolik olarak aktif bölgelerden olan oksipital loblar seçici şekilde zarar görür. İlk resüsitasyon işlemi spontan dolaşımı geri kazandırsa da, ikincil hasar mekanizmaları gecikmiş ve ilerleyici nörolojik hasara katkıda bulunabilir. Bu yazıda, başarılı kardiyopulmoner resüsitasyon sonrası ani kortikal körlük ve belirgin anozognozi ile ortaya çıkan çarpıcı bir Anton-Babinski sendromu vakası sunulmuştur. Nörogörüntülemesinde bilateral oksipital iskemi ile doğrulanan belirgin görme kaybına rağmen hasta görebildiğini iddia etmiş ve çevresini hayali şekilde tanımlayarak konfabülasyon yapmıştır. Bu vaka, Anton-Babinski sendromu üzerine sınırlı veri içeren literatüre özgün bir katkı sağlamakta ve nadir görülen post-hipoksik komplikasyonların ortaya çıkarılmasında erken tanı ve kapsamlı değerlendirmenin kritik önemini vurgulamaktadır.
Anahtar kelimeler: Kardiyak arrest; hipoksi; kortikal körlük; beyin iskemisi; hipoksik-iskemik ensefalopati; iskemi-reperfüzyon hasarı; Anton-Babinski sendromu.

INTRODUCTION

Hypoxic brain injury is a significant cause of morbidity and mortality, particularly in the context of cardiac arrest, where global cerebral ischemia can lead to extensive neurological damage. The occipital cortex is particularly vulnerable to hypoxic injury

Presented as a poster at the 60th National Neurology Congress (November 26-December 2, 2024; Antalya, Türkiye)

due to its high metabolic demand, and even brief periods of oxygen deprivation can result in significant and sometimes irreversible neurological damage (1). Although prompt resuscitation following hypoxic events like cardiac arrest can restore circulation, it also introduces secondary injury mechanisms, including oxidative stress, inflammation, and excitotoxicity, which contribute to delayed neuronal damage and functional deficits (2).

Delayed post-hypoxic cortical blindness is a rare but serious neurological complication that may manifest hours to days after the initial hypoxic insult. Despite severe visual impairment, patients often retain pupillary light reflexes due to the preservation of anterior visual pathways. However, in cases where only partial damage to the occipital cortex occurs, patients may experience visual field deficits rather than complete blindness (3).

Anton-Babinski syndrome, characterized by cortical blindness, anosognosia (denial of blindness), and confabulation, is an uncommon condition in clinical practice and even rarer as a complication following cardiopulmonary resuscitation (CPR). The limited literature on post-CPR Anton-Babinski syndrome underscores a significant gap in understanding its pathophysiology, clinical course, and management (4). Early recognition of this condition is crucial, as with other delayed neurological deficits, where postponed diagnosis can significantly impede timely intervention and optimal rehabilitation outcomes (5).

This report aimed to present a case of an 80-year-old female who developed delayed-onset Anton-Babinski syndrome following successful CPR. By detailing this case, we aimed to contribute to the limited literature and emphasize the importance of early recognition, comprehensive evaluation, and multidisciplinary management of this rare but critical complication in post-hypoxic patients.

CASE REPORT
An 80-year-old female with a history of controlled hypertension and atrial fibrillation, but no prior neurological deficits, was brought to the emergency department following a witnessed cardiac arrest. Immediate CPR was initiated by bystanders, and emergency services continued advanced cardiac life support. Return of spontaneous circulation was achieved after approximately 10 minutes of resuscitation. Upon arrival at the hospital, the patient underwent coronary angiography due to electrocardiographic evidence of an acute myocardial infarction. Angiography revealed critical stenosis of the left anterior descending artery, necessitating immediate percutaneous coronary intervention with stent placement. Neurologically, the patient showed no deficits in the immediate postoperative period, exhibiting full motor and sensory function and following commands. On the second postoperative day, the patient reported diminished vision, describing her surroundings as "dim" and "blurred." However, family members observed that she was unable to see, frequently colliding with objects and showing no visual response to stimuli. Despite this, the patient insisted she could see and provided inaccurate descriptions of her environment. This discrepancy, combined with confabulation, led to the suspicion of cortical blindness. Neurological examination revealed no

visual response to light, and there were no signs of motor or sensory deficits. Despite her blindness, the patient's pupillary reflexes were intact. During the initial evaluation, laboratory analysis revealed elevated serum lactate levels of 3.8 mmol/L (reference, 0.5-2.2 mmol/L) and a mild metabolic acidosis with a pH of 7.32 and bicarbonate level of 18 mmol/L, indicating significant tissue hypoxia and supporting the diagnosis of acute hypoxic injury. Brain magnetic resonance imaging (MRI) demonstrated bilateral ischemic lesions localized to the occipital cortices, providing definitive radiological confirmation of cortical blindness (Figure 1). Although visual evoked potentials (VEP) and electroencephalography (EEG) were initially planned to assess the functional integrity of the visual pathways and cortical activity, these procedures could not be completed due to the patient's cognitive confusion and restlessness. To objectively support the preliminary diagnosis, an ophthalmologic evaluation was conducted, which confirmed the cortical nature of the visual loss by demonstrating intact anterior visual pathways and ruling out ocular or optic nerve pathologies as potential causes of the blindness. A comprehensive supportive management approach, including structured neurological rehabilitation and close clinical monitoring, was initiated to optimize neurological recovery and functional outcomes. The patient experienced significant visual recovery one month later, with visual field deficits nearly resolved.

DISCUSSION
Anton-Babinski syndrome is characterized by cortical blindness accompanied by anosognosia and confabulation (4). The denial of visual loss, a hallmark of the syndrome, is believed to result from damage to neural pathways responsible for visual awareness, while primary visual input pathways remain unaffected. This explains why patients, despite profound blindness, confidently assert they can see and provide vivid but incorrect descriptions of their environment (6). In our case, the patient persistently claimed to see her surroundings, offering inaccurate visual details, despite clear evidence of blindness and frequent collisions with objects. Notably, pupillary reflexes remained intact, as the anterior visual pathways, including the optic nerves and brainstem structures, were preserved. This dissociation between visual perception and pupillary response is a critical diagnostic clue for cortical blindness (7). The patient's confabulation and denial of blindness further confirmed the diagnosis of Anton-Babinski syndrome, emphasizing the importance of thorough neurological assessment in post-hypoxic patients presenting with visual disturbances.

Anton-Babinski syndrome can arise from various etiologies, including bilateral occipital lobe infarction, traumatic brain injury, hypoxic-ischemic events, and, less commonly, neoplastic or inflammatory processes affecting the visual cortex (4). In evaluating the etiology of cortical blindness in this case, several differential diagnoses were considered, including hypoxic injury, cardiac embolism, posterior circulation stroke, vasculitis, and metabolic disturbances. However, the bilateral and symmetrical nature of the occipital ischemic lesions, along with the absence of focal neurological deficits typically associated with embolic events, favored hypoxic injury as the primary
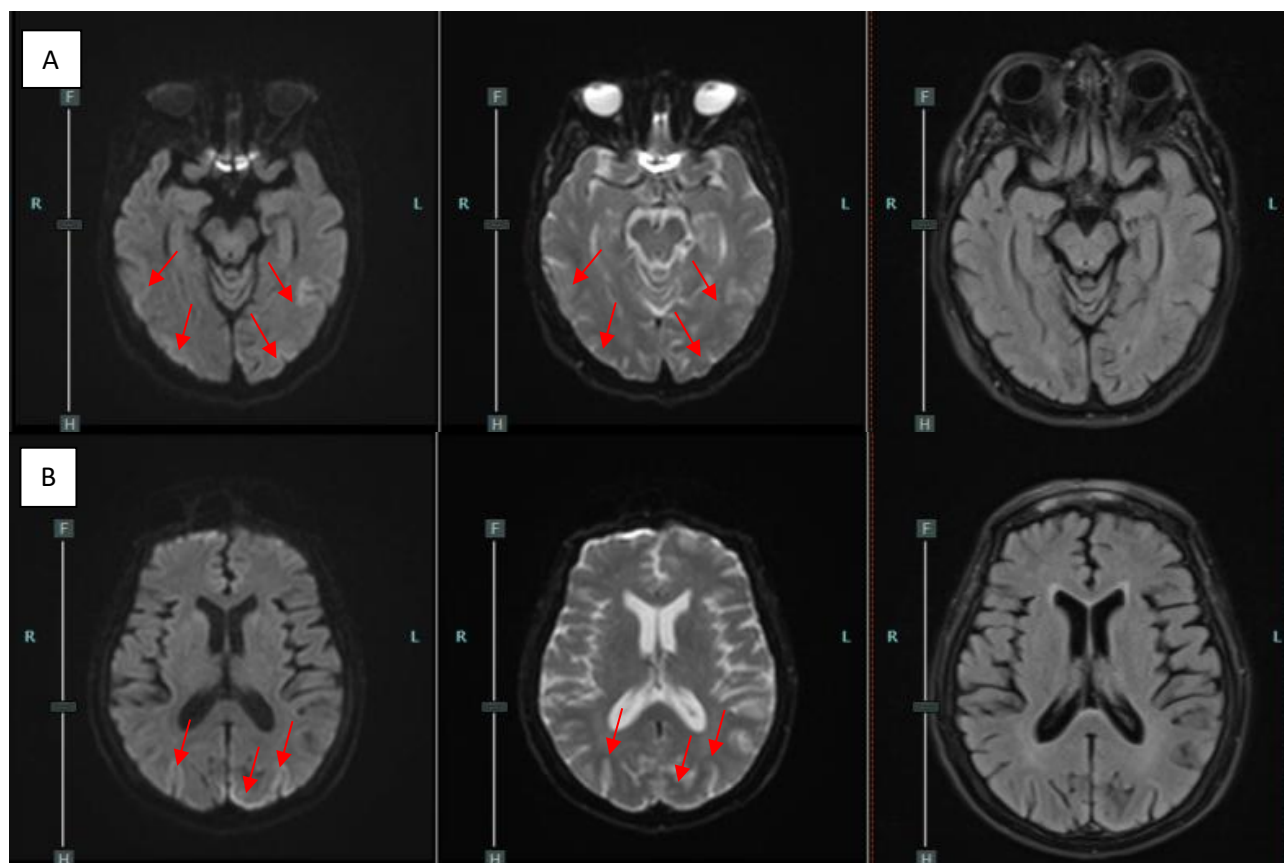
Figure 1. The figure presents axial magnetic resonance imaging (MRI) images obtained at different levels from the occipital regions using various sequences. Diffusion-weighted imaging (DWI) reveals restricted diffusion in the affected areas bilaterally. Corresponding apparent diffusion coefficient (ADC) maps show these regions as hypointense to isointense. T2-weighted fluid-attenuated inversion recovery (FLAIR) sequences demonstrate predominantly isointense lesions with limited focal areas of hyperintensity

cause. Elevated lactate levels and metabolic acidosis observed during the initial evaluation further supported the presence of significant global hypoxia. Moreover, imaging studies revealed no evidence of vascular occlusion, malignancy, or inflammatory processes that would indicate an embolic, neoplastic, or vasculitic origin. Taken together, these clinical and radiological findings reinforced the conclusion that hypoxia, rather than embolic phenomena, was the predominant factor contributing to the development of cortical blindness in this patient.

Anton-Babinski syndrome is an exceptionally rare but clinically significant neurological complication that may develop in elderly individuals who are more susceptible to post-hypoxic cortical injury due to factors such as reduced cerebrovascular reserve, age-related neuronal vulnerability, and comorbid conditions that can exacerbate ischemic damage (6). Although delayed post-hypoxic leukoencephalopathy secondary to white matter injury is infrequent, it has been documented in 2.75% to 10% of patients following carbon monoxide poisoning, emphasizing the potential for delayed neurological sequelae after hypoxic insults (5). Cortical blindness, another rare yet impactful complication, can result from hypoxic-ischemic injury to the occipital lobes. In this context, Anton-Babinski syndrome, defined by the coexistence of cortical blindness and anosognosia, has been specifically associated with bilateral occipital lobe damage, further underscoring the vulnerability of this region to hypoxic injury (8).

In this case, the development of Anton-Babinski syndrome following a hypoxic event underscores the complexity of post-hypoxic neurological outcomes, particularly in elderly patients with vascular comorbidities such as hypertension and atrial fibrillation. Although the initial neurological examination post-resuscitation was unremarkable, the patient later developed delayed-onset cortical blindness accompanied by anosognosia and confabulation, consistent with Anton-Babinski syndrome. The occipital lobes, being metabolically active, are particularly vulnerable to oxygen deprivation. While reperfusion restores oxygen supply, it also introduces reactive oxygen species, leading to oxidative damage, mitochondrial dysfunction, and calcium overload. These processes can initiate apoptosis, contributing to delayed neuronal injury and the subsequent onset of cortical symptoms days to weeks after the initial hypoxic insult (9). The pathophysiology of this case can be attributed to a combination of the initial hypoxic insult and secondary injuries triggered by reperfusion. Elevated lactate levels and metabolic acidosis observed during the initial evaluation indicated significant tissue hypoxia, underscoring the severity of the cerebral injury. The abrupt restoration of blood flow post-resuscitation likely initiated a cascade of secondary damage mechanisms, including oxidative stress, mitochondrial dysfunction, and excitotoxicity, which are known to contribute to delayed neuronal injury, particularly in the metabolically vulnerable occipital cortex (10). These pathophysiological

processes provide a plausible explanation for the delayed onset of cortical blindness, which emerged despite an initially uneventful neurological recovery following resuscitation. The onset of visual symptoms two days after resuscitation aligns with known patterns of delayed post-hypoxic cortical blindness, which can emerge after an initial recovery period (11).

The patient's partial visual recovery following comprehensive supportive care and structured neurological rehabilitation highlights the potential for neuroplasticity and functional improvement, even in elderly individuals with severe cortical injury. This case underscores the importance of early diagnosis and multidisciplinary management in optimizing outcomes for post-hypoxic complications. Consistent with previous reports, Anton-Babinski syndrome emerged as a delayed complication of post-hypoxic cortical injury (6-8). While some cases in the literature describe persistent visual deficits, others, like our patient, demonstrate significant recovery over time.

The observed improvement, characterized by the gradual resolution of visual field deficits over one month, was likely facilitated by early initiation of targeted rehabilitation, including visual scanning exercises, orientation training, and environmental adaptations to enhance visual perception and compensatory strategies. Additionally, psychological support was integral in addressing anosognosia and confabulation, core features of Anton-Babinski syndrome (12).

This case contributes to the limited literature by emphasizing that early and individualized rehabilitation can significantly influence visual outcomes, even after severe cortical injury. It also reinforces the necessity for long-term, multidisciplinary follow-up to monitor neurological progress and adapt rehabilitation strategies accordingly. Ultimately, this case highlights the value of a proactive, patient-centered approach in managing delayed post-hypoxic neurological deficits to optimize functional recovery.

REFERENCES
1. Goodall S, Twomey R, Amann M. Acute and chronic hypoxia: implications for cerebral function and exercise tolerance. Fatigue. 2014;2(2):73-92.
2. Jurcau A, Ardelean AI. Oxidative stress in ischemia/reperfusion injuries following acute ischemic stroke. Biomedicines. 2022;10(3):574.
3. Diana L, Casati C, Melzi L, Bianchi Marzoli S, Bolognini N. The effects of occipital and parietal tDCS on chronic visual field defects after brain injury. Front Neurol. 2024;15:1340365.
4. Ziaul YH, Mittal J, Afroze T, Kumar V. Anton-Babinski syndrome: A visual anosognosia. Cureus. 2024;16(3):e55679.
5. Önder Ö, Kılıçaslan R. Delayed neuropsychiatric syndrome following carbon monoxide poisoning: Report of a rare case with response to treatment. J Emerg Med Case Rep. 2021;12(1):16-8.
6. Chen JJ, Chang HF, Hsu YC, Chen DL. Anton-Babinski syndrome in an old patient: a case report and literature review. Psychogeriatrics. 2015;15(1):58-61.
7. Yasir ZH, Sharma R, Khandekar R, Kesarwani D. Posterior cerebral artery stroke with visual manifestation during COVID pandemic. Indian J Clin Exp Ophthalmol. 2023;9(3):287-93.
8. Majoulet A, Audo I, Goujard C, De Menthon M, Chaix F, Safar P, et al. Delayed-onset hypoxic cortical blindness: coming back from the abyss. Doc Ophthalmol. 2022;144(2):147-52.
9. Sekhon MS, Stukas S, Hirsch-Reinshagen V, Thiara S, Schoenthal T, Tymko M, et al. Neuroinflammation and the immune system in hypoxic ischaemic brain injury pathophysiology after cardiac arrest. J Physiol. 2024;602(21):5731-44.
10. Rae CD, Baur JA, Borges K, Dienel G, Díaz-García CM, Douglass SR, et al. Brain energy metabolism: A roadmap for future research. J Neurochem. 2024;168(5):910-54.
11. Buonfiglio F, Böhm EW, Pfeiffer N, Gericke A. Oxidative stress: A suitable therapeutic target for optic nerve diseases? Antioxidants (Basel). 2023;12(7):1465.
12. Saionz EL, Busza A, Huxlin KR. Rehabilitation of visual perception in cortical blindness. Handb Clin Neurol. 2022;184:357-73.

A Rare Case: Primary Pulmonary Amyloidosis

Nadir Bir Olgu: Primer Pulmoner Amiloidoz

Mustafa KUZUCUOĞLU[1]
[0000-0001-9889-0061]
Ceyda CEYLAN[1]
[0009-0004-1834-0203]
Arslan Hirad GANİ[1]
[0009-0000-3561-6831]
Gülay TURAN[2]
[0000-0002-3702-8811]

ABSTRACT

Amyloidosis is a rare disorder characterized by the extracellular deposition of insoluble protein aggregates. There are two common types of amyloidosis: Amyloid A (AA) and amyloid light chain (AL). AA amyloidosis typically occurs secondary to chronic inflammatory processes such as tuberculosis and rheumatoid arthritis, with pulmonary involvement being a rare manifestation. AL amyloidosis, on the other hand, is often associated with conditions like multiple myeloma, gammopathies, and idiopathic primary amyloidosis. While kidney involvement is common, pulmonary involvement can also occur as part of systemic amyloidosis or, more rarely, in an isolated form. Pulmonary amyloidosis can present in three forms: nodular, diffuse, and tracheobronchial. This study presented a case of primary pulmonary amyloidosis in the nodular form, identified in a 69-year-old female patient.
Keywords: Nodular amyloidosis; amyloid; light chain; wedge.

[1]Department of Thoracic Surgery, İzmir Katip Çelebi University Faculty of Medicine, İzmir, Türkiye

[2]Department of Medical Pathology, Balıkesir University Faculty of Medicine, Balıkesir, Türkiye

ÖZ

Amiloidoz suda çözünmeyen proteinöz yapıların hücre dışında birikimi ile karakterize nadir görülen bir hastalıktır. Amiloid A (AA) ve amiloid hafif zincir (AL) olmak üzere iki yaygın amiloidoz tipi mevcuttur. AA tipi amiloidoz tüberküloz ve romatoid artrit gibi kronik inflamatuar süreçlere sekonder olarak ortaya çıkar ve pulmoner tutulum nadir bir bulgudur. Öte yandan, AL tipi amiloidoz ise sıklıkla multiple miyelom, gamopatiler ve idiyopatik olarak ortaya çıkan primer amiloidoz gibi durumlarla ilişkilidir. Böbrek tutulumu yaygın olmakla birlikte pulmoner tutulum sistemik amiloidozun bir parçası olarak veya daha nadiren izole bir formda da ortaya çıkabilir. Pulmoner amiloidoz nodüler, diffüz ve trakeobronşiyal olmak üzere üç formda ortaya çıkabilir. Bu çalışmada, 69 yaşında bir kadın hastada saptanan nodüler formdaki primer pulmoner amiloidoz vakası sunulmuştur.
Anahtar kelimeler: Nodüler amiloidoz; amiloid; hafif zincir; wedge.

Corresponding Author
Sorumlu Yazar
Mustafa KUZUCUOĞLU
mustafakuzucuoglu@hotmail.com

INTRODUCTION

Amyloidosis is a rare disease characterized by the extracellular accumulation of water-insoluble, proteinaceous substances called amyloid, first described by Virchow in 1854 (1,2). While amyloid deposits can occur in any organ, they most commonly affect the kidneys. There are two main types of amyloidosis: Amyloid A (AA) and amyloid light chain (AL). AA amyloidosis typically develops as a secondary complication of chronic inflammatory conditions, while AL amyloidosis is often idiopathic and represents primary amyloidosis. Pulmonary amyloidosis may manifest as part of primary systemic amyloidosis or as an isolated condition (1,3).

Presented as a poster at the 10th National Thoracic Surgery Congress (April 25-28, 2019; Antalya, Türkiye).

Amyloid accumulation in the respiratory tract was first described by Lesser in 1877. Pulmonary amyloidosis can present in three forms: nodular, diffuse, and tracheobronchial. Localized forms are often seen as tracheobronchial disease (2,4).

In this report, a rare case of primary pulmonary amyloidosis, along with a review of the relevant literature, was presented.

CASE REPORT

A 69-year-old female was admitted with progressively worsening dyspnea. The patient's physical examination findings revealed a dyspneic appearance, mild retractions in the intercostal muscles, and coarse crackles in the breath sounds. Peripheral non-invasive oxygen saturation without supplemental oxygen was measured at 92%. Her laboratory results revealed a white blood cell count of 10,500 /mm³, an eosinophil level of 3%, and a C-reactive protein (CRP) level of 35 mg/L. A chest X-ray showed bilateral, patchy consolidations with nodular features, leading to a presumptive diagnosis of pneumonia (Figure 1). Intravenous moxifloxacin was administered for 14 days however, despite partial clinical improvement, the patient's dyspnea persisted.

Further evaluation suggested interstitial lung disease, and a computed tomography (CT) scan of the thorax revealed bilateral nodular consolidations, more pronounced on the right side (Figure 2). A tissue biopsy was planned for differential diagnosis, and a wedge resection was performed via mini-thoracotomy with general anesthesia, 3 weeks after medical treatment. Pathological evaluation revealed nodular areas stained with Congo red, which appeared green under polarized light, leading to the diagnosis of nodular amyloidosis (Figure 3).

The patient underwent biochemical tests to evaluate liver and kidney functions, specifically for systemic amyloidosis screening. No pathological findings were observed in the conducted tests. During the systemic screening for amyloidosis, ultrasound and CT did not reveal any involvement of other organs. The patient was diagnosed with primary pulmonary amyloidosis, and colchicine therapy was initiated. After six months of treatment, a clinical response was observed, although follow-up thoracic CT scans showed no significant radiological regression (Figure 4). Clinically, there was improvement in exertional capacity and reduced oxygen requirements, and the patient no longer required regular oxygen support during follow-up.

DISCUSSION

Amyloidosis has an incidence of approximately 1 in 100,000 annually (4,5). AA amyloidosis typically occurs as a secondary complication of chronic inflammatory diseases, such as tuberculosis and rheumatoid arthritis, with pulmonary involvement being rare. In contrast, AL amyloidosis is more commonly associated with multiple myeloma, gammopathies, and idiopathic cases, representing primary amyloidosis. While primary systemic amyloidosis can affect all organs, primary localized amyloidosis specifically leads to pulmonary involvement (1,4). In a study by Hui et al. (6) involving 48 cases of pulmonary amyloidosis, 28 patients had the nodular form, 14 had tracheobronchial involvement, and 6 had diffuse disease.

Nodular pulmonary amyloidosis is often asymptomatic, while diffuse and tracheobronchial forms typically present with respiratory symptoms. In the tracheobronchial form, dyspnea and hemoptysis are common (1,2,4). Peng et al. (7) reported a case of a 59-year-old patient with calcifications and atelectasis around the bronchi on radiological evaluations. The patient presented with cough, dyspnea, stridor, hemoptysis, and fever. Our patient had the nodular
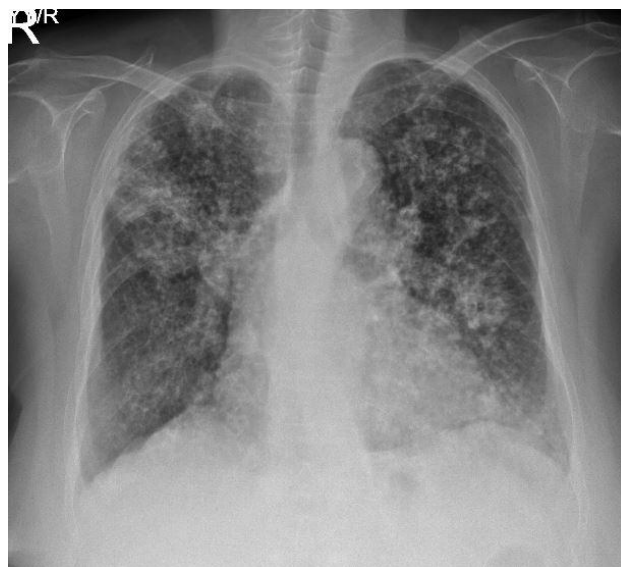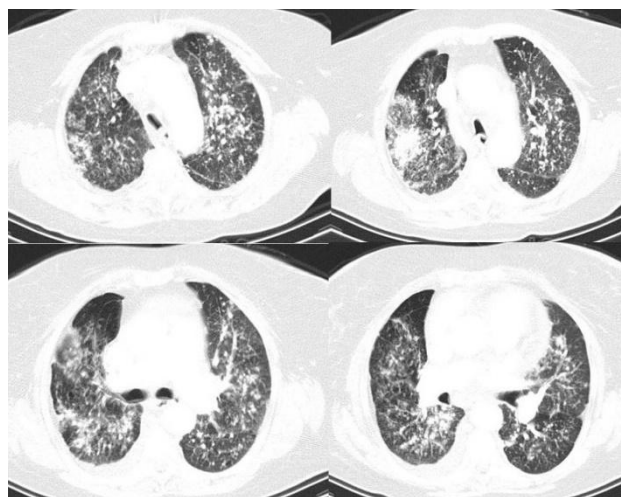

Figure 1. Amyloid deposition on chest X-ray

Figure 2. Chest computed tomography prior to surgery showing nodular amyloid deposition in the lungs
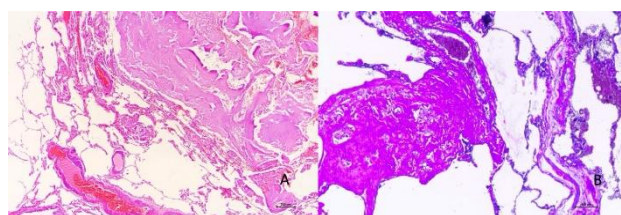

Figure 3. A) Acellular, eosinophilic amyloid accumulation in the alveolar septum, positively stained with Congo red on pathological examination (100x). **B)** Amyloid accumulation in the alveolar septum, stained positively with histochemical crystal violet (200x).

form, with dyspnea as the predominant symptom, and pulmonary function tests revealed a restrictive pattern.

The diagnosis of pulmonary amyloidosis is often made incidentally or based on respiratory symptoms, with chest X-rays and thoracic CT scans playing a crucial role. Imaging studies may show single or multiple nodular lesions in the nodular type, while the diffuse form presents with non-specific consolidations. Amyloid nodules can reach sizes of up to 15 cm and typically have lobulated contours. Tracheobronchial amyloid deposits can be detected via bronchoscopy (2,4,5). Amyloid nodules can radiologically mimic lung cancer. Oki et al. (8) presented a case of a 59-year-old female patient with an amyloid nodule located in the anterior upper lobe of the left lung, which radiologically mimicked lung cancer, and was diagnosed with an amyloid nodule in the pathological examination performed after wedge resection. In our case, thoracic CT scans revealed bilateral nodular lesions, consistent with findings reported in the literature.

Pathological evaluation is considered the gold standard for diagnosing amyloidosis. Congo red staining highlights amyloid deposits, which exhibit green birefringence under polarized light (2,4).

Although there is no definitive treatment for pulmonary amyloidosis, colchicine and steroid therapy have been used for both diffuse and nodular forms. Studies have shown symptomatic relief with colchicine, although no improvement in survival has been demonstrated. In tracheobronchial amyloidosis, bronchoscopic interventions, including laser therapy and stent placement,
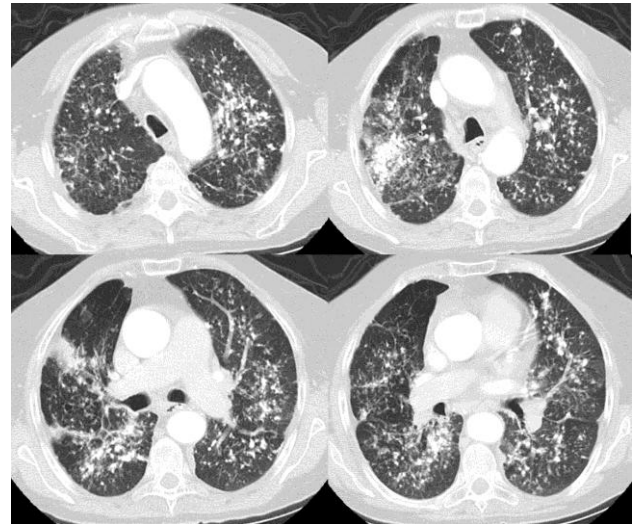

Figure 4. No significant change in amyloid deposition on follow-up chest computed tomography after treatment.

have been reported to yield successful outcomes (1,2,4). In our patient with nodular amyloidosis, colchicine therapy was initiated, resulting in symptomatic improvement, although no radiological response was observed.

In conclusion, pulmonary amyloidosis should be considered in the differential diagnosis of diffuse or nodular parenchymal lesions in patients with interstitial lung disease.

REFERENCES
1. Canbakan SÖ, Soylu B, Pelit A, Demirağ F, Başer Y. Primary pulmonary amyloidosis: Case report. Ankara Patoloji Bülteni. 1998;15(2):34-6. Turkish.
2. Şenol T, Günay Ş, Eser İ, Erkilet E. A case of tracheobronchial amyloidosis. Dicle Med J. 2014;41(3):581-4. Turkish.
3. Engineer DP, Kute VB, Patel HV, Shah PR. Clinical and laboratory profile of renal amyloidosis: a single center experience. Saudi J Kidney Dis Transpl. 2018;29(5):1065-72.
4. Al-Umairi RS, Al-Lawati F, Al-Busaidi FM. Nodular pulmonary amyloidosis mimicking metastatic pulmonary nodules: A case report and review of the literature. Sultan Qaboos Univ Med J. 2018;18(3):e393-6.
5. Baumgart JV, Stuhlmann-Laeisz C, Hegenbart U, Nattenmüller J, Schönland S, Krüger S, et al. Local vs. systemic pulmonary amyloidosis-impact on diagnostics and clinical management. Virchows Arch. 2018;473(5):627-37.
6. Hui AN, Koss MN, Hochholzer L, Wehunt WD. Amyloidosis presenting in the lower respiratory tract. Clinicopathologic, radiologic, immunohistochemical, and histochemical studies on 48 cases. Arch Pathol Lab Med. 1986;110(3):212-8.
7. Peng X, Wang X, Luo D, Zuo W, Yao H, Zhang W. Atypical primary pulmonary amyloidosis: A rare case report. Medicine (Baltimore). 2020;99(26):e20828.
8. Oki T, Izuka S, Otsuki Y, Katayama M, Nakamura T. Localized nodular pulmonary amyloidosis mimicking primary lung cancer associated with cystic airspaces: A case report. Radiol Case Rep. 2024;19(9):3719-23.

Comment on "Comparison of Nasal Anthropometric Measurements of Turks Living in Different Geographical Regions"

"Farklı Coğrafi Bölgelerde Yaşayan Türklerin Nazal Antropometrik Ölçümlerinin Karşılaştırılması" Başlıklı Yazı Üzerine

Helin YÜCEDAĞ GÜNDOĞDU
0000-0001-7724-6031
Bahattin PASLI
0000-0002-4354-3238

Department of Anatomy, Hacettepe University Faculty of Medicine, Ankara, Türkiye

Corresponding Author
Sorumlu Yazar
Helin YÜCEDAĞ GÜNDOĞDU
yucedaghelin@gmail.com

Dear Editor,

We read with great interest the article "Comparison of Nasal Anthropometric Measurements of Turks Living in Different Geographical Regions" by Kanter et al. (1) published on pages 139-145 of the 26(2) issue of the Duzce Medical Journal in 2024. We are writing to offer additional comments and discussion on the article. While the study presents valuable insights into the nasal morphology of two distinct populations of Turkish populations that have inhabited different geographical regions for 1000 years, we would like to express a few thoughts about the study.

Firstly, the article attributes differences in nasal measurements primarily to ethnicity, which is a valid consideration. However, it is important to acknowledge that factors such as climate and environmental conditions may play a significant role in shaping of external nasal structures. For instance, variations in nasal morphology across populations could be influenced by adaptive mechanisms to different climates, particularly temperature and humidity (2). We think that the difference in nasal measurements observed between the Türkiye Turks and the Kazakh Turks populations may be modest evidence of the influence of climatic factors. It is also known that nasal anthropometry shows significant differences in geographical regions of Türkiye with different climate characteristics (3).

Secondly, given the paucity of large-scale studies in the extant literature that can confirm racial differences and the existence of multifaceted interactions between societies, it may be more appropriate to use terms such as "a sample of the Turkish population", "from the Turkish subpopulation", "among Turkish individuals" articles, thus emphasizing that these observations do not generalize to the entire race. The use of these sample expressions has the potential to increase the quality of scientific studies by eliminating problems related to sample representation.

Thirdly, as a consequence of the natural process of ageing, a number of changes may be observed in the nasal region. These include the loss of fibrous tissue between the lateral and major alar cartilages, the weakening of the supporting ligament of the medial crus of the major alar cartilage, and the thickening of the subcutaneous tissue of the nasal tip. These changes can result in the drooping of the tip of the nose and the convexity of the dorsum. Consequently, the

dorsum of the nose length and nasolabial angle are subject to change with age (4). In the discussion of the present article, a comparison is made between the findings of the study and the findings reported by Garandawa et al. (5) and Mehta et al (6). However, the sample age ranges in these studies were 18-70 and 20-60, respectively. We believe that this comparison will not be optimal due to the possibility that these parameters may change with age, and the inclusion of this detail in the article would be more accurate and appropriate.

We hope that our comments and discussions will be taken into account in the ongoing discourse on this fascinating topic. We would be grateful for any additional input or suggestions from your side. Thank you for your consideration and attention.

REFERENCES

1. Güler Kanter A, Saruarov Y, Kamaşak Arpaçay B, Ülger H. Comparison of nasal anthropometric measurements of Turks living in different geographical regions. Duzce Med J. 2024;26(2):139-45.
2. Zaidi AA, Mattern BC, Claes P, McEvoy B, Hughes C, Shriver MD. Investigating the case of human nose shape and climate adaptation. PLoS Genet. 2017;13(3):e1006616.
3. Borman H, Özgür F, Gürsu G. Evaluation of soft-tissue morphology of the face in 1,050 young adults. Ann Plast Surg. 1999;42(3):280-8.
4. Rohrich RJ, Hollier LH Jr, Janis JE, Kim J. Rhinoplasty with advancing age. Plast Reconstr Surg. 2004;114(7):1936-44.
5. Garandawa H, Nwaorgu O, Oluwatosin O. Morphometric nose parameters in adult Nigerians. Internet J Otorhinolaryngol. 2009;10(2):1-6.
6. Mehta N, Srivastava RK. The Indian nose: An anthropometric analysis. J Plast Reconstr Aesthet Surg. 2017;70(10):1472-82.

SCIENTIFIC RESPONSIBILITY

In terms of scientific publishing standards, articles to be submitted should be prepared in accordance with the criteria of the International Committee of Medical Journal Editors (ICMJE), the World Association of Medical Editors (WAME) and the Committee of Publication Ethics (COPE).

- All articles must be complied with the research and publication ethics. The responsibility of the articles belongs to the authors.
- Articles are required to have not been published in anywhere previously, and/or are not in the evaluation process for publication.
- Articles must be submitted with the Copyright Transfer Form signed by all authors to begin the evaluation process. For authors' order, the signature order in the Copyright Transfer Form is based on.
- The corresponding author is responsible for the final version of the article on behalf of all authors.

ETHICAL RESPONSIBILITY

- Compliance with The Principles of Helsinki Declaration (https://www.wma.net/what-we-do/medical-ethics/declaration-of-helsinki/) is required in all studies including "human" factor. In this kind of studies, authors must state that they perform the study in compliance with these principles, they have taken the approval from ethics committee of their institution and the "informed consent" from people participating the study, in the MATERIAL AND METHODS section.
- If "animal" factor was used in the study, authors must state that they have protected the animal rights in line with the principles of Guide for the Care and Use of Laboratory Animals (https://grants.nih.gov/grants/olaw/guide-for-the-care-and-use-of-laboratory-animals.pdf) and they have taken the approval from ethics committee of their institution, in the MATERIAL AND METHODS section.
- In case reports, informed consent must be taken from patients.
- The information of the ethics committee approval should be indicated together with the name of the committee, approval date and number, in the MATERIAL AND METHODS section.
- If there is a direct-indirect commercial relation or an institution giving financial support in the study, authors must state that they have no commercial relationship with the commercial product, medicine, company etc. used, or if any, what kind of a relationship they have (consultant, other agreements), in the cover letter to the editor.
- The authors are responsible for reporting all personal and financial relationships that may be related with the study. It is necessary to state clearly whether there is any conflict of interest related to the submission and/or evaluation of the article.
- Compliance of the articles with the scientific and ethical rules is responsibility of authors.

SUBMISSION FILES

Articles must be uploaded to the system as separate files as described below.

Copyright Transfer Form: The Copyright Transfer Form to be obtained from the system during the submission must be signed by all authors in accordance with the authorship order in the article.

Cover Letter: Type of the article, the statement that has not been published previously in anywhere before, and/or not in the evaluation process for publication, if any, the people and institutions supporting the study financially and the relationship of these institutions with authors (if not, there is no relationship) must be stated. The names, academic titles, institutions, contact information and e-mail addresses of at least two reviewers suggested in relation to the subject of the article and not related to the authors and their institutions should be written. Editors' right to choose the reviewers are reserved.

Title Page: It must include the title of article (English and Turkish), short title not exceeding 40 characters, names, academic titles, ORCID® numbers, institutions, e-mail addresses of all authors, and also name, correspondence address, phone number, email address of the corresponding author. If the article has been presented previously in a scientific meeting; the name, date and place of the meeting (if not, not presented) should be stated.

Main Text: The title of the article (English and Turkish), short title not exceeding 40 characters, Abstract (English and Turkish), Keywords (English and Turkish), Main Text (sectioned according to the type of article submitted), References, Tables and Figures should be included.

Ethics Committee Approval Document: Ethics Committee Approval Document should be uploaded as a separate file for all research articles.

Note: If there are figures, pictures or photographs in the article, each of them must be uploaded as separate files.

SECTIONS THAT SHOULD BE USED ACCORDING TO THE TYPE OF ARTICLE

Research Article
TITLE (English and Turkish), SHORT TITLE, ABSTRACT (English and Turkish), Keywords (English and Turkish), INTRODUCTION, MATERIAL AND METHODS, RESULTS, DISCUSSION, CONCLUSION, REFERENCES
ABSTRACT and ÖZ should be compatible in terms of translation and each should be between 200-250 words.
ABSTRACT should be structured as "Aim, Material and Methods, Results, Conclusion".
ÖZ, should be structured as "Amaç, Gereç ve Yöntemler, Bulgular, Sonuç".

Review (Invited Only)
TITLE (English and Turkish), SHORT TITLE, ABSTRACT (English and Turkish), Keywords (English and Turkish), INTRODUCTION, Subtitles Related to the Subject, CONCLUSION, REFERENCES
ABSTRACT and ÖZ should be compatible in terms of translation and each should be between 150-200 words.

Case Report
TITLE (English and Turkish), SHORT TITLE, ABSTRACT (English and Turkish), Keywords (English and Turkish), INTRODUCTION, CASE REPORT, DISCUSSION, REFERENCES
ABSTRACT and ÖZ should be compatible in terms of translation and each should be between 100-150 words.

Other
The general writing rules are applied for the preparation of the writings (letter to the editor, editorial comment/discussion, etc.) except these three basic types of article. There is no title and abstract sections in these writings. The number of references is limited to 5. The dedicated article should be specified by giving the number and date. The name, institution and address of the author should be included at the end of writing. Answer to the letter is given by the editor, or authors of the dedicated article, by publishing again in the journal.

WRITING RULES
- Articles should be prepared as Microsoft Word® document.
- The required margins are 2.5 cm on all sides.
- Page numbers should be placed to bottom right corner of pages.
- All texts must be typed with double-space as left-aligned using 12 point Times New Roman font.

KEYWORDS
- Number of the keywords must be at least 2, words should be separated from each other by a semicolon (;).
- Keywords in Turkish must be given in accordance with Türkiye Bilim Terimleri (TBT) (http://www.bilimterimleri.com), and keywords in English must be given in accordance with Medical Subject Headings (MESH) (http://www.nlm.nih.gov/mesh/MBrowser.html).

STATISTICAL METHODS
- All research articles should be assessed in terms of biostatistics and indicated with appropriate plan, analysis and report. In these articles last subtitle of the MATERIAL and METHODS section should be the "Statistical Analysis".
- In this section, the statistical methods used in the study should be written by indicating the purpose of use, package programs and versions used for statistical analysis should be specified.
- p values should be given in three decimal digits (p=0.038; p=0.810 etc.).
- Further information to control the convenience of articles in terms of biostatistics, can obtained from www.icmje.org.

ABBREVIATIONS
- The term should be written in full words with the abbreviation in parenthesis where first mentioned, and the same abbreviation should be used throughout the entire text.
- Abbreviations used internationally should be used in accordance with the Scientific Writing Rules.

TABLES AND FIGURES
- Should be indicated at the end of the relevant sentence in the text as (Table 1) and/or (Figure 1).
- Tables (with headings) and figures (with captions) must be added after references at the end of the text as each to be on a separate page.
- The table headings should be written at top of the table (Table 1. Table heading) and the figure captions should be written below the figure (Figure 1. Figure caption) as their first letters being upper case.
- If any abbreviation or symbol is used in tables and figures, it should be explained as a footnote below.
- The figures and photographs should be upload as separate files in .png, .jpg, etc. format and at least 300 dpi resolution.
- Captions of figure and photograph should be given on a separate page respectively, after the page including last table.
- If figure, picture, table, graphic etc. which have been published before is used, written permission must be taken and it should be stated in the explanation of figures, pictures, tables, graphics. The legal responsibility in this regard belongs the authors.

ACKNOWLEDGEMENT
- If any conflict of interest, financial support, donation and other editorial (English/Turkish evaluation) and/or technical support, it must be stated in this section before the REFERENCES section.

REFERENCES
- References should be numbered according to the order of use and stated with numbers in parentheses as (1) or (1,2) or (3-5) at the end of the relevant sentence in the text.
- Reference list should be formed according to the reference order used in the text.
- If the number of authors are 6 or less, all authors should be specified, if there are 7 or more "et al." should be added after the first 6 authors are specified.
- The conference papers, personal experiences, unpublished papers, theses and internet addresses should not be used as references.
- DOI is the only acceptable online reference.

Article:
Al-Habian A, Harikumar PE, Stocker CJ, Langlands K, Selway JL. Histochemical and immunohistochemical evaluation of mouse skin histology: comparison of fixation with neutral buffered formalin and alcoholic formalin. J Histotechnol. 2014;37(4):115-24.

Aho M, Irshad B, Ackerman SJ, Lewis M, Leddy R, Pope T, et al. Correlation of sonographic features of invasive ductal mammary carcinoma with age, tumor grade, and hormone-receptor status. J Clin Ultrasound. 2013;41(1):10-7.

Book:
Buckingham L. Molecular diagnostics: fundamentals, methods and clinical applications. 2nd ed. Philadelphia: F.A. Davis; 2012.

Book Chapter:
Altobelli N. Airway management. In: Kacmarek R, Stoller JK, Heuer AJ, editors. Egan's fundamentals of respiratory care. 10th ed. St. Louis: Saunders Mosby; 2013. p.732-86.

BİLİMSEL SORUMLULUK

Bilimsel yayıncılık standartları açısından, gönderilecek makaleler, Uluslararası Tıbbi Dergi Editörler Kurulu (ICMJE), Dünya Tıbbi Editörler Birliği (WAME) ve Yayın Etik Kurulu (COPE) kriterlerine uygun olarak hazırlanmalıdır.

- Gönderilecek makalelerde araştırma ve yayın etiğine uyulması zorunludur. Makalelerin sorumluluğu yazarlarına aittir.
- Makalelerin daha önce hiç bir yerde yayınlanmamış ve/veya yayınlanmak üzere değerlendirme sürecinde olmaması gerekir.
- Değerlendirme sürecinin başlaması için makaleler, tüm yazarlar tarafından imzalanmış Telif Hakkı Devir Formu ile birlikte gönderilmelidir. Yazar sıralaması için Telif Hakkı Devir Formu'ndaki imza sırası dikkate alınır.
- Sorumlu yazar, tüm yazarlar adına makalenin son halinin sorumluluğunu taşır.

ETİK SORUMLULUK

- "İnsan" öğesini içeren tüm çalışmalarda Helsinki Deklerasyonu Prensipleri'ne (https://www.wma.net/what-we-do/medical-ethics/declaration-of-helsinki/) uygunluk aranır. Bu tip çalışmalarda yazarların, GEREÇ VE YÖNTEMLER bölümünde çalışmayı bu prensiplere uygun olarak yaptıklarını, kurumlarının etik kurullarından onay ve çalışmaya katılmış insanlardan "bilgilendirilmiş olur" (informed consent) aldıklarını belirtmeleri gerekmektedir.
- Çalışmada "Hayvan" öğesi kullanılmış ise yazarların, GEREÇ VE YÖNTEMLER bölümünde Guide for the Care and Use of Laboratory Animals (https://grants.nih.gov/grants/olaw/guide-for-the-care-and-use-of-laboratory-animals.pdf) prensipleri doğrultusunda çalışmalarında hayvan haklarını koruduklarını ve kurumlarının etik kurullarından onay aldıklarını belirtmeleri gerekmektedir.
- Olgu sunumlarında hastalardan "bilgilendirilmiş olur" (informed consent) alınmalıdır.
- Etik kurul onay bilgisi GEREÇ ve YÖNTEMLER bölümünde kurul adı, onay tarihi ve sayısı ile birlikte belirtilmelidir.
- Eğer çalışmada direkt-indirekt ticari bağlantı veya maddi destek veren kurum mevcut ise yazarlar; kullanılan ticari ürün, ilaç, firma vb. ile ticari hiçbir ilişkisinin olmadığını veya varsa nasıl bir ilişkisinin olduğunu (konsültan, diğer anlaşmalar), editöre sunum sayfasında belirtmelidirler.
- Yazarlar çalışma ile ilgili kişisel ve finansal tüm ilişkilerin bildirilmesinden sorumludur. Makalenin başvurusu ve/veya değerlendirmesi ile ilişkili herhangi bir çıkar çatışması olup olmadığının açıkça beyan edilmesi gerekmektedir.
- Makalelerin bilimsel ve etik kurallara uygunluğu yazarların sorumluluğundadır.

BAŞVURU DOSYALARI

Makaleler aşağıda belirtilen şekilde ayrı dosyalar halinde sisteme yüklenmelidir.

Telif Hakkı Devir Formu: Başvuru sırasında sistemden alınacak Telif Hakkı Devir Formu tüm yazarlar tarafından makaledeki yazar sıralamasına uygun şekilde imzalanmış olmalıdır.

Başvuru Mektubu: Makalenin türü, daha önce hiç bir yerde yayınlanmamış ve/veya yayınlanmak üzere değerlendirme sürecinde olmadığı, varsa çalışmayı maddi olarak destekleyen kişi ve kuruluşlar ve bu kuruluşların yazarlarla olan ilişkileri (yoksa olmadığı) belirtilmelidir. Makalenin konusuyla ilgili olarak önerilen, yazarlarla ve kurumlarıyla ilgisi olmayan en az iki hakemin adları, akademik unvanları, kurumları, iletişim bilgileri ve e-posta adresleri yazılmalıdır. Editörlerin hakemleri seçme hakkı saklıdır.

Başlık Sayfası: Makalenin başlığını (İngilizce ve Türkçe), 40 karakteri geçmeyen kısa başlık, tüm yazarların adlarını, akademik unvanlarını, ORCID® numaralarını, kurumlarını, e-posta adreslerini ve ayrıca sorumlu yazarın adını, yazışma adresini, telefon numarasını, e-posta adresini içermelidir. Makale daha önce bilimsel bir toplantıda sunulmuş ise toplantı adı, tarihi ve yeri (yoksa sunulmadığı) belirtilmelidir.

Ana Metin: Makalenin başlığı (İngilizce ve Türkçe), 40 karakteri geçmeyen kısa başlık, Öz (İngilizce ve Türkçe), Anahtar kelimeler (İngilizce ve Türkçe), Ana Metin (gönderilen makalenin türüne uygun olarak bölümlere ayrılmış), Kaynaklar, Tablolar ve Şekil açıklamaları yer almalıdır.

Etik Kurul Onay Belgesi: Tüm araştırma makaleleri için Etik Kurul Onay Belgesi ayrı bir dosya olarak yüklenmelidir.

Not: Makalede şekil, resim veya fotoğraf varsa bunların da her biri ayrı birer dosya olarak yüklenmelidir.

MAKALE TÜRÜNE GÖRE KULLANILMASI GEREKEN BÖLÜMLER

Araştırma Makalesi

BAŞLIK (İngilizce ve Türkçe), KISA BAŞLIK, ÖZ (İngilizce ve Türkçe), Anahtar kelimeler (İngilizce ve Türkçe), GİRİŞ, GEREÇ VE YÖNTEMLER, BULGULAR, TARTIŞMA, SONUÇ, KAYNAKLAR

ÖZ ve ABSTRACT çeviri açısından uyumlu olmalı ve her biri kendi içinde 200-250 kelime arasında olmalıdır.
ABSTRACT, "Aim, Material and Methods, Results, Conclusion" şeklinde yapılandırılmalıdır.
ÖZ, "Amaç, Gereç ve Yöntemler, Bulgular, Sonuç" şeklinde yapılandırılmalıdır.

Derleme (Sadece Davetli)

BAŞLIK (İngilizce ve Türkçe), KISA BAŞLIK, ÖZ (İngilizce ve Türkçe), Anahtar kelimeler (İngilizce ve Türkçe), GİRİŞ, Konu ile İlgili Alt Başlıklar, SONUÇ, KAYNAKLAR

ÖZ ve ABSTRACT çeviri açısından uyumlu olmalı ve her biri kendi içinde 150-200 kelime arasında olmalıdır.

Olgu Sunumu

BAŞLIK (İngilizce ve Türkçe), KISA BAŞLIK, ÖZ (İngilizce ve Türkçe), Anahtar kelimeler (İngilizce ve Türkçe), GİRİŞ, OLGU SUNUMU, TARTIŞMA, KAYNAKLAR

ÖZ ve ABSTRACT çeviri açısından uyumlu olmalı ve her biri kendi içinde 100-150 kelime arasında olmalıdır.

Diğer

Bu üç temel makale türü dışındaki (editöre mektup, editöryel yorum/tartışma vb.) yazıların hazırlanmasında da genel yazım kuralları geçerlidir. Bu tür yazılarda başlık ve öz bölümleri yoktur. Kaynak sayısı 5 ile sınırlıdır. İthaf olunan makale sayı ve tarih verilerek belirtilmelidir. Yazının sonunda yazarın ismi, kurumu ve adresi yer almalıdır. Mektuba cevap, editör veya makalenin yazarları tarafından, yine dergide yayınlanarak verilir.

YAZIM KURALLARI
- Makaleler Microsoft Word® belgesi olarak hazırlanmalıdır.
- Sayfa kenarlarında 2,5 cm boşluk bırakılmalıdır.
- Sayfa numaraları sayfanın sağ alt köşesine yerleştirilmelidir.
- Tüm metinler 12 punto Times New Roman karakteri kullanılarak çift satır aralığı ile sola hizalanmış olarak yazılmalıdır.

ANAHTAR KELİMELER
- Anahtar kelime sayısı en az 2 olmalı, kelimeler birbirlerinden noktalı virgül (;) ile ayrılmalıdır.
- Türkçe anahtar kelimeler Türkiye Bilim Terimleri (TBT)'ne (http://www.bilimterimleri.com), İngilizce anahtar kelimeler Medical Subject Headings (MESH)'e (http://www.nlm.nih.gov/mesh/MBrowser.html) uygun olarak verilmelidir.

İSTATİSTİKSEL YÖNTEMLER
- Tüm araştırma makaleleri biyoistatistik açıdan değerlendirilmeli ve uygun plan, analiz ve raporlama ile belirtilmelidir. Bu makalelerde, GEREÇ VE YÖNTEMLER bölümünün son alt başlığı "İstatistiksel Analiz" olmalıdır.
- Bu bölümde çalışmada kullanılan istatistiksel yöntemler ne amaçla kullanıldığı belirtilerek yazılmalı, istatistiksel analiz için kullanılan paket programlar ve sürümleri belirtilmelidir.
- p değerleri ondalık üç basamaklı (p=0,038; p=0,810 vb.) olarak verilmelidir.
- Makalelerin biyoistatistik açıdan uygunluğunun kontrolü için ek bilgi www.icmje.org adresinden temin edilebilir.

KISALTMALAR
- Terim ilk kullanıldığında parantez içinde kısaltmayla birlikte açık olarak yazılmalı ve tüm metin boyunca aynı kısaltma kullanılmalıdır.
- Uluslararası kullanılan kısaltmalar Bilimsel Yazım Kurallarına uygun şekilde kullanılmalıdır.

TABLOLAR VE ŞEKİLLER
- Metinde ilgili cümlenin sonunda (Tablo 1) ve/veya (Şekil 1) şeklinde belirtilmelidir.
- Tablolar (başlıklarıyla birlikte) ve şekiller (açıklamalarıyla birlikte) kaynaklardan sonra ve her biri ayrı bir sayfada olacak şekilde metnin sonuna eklenmelidir.
- Tablo başlıkları tablo üstünde (Tablo 1. Tablo başlığı), şekil açıklamaları ise şeklin altında (Şekil 1. Şekil açıklaması), ilk harfleri büyük olacak şekilde yazılmalıdır.
- Tablolarda ve şekillerde kısaltma veya sembol kullanılmış ise altında dipnot olarak açıklanmalıdır.
- Şekiller ve fotoğraflar, .png, .jpg vb. formatta ve en az 300 dpi çözünürlükte ayrı dosyalar halinde yüklenmelidir.
- Şekil ve fotoğraf alt yazıları, son tablonun olduğu sayfadan sonra, ayrı bir sayfada sırasıyla verilmelidir.
- Daha önce basılmış şekil, resim, tablo, grafik vb. kullanılmış ise yazılı izin alınmalı ve açıklama olarak belirtilmelidir. Bu konudaki hukuki sorumluluk yazarlara aittir.

TEŞEKKÜR
- Eğer çıkar çatışması/çakışması, finansal destek, bağış ve diğer bütün editöryel (İngilizce/Türkçe değerlendirme) ve/veya teknik yardım varsa, bu bölümde, KAYNAKLAR bölümünden önce belirtilmelidir.

KAYNAKLAR
- Kaynaklar, kullanım sırasına göre numaralandırılmalı ve metin içinde ilgili cümlenin sonunda parantez içinde numaralarla (1) veya (1,2) veya (3-5) şeklinde verilmelidir.
- Kaynaklar dizini, metin içinde kaynakların kullanıldığı sıraya göre oluşturulmalıdır.
- Yazar sayısı 6 veya daha az ise tüm yazarlar belirtilmeli, 7 veya daha fazla ise ilk 6 yazar belirtildikten sonra "et al." eklenmelidir.
- Kongre bildirileri, kişisel deneyimler, basılmamış yayınlar, tezler ve internet adresleri kaynak olarak gösterilmemelidir.
- DOI tek kabul edilebilir online referanstır.

Makale:
Al-Habian A, Harikumar PE, Stocker CJ, Langlands K, Selway JL. Histochemical and immunohistochemical evaluation of mouse skin histology: comparison of fixation with neutral buffered formalin and alcoholic formalin. J Histotechnol. 2014;37(4):115-24.

Aho M, Irshad B, Ackerman SJ, Lewis M, Leddy R, Pope T, et al. Correlation of sonographic features of invasive ductal mammary carcinoma with age, tumor grade, and hormone-receptor status. J Clin Ultrasound. 2013;41(1):10-7.

Kitap:
Buckingham L. Molecular diagnostics: fundamentals, methods and clinical applications. 2nd ed. Philadelphia: F.A. Davis; 2012.

Kitap Bölümü:
Altobelli N. Airway management. In: Kacmarek R, Stoller JK, Heuer AJ, editors. Egan's fundamentals of respiratory care. 10th ed. St. Louis: Saunders Mosby; 2013. p.732-86.

DÜZCE
ÜNİVERSİTESİ